Synthesis and Biophysical Studies of PNA Analogues Derived from 4-Substituted Proline and 1,2,3-Triazole in the Backbone

Thesis Submitted to
The University of Pune for the degree of
Doctor of Philosophy
in
Chemistry

By

Gitali Devi

Research Supervisor

Prof. Krishna N. Ganesh

DIVISION OF ORGANIC CHEMISTRY
NATIONAL CHEMICAL LABORATORY
PUNE-411008

October, 2009

CERTIFICATE

This is to certify that the work presented in the thesis entitled **"Synthesis and biophysical studies of PNA analogues derived from 4-substituted proline and 1,2,3-triazole in the backbone"** submitted by **Gitali Devi**, was carried out by the candidate at National Chemical Laboratory, Pune, under my supervision. Such materials as obtained from other sources have been duly acknowledged in the thesis.

Prof. K. N. Ganesh, FNA, FNASc **October, 2009**
(Research Supervisor)
Director, IISER Pune
Pune -411008

J. C. Bose Fellow
National Chemical Laboratory
Pune -411 008

CANDIDATE'S DECLARATION

I hereby declare that the thesis entitled **"Synthesis and biophysical studies of PNA analogues derived from 4-substituted proline and 1,2,3-triazole in the backbone"** submitted for the award of degree of ***Doctor of Philosophy*** in Chemistry to the University of Pune has not been submitted by me to any other university or institution. This work was carried out by me at the National Chemical Laboratory, Pune, India. Such materials as obtained from other sources have been duly acknowledged in the thesis.

Gitali Devi **October, 2009**
National Chemical Laboratory
Pune- 411 008

Dedicated to my beloved parents

and family members

Acknowledgement

It gives me an immense pleasure to express my deepest gratitude to my supervisor Prof. K. N. Ganesh, whose encouragement, guidance and support from the initial to the final level of my research enabled me to develop a proper understanding of the subject. I am thankful for the confidence he had on me which encouraged me to pursue different scientific ideas during my research period. During my tough time in professional as well as personal life he always supported me wholeheartedly. His receptive behaviour was a source of encouragement for me.

I am also grateful to Dr. V. A. Kumar without whose support, this thesis would not have been possible. Her suggestions and encouragement has been an immense help during my research period.

My deepest gratitude goes to my family for their unflagging love and support throughout my life, this dissertation is simply impossible without them. I am indebted to my father, who spared no effort to provide the best possible environment for me to grow up. I am thankful for my mother, brother and sisters for giving me unconditional love all the way. Special mention must be made of my husband Khagen, whose love and rock solid support gave me enough strength to complete my research.

I sincerely thank Mrs Anita Gunjal and Dr. Moneesha D'Costa for all the scientific discussions and help, Mrs Mane for HPLC experiments. My thanks are also due to Dr S. Hotha for helping me during the initial period of my research, Dr. N. P. Argade for providing me the initial infrastructure, and Dr H. V. Thulshiram for providing all the necessary help. Also special thanks to Dr Mahesh Kulkarni and Mrs Shanta Kumari for the MALDI-TOF and LC-MS experiments.

My heartfelt thank goes to Madhuri and her family. From the beginning of my Ph. D, they are the ones who supported me during the ups and downs and never left me alone. Also special thanks to Maitri, Indu and Madhuri Patil for giving me all the love and support and the good times we spent together.

I admire the co-operation of my seniors and colleagues who have taught me many things. I thank Dr Pallavi, Dr Raman, Dr Umashankara, Dr Govidaraju, Dr Nagendra, Dr Sunil, , Dr Gaurishankar, Dr Pravin, Amit, Ashwani, Shridhar, Roopa,

Pradnya, Manaswini, Mahesh, Deepak, Nitin, Vijay, Sachin, Namrata, Seema, Parameswar, Kiran, Venu, Manoj and Anjan for your cheerful company. Pawar and Bhumkar deserve a big thank for the laboratory assistance provided to me.

I wish to thank the many friends and colleagues who have helped in one way or other, especially Manash, Pranjal Kalita, Sanjeev, Diganta, Pranjal Barua, Sasanka, Lakhi, Khirud, Rahul, Ankur, Sofia, Meera, Shweta and Deepak. Also Prity, Gitanjali, Debashish, Bornali, Parasha, Bagmita, Barsha, Bristi, Dolly and Ashim da.

I take this opportunity to thank all those who have helped and supported me throughout my education period. I thank director NCL, for allowing me to work in this premier research institute and providing the entire necessary infrastructure. Also, my sincere thanks to IISER, Pune for providing all necessary facilities and CSIR, New Delhi for the financial support.

Gitali Devi

Contents

Chapter 2: Design, synthesis and biophysical evaluation of backbone extended *prolyl*PNA

Chapter 3: Synthesis of 1,2,3-triazole des-peptidic analogues of PNA and its biophysical studies

Chapter 4: Synthesis and enzyme mimetic hydrolytic studies of imidazolyl PNA

Abbreviations

A	Adenine
Ac_2O	Acetic anhydride
aeg	Aminoethylglycine
aep	Aminoethylprolyl
ap	Antiparallel
aq.	Aqueous
Bz	Benzoyl
C	Cytosine
Calc.	Calculated
Cbz	Benzyloxycarbonyl
CD	Circular Dichroism
ch	Cyclohexyl
cp	Cyclopentyl
DCC	Dicyclohexylcarbodiimide
DCM	Dichloromethane
DCU	Dicyclohexyl urea
DIAD	Diisopropyl azodicarboxylate
DIPEA/DIEA	N,N-Diisopropylethylamine
DMAP	N,N-Dimethyl-4-aminopyridine
DMF	N,N-dimethylformamide
DMSO	N,N-Dimethyl sulfoxide
DNA	2’-deoxyribonucleic acid
ds	Double stranded
eda	Ethylenediamine
EDTA	Ethylene diamine tetraacetic acid
Et	Ethyl
EtOAc	Ethyl acetate
Fmoc	9-Fluorenylmethoxycarbonyl

g	gram
G	Guanine
gly	Glycine
hrs	Hours
his	Histidine
HBTU	2-(1H-Benzotriazole-1-yl)-1,1,3,3 tetramethyl-uronum-hexafluoro-phosphate
HIV	Human Immuno Difficiency Virus
HOBt	N-Hydroxybenzotriazole
HPLC	High Performance Liquid Chromatography
IR	Infra red
L-	Levo-
LC-MS	Liquid Chromatography-Mass Spectrometry
Lys	Lysine
MALDI-TOF	Matrix Assisted Laser Desorption Ionisation-Time of Flight
MBHA	4-Methyl benzhydryl amine
mg	milligram
MHz	Megahertz
min	minutes
µL	Microliter
µM	Micromolar
mL	milliliter
mM	millimolar
mmol	millimoles
m.p.	melting point
MS	Mass spectrometry
MW	Molecular weight
N	Normal
nm	Nanometer
NMR	Nuclear Magnetic Resonance

p	Parallel
PCR	Polymerase chain reaction
ppm	Parts per million
PNA	Peptide Nucleic Acid
PS-oligo	Phosphorothioate-oligo
R	Rectus
R_f	Retention factor
RNA	Ribonucleic Acid
RP	Reverse Phase (-HPLC)
rt	Room temperature
RT	Retention time
S	Sinister
SPPS	Solid Phase Peptide Synthesis
ss	Single strand
T	Thymine
TEA/Et_3N	Triethylamine
TFA	Trifluoroacetic acid
TFMSA	Trifluoromethane sulfonic acid
THF	Tetrahydrofuran
Tm	Melting temperature
TPP	Triphenylphosphine (PPh_3)
UV-Vis	Ultraviolet-Visible

Abstract

The thesis entitled **"Synthesis and biophysical studies of PNA analogues derived from 4-substituted proline and 1,2,3-triazole in the backbone"** comprises studies towards the design, synthesis and biophysical studies of modified PNA oligomers towards the DNA binding. The thesis has been divided into four chapters.

Chapter 1: The first chapter gives an overview on background literature for the undertaking research work, briefly reviews the literature and recent advancements in the area of peptide nucleic acid and their applications.

Chapter 2: This chapter describes design, synthesis of backbone extended *prolyl*PNA monomer and binding studies of the corresponding oligomers towards complementary DNA.

Chapter 3: In this chapter we have explored the replacement of the amide functions in polyamide backbone of PNA with the triazole rings to examine its effect on PNA hybridization properties.

Chapter 4: This chapter presents the synthesis, biophysical studies of catalytic antisense PNA and its enzyme mimetic hydrolytic studies towards the complementary RNA oligonucleotide.

Chapter 1: Introduction to Nucleic Acids

The recognition of DNA and RNA sequences by complementary oligonucleotides is a central feature of biotechnology and is important for hybridization based biological applications. This is vital to make antisense- or antigene-based inhibition as a practical approach to therapeutics. Zamecnik and Stephensen were the first to propose the use of synthetic antisense oligonucleotides for therapeutic purposes. The specific inhibition is based on the Watson-Crick base-pairing between the heterocyclic bases of the antisense oligonucleotide and of the target nucleic acid. In order to meet all the requirements of a successful medicinal agent, it is necessary for normal oligonucleotides to be

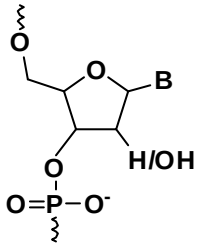

DNA/RNA

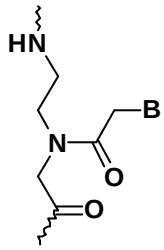

PNA

chemically modified in a suitable manner. To address the combined task of improving the rate, affinity or specificity of oligonucleotide recognition, while the enhancing membrane permeability and resistance to nuclease digestion, several chemical modifications of DNA have been attempted.

The most fundamental change to the natural structure was introduced by Nielsen *et.al,* who replaced the entire sugar phosphate backbone by an *N*-(2-aminoethyl) glycine-based polyamide structure. The basic PNA structure (Figure1) consists of *N*-(2-aminoethyl) glycyl backbone carrying nucleobases through an acetyl linker. Peptide Nucleic Acids (PNAs) bind with higher affinity to complementary DNA/RNA than their natural counterparts obeying Watson-Crick base pairing rule. PNAs and their analogues are resistant to proteases and nucleases. Due to these exceptional properties PNAs have major applications as a tool in molecular biology, as lead compounds for development of gene targeted drugs via antisense/antigene technology, for diagnostics and biosensors, and as building blocks for designing PNA supramolecular constructs.

The current limitations in PNA properties are its poor water solubility and lack of cell permeability coupled with ambiguity in DNA/RNA recognition arising from its equally facile binding in a parallel/antiparallel fashion with the complementary nucleic acid sequences. These limitations are being systematically addressed with rationally modified PNA analogues. The solubility of PNAs was improved through conjugation with cationic ligands such as polyamines. The cell penetrability has been improved by conjugation with various transfer molecules such as cell-penetrating peptides. The equal binding of PNA in parallel and antiparallel orientations to DNA/RNA reduces its target specificity by a factor of 2, which can have serious implications for therapeutic applications depending on the other gene that gets affected. This issue was addressed by introduction of chirality into achiral PNA backbones to affect orientational selectivity in complementary DNA/ RNA binding.

Chapter 2: Design, synthesis and biophysical evaluation of backbone extended *prolyl*PNA

The rationale for the present work is to design peptide nucleic acid analogues that can bind selectively to RNA or DNA. Constraining of backbone in classical PNA leads to a low energy conformation different from the conformation preferred for the formation of a stable PNA-DNA complex. This may be achieved if the conformational freedom in *aeg*PNA is curtailed by bridging the aminoethyl, or glycyl acetyl linker arms leading to cyclic analogues (Figure 1) and thus achieving orientation selective binding by virtue of chirality and rigidity in the backbone of complementary DNA *via* hydrogen bonding. Keeping these in view the backbone extended (2*S*,4*S*)-*prolyl*PNA **I** and (2*S*,4*R*)-*prolyl*PNA **II** (Figure 1) has been designed and these were synthesized following the reaction sequences mentioned in Scheme 1 and Scheme 2 respectively.

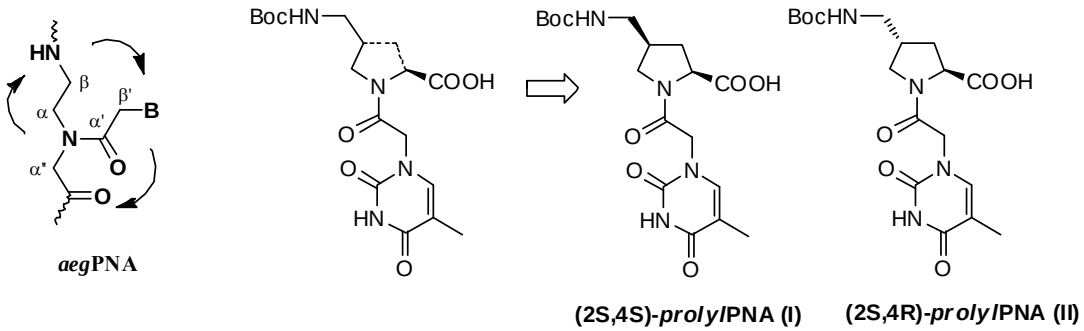

Figure 1: Chemical structure of modified PNA monomers

Synthesis of (2*S*,4*S*) and (2*S*,4*R*)-backbone extended *prolyl*PNA monomer: *trans*-4-hydroxy-L- proline was the starting material for the synthesis of backbone extended *prolyl*PNA monomer **I** and **II**. *trans*-4-hydroxy-L-proline was converted to the compound **2** and further converted to the final monomer following the reaction sequence mentioned in the Scheme 1. The same reaction sequence was followed for the synthesis of (2*S*,4*R*)- backbone extended *prolyl*PNA monomer after inversion of configuration through Mitsunobu condition.

Biophysical studies of PNA oligomers

The synthesis of the oligomers (**PNA2-PNA18**) incorporating the conformationally constrained chiral modified units **8** and **11** at specific positions in the *aeg*PNA oligomer was done on the solid support using solid phase peptide synthesis method. Homopyrimidine (thymine) octamers (**PNA1-PNA9**) are synthesized to study the effect of the two prolyl isomers (2*S*,4*S*) and (2*S*,4*R*), for their triplex forming ability. The mixed purine-pyrimidine oligomers (**PNA11-PNA18)** were synthesized for comparative studies with mixed *aeg*PNA (**PNA10**) oligomer. The binding stoichiometry of the oligomers were determined by Job's method which was found to be 2:1 for homopyrimidine oligomers and 1:1 for mixed purine-pyrimidine mixed oligomers.

Scheme1: Synthesis of (2*S*,4*S*)-backbone extended *prolyl*PNA monomer

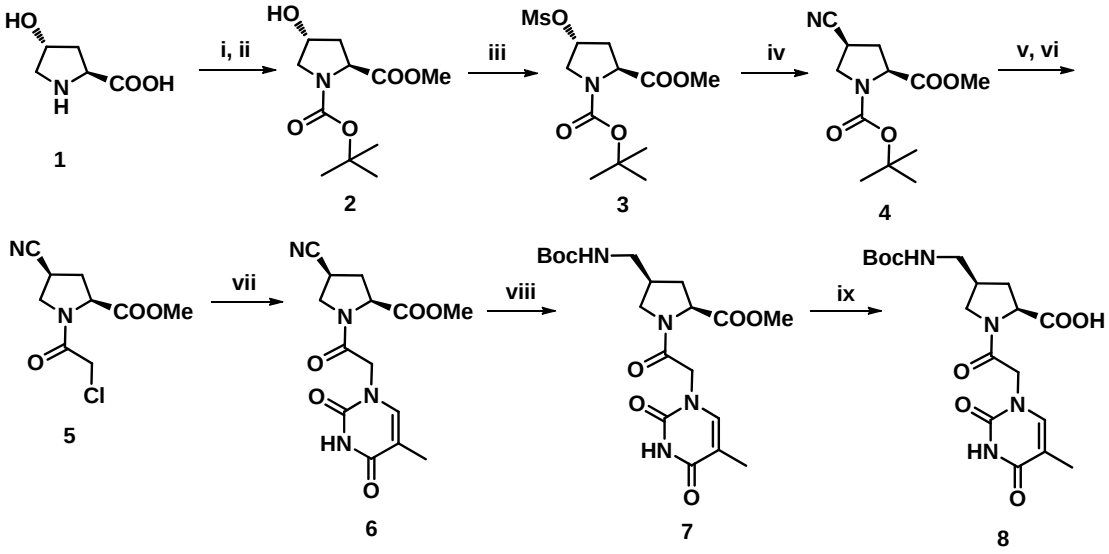

Reagents and condition: (i) $SOCl_2$, MeOH, 0-60^oC (ii) $(Boc)_2O$, Et_3N, ACN:H_2O, 85% (iii) Mesyl chloride, pyridine, 0^oC, 92% (iv) NaCN, DMSO, 60^oC, 35% (v) 50% TFA in DCM, 25% ammonia solution (vi) $ClCH_2COCl$, Et_3N, DCM, 0^oC, 72% (vii) Thymine, K_2CO_3, DMF, 60^oC, 81% viii) 10 mol% Pd/C, Et_3N, $(Boc)_2O$, MeOH, 87% (ix) 1N aq LiOH, THF, 80%.

Scheme 2: Synthesis of (2*S*,4*R*)-backbone extended *prolyl*PNA monomer

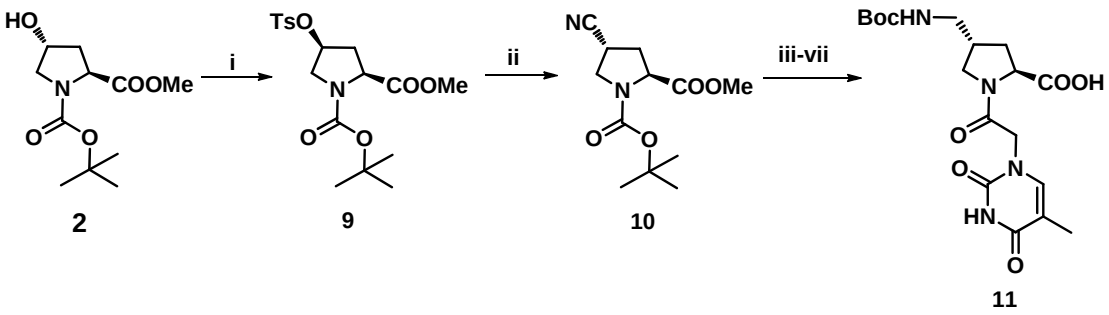

Reagents and condition: (i) *p*-toluene sulphonic acid, PPh_3, DIAD, THF, 54% (ii) NaCN, DMSO, 60°C, 28% (iii) 50% TFA in DCM, 25% ammonia solution (iv) $ClCH_2COCl$, Et_3N, DCM, 0°C, 73% (v) Thymine, K_2CO_3, DMF, 60°C, 81% (vi) 10 mol% Pd/C, MeOH, $(Boc)_2O$, Et_3N, 81% (vii) 1N aq LiOH, THF, 83%

Table 1: Melting studies of backbone extended *prolyl*PNA oligomers

S No	Entry	PNA composition	UV-T_m DNA1	
1	**PNA1**	H. TTTTTTTT-LysNH_2	45.0	
2	**PNA2**	H. **t$_{SS}$**TTTTTTT-LysNH_2	47.4	
3	**PNA3**	H. TTT**t$_{SS}$**TTTT-LysNH_2	30.5	
4	**PNA4**	H. TTT**t$_{SS}$**TTT**t$_{SS}$**-LysNH_2	28.1	
5	**PNA5**	H. TTTTTTT**t$_{SS}$**-LysNH_2	31.4	
6	**PNA6**	H. **t$_{SR}$**TTTTTTT-LysNH_2	48.9	
7	**PNA7**	H. TTT**t$_{SR}$**TTTT-LysNH_2	37.3	
8	**PNA8**	H. TTT**t$_{SR}$**TTT**t$_{SR}$**-LysNH_2	24.4	
9	**PNA9**	H. TTTTTTT**t$_{SR}$**-LysNH_2	28.3	
Mixed sequences			**DNA2***	**DNA3***
10	**PNA10**	H. T ATT ATT ATT-LysNH_2	10.2	23.9
11	**PNA11**	H. **t$_{SS}$** ATT ATT ATT-LysNH_2	NB	33.9
12	**PNA12**	H.T ATT A**t$_{SS}$**T ATT-LysNH_2	34.1	48.1
13	**PNA13**	H. **t$_{SS}$** ATT A**t$_{SS}$**T ATT-LysNH_2	34.4	50.6
14	**PNA14**	H.T ATT ATT AT**t$_{SR}$**-LysNH_2	NB	NB
15	**PNA15**	H.**t$_{SR}$** ATT ATT ATT-LysNH_2	NB	28.3
16	**PNA16**	H.T ATT A**t$_{SR}$**T ATT-LysNH_2	18.0	33.4
17	**PNA17**	H.**t$_{SR}$** ATT A**t$_{SR}$**T ATT-LysNH_2	NB	23.7
18	**PNA18**	H. T ATT ATT AT**t$_{SR}$**-LysNH_2	NB	19.3

[a]NB indicates non-binding to complementary DNA; **DNA2** is 5' A TAA TAA TAA 3' **DNA3** is 5' AAT AAT AAT A 3'

The UV-T_m studies show the destabilization for the modified homopyrimidine oligomers for both the isomers as compared to *aeg*PNA homopyrimidine oligomers.

Mixed purine-pyrimidine oligomers show the position dependent stability towards complementary DNA (Table 1) binding.

Chapter 3: Synthesis of 1,2,3-triazole des-peptidic analogues of PNA and its biophysical studies

Triazoles have been shown to be good isosteres of peptide bond and hence used to design backbone of cyclotetrapepeptide mimics, peptoid oligomers and even to replace the phosphate linkage in DNA. These non-peptidic links that adopt well-defined conformations are alternative to peptide bond in design of peptidomimetic drugs. Triazoles can be easily accessed synthetically through copper catalysed version of Huisgen (3+2) cycloaddition reaction ("click" reaction). In the above context of literature, we have explored the replacement of the amide functions in polyamide backbone of PNA with the triazole rings to examine its effect on PNA hybridization properties. The triazole link in **V** was generated from click reaction of the polymer supported azido component **III** with the acetylenic component **IV** synthesized in solution (Figure 2).

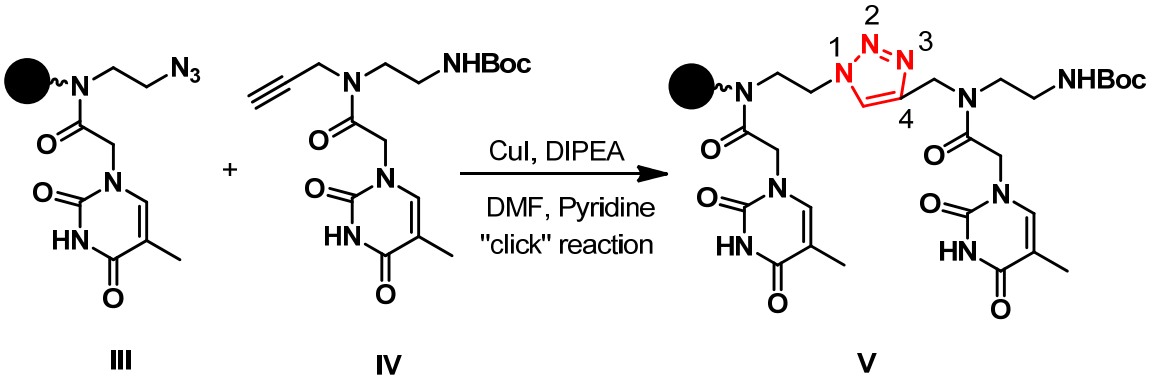

Figure 2: Schematic diagram for triazole synthesis on solid support

Synthesis of acetylenic monomer: The alkyne functionalized fragment **16** was synthesized starting from1,2-diaminoethane **12** using the reaction sequence mentioned in Scheme 3

Scheme 3: Synthesis of alkyne functionalized monomer

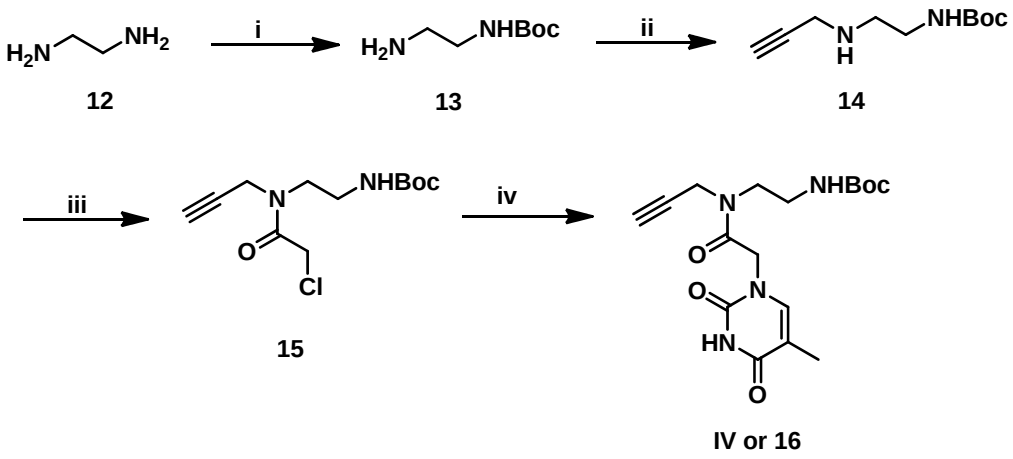

Reagents and conditions: i. $(Boc)_2O$, THF, 60% ii. Propargyl bromide, K_2CO_3, CH_3CN, 56% iii. $ClCH_2COCl$, Et_3N, DCM, 81% iv. Thymine, K_2CO_3, DMF, 83%

Synthesis of 1,2,3-triazole on solid support: The synthesis of PNA analogues (Table 2) in which the amide bond is replaced by 1,2,3-triazole unit was achieved on solid phase (Scheme 4) using the Huisgen 1,3-dipolar cycloaddition reaction catalyzed by Cu (I). The solid supported amine was converted to azide using triflyl azide (TfN_3). The resulting azide was subjected to 1,3 dipolar cycloaddition reaction with the acetylenic component **16**, synthesized on solution phase to incorporate 1,2,3-triazole unit in the PNA backbone. Cu(I) was used as the catalyst to obtain the regioselectivity . The oligomers synthesized are depicted in Table 2.

Table 2: UV-T_m of *triazolyl* PNA oligomers

Entry	PNA	UV-T_m Single strand	UV-T_m (^oC)	ΔT_m (^oC)
PNA24	H-TTTTTT-$LysNH_2$	---	20.5	---
PNA25	H-TTTTT*T-$LysNH_2$	---	29.8	+8.4
PNA26	H-T*TTTTT-$LysNH_2$	---	31.9	+11.4
PNA27	H- TT*TT*TT-$LysNH_2$	---	34.3	+13.8
PNA28	H- T*TT*TT*T-$LysNH_2$	42.9	43.6	---
PNA29	H-T*T*T*T*T*T-$LysNH_2$	48.1	47.9	---

Complementary DNA is 5’ CG A_8 GC 3’

Scheme 4: Synthesis of 1,4 substituted 1,2,3-triazole on solid support

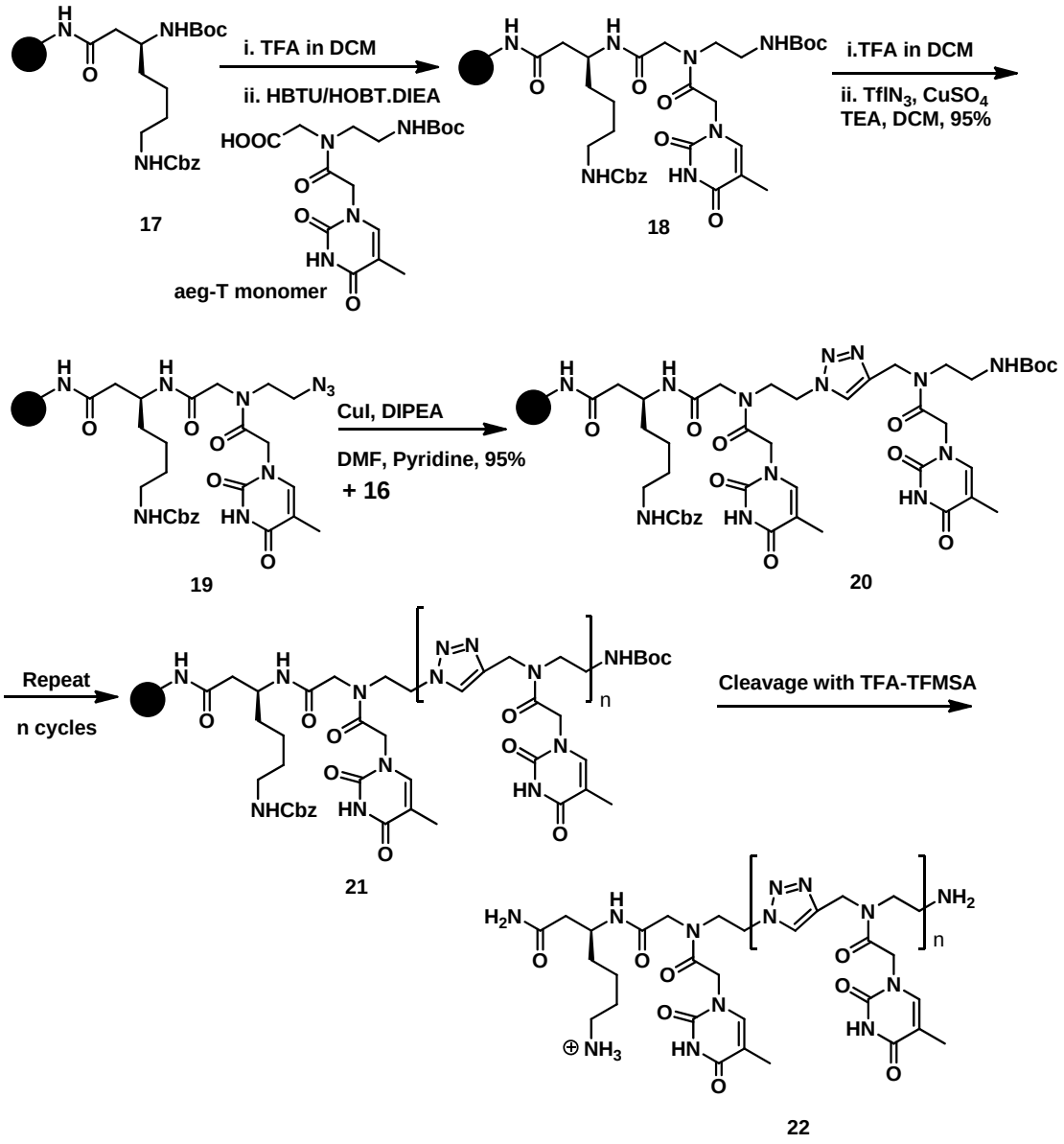

It is demonstrated here that 1,2,3-triazole analogues of PNA wherein the amide link in backbone is replaced by triazole (**V**) systematically and significantly stabilize the derived PNA_2:DNA triplexes With increasing number of triazole unit the single stranded PNA undergo self organized structure.

Chapter 4: Synthesis and enzyme mimetic hydrolytic studies of imidazolyl PNA

A number of approaches to synthetic artificial ribonucleases have been developed over the last decade. Apart from the scientific challenge in designing and synthesizing these artificial enzymes, the simultaneous development of antisense therapy leads to the possibility of combining these two concepts and thus using the artificial nuclease for medical applications. In the protein universe, the ribonucleases cleave RNAs using amino acids such as histidine, which carries an imidazole side chain that has a nitrogen atom with a p*K*a around 6. Hence it has been designed to synthesize the PNA monomers **VI**, **VII** and PNA oligomer **VIII** (Figure 4) containing imidazole as the catalytic unit. This catalytic moiety can cleave the complementary DNA/RNA sequence through hydrolysis of phosphodiester units. An efficient antisense artificial ribonuclease consists of two moieties, a catalytic group and a probe for sequence recognition. The catalytic group cleaves the phosphodiester bond and the oligonucleotide moiety brings the sequence selectivity for hybridization.

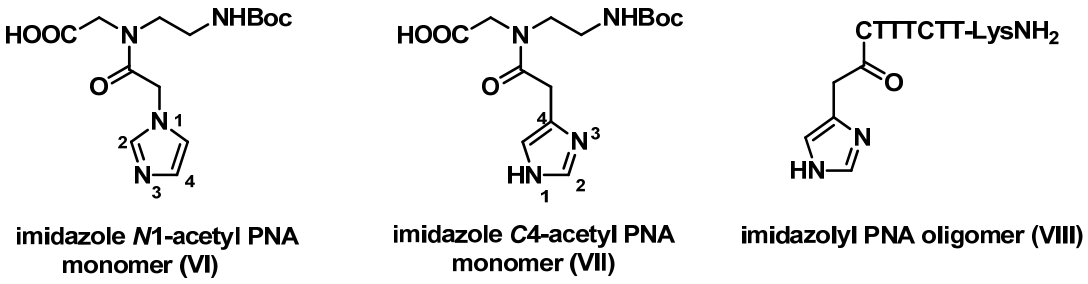

Figure 4: Chemical structure of imidazole based monomer and oligomer

Synthesis of imidazole *N*1-acetyl PNA and imidazole *C*4-acetyl PNA monomer: The synthesis of imidazole *N*1-acetyl PNA monomer **VI** starts from commercially available 1,2-diaminoethane **23** (Scheme 5). After obtaining the mono alkylated product **25** as mentioned in Scheme **5**, acylation was done with chloroacetyl chloride in presence of triethylamine to get the product **26**, which was further alkylated using imidazole to obtain product **27**. This upon hydrolysis using 1N aqLiOH gives the monomer acid **28** or **VI**. Compound **25** was subjected to

EDC/DIPEA coupling (Scheme 6) followed by hydrolysis, for the synthesis of compound **VII** or **30** where imidazole *C*4-acetyl unit is attached to the PNA backbone.

Scheme 5: Synthesis of imidazole *N*1-acetyl PNA monomer

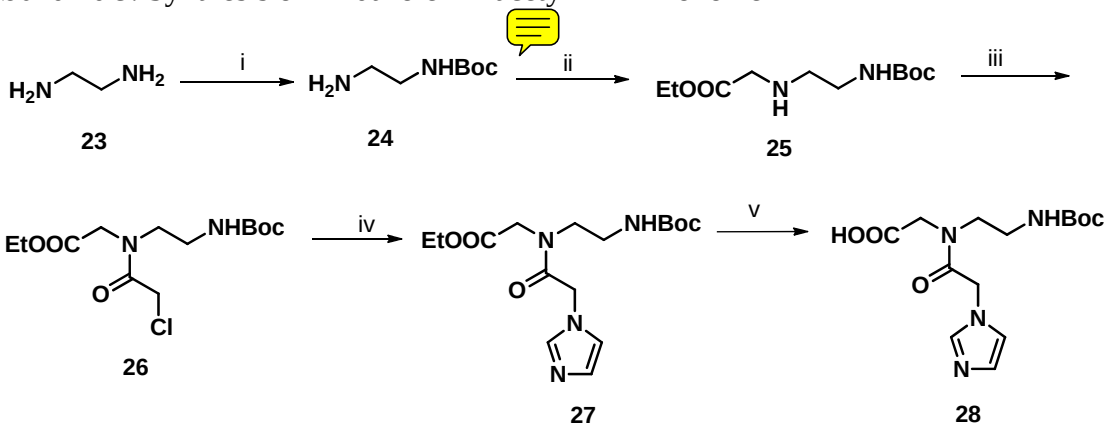

Reagents and conditions: i. $(Boc)_2O$, THF, 60% ii. $BrCH_2COOEt$, Et_3N, ACN, 81% ii. $ClCH_2COCl$, Et_3N, DCM, 80% iii. Imidazole, K_2CO_3, 60°C, 79%, iv. 1N aq LiOH, THF, 86%

Scheme 6: Synthesis of imidazole *C*4-acetyl PNA monomer

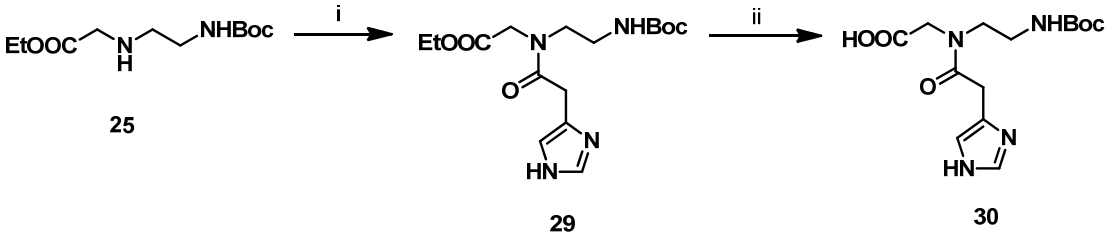

Reagents and conditions: i. imidazole-4-acetic acid monohydrochloride, EDC, DIPEA, DMF, 22% ii. 1N LiOH, THF, 78%

To study the binding selectivity, specificity and discrimination of the modified imidazole-*N*1-acetyl PNA oligomers towards complementary DNA, temperature dependent UV-absorbance experiments were carried out with all the synthesized oligomers (**PNA31-PNA36**, Table 3 and Table 4) and the T_m data was compared with the control *aeg*PNA (**PNA1, PNA10**). The stability of the imidazole *N*1-acetyl PNA duplexes (**PNA33-36**) with DNA was also studied.

Table 3: UV melting data for homopyrimidine and oligomers

S. No.	Entry	Triplex PNA$_2$:DNA	UV-T_m (^oC)	ΔT_m (^oC)
1	**PNA1**	H. TTTTTTTT-LysNH$_2$	45.0	-----
	DNA1	5' CGAAAAAAAAGC 3'		
	PNA1	H$_2$N Lys-TTTTTTTT.H		
2	**PNA31**	H. **I$_m$**TTTTTTT-LysNH$_2$	28.3	-16.7
	DNA1	5' CGAAAAAAAAGC 3'		
	PNA31	H$_2$N Lys-TTTTTTT**I$_m$**.H		
3	**PNA32**	H. TTT **I$_m$** TTTT-LysNH$_2$	28.3	-16.7
	DNA1	5' CGAAAAAAAAGC 3'		
	PNA32	H$_2$N Lys-TTTT**I$_m$**TTT.H		

T_m = melting temperature PNA:DNA complexes (measured in the buffer 10 mM sodium phosphate, 100 mM NaCl, pH = 7.4), **I$_m$** indicates imidazole *N*1-acetyl PNA monomer **28**

Table 4: UV-T_m of mixed purine/pyrimidine oligomers

S. No.	PNA	Duplex PNA:DNA	Binding orientation	UV-T_m	ΔT_m
1	**PNA 10**	H. T ATT ATT ATT-LysNH$_2$	Antiparallel	23.9	-----
2	**PNA 10**	H. T ATT ATT ATT-LysNH$_2$	Parallel	10.2	-----
3	**PNA 33**	H. **I$_m$**ATT ATT ATT- LysNH$_2$	Antiparallel	23.3	-0.6
4	**PNA 33**	H. **I$_m$** ATT ATT ATT- LysNH$_2$	Parallel	23.1	+12.9
5	**PNA 34**	H.T ATT A**I$_m$**T ATT- LysNH$_2$	Antiparallel	31.2	+7.3
6	**PNA 34**	H.T ATT A**I$_m$**T ATT- LysNH$_2$	Parallel	25.0	+14.8
7	**PNA 35**	H. **I$_m$** ATT A**I$_m$**T ATT- LysNH$_2$	Antiparallel	26.7	+2.8
8	**PNA 35**	H. **I$_m$** ATT A**I$_m$**T ATT- LysNH$_2$	Parallel	21.8	+11.6
9	**PNA 36**	H.T ATT ATT AT**I$_m$**- LysNH$_2$	Antiparallel	24.0	-0.7

T_m = melting temperature PNA:DNA complexes (measured in the buffer 10 mM sodium phosphate, 100 mM NaCl, pH = 7.4), **I$_m$** indicates imidazole *N*1-acetyl PNA monomer **28**

None of the oligomers synthesized from imidazole *N*1-acetyl PNA monomer exhibited stabilization towards the complementary DNA oligomers for triplex formation. However duplex from the mixed purine-pyrimidine PNA oligomers with middle and double modifications exhibited some stabilization.

Enzyme mimetic hydrolytic studies

PNA oligomers (**PNA38** and **PNA39**, Table 5) having imidazole unit at side chain and in the middle of the oligomer were specifically designed and synthesized.

Table 5 : oligomers synthesized for enzyme catalysis study

S. No.	Entry	PNA sequence
1	**PNA37**	H. C TTT CTT-LysNH_2
2	**PNA38**	H. $\mathbf{I_{mC4}}$-C TTT CTT-LysNH_2
3	**PNA39**	H. G$\mathbf{I_m}$A GAT CAC T-LysNH_2
		RNA sequence
4	**RNA40**	5' AAG AAA GAG A 3'
5	**RNA41**	5' AGU GAU CUA C 3'

RNA40 is complementary to **PNA37** and **PNA38**
RNA41 is complementary to **PNA39**

$\mathbf{I_{mC4}}$ =

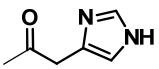

$\mathbf{I_m}$ =

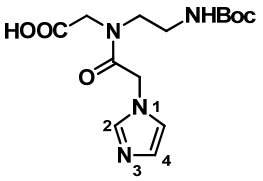

imidazole *N*1-acetyl PNA monomer (28)

RNA cleavage experiments were performed for catalytic **PNA38** under different reaction conditions, which bears an imidazole moiety at the N-terminus of the oligomer. RNA cleavage was not observed for any reaction condition. Under slightly high Zn^{2+} concentration, RNA got completely degraded. Hence further studies are required in terms of different RNA sequences (longer), PNA sequence (mixed purine-pyrimidine) to optimize and test the hypothesis.

Chapter 1

Introduction to Nucleic Acids

1 Introduction to Nucleic Acids

The nucleic acids are macro biopolymers made up of a linear array of repeating units called nucleotides. Each nucleotide consists of three components: a nitrogenous heterocyclic base (nucleobase), which is either a purine or a pyrimidine; a pentose sugar; and a phosphate group. Nucleobases are connected to the pentose sugar via a *β*-glycosidic linkage to give rise to nucleoside[1] upon phosphorylation become nucleotides. These are the components of both ribonucleic acid (RNA) and deoxyribonucleic acid (DNA) (Figure 1). RNA is made up of ribonucleotides while the monomers of DNA are 2'-deoxyribonucleotides.

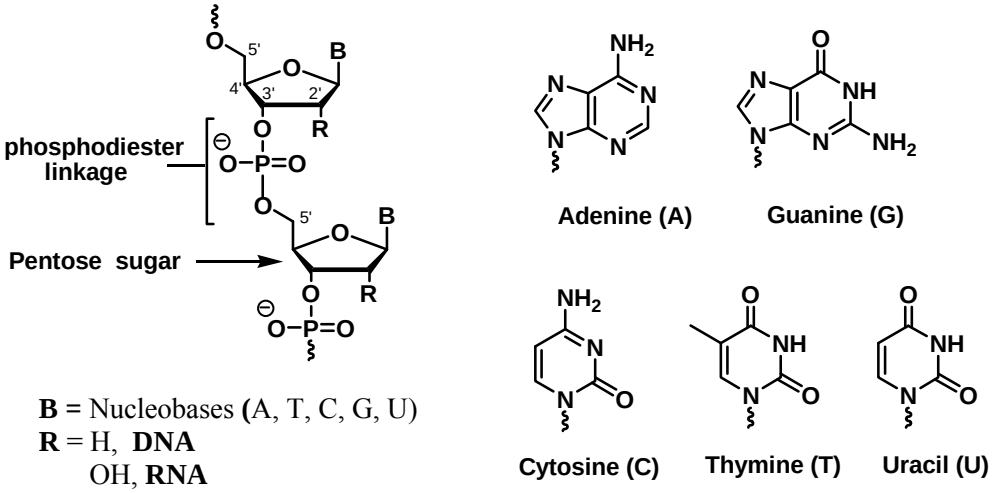

Figure 1: Chemical constituents of DNA and RNA

DNA present in the nucleus of organisms contains the genetic instructions which specify the biological development of all cellular forms of life and many viruses. The molecular architecture of DNA consisting of two helical chains each coiled round the same axis with a right handed twist was proposed by Watson and Crick in 1953[2] (Figure 2a). The phosphodiester group joins the *β*-D-deoxyribofuranose residues through 3'-5' linkages forming a helical chain (Figure 1) in which they are pointed towards the outside of the helix. The other main constituent of DNA is the nitrogenous bases e.g. adenine (A), thymine (T), guanine (G) and cytosine (C) which are pointed towards the center of the helix. The hydrogen bonds between complementary base pairs (A:T, G:C) hold the two strands together by Watson-Crick base pairing to form an

antiparallel double helical structure for DNA (Figure 2). RNA contains ribose sugar rather than the 2'-deoxyribose sugar and the base composition is guanine, adenine, cytosine and uracil (instead of thymine in DNA).

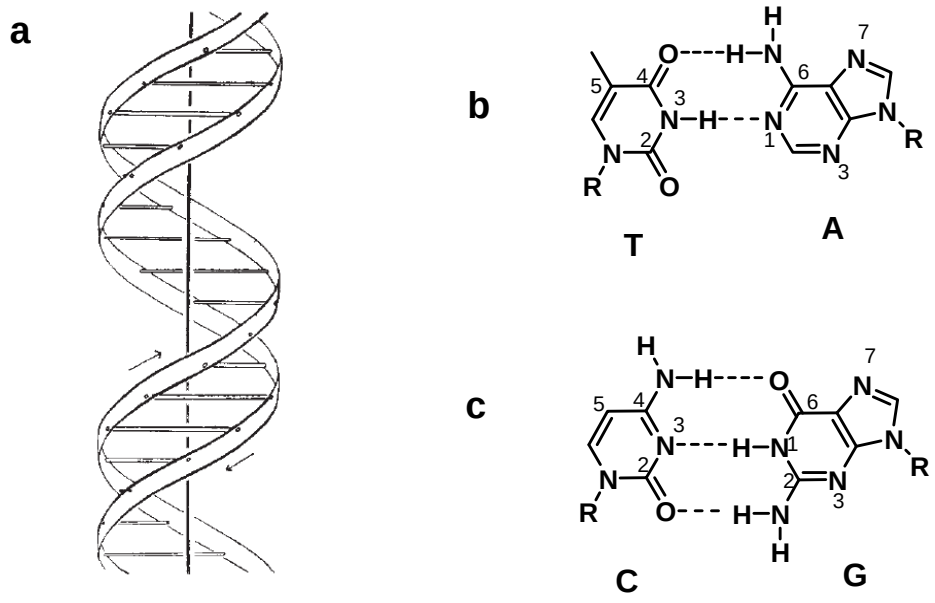

Figure 2: (a) Structure of DNA double helix (b) AT base pairing (c) GC base pairing

1.1 Hydrogen bonding in DNA

The N-H groups of the bases are potent hydrogen donors, while the sp^2-hybridized electron pairs on the oxygens of the C=O groups and on the ring nitrogens are hydrogen bond acceptors, better than the oxygens of either the phosphate or the pentose sugar. In Watson-Crick pairing, two hydrogen bonds in A:T base pair and three hydrogen bonds a G:C base pair (Figure 2b-c) hold together and other significant H-bond pairings are the Hoogsteen[3] (HG) and Wobble[4] base pairs (Figure 3). Hoogsteen base pairing is not isomorphous with Watson-Crick base pairing and has importance in triple helix formation. In Wobble base pairing, a single purine is able to recognize a noncomplementary pyrimidine (e.g. GU, where U=Uracil) and these have importance in the interaction of messenger RNA (mRNA) with transfer RNA (tRNA) on the ribosome during protein synthesis (codon-anticodon interactions).

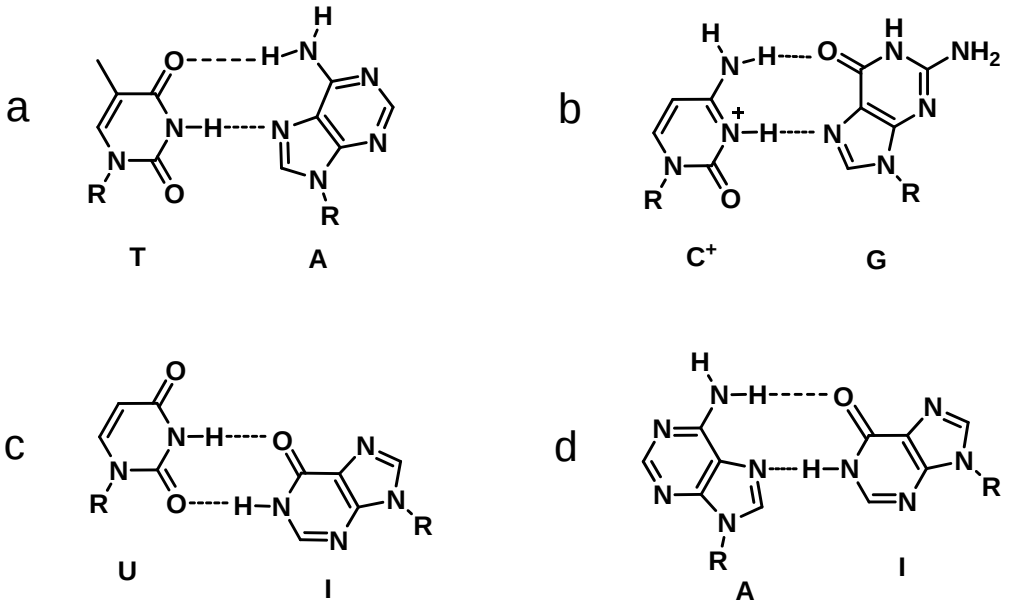

Figure 3: Hoogsteen base paring (a-b), Wobble base paring (c-d)

1.2 Secondary structures of Nucleic acids

Out of the several conformations of DNA which were confirmed by fiber and single crystal x-ray diffraction studies[5] the most common is the B-DNA (Figure 4) which is a right-handed double helix. It is endowed with a wide major-groove and a narrow minor-groove wherein the bases lie perpendicular to the helical axis. DNA also forms the A-form, a right-handed helix in which the major-groove is very deep and the minor-groove is quite shallow. At low humidity and high salt, the favored form is the highly crystalline A-DNA while at high humidity and low salt, the dominant structure is B-DNA. In both A and B forms of DNA, the Watson-Crick base pairing is maintained along with *anti*-glycosidic conformation.

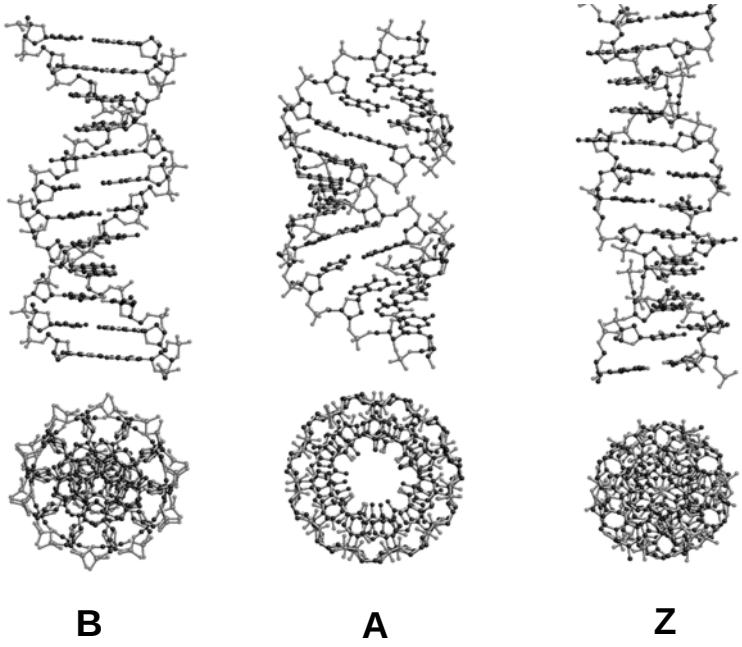

Figure 4: Top: Molecular models of B, A and Z form DNA. Bottom: views along the helical axis.

The sugar conformation is however different in both forms with the B form showing C2'-*endo* puckered sugar and the A form DNA exhibiting C3'-*endo* sugar-pucker (Figure 5). A very unusual form of DNA-duplex is the left-handed Z-DNA. This conformation of DNA is stabilized by high concentrations of $MgCl_2$, NaCl and ethanol and is favored for alternating G:C/C:G sequences. Z-DNA has a characteristic zig-zag phosphate backbone and the Watson-Crick base pairing is achieved by purines adopting *syn*-glycosidic conformation with C3'-*endo* sugar-pucker.

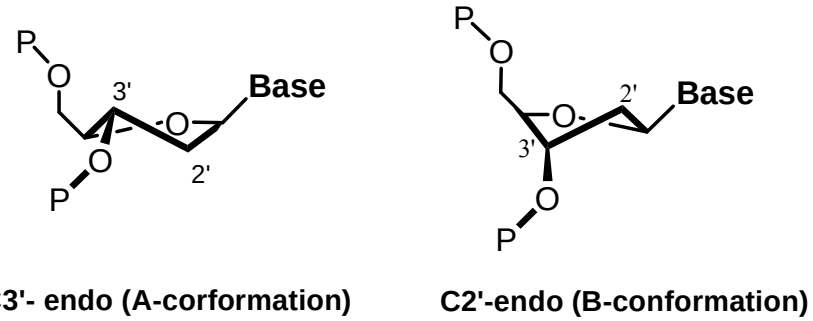

Figure 5: Structures of C3'-endo and C2'-endo sugar puckering

RNA can form double stranded RNA:RNA and RNA:DNA duplexes. These duplexes are in the A conformation because of the presence of 2'-OH which results in

C3'-*endo* sugar-pucker thus precluding the B conformation. More commonly, RNA is single stranded and can form complex and unusual shapes such as stem and bubble structures, which occur due to the intramolecular chain folding (intramolecular base pairing). An example is tRNA, the key molecule involved in the translation of genetic information to proteins. It contains about 70 bases that are folded such that there are base paired stems and open loops, with the overall shape of the completely folded tRNA being L shaped.

1.3 Applications of Nucleic Acid

The double helix of DNA is nature's simple and elegant solution to the problem of storing, retrieving, and communicating the genetic information of living organism. Recognition of DNA and RNA sequences by complementary oligonucleotides is a central feature of biotechnology and is important for hybridization based biological applications.[5] The study of such complementary recognition is possible with the widely used experimental techniques and diagnostic protocols.

1.3.1 Oligonucleotides as therapeutic agent

Designing a drug against a protein target requires a specific understanding of 3D structure of the protein. Although recent advances in X-ray crystallography, NMR and computer modeling of proteins have accelerated the drug design process, this method lacks generality. In contrast, the base sequence in RNA and DNA is universal and this generality is very appealing from the drug-design point of view. In principle, one can design a drug that, like nucleic acids, is repetitive in its primary structure and binds sequence specifically to these drug targets. In order for the sequence specific recognition to happen, such drug should contain nucleobases that are fundamental units of nucleic acid recognition.

Two innovative strategies are being tested for inhibiting the production of disease related proteins using such sequence specific DNA fragments as gene expression inhibitors. The first strategy known as *antisense strategy*[6] aims to selectively impede translation by inhibiting the protein synthesis. Antisense oligonucleotides (Figure 6) recognize a complementary sequence on target mRNA through Watson-Crick base pairing and form a duplex (RNA:DNA hybrid) that is not

processed by the protein synthesis machinery and hence would retard the expression of the corresponding protein. When target proteins are disease related, this will have a therapeutic value.

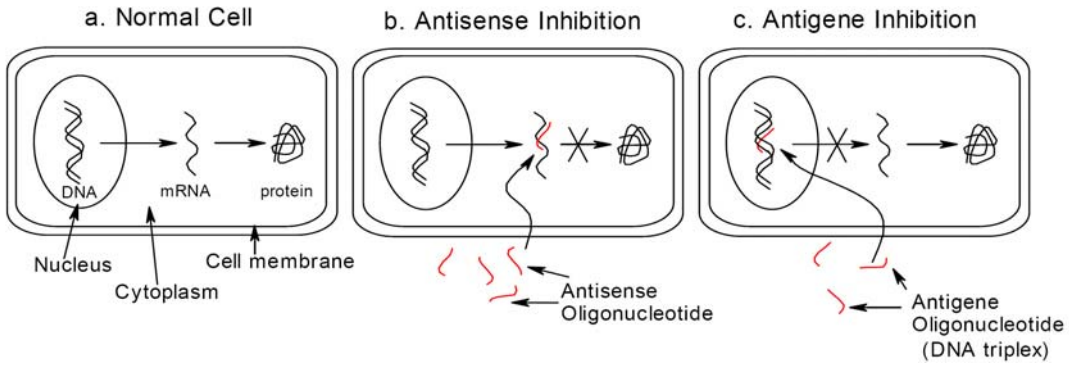

Figure 6: Principle of action of antisense and antigene oligonucleotides.

In the second strategy which is known as *antigene strategy*, aims to stop the production of an unwanted protein by selectively inhibiting transcription of gene. In this method, oligonucleotides target the major groove of DNA where it winds around the double-helical DNA to form triplex involving HG hydrogen bonds[7] (Figure 7). Thus the double stranded DNA itself can act as a target for the third strand oligonucleotides or their analogue, and the limitation for triplex formation is that it is possible only at homopurine stretches of DNA, since it requires purine to be the central base

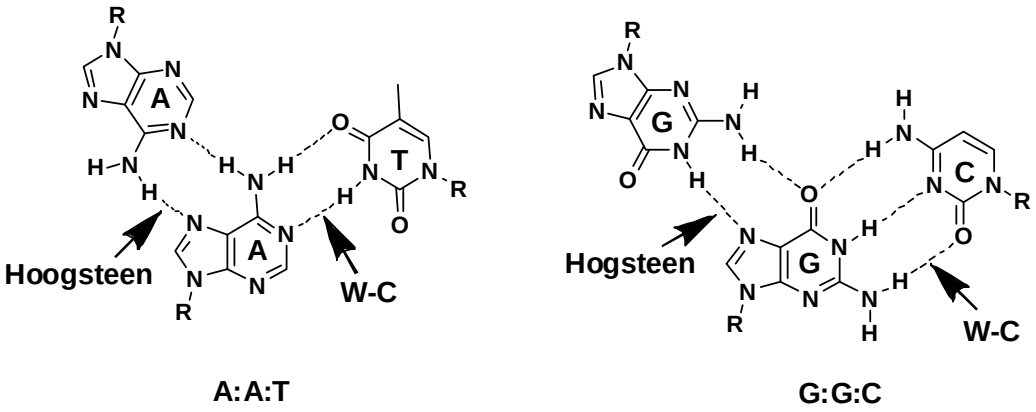

Figure 7: Watson-Crick (W-C) and Hoogsteen (HG) hydrogen bonds of A:A:T and G:G:C triads

This is vital to make antisense or antigene based inhibition as a practical approach to therapeutics. Various cellular processes can be inhibited depending on the site at which the antisense oligonucleotide hybridizes to the target nucleic acid. For an 'antisense' oligonucleotide to be able to inhibit translation, it must reach the interior of the cell unaltered. The requirements for this are the stability of the oligonucleotide towards extra and intra-cellular enzymes and equally important is its ability to traverse the cell membrane. After reaching the cytoplasm, it must bind the target mRNA with sufficient affinity and high specificity. In addition, it must possess an adequate half-life in order to elicit its action. The toxicity of the oligonucleotide should also be negligible to the cell. The unmodified antisense oligonucleotides are intended to enter the cell where they can pair with, and so inactivate, the complementary mRNA sequences. But their inability to permeate cell membrane as they carry anionic charge results from repulsive interaction with the cell lipid layer. Further, they are degraded by intracellular enzymes such as exo-nucleases. In order to meet all the requirements of a successful medicinal agent, it is necessary for normal oligonucleotides to be chemically modified in a suitable manner.

1.4 Chemical modifications of DNA

Zamecnik and Stephensen[8] were the first to propose the use of synthetic antisense oligonucleotides for therapeutic purposes. The specific inhibition is based on the Watson-Crick base-pairing between the heterocyclic bases of the antisense oligonucleotide and of the target nucleic acid. To address the combined task of improving the rate, affinity or specificity of oligonucleotide recognition, while the enhancing membrane permeability and resistance to nuclease digestion, several chemical modifications of DNA have been attempted (Figure 8). These can be broadly distinguished as i) analogs with unnatural bases ii) modified sugars (especially at the position of the ribose iii) altered sugar-phosphate backbone

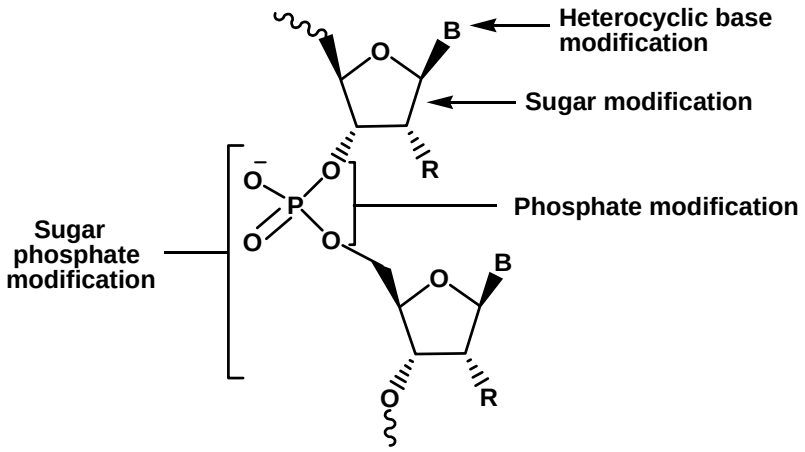

Figure 8: Different sites of modification for DNA

1.4.1 First generation antisense oligonucleotides

1.4.1a Alternative phosphate containing linkages

The modifications of phosphate moiety resulting in phosphorothioates[9] **1**, methylphosphonates[10] **2**, phosphoramidates[11] **3** and phosphotriesters[12] **4** and boranophosphonate[13] **5** have lead to the first generation 'antisense' oligonucleotides (Figure 9). These have shown promising results with one drug Vitravene (ISIS) based on the phosphorothioate backbone has already been approved by FDA for retinitis.

Phosphorathioates: In phosphorothioates (PS-oligos) negatively charged oxygen has been substituted by a sulfur atom at phosphorus centre, and the linkage thus retains a formal negative charge, which is however reduced compared to the phosphodiester homologue. PS-oligos are easily synthesized on a commercial DNA synthesizer, as a mixture of diastereomers at the phosphorus atom, and are resistant to nuclease cleavage. PS oligomers can act as substrates to RNase H and these first generation antisense agents have been extensively tested in various human clinical trials against numerous targets. However, these oligomers have a tendency to induce non-specific effects, through binding to extra cellular and cellular proteins as well as cleavage of non target mRNAs that are only partially complementary.

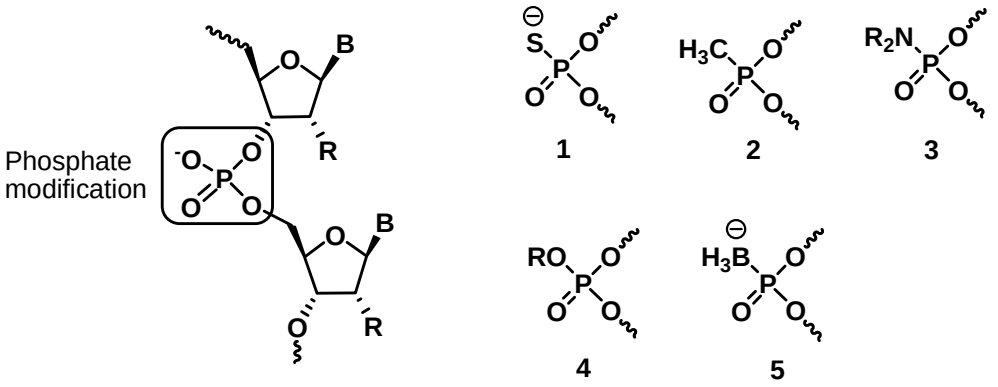

Figure 9: Structure of alternative phosphate containing linkages

1.4.1b Non-phosphorus backbone

Out of all the backbone modifications, those involving the replacement of the phosphodiester group with neutral linkers which are more lipophilic than the unmodified one, might increase the efficiency of passage into the cells, decrease the electrostatic repulsion with target nucleic acids and therefore improve affinity. Affinity can be improved with neutral linkages, provided that the linkage is pre-organized into the correct conformation for binding and is favorably hydrated in the duplex state.

In the first group, four atoms are present in the backbone[14] (Urea **6**, guanidine **7,** Figure 10). Because of the conjugation of lone pairs of electrons from nitrogen and oxygen atoms with a carbonyl (or imine) group, three atoms are maintained in the same plane. As a consequence, a rather severe destabilization of the duplexes was observed when these modifications were introduced into DNA strand.

The second group of modifications (hydroxylamine[15] **8**, thioformacetal[16] **9**; Figure 10), introduce less pronounced conformational restrictions. Interestingly, an increase in the size of the substituents on the nitrogen atom does not substantially destabilize the duplexes, when the amide group is located in the middle of the backbone.

In the third group of modifications (ketone **10**, thioether **11**; Figure 10), the backbone has a high degree of conformational freedom.[17] Consequently, much lower T_ms were obtained for the corresponding duplexes because of an increased negative entropy contribution to the hybridization process.

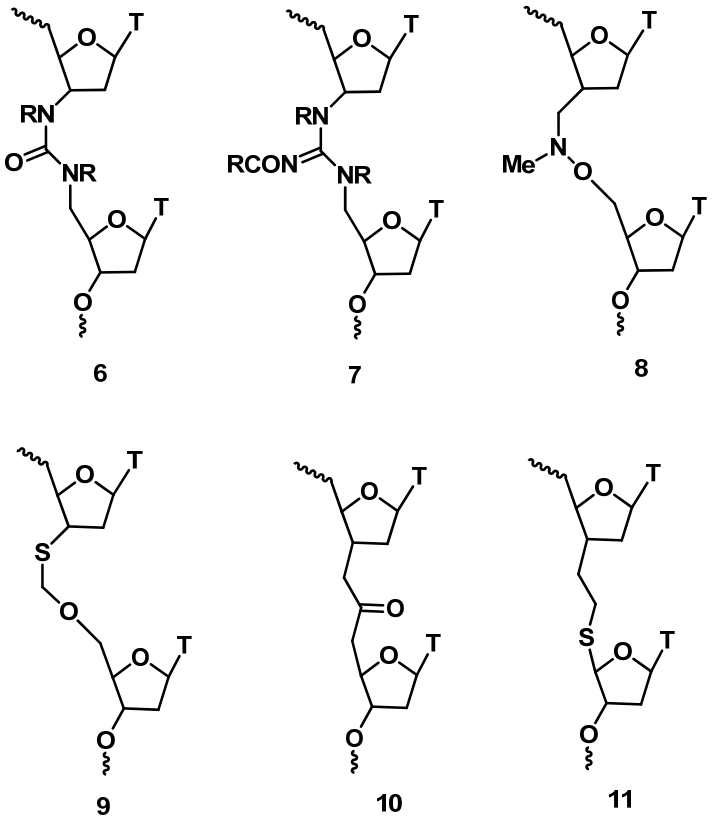

Figure 10: Structure of non-phosphorous backbone containing linkages

1.4.2 Second generation antisense-oligonucleotides

2'-modification

The instability of oligoribonucleotides under physiological conditions led to the synthesis of their 2'-modified analogues. The problems associated with phosphorothioate oligodeoxynucleotides are solved to some degree by this type of *O*-alkyl modifications at the 2' position of the ribose. 2'-*O*-methyl **12** and 2'-*O*-methoxyethyl RNA **13** (Figure 11) are the most important members of this class of oligonucleotides.[18] The oligonucleotides containing these building blocks are less toxic than phosphorothioate DNAs and have a slightly enhanced affinity towards their complementary RNAs. This class of compounds is attractive for antisense applications because ribonucleosides are much less costly as starting materials than their deoxy analogues and because of the greater thermal stability of the hybrids of 2'-*O*-methylribonucleotides with complementary RNA than that of corresponding unmodified DNA:RNA duplexes.

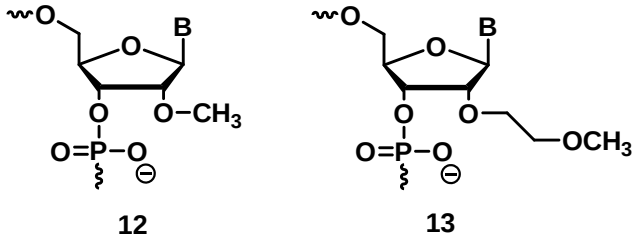

Figure 11: Structures of 2'-modified deoxyribonucleic acid

1.4.3 Third generation antisense oligonucleotide

The replacement of the ribose sugar by hexose or carbocycles has not been very successful in terms of specificity of binding/hybridization. However, morpholino oligomers,[19] where the monomers are linked through neutral carbamate linkages **14** or through phosphoramidate linkages[20] **15** (Figure 12), have shown promising antisense activity as they have superior permeability properties.

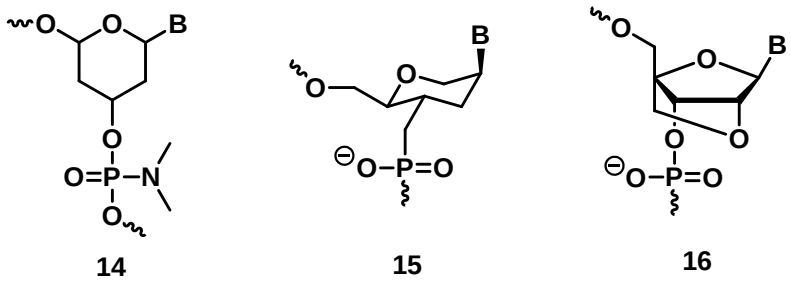

Figure 12: Structures of pentose sugar modified deoxyribonucleic acid

The locked nucleic acids (LNAs)[21] **16** (Figure 12) are oligonucleotides containing one or more 2'-O, 4'-C-methylene-*β*-D-ribofuranosyl nucleotides. These were found to exhibit unprecedented stability of their complexes with complementary DNA and RNA. They are also stable to 3'-exonucleolytic degradation and possess good water solubility. The conformational preorganization of LNA could be helpful in imparting the enhanced binding affinity to DNA.

Threofuranosyl Nucleic Acids (TNAs)[22] **17** (Figure 13) containing vicinally connected (3'→2') phosphodiester bridges undergo informational base pairing in antiparallel strand orientation and are capable of cross-pairing with RNA and DNA.

Being derived from a sugar containing only four carbons, TNA is structurally the simplest of all potentially natural oligonucleotide-type nucleic acid alternatives.

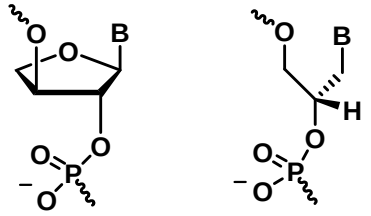

17 18

Figure 13: Structures of α-threofuranosyl nucleic acid (TNA) and glycol nucleic acid (GNA)

Inspired by TNA structure, structurally simplified nucleic acid containing acyclic glycol nucleoside backbones has been synthesized in order to improve synthetic accessibility of artificial duplexes. The resulted Glycol Nucleic Acid (GNA)[23] **18** (Figure 13) forms highly stable antiparallel helical duplex structures following the Watson-Crick base pairing rules. Being the most atom economical solution for a functional nucleic acid backbone, GNA has been proposed as potential predecessor of RNA as a genetic material and catalyst for Earth's earliest organisms.

1.4.4 Gene silencing by RNA interference

RNA interference (RNAi), is a technique in which exogenous, double stranded RNAs (dsRNAs) that are complementary to known mRNAs, are introduced into a cell to specifically destroy that particular mRNA, thereby diminishing or abolishing gene expression.[24] RNA interference has been used in the nematode *Caenorhabditis elegans* to manipulate gene expression.[25] Two types of small RNA molecules, microRNA (miRNA) and small interfering RNA (siRNA) are central to RNA interference.

Formation of small interfering RNA (siRNA) occurs in two steps involving binding of the RNA nucleases to a large double-stranded RNA (dsRNA) and its cleavage by the enzyme Dicer into discrete 21- to 25-nucleotide RNA fragments called siRNA (Figure 14). In the second step, these siRNAs incorporated into the RNA-induced silencing complex (RISC) and binds to the target mRNA by complementary base pairing, which subsequently suppresses gene expression either by cleavage or by translational repression. siRNA delivered by microinjection into the intestine exerts

interference effects in tissues in both the injected animal and its progeny.[25] This technology is an extremely useful tool for identifying gene functions and evaluating potential therapeutic targets. So, an increasing number of biotechnological and pharmaceutical companies are attempting to develop siRNA-based drugs for the prevention and treatment of human disease such as cardiovascular diseases, neurological diseases, viral infections, cancer etc.[26]

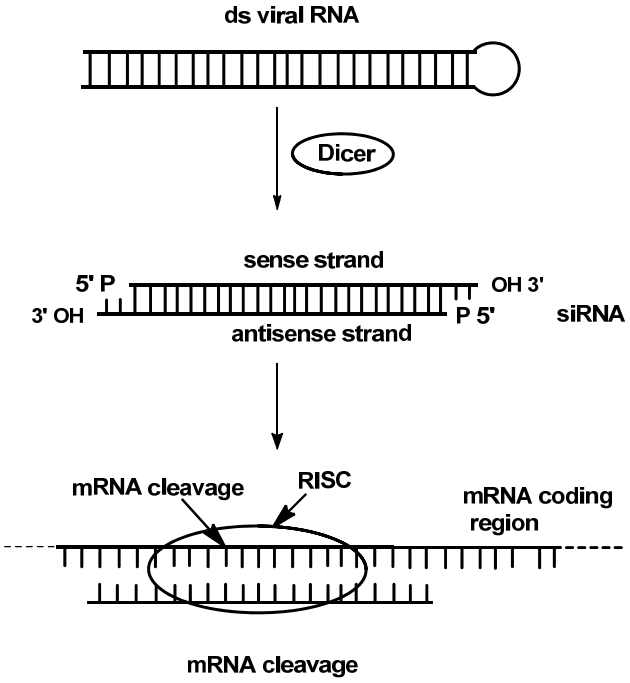

Figure 14: Process of double-stranded viral RNA to form siRNA

Primary RNA transcripts in the nucleus have been found to contain hundreds of endogenous sequences known as microRNAs that can fold into hairpins that contain imperfect matches. These RNA transcripts are processed in the nucleus into hairpin RNAs of 70-100 nt by the dsRNA-specific ribonuclease Drosha, which contains an RNase III activity. The hairpin RNAs are transported to the cytoplasm and are digested by a second, double-strand specific ribonuclease Dicer. The resulting 19-23 mer miRNA is bound by a complex that is similar to the RNA-induced silencing complex (RISC), which directs one of the two RNA strands to bind to a selected sequence in the 3'-untranslated region of a gene resulting in block of translation.[27]

The attempts to optimize the properties of oligonucleotides have resulted in the synthesis and analysis of a huge variety of new oligonucleotide derivatives with

modifications to the phosphate group, the ribose, or the nucleobase, as some of them has been mentioned in the above section. Most of the analogues being investigated so far are closely related to natural oligonucleotides and only few attempts to radically modify the backbone of DNA have been successful. The most radical change to the natural structure is the replacement of the entire sugar-phosphate backbone which is known as peptide nucleic acid (PNA) will be discussed in detail in the following section.

1.5 Peptide Nucleic Acid

1.5.1 Introduction

Peptide Nucleic Acids (PNAs) are DNA analogues first introduced by Nielsen et al. in 1991 where the sugar-phosphate backbone has been replaced by a polyamide chain composed of *N*-2-aminoethylglycine repeating units, covalently linked to nucleobases through a carboxymethyl spacer[28] (Figure 15). They contain the natural nucleobases and are therefore able to bind to complementary DNA through the classical Watson-Crick base pairing rule, although some non-specific interactions were also recently revealed.[29] The PNA backbone is constituted by six atoms for each repeating unit and a two atom spacer between the backbone and the nucleobase, similar to the natural DNA.

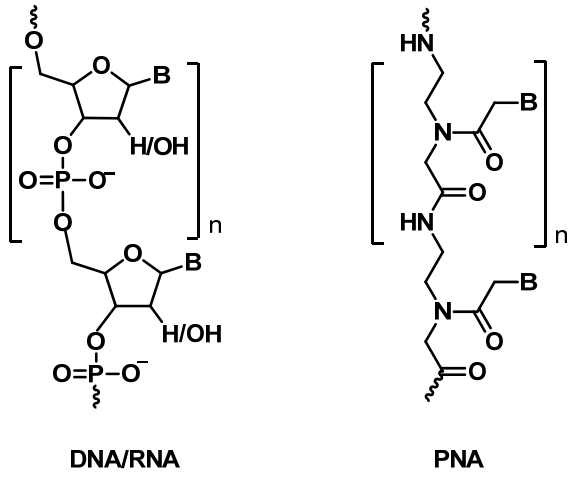

Figure 15: Chemical structures of DNA/RNA and PNA

1.5.2 Chemical and physical properties of PNA

1.5.2a Duplex formation with complementary oligonucleotides

PNAs hybridize to complementary oligonucleotides obeying Watson-Crick base pairing rule. The internucleobase distances in PNA are conserved such that they complement the internucleobase distances in DNA for effective recognition of the base sequences. Therefore PNA is a true DNA mimic in terms of base pair recognition. Though in DNA:DNA duplexes the two strands are always in an antiparallel orientation (with the 5'-end of one strand opposed to the 3' end of the other), PNA:DNA adducts can be formed in two different orientations, arbitrarily termed parallel and antiparallel (Figure 16) both adducts being formed at room temperature, with the antiparallel orientation showing higher stability.[30] This creates the possibility for PNAs to bind two DNA tracts of opposite sequence.

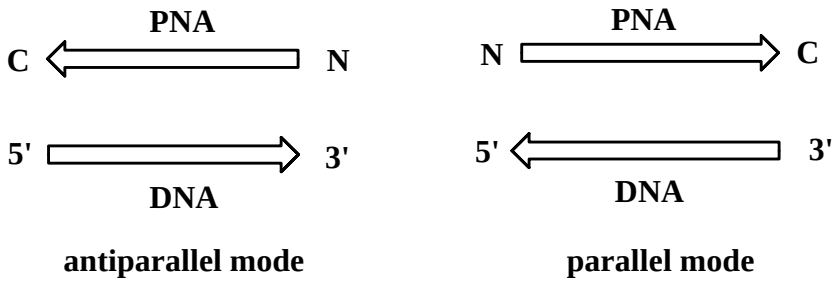

Figure 16: Parallel and antiparallel modes of PNA-DNA binding

A kinetic study of PNA complex formation using capillary electrophoresis,[31] showed that the antiparallel complex was formed immediately (<30s), whereas the formation of the parallel complex required several hours. The stability of DNA:DNA hybrids was shown to increase with increasing salt concentration, whereas in case of PNA:DNA duplex the stability remains same.[32] The contrasting effect of ionic strength on duplex formation can be explained by the association of counter ions in case of DNA:DNA duplex formation and by displacement of counter ions in the case of PNA:DNA duplex formation. One of the most important features of the PNA:DNA duplexes is that their stability is highly sensitive to the presence of a single mismatched base pair.[33] Thus PNA probes are very sequence-selective and are superior to DNA probes in recognizing single-base mispairing.

1.5.2b Triple Helix formation of PNA

Polypyrimidine PNAs are able to form stable adducts with complementary polypurine DNA, through the formation of PNA_2:DNA triplexes.[28a] However, in case of C- rich PNAs and GC- rich DNA duplexes, PNA:DNA_2 triple helices are observed. The base pairing in these complexes occurs via Watson-Crick and Hoogsteen hydrogen bonds. If only one PNA sequence is used to form a PNA_2:DNA triple helix then both strands are necessarily either parallel or antiparallel to DNA strand. When two different homopyrimidine PNA sequences are used the most stable complex is formed when the Watson-Crick PNA strand is oriented antiparallel and the Hoogsteen strand is parallel to the purine strand of the DNA. The sequence specificity of triple helix formation is based on the selectivity of formation of the intermediate PNA:DNA duplex, whereas binding of the third strand contributes only slightly to selectivity. The stability of these structures enables PNA to perform strand invasion,[28a,34] a property which is uniquely shown by PNAs.

Strand invasion: This unique property of PNAs to displace one strand of DNA double helix to form strand invasion complexes[35] (Figure 17), which is favorable attribute for their application as antisense/antigene agents. The tendency of homopyrimidine PNAs to form PNA_2:DNA triple helices is so strong that under certain conditions they can bind as a triple helix to one strand of double-stranded DNA (ds-DNA), while the second DNA strand is displaced and forms a single stranded loop structure (P loop). The prerequisites for strand displacement by PNA are (i) a DNA duplex that is not too stable and (ii) low salt concentration.

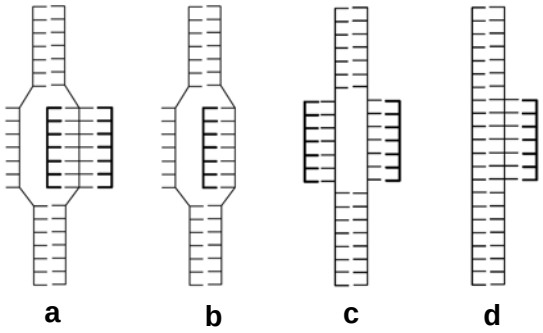

Figure 17: PNA binding modes for targeting double stranded DNA (a) Triplex invasion (b) Duplex invasion (c) Double duplex invasion (d) Triplex

For triple helix formation, strand displacement is independent of the orientation (parallel or antiparallel) of the pyrimidine PNA strand in relation to the purine strand of the complementary DNA. Strand invasion is highly sequence specific. The original studies of strand invasion were carried out on homopyrimidine PNAs at low salt concentrations.

1.5.3 Structures of PNA-DNA and PNA-RNA complexes

Three-dimensional structures have been determined for the major families of PNA complexes (Figure 18). Two duplex structures, a PNA:RNA and a PNA:DNA duplex, were solved by NMR, and a PNA_2:DNA triplex and a PNA:PNA duplex were solved by x-ray crystallography.

PNA:DNA duplexes: The structural information obtained from the NMR spectroscopic study of two antiparallel PNA-DNA duplexes[36] (8-mer and 10-mer) suggest that the DNA strand is in a conformation similar to the B form, binding through Watson-Crick base-pairing with a glycosidic anti-conformation, and the deoxyribose in the C2'-endo form. The NMR study of an octameric antiparallel PNA-DNA duplex showed the presence of elements for both A-form and B-form DNA. The right-handed helix contains approximately 13 base-pairs per turn compared to 10 base pairs for B-form DNA with widened major groove and shallow and narrow minor groove. The primary amide bonds of the PNA backbone are in the *trans*-conformation and directed towards the solvent while the carbonyl oxygen atoms of the backbone-nucleobase linker point towards the carboxy terminus of the PNA strand. There is no evidence for the formation of hydrogen bonds between the amide and carbonyl groups in the backbone. CD spectra indicates that the antiparallel PNA-DNA duplexes forms a right-handed helix,[37] however parallel PNA-DNA duplexes shows a structure that differs considerably from that of either the B and A form.

PNA:RNA Duplexes: ^{1}H NMR spectroscopy for PNA-RNA duplexes[38] indicate that all bases form Watson-Crick base pairs, the glycosidic torsion angle in the RNA strand indicates an *anti*-conformation, and the ribose sugars are in the 3'-endo form which resembles an A-form structure. The tertiary amide bonds of PNA are all in the *cis*-conformation and being the carbonyl group of the tertiary amide in the PNA backbone isosteric to the C2'-hydroxyl group, it increases the solvent contact of the

carbonyl oxygen atom. The secondary amide protons of the backbone do not participate in any form of hydrogen bonding. The CD spectra of antiparallel PNA-RNA duplexes indicate the formation of a right-handed helix with a geometry similar to the A or B form.

PNA_2: DNA triplexes: The structure of PNA_2:DNA triple helices was obtained from an X-ray crystal structure analysis of the complex formed by a bis-PNA and its complementary antiparallel DNA.[39] The structure is different from both A-form and B-form DNA, and forms a P helix with 16 bases per turn. The nucleobases of the PNA strand bind to the DNA by Watson-Crick and Hoogsteen base pairing and lie almost perpendicular to the helix axis, which is the characteristic of B-form DNA. The helix is considerably widened as compared to A-form DNA. The phosphate groups of DNA are hydrogen bonded to the PNA backbone amide protons of the Hoogsteen strand. These hydrogen bonds, together with additional van der Waals contacts and the lack of electrostatic repulsion, are the main factors responsible for the enormous stability of the triple helix. The deoxyribose of the DNA strand is in the C3'-endo conformation. The CD spectra of PNA_2:DNA triple helices indicate the presence of a right-handed helix and a geometry similar to that of the pure DNA triple helix.[40]

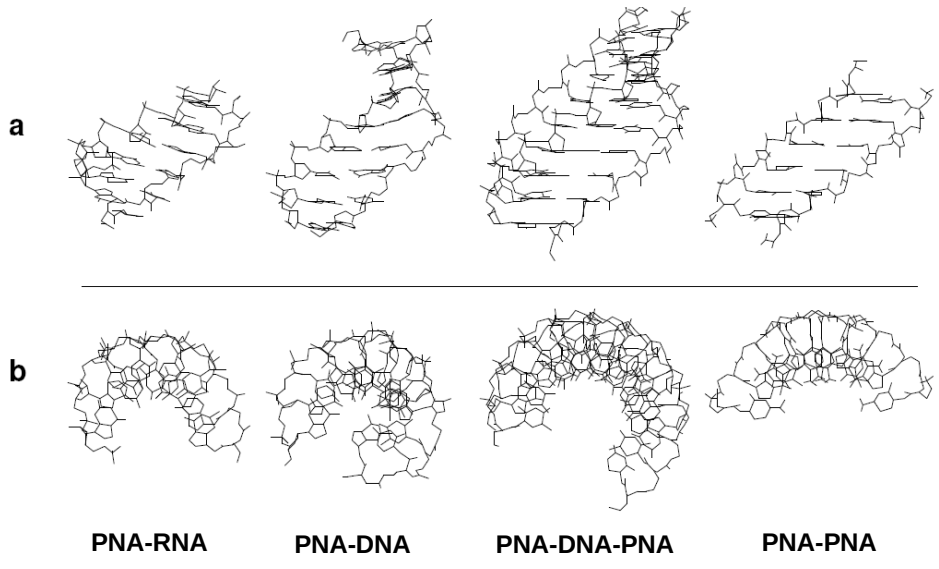

Figure 18: Structures of various PNA complexes shown in side view (upper panel), top view (lower panel).

PNA:PNA duplex: The existence both right and left handed helices, which are stacked coaxially and alternately in the crystal by forming a continuous pseudohelix,

was confirmed by the X-ray crystal structure analysis of a self-complementary PNA:PNA duplex (H-cgtacg-NH_2).[40] The nucleobase-pairing is of Watson- Crick-type, where the bases lie almost perpendicular to the helix axis, with a propeller twist of 5-9^o with 18 bases per turn compared to the 11 and 10 bases per turn in A- and B-form DNA, respectively. The amide groups of the backbone are in the *trans*-conformation and the carbonyl groups of the linkers point towards the carboxy terminus. Thus, the structure bears a strong similarity to the P form of PNA_2:DNA helices.[39]

All the structures of PNA-DNA and PNA-RNA discussed above, clearly demonstrate that the PNA have the flexibility to adapt the A-and B-form helices preferred by RNA and DNA, but the results also clearly show that the structure preferred by PNA is much wider and more slowly winding helix (18 base pair pitch), which is referred to as the P-form.

1.5.4 Applications of PNA

1.5.4a Antisense effect or inhibition of translation

The mechanism of antisense effects by oligonucleotides (ODNs) is believed to be either a ribonuclease H (RNase H)-mediated cleavage of the RNA strand in ODN-RNA hybrids or a physical blocking of the translation machinery at the ODN-RNA complex.[35b] The ability of oligonucleotides to stimulate RNA cleavage by RNase H is largely dependent upon their chemical structure. PNAs belong to the group of nucleic acid analogues that do not stimulate RNase H on duplex formation with RNA. Therefore the mechanism for inhibition of transcription process is probably due to physical blocking and not RNase H-mediated mRNA degradation. Translation experiments performed in cell-free extracts showed that duplex-forming PNA blocked translation in a dose-dependent manner when the target was 5'-proximal to the AUG start codon on the RNA, whereas PNAs had no effect when targeted towards sequences in the coding region.[41] Triplex-forming PNAs were efficient and specific antisense agents with a target overlapping the AUG start codon and caused arrest of ribosome elongation with a target positioned in the coding region of the mRNA.

1.5.4b Antigene effect or inhibition of transcription

Homopyrimidine PNA oligomers bind to the homopurine sequence of the template strand resulting efficient inhibition of transcription either by triple helix formation, or by a strand invasion. A high thymine content in the pyrimidine PNA shows more efficiency in blocking transcription process. Homopurine regions of eight base pair or more in length in double-stranded DNA (dsDNA) can be targeted by homopyrimidine PNAs via the formation of extremely stable PNA triplex strand invasion complexes.[42] For the formation of these complexes two PNAs are required where one of them is Watson-Crick bound and the other Hoogsteen bound, more often bis-PNAs in which the two parts are chemically linked are employed for dsDNA targeting. The main obstacle to therapeutic use of the strand displacement principle is the stability of the GC-rich natural DNA double strand, under physiological salt conditions. Kinetics of strand invasion during the active transcription process increases when the PNA oligomer was targeted against a transcriptionally active DNA fragment or DNA polymerase and thereby making PNAs good candidates for antigene reagents.

1.5.4c Inhibition of Replication

In the DNA replication process, the elongation of DNA primers by DNA polymerases can be inhibited by PNAs *in vitro*. As a consequence, DNA replication can be inhibited by PNAs if the DNA duplex is susceptible to strand invasion under physiological salt conditions, or if the DNA is single-stranded during the replication process. In fact, in the case of extrachromosomal mitochondrial DNA, which is largely single-stranded during replication, efficient inhibition of replication by PNAs is possible.

1.5.4d Interactions with Enzymes

Ribonuclease H (RNase H): RNA becomes a substrate for cleavage by the ubiquitous intracellular enzyme RNase H when it forms a double strand with unmodified oligodeoxyribonucleotides. It is well known that antisense oligonucleotides with the ability to activate RNase H are generally much better antisense inhibitors than those without this ability. The DNA/PNA chimeras are able to stimulate RNA cleavage by RNase H (Figure 19) on formation of a chimera-RNA double strand.[43] RNA

cleavage occurs at the ribonucleotides which base-pair with the DNA part of the chimera. The cleavage is sequence specific, as random sequence DNA/PNA chimeras do not cleave the RNA under the same conditions.

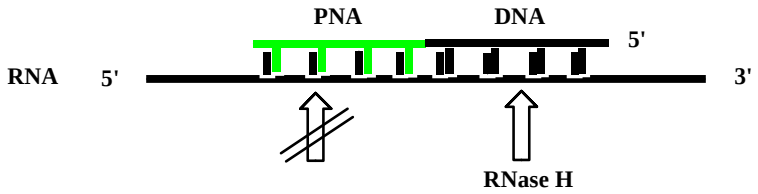

Figure 19: Schematic representation of RNase H-mediated cleavage of activity after the binding of a PNA-DNA chimera to an RNA target.

Inhibition of Telomerase activity: Long $(TTAGGG)_n$ repeats at the 3'-end of DNA strands, is synthesized by human telomerase.[44] The ribonucleoprotein telomerase are composed of a protein component with DNA polymerase activity, and an RNA component that acts as a primer binding site. The telomerase activity can be inhibited by PNA sequences that are complementary to the RNA primer binding site better than the corresponding phosphorothioate oligonucleotides because of their higher binding affinity. The activity is dependent upon the binding site and base composition of the PNA oligomer.

PNA directed PCR clamping: PNAs do not normally interact directly with DNA polymerases and reverse transcriptases. They can, however, terminate the elongation of oligonucleotide primers by binding to the template strand, or even compete directly with the oligonucleotide primer for binding to the template. PNA can either be directed towards the primer binding site, the region adjacent to the primer, or towards the middle of the PCR region. Competition between the primer and PNA for binding to the primer site resulted in decreased amplification since PNA cannot function as a primer for DNA polymerase because of their structure. When the PNA target site is located adjacent to the primer site the observed clamping is likely to reflect that the polymerase cannot access the PCR primer or that primer elongation is prevented. Conversely, PNA binding at a distance from the primer site is expected to cause elongation arrest of the polymerase. The most efficient and discriminative clamping was observed with homopyrimidine PNA decamers. Formation of the

extraordinary stable $(PNA)_2$:DNA triplexes caused inhibition of the polymerase at PNA binding site.

PNA as artificial restriction enzyme: PNAs in combination with nuclease S1 has been used as the artificial restriction enzyme.[45] The first model illustrates the hybridization of homopyrimidine PNA decamer to complementary target on double stranded DNA via a strand invasion mechanism leading to the formation of looped-out noncomplementary DNA strands (Figure 20). The enzyme nuclease S1 can degrade this single-stranded DNA part into well-defined fragments. It was suggested that the enzyme first digested the displaced strand, and then the gap was enlarged to some extent, thereby allowing the opposite strand to act as a substrate for nuclease S1. When PNAs with a single mismatch were employed very weak cleavage was observed. This difficulty could be eliminated by the use of dimeric targets either in *cis* or *trans*.[46] The binding of PNA to two adjacent targets in *cis* lead to an opening of the entire region, thereby provided an easily accessible substrate for the nuclease. This considerably increases the sensitivity to cleave and even more favourable situation arises if two PNA targets were on opposite strands.

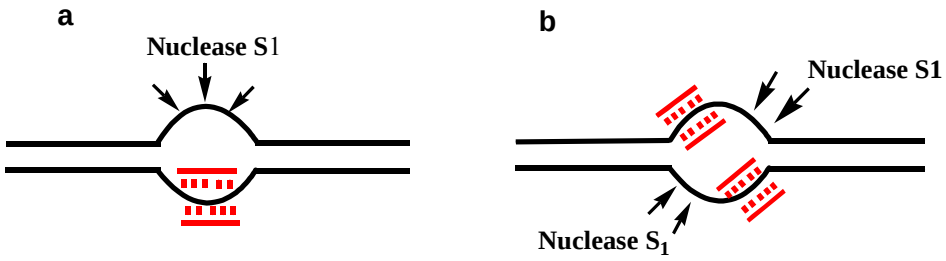

Figure 20: Artificial restriction enzymes a) single strand cleavage by PNA b) double strand cleavage by double PNA clamping.

1.5.5 Chemical modifications of PNA

Since their discovery, many modifications[47] of the basic PNAs structure have been proposed, in order to improve their performances in term of affinity and specificity towards complementary oligonucleotides. A modification introduced in the PNA structure can improve its pharmacological potential generally in three different ways: i) improving DNA binding affinity; ii) improving sequence specificity, in

particular for directional preference (antiparallel vs parallel) and mismatch recognition; iii) improving bioavailability (cell internalization, pharmacokinetics, etc.).

The main strategies which have been used for achieving this goal are summarized in Figure 21. Preorganization was achieved either by cyclization of the PNA backbone (in the aminoethyl side or in the glycine side), by adding substituents in the α'' or β carbon of the monomer or by inserting the aminoethyl group into cyclic structures. The addition of substituents at α'' or β carbon of the monomers can also preorganize the PNA strand, but mainly it has the effect of shifting the PNA preference towards a right-handed or left-handed helical conformation, according to the configuration of the new stereogenic centers, in turn affecting the stability of the PNA-DNA duplex through a control of the helix handedness.

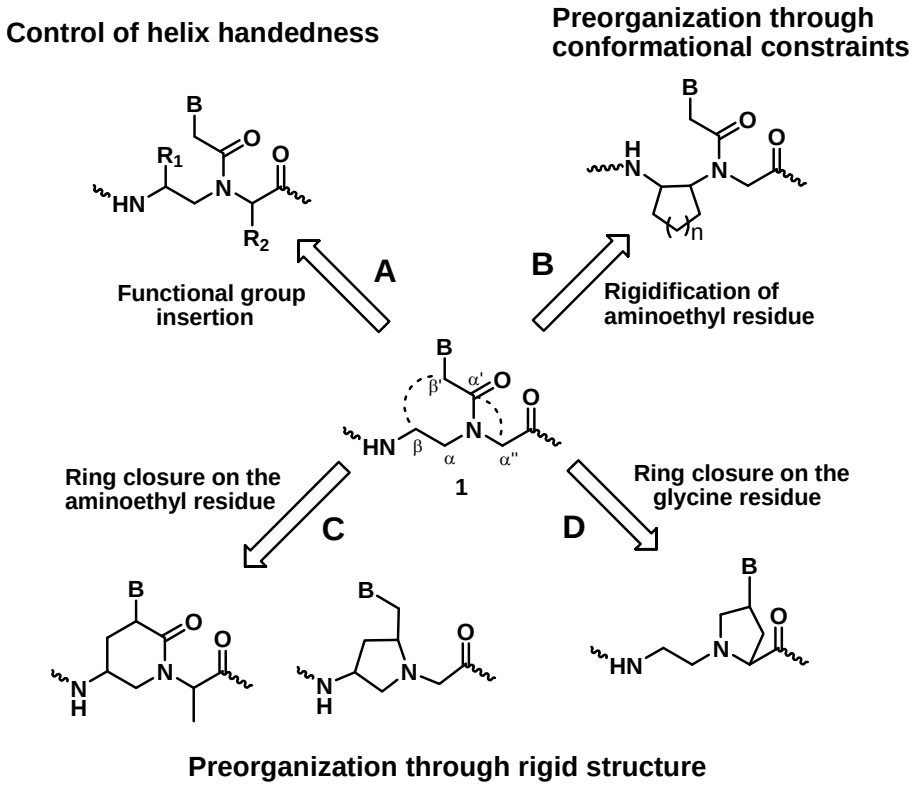

Figure 21: Strategies for inducing preorganization in the PNA monomers.

1.5.5a Preorganization through conformational constraints

The earliest modifications mentioned in route A and B (Figure 21) were reported with extension of the PNA structure with a methylene group individually in

each of the structural sub-units (aminoethyl, glycine and base linker) of the PNA monomer which results in PNAs with *N*-(2-aminoethyl)-β-alanine[48] **20** and *N*-(3-aminopropyl)glycine[48] **21** backbone and ethylene carbonyl linked nucleobase[48] **22** (Figure 22). These modifications resulted in a significant lowering of T_m of the derived PNA:DNA hybrids. The consequences of such small changes to the PNA structure suggested the high structural organization to which the original PNA structure is inherently tuned for interaction with DNA.

The replacement of the tertiary amide carbonyl by a methylene group leading to a flexible, cationic tertiary amine monomer **23** resulted in a large destabilization of the PNA:DNA hybrids.[49] The necessity of such a pseudo rigid amide group pointed to the importance of constrained flexibility in the backbone. Further rigidification of the PNA backbone has been attempted by introduction of alkyl substituents individually or simultaneously in the aminoethyl or glycine segments or in both **24**.[50] Number of modifications generated by substitution of glycine component by other α-amino acids, leading to chiral PNA **24** (R_1=H) having hydrophobic, hydrophilic or charged α-substituents have been reported.

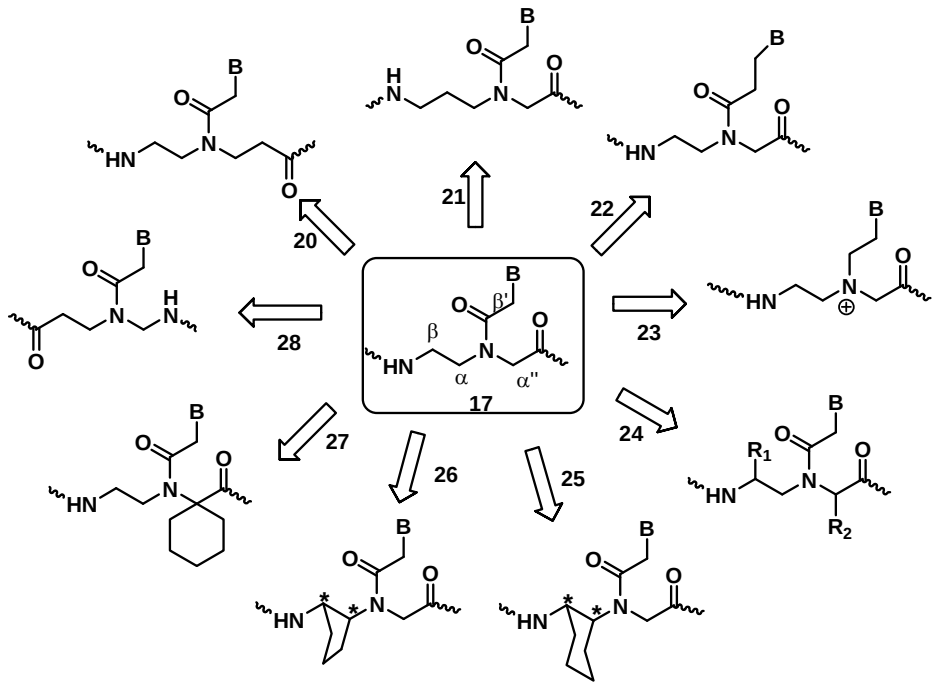

Figure 22: Structures of conformationally constraint peorganized modified PNA monomers

PNA oligomers incorporating chiral monomers retained the hybridization properties though less efficiently, with tolerance for small and medium substituents at the glycine α"- position. Suitable substitutions may also lead to generation of cyclic structures with 1,2-cyclohexylamino[51] **25,** 1,2-cyclopentylamino[52] **26** and spirocyclohexyl[53] **27** rings in monomers. Several papers have reported a systematic approach in the design of monomers exhibiting DNA/RNA selectivity. The *trans*-cyclopentane (*tcyp*-PNA) modified PNA structure **26**, which is equivalent to covalently closing the aminoethyl glycine PNA backbone, has been successfully utilized as a target capture strand to improve the detection limit of a known DNA detection assay, and provided to high levels of mismatch discrimination. c*is*-(1*R*,2*S*)-cyclopentyl PNA analogues **26**, (the same as *tcyp*-PNA, except for stereochemistry) hybridize to DNA/RNA without discrimination because the ring puckering of the cyclopentane ring.

In contrast to the rigid locked chair conformation of a cyclohexane system, in fact the cyclopentane ring is more flexible and can be easily conformationally adjusted. The *ch*PNAs **25** shows remarkable differences in duplex stability with their DNA and RNA complexes, depending on number of modification and stereochemistry. There is a highly significant preference to form a duplex with RNA as compared to DNA. PNAs that bear (*S,S*) cyclohexyl ring **25** in the aminoethyl part hybridize with complementary DNA similar to the unmodified PNA, those derived from (*R,R*) cyclohexyl **25** moiety lacked such a property.

Another type of modification involved interchange of various CO and NH groups on the peptide linkages leading to retro inverse analogue **28**.[54] The inter-base residue separations are similar to the unmodified PNA, but accompanied by inversion of intra and inter residue amide bonds. This exhibited a lower potency for duplex formation with complementary DNA/RNA suggesting that in addition to geometric factors, other subtle requirements such as hydration and dipole-dipole interactions, etc influencing the microenvironment of the backbone, may be involved in effecting efficient PNA:DNA hybridization.

1.5.5b Preorganization through rigid five membered heterocycles

Some of the relatively successful conformationally preorganized modifications[55] so far are based on introduction of methylene/ethylene groups to bridge

the aminoethyl-glycyl backbone and methylene carbonyl side chain to generate diverse five or the six- membered nitrogen hetetocyclic analogues (route C ans D; Figure 21). The cyclic analogues where the nucleobases are directly attached to the ring have defined nucleobase orientation, overcoming the rotamer problem. It also concomitantly introduces chiral centers, which may impart directional selective binding of PNA with chiral DNA/RNA.

The naturally occuring amino acid *trans*-4-hydroxy-L-proline, a five-membered nitrogen heterocycle, is a versatile, commercially available starting material for creating structural diversity to mimic DNA/PNA structures. From this amino acid a wide variety of chiral, constrained and structurally preorganized PNAs have been synthesized. Depending on the synthetic approach and on the presence of the tertiary amine group in the monomers, the modifications afford either positively charged or uncharged cyclic PNA analogs. The different cyclic PNAs proposed showed that the right stereochemistry and conformation is really important for binding abilities towards nucleic acids and in some cases even for discriminate between RNA and DNA. For example, in the case of the cyclic PNA analogue *N*-(thymin-1-yl-acetyl)-4-aminoproline[56] **29** (Figure 23), all steroisomers were synthesized, and the L-*trans*-4-aminoprolyl isomer, was shown to bind to DNA with higher affinity, while the L-*cis* isomer and the D-*trans*, which could not adopt the same spatial arrangement, showed reduced performances. The same model can be applied to the (2*R*,4*S*)-stereoisomer of the aminoethylprolyl PNA[57] **30** (*aep*PNA), Effect of a chiral monomer on DNA affinity might be dependent on whether it is used for the synthesis of all the PNA oligomer or it is inserted in an oligomer made of achiral monomers.

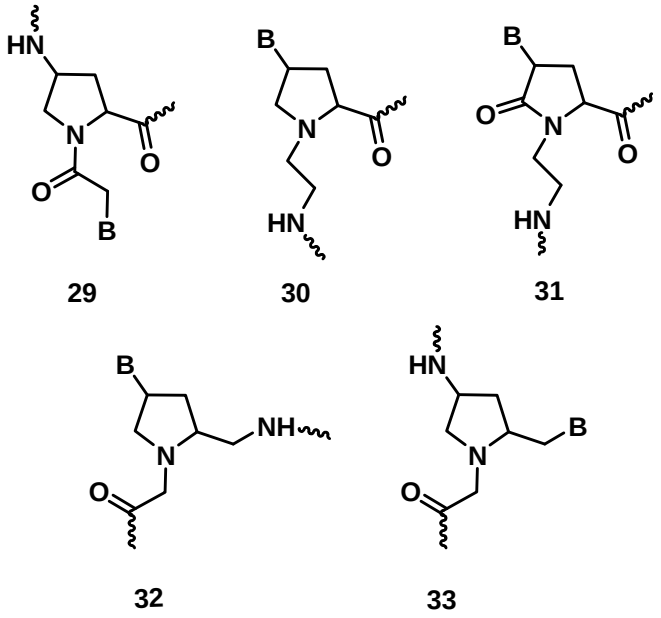

Figure 23: Stuctures of conformationally preorganized five and six membered heterocyclic PNA monomers

The aminoethylprolyl-5-one (*aepone*) thymine monomers[58] **31** were synthesized and incorporated into *aeg*-PNA-T_8 backbone at different positions. The *aepone*-PNAs showed remarkable stabilization of derived PNA_2:DNA triplexes compared to *aeg*-PNA. In particular the synthesis of pyrrolidine-based chiral positively charged PNA[59] **32** (Figure 23) the derived (2*R*,4*S*) stereomeric homoadenylate oligomer formed a stable complex with both DNA and RNA. PNAs containing the other pyrrolidine stereoisomers are reported but they do not show any considerable improvement in binding affinity.

Introduction of a methylene bridge between the α' and β carbon yields another pyrrolidine-PNA[60] **33**. Diastereomeric monomers bearing T, A, C, G, nucleobases were introduced in PNA oligomers and the complexation with DNA and RNA sequences was studied. It was found that: (2*R*,4*S*) homopyrimidine PNA stabilize PNA_2:DNA triplexes, (2*S*,4*R*) stereoisomers in mixed sequences affects enhanced DNA duplex stability, (2*S*,4*S*) and (2*R*,4*R*) remarkably enhance PNA:RNA duplex stability. All the pyrrolidine modifications show preference for the anitparallel DNA binding. Thus in this case the effect of stereochemistry is not very clear, and relative conformational freedom of the five-membered ring can account for this.

1.5.5c Preorganization through rigid six membered heterocycles

The behaviour of two stereoisomers of a 6-membered ring PNA is the discrimination between the parallel versus antiparallel DNA reported for a single modified (2*S*,5*R*) aminoethyl pipecolic PNA[61] unit **34** (Figure 24) inserted in the middle of the strand. The effect is highly dependent on the position of the stereocenters, as it has been already seen for flexible chiral PNAs. PNAs derived from piperidinone[62] **35** were also reported, though the rigidity of the ring and their particular geometry led to a decrease of PNA:DNA duplex stability; however, the best performing was the (3*R*,6*R*)-isomer, which is in line with proper group arrangement.

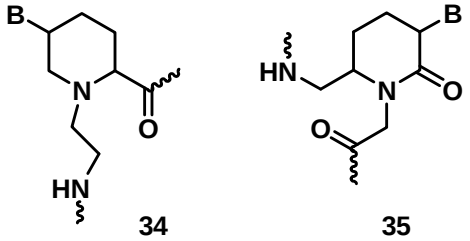

Figure 24: Structures of pipecolic PNA and piperidinone PNA

1.5.5d Modified Nucleobases

There is increasing interest in modulating and expanding the recognition motifs of standard base pairs. Employing non-natural nucleobase ligands in place of natural nucleobases would help understand the recognition process in terms of various factors contributing to the event such as hydrogen bonding and internucleobase stacking. Further, new recognition motifs may also have potential applications in diagnostics and nanomaterial chemistry. This when coupled with high affinity and strand invasion properties offered by PNA would add a new dimension to PNA applications. The non-standard nucleobases employed so far with PNA are limited, compared to the repertoire of backbone modifications described earlier. 2,6-Diaminopurine[63] (**36**, Figure 25) offers increased affinity and selectivity for thymine and pseudoisocytosine[64] **37** is a very efficient mimic of protonated cytosine for triplex formation. 2-Aminopurine[65] **38** hydrogen bonds with U and T in reverse Watson-Crick mode and has the advantage of being inherently fluorescent to enable study of kinetic events associated in

hybridization. The E-base[66] **39** was rationally designed for recognition of A:T base pair in the major groove and form a stable triad with T in the central position.

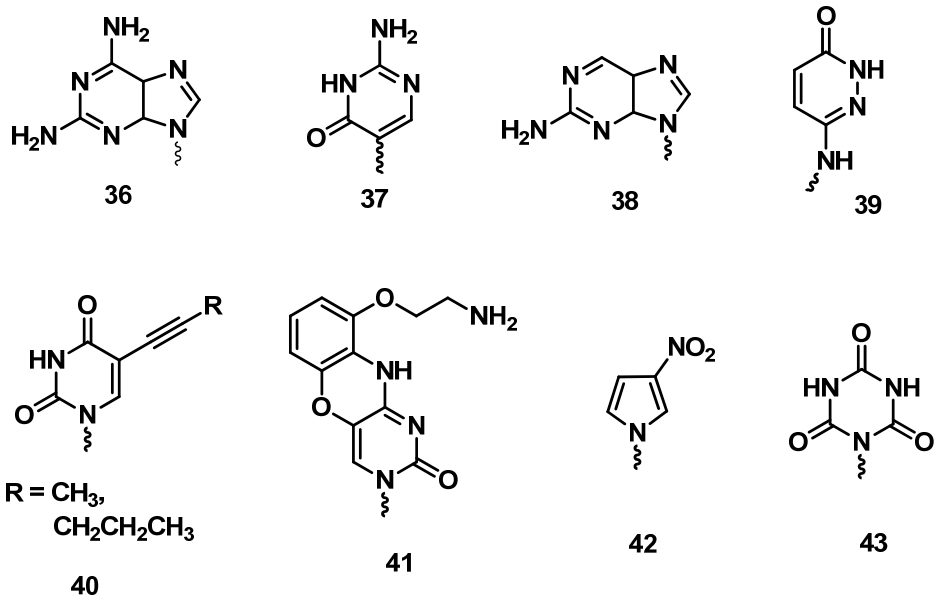

Figure 25: Structures of modified nucleobases

In order to increase the stability of complexes formed by PNA with target nucleic acids, bases that possess a larger surface area (for greater hydrophobic/stacking interactions), make additional H-bonds or that are positively charged have been prepared. A wide variety of 5-substituted uracils were synthesized and their ability for triplex formation has been studied[67] (**40,** Figure 25). The G-clamp base **41** was developed to build in specific, additional bonding interactions with guanine.[68] Unnatural heterocycles 3-nitropyrrole **42** have been used as potential universal bases in PNA.[69] The synthesis of cyanuryl PNA monomer containing cyanouric acid **43** as the base was achieved by direct N-monoalkylation of cyanuric acid with *N*-(2-Boc-aminoethyl)-*N*′-(bromoacetyl)glycyl ethyl ester.[70] The monomer was incorporated as a T-mimic into PNA oligomers and biophysical studies on their triplexes/duplex complexes with complementary DNA oligomers indicated unusual stabilization of PNA:DNA hybrids when the cyanuryl unit was located in the middle of the PNA oligomer.

1.5.6 Stability in cells and cellular uptake of PNA

The use of PNAs as antisense or antigene therapeutics requires that they show sufficiently high biological stability in serum and in cells. The unmodified PNA oligonucleotides, having the peptide-like structure make their potential degradation by peptidases or proteases in serum. However, PNAs have a remarkably high biostability in both human serum and in cell extracts. The experiment was carried out with homopolymer H-$(t)_{10}$-Lys-NH_2 where no significant degradation could be detected by HPLC after a two hour incubation of the human serum, or in cytoplasmic, or nuclear fractions of mouse tumour cells. Due to the low cellular uptake of PNAs so far there are no reports of antisense activity of pure PNAs in cell culture without the use of techniques that help to bypass the membrane barrier. Antisense and antigene activity of PNAs has been studied by direct intracellular microinjection of the PNAs.[71] Pure PNAs, such as H-t_8-Lys-NH_2, could only be detected in cells at high concentrations (>50mm), where cytotoxic effects could also be observed.[72] The cellular uptake may improve by attachment of lipophilic or other helper groups to PNA that bind selectively to cell surface receptors, by formation of PNA-DNA chimeras, PNA-peptide conjugates or alternatively, the transporter-drug conjugate can be designed as a prodrug, i.e., with a linker that is chemically or biochemically cleaved after passage through a barrier, allowing for release of the free drug in targeted cells or tissue.

1.5.6a PNA-DNA Chimerae

The successful applications of the remarkable DNA binding properties of PNAs are sometimes (sequence/length dependent) hampered by their tendency to self-aggregate and poor aqueous solubility. Overcoming these limitations and imparting other abilities for therapeutic applications such as cellular uptake, RNase H activation properties, have been addressed by designing covalent hybrids or chimaeras of PNA with DNA, functional peptides and other effector molecules. Three types of PNA-DNA chimeras (Figure 26) are in place (i) 5'-DNA-linker X-PNA-*pseudo*-3'[73] **44** (ii) *pseudo*-5'-DNA-linker X-DNA-3'[74] **45** and (iii) *pseudo* -5'-PNA-linker X- DNA-3'[73]**46**.

Synthetic protocols have been developed with protecting groups compatible for carrying out on-line synthesis of both PNA and DNA to generate the chimeras. Several interesting properties were noticed in such covalent hybrids such as co-operative

stabilizing effects against proteases and nucleases, enhanced water solubility and duplex/triplex stabilities dependent on the structure of chimerae and the linker. The linker can also be a fragment of DNA to generate PNA-(5')-DNA-(3')- PNA chimera which formed stable duplexes with both DNA and RNA with a lower stability than corresponding DNA:DNA and DNA:RNA duplexes.

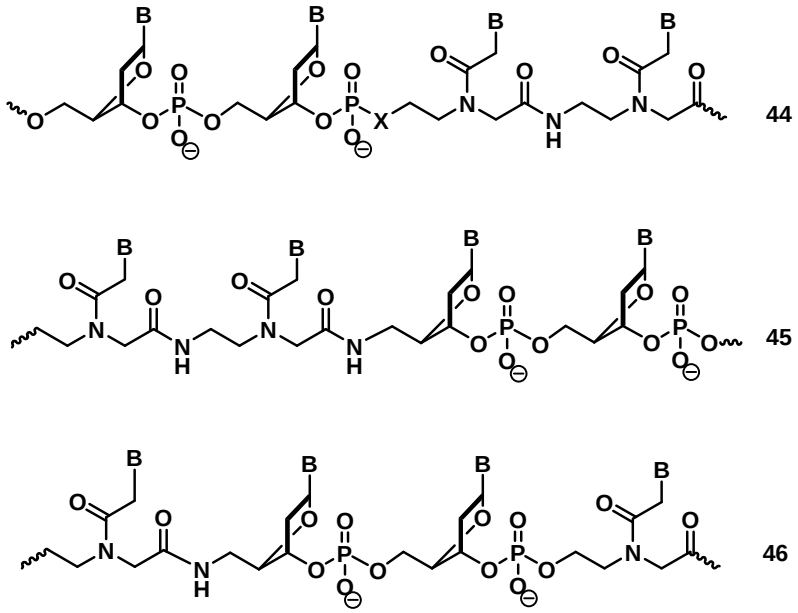

Figure 26: Structures of DNA-PNA chimera

ONs based on locked nucleic acids (LNAs) have been shown to have extremely strong RNA binding ability, which has led recently to the application to microRNA inhibition of LNA/DNA mixmers, which have higher sequence specificity than all LNA ONs and such reagents are now available commercially.[75,76]

1.5.6b PNA-peptide conjugates

In order to evaluate the potential of PNAs for microRNA inhibition in cells R6-Penetratin (in which arginine-residues were added to the N-terminus of Penetratin) was synthesized and found to be the most active of all CPPs tested so far in a splicing correction assay in which masking of a cryptic splice site allows expression of a luciferase reporter gene.[77] Efficient and sequence-specific correction occurs at 1 μM concentration of the R6Pen-PNA705 conjugate as monitored by luciferase luminescence.

PNA containing arginine side chains (guanidinium functional group) exhibited remarkable uptake properties into mammalian cells, not only in cultures but also in intact mammalian organisms by maintaining Watson-Crick recognition with complementary DNA strands (Figure 27). The GPNA was found to be highly soluble in water compared to the unmodified PNA, which has a strong tendency to aggregate in solution despite the positive charged side chains and retains high level of sequence specificity normally exhibited by PNA.

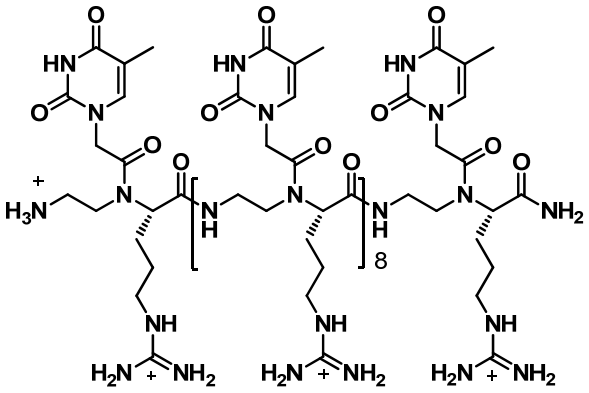

Figure 27: Structure of Guanidinium PNA oligomers

A PNA pentadecamer with a heptapeptide attached to N-terminus through *tris*-(8-amino-3,6-dioxaoctanoic acid) was found to have a higher Tm on hybridization with DNA perhaps due to the presence of two positively charged arginine units.[78]A PNA-peptide-PNA chimera consisting of two oligopyrimidine PNA nonamers linked by His-Gly-Ser-Ser-Gly-His formed a stable triple helix with oligopurine DNA strand.[79] Similarly, cationic *tris*-PNA structures involving a positively charged lysine in hairpin region.[80] 2'-5'-Oligoadenylates are known to activate 2-5A dependent RNase L and hence their PNA conjugates have been used to cause degradation of RNA substrates by RNase L. A PNA peptide chimerae involving linking a 10-mer peptide containing serine, which is a substrate for protein kinase A was used in an assay for phosphorylation of serine by kinase.[78] The 5-mer PNA sequence H_2N-TAGGG-COOH linked to the N-terminus of various homooligomeric peptides of cationic amino acids lysine, ornithine and arginine are shown to inhibit human telomerase.[81]

1.6 Present Work

The preceding section has given an overview on the concept of peptide nucleic acids (PNAs) which is a successful mimic of DNA. These are having the properties of natural oligonucleotides and are important for the development of therapeutics in the form of antisense and antigene oligonucleotides. The major drawbacks of PNA like poor water solubility, inefficient cell uptake, self aggregation and ambiguity in directionality of binding restrict its applications. Hence various modifications of PNA for improving the activity which were attempted by different research groups described in the previous section.

Chapter 2: The ambiguity in DNA/RNA binding of PNA may lead to recognition of nonspecific target sequences, and achieving PNA specificity in binding is a desirable goal for successful therapeutic applications. This problem can overcome by introduction of chirality into achiral PNA backbones. This chapter describes the synthesis of modified backbone extended *prolyl*PNA monomers with (2*S*,4*S*) and (2*S*,4*R*) stereochemistry with two chiral centers at *C*2 and *C*4 position (Figure 28), which was envisaged to confer the combined effect of controlled rigidity and flexibility on the relatively more flexible *aeg*PNA backbone to modulate the physico-chemical properties. The introduction of methylene bridge between the *β*-carbon atom of the aminopropyl segment and the *α*''-carbon atom of the glycine segment of the *apg*PNA resulted in the desired backbone extended *prolyl*PNA monomers.

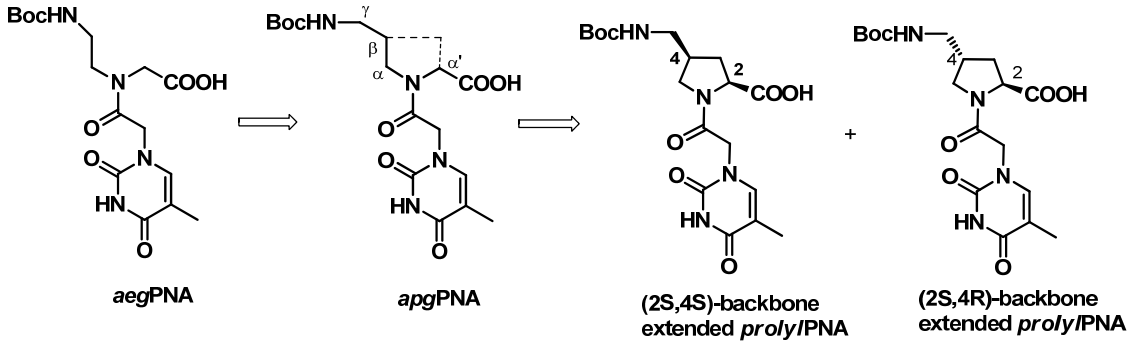

Figure 28: Chemical structures of modified backbone extended *prolyl*PNA monomers.

These (2*S*,4*S*) and (2*S*,4*R*)-backbone extended *prolyl*PNA have been incorporated into PNA oligomeric sequences by solid phase peptide synthesis. Cleavage of the synthesized oligomers from the solid support, their subsequent purification procedures, followed by suitable characterization is also described in detail in this chapter.

Chapter 3: We have explored the replacement of the amide functions in polyamide backbone of PNA with the triazole rings to examine its effect on PNA hybridization properties. It is demonstrated here that 1,2,3-triazole analogues of PNA (TzNA) wherein the amide link in backbone is replaced by triazole (**C**) can be synthesized on solid phase by 'click' chemistry (Figure 29). The triazole link in **C** was generated from click reaction of the polymer supported azido component **A** with the acetylenic component **B** in solution phase. Further the biophysical studies of corresponding oligomers have been presented in this chapter.

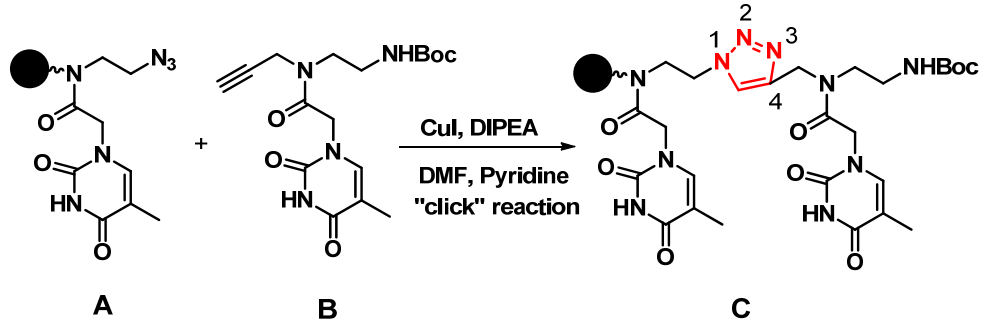

Figure 29: Synthetic protocol for introduction of triazole unit in PNA backbone

Chapter 4: The Gene silencing by antisense oligonucleotides could benefit from artificial ribonucleases due to the reason that the oligodeoxyribonucleotides (ODN) and their phosphorothioate analogs activate an intracellular enzyme, RNase H, which degrades the RNA component of RNA-ODN duplex, releasing the antisense ODN. In view of this concept, an artificial catalytic PNA oligomer has been designed based on imidazole-N-acetyl PNA **1** and imidazole *C*4-acetyl PNA **2** monomers (Figure 30). These monomers can be incorporated at the desired positions of the *aeg*PNA oligomer which will bind to the complementary RNA oligonucleotide and the imidazole unit acts as acid and base catalyst for RNA cleavage. PNA oligomer containing imidazole unit at the N-terminus also designed for RNA catalytic study.

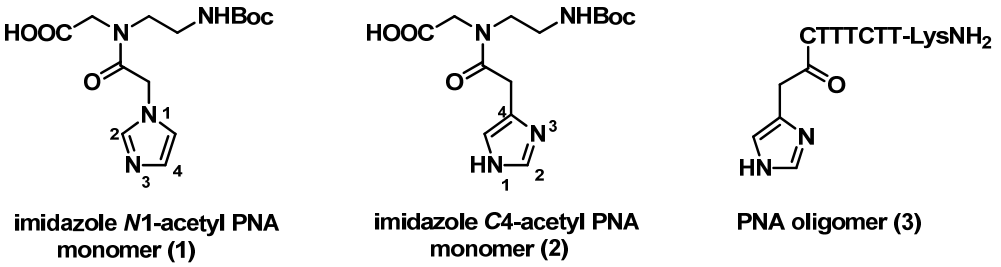

Figure 30: Chemical structures of imidazolyl PNA monomers and oligomer

1.7 References

1. Alberts, B.; Johnson, A.; Lewis, J.; Raff, M.; Roberts, K.; Wlater, P. *Molecular Biology of the Cell* (4th ed.). Garland Science. **2002**, pp. 120-121.
2. Watson, J. D.; Crick, F. H. C. Molecular structure of nucleic acid. A structure for deoxyribose nucleic acid. *Nature*, **1953**, *171*, 737-738.
3. Hoogsteen, K. The crystal and molecular structure of a Hydrogen-bonded complex between 1-Methyl thymine and 9-methyl adenine. *Acta. Crystal.* **1963**, *16*, 907-916.
4. (a) Crick, F. H. C. Codon-Anticodon pairing. The Wobble Hypothesis. *J. Mol. Biol*. **1966**, *19*, 548-555. (b) Soll, D.; Cherayil, J. D.; Bock, R. M.; Studies on polynucleotides. LXXV. Specificity of tRNA for codon recognition as studied by the ribosomal binding technique. *J. Mol. Biol.* **1967**, *29*, 97-112.
5. (a) Brahms, J.; Mommaerts, W. F. H. M. A study of conformation of nucleic acids in solution by means of circular dichroism. *J. Mol. Biol*. **1964**, *10*, 73-85. (b) Fuller, W.; Wilkins, M. H. F.; Wilson, H. R.; Hamilton, L. The molecular configuration of deoxyribonucleic acid IV. X-ray diffraction study of the A-form. *J. Mol. Biol*. **1965**, *12*, 60-80. (c) Dickerson, R. E. DNA structure from A-Z. *Methods in Enzymol.* **1992**, *211*, 67-111. (d) Saenger, W. (Ed) Principles of Nucleic Acids structure. Springer-Verlag, New York, **1984**. (e) Wang, A. H. J.; Quigley, G. J.; Kolpak, F. J.; Van der M. G.; Van Boom, J. H.; Rich, A. Left-handed double helical DNA: variations in the backbone conformation. *Science*, **1981**, *211*, 171-176.
6. (a) Toule, J-J. in Antisense oligonucleotides and antisense RNA: Novel Pharmacological and Therapeutic Agents. (Weiss, B., ed), CRC press, **1997**, 1-16. (b) Wagner, R. W. The state of the art in antisense research. *Nat. Med*. **1995**, *1*, 1116-1118.
7. (a) Soyfer, V. N.; Potamann, V. N. *Triple Helical Nucleic Acids*, **1996**, Springer-Verlag, NY. (b) Chan, P. P.; Glazer, P. M. *J. Mol. Med*. **1997**, *75*, 267.
8. Zamecnik, P. C.; Stephenson, M. L. Inhibition of Rous sarcoma virus replication and cell transformation by a specific oligodeoxynucleotide. *Proc. Natl. Acad. Sci*. **1978**, *75*, 280-284.

9. Stein, C. A.; Cohen, J. S. Phoshorothioate oligodeoxynucleotide analogues. In Cohen J. S. (ed.): Oligodeoxynucleotides-Antisense Inhibitors of Gene Expression. London: Macmillan Press, **1989**, p. 97.

10. Millar, P. S. Non-ionic antisense oligonucleotides. In Cohen, J. S. (ed.): Oligodeoxynucleotides-antisense ihibitors of gene expression. London: Macmillan Press, **1989**, p. 79.

11. Froehler, B.; Ng, P.; Matteucci, M. Phosphoramidate analogs of DNA: Synthesis and thermal stabilities of heteroduplexes. *Nucleic Acids Res*. **1988**, *16*, 4831-4839.

12. Summers, M. F.; Powell, C.; Egan, W.; Byrd, R. A.; Wilson, W. D.; Zon, G. Alkyl phospotriester modified oligodeoxyribonucleotides. VI. NMR and UV spectroscopic studies of ethyl phosphotriester (Et) modified Rp-Rp and Sp-Sp duplexes, $(d(GGAA(Et)TTCC))_2$. *Nucleic Acids Res*. **1986**, *14*, 7421-7437.

13. (a) Sood, S.; Shaw, B. R.; Spielvogel, B. F.; Boron-containing nucleic Acids. Synthesis of oligonucleoside boranophosphates. *J. Am. Chem. Soc*. **1990**, *112*, 9000-9001. (b) Shaw, B. R.; Madison, J.; sood, S.; Spielvogel, B. F; Oligonucleotide boranophosphate (borane phosphate). In Agrawal, S. (ed): *Methods in Molecular biology*, vol 20: Protocols for Oligonucleotides and Analogs. Synthesis and properties. Totowa, NJ. Humana Press, Inc. **1993**, 225-243. (c) Sergueev, D. S.; Shaw, B. R. H-phophonate approach for solid phase synthesis of oligodeoxyribinucleotide boranophosphates and their characterization. *J. Am. Chem. Soc*. **1998**, *120*, 9417-9427.

14. Mesmaeker, A. D.; Walder, A.; Lebreton, J.; Hoffmann, P.; Fritsch, V.; Wolf, R. M.; Frier, S. M. Amide bridging, a new type of modification of oligonucleotide backbones. *Angew. Chem. Int. Ed. Eng*. **1994**, *33*, 226-229.

15. Metteuci, M. D. Deoxunucleotide analogues based on formacetal linkages. *Tetrahedron Lett*. **1990**, *31*, 2385-2388.

16. Jones, R. J.; Lin, K.-Y.; Miligan, J. F.; Wadwani, S.; Matteucci, M. D. Synthesis and binding properties of pyrimidine oligodeoxynucleoside analogs containing neutral phosphodiester replacements: the formacetal and 3'-thioformacetal internucleoside linkages. *J. Org. Chem*. **1993**, *58*, 2983-2991.

17. Lebreton, J.; Waldner, A.; Fritsch, V.; Wolf, R. M.; Mesmaeker, A. D. Comparison of two amides as backbone replacement of the phosphodiester linkage in oligodeoxynucleotides. *Tetrahedron Lett*. **1994**, *35*, 5225-5228.

18. Crooke, S. T.; Lemonidis, K. M.; Neilson, L.; Griffey, R.; Lesnik, E. A.; Monia, B. P. Kinetic characteristics of *Escherichia coli* RNase H: cleavage of various antisense oligonucleotide- RNA duplexes. *Biochem. J.* **1995**, *312*, 599-608.

19. (a) Summerton, J.; Weller, D. Morpholino antisense oligomers: design, preparation, and properties. *Antisense Nucleic Acid Drug Dev*. **1997**, *7*, 187-195. (b) Summerton,

J.; Weller, D. Antisense properties of morpholino oligomers. *Nucleosides & Nucleotides.* **1997**, *16*, 889-898.

20. Hendrix, C.; Rosemeyer, H.; Verheggen, I.; Seela, F.; Aerschot, A-V.; Herdewijn, P. 1', 5'-anhydrohexitol oligonucleotides: Synthesis, base pairing and recognition by regular oligodeoxyribonucleotides and oligoribonucleotides. *Chem. Eur. J.* **1997**, *3,* 110-120.

21. (a) Petersen, M.; Wengel, J. LNA: A versatile tool for therapeutic and genomics. *Trends Biotechnol*. **2003**, *21,* 74-81 (b) Koshkin, A.; Singh, S. K.; Nielsen, P.; Rajwanshi, V. K.; Kumar, R.; Meldgaard, M.; Olsen, C. E.; Wengel, J. LNA (locked nucleic acid): synthesis of the adenine, cytosine, guanine, 5-methylcytosine, thymine and uracil bicyclonucleotide monomers, oligomerization and unprecedented nucleic acid recognition. *Tetrahedron*, **1998**, *54*, 3607-3630. (c) Singh, S. K.; Nielsen, P.; Koshkin, A. A.; Wengel, J. LNA (locked nucleic acid): Synthesis and high affinity nucleic acid recognition. *Chem. Commun*. **1998**, 455-456.

22. (a) Allart, B.; Khan, K.; Rosemeyer, A. H.; Schepers, G.; Hendrix, C.; Rothenbacher. K.; Seela. F.; Aerschot, V.; Herdewijn. P. Synthesis of protected D-altritol nucleosides as building blocks for oligonucleotide synthesis. *Tetrahedron*, **1999**, *55*, 6527-6546.

23. Lilu, Z.; Adam, P.; Eric, M. A simple Glycol Nucleic Acid. *J. Am. Chem. Soc.* **2005**, *127*, 4174-4175.

24. (a) Izant, J.; Weintraub, H. Inhibition of thymidine kinase gene expression by antisense RNA: a molecular approach to genetic analysis. *Cell*, **1984**, *36*, 1007-1015. (b) Nellen, W.; Lichtenstein, C.; What makes an mRNA anti-sense-itive? *Trends Biochem. Sci.* **1993**, *18*, 419- 423.

25. Fire, A.; Xu, S.; Montgomery, M. K.; Kostas, S. A.; Driver, S. E.; Mello, C. C. Potent and specific genetic interference by double-stranded RNA in *Caenorhabditis elegans. Nature*, **1998**, *391*, 806-811.

26. (a) Yin, J. Q.; Gao, J.; Shao, R.; Tian, W. N.; Wang, J.; Wan, Y. siRNA agents inhibit oncogene expression and attenuate human tumor cell growth. *J. Exp. Ther. Oncol.* **2003**, *3*, 194-204. (b) Drosett, Y.; Tuschl, T. siRNAs: applications in functional genomics and potential as therapeutics. *Nat. Rev. Drug. Discov*. **2004**, *3*, 318-329. (c) de Francesco, R.; Migliaccio, G. Challenges and successes in developing new therapies for hepatitis C. *Nature*, **2005**, *436*, 953-960.

27. (a) Carrington, J. C.; Ambros, V. Role of microRNAs in plant and animal development. *Science*, **2003**, *301*, 336-338. (b) Ambros, V. MicroRNA pathways in flies and worms: growth, death, fat, stress, and timing. *Cell*, **2003**, *113*, 673-676. (c) Xu, P.; Vernooy, S. Y.; Guo, M.; Hay, B. A. The Drosophila microRNA mir-14

suppresses cell death and is required for normal fat metabolism. *Curr. Biol*. **2003**, *13*, 790-795.

28. (a) Nielsen, P. E.; Egholm, M.; Berg, R. H.; Buchardt, O. Sequence-selective recognition of DNA by strand displacement with a thymine-substituted polyamide. *Science*, **1991**, *254*, 1497-1501. (b) Egholm, M.; Nielsen, P. E.; Buchardt, O.; Berg, R. H. Recognition of guanine and adenine in DNA by cytosine and thymine containing peptide nucleic acids (PNA). *J. Am. Chem. Soc*. **1992**, *114*, 9677-9678. (c) Egholm, M.; Buchardt, O.; Nielsen, P. E.; Berg, R. H. Peptide nucleic acids (PNA). Oligonucleotide analogs with an achiral peptide backbone. *J. Am. Chem. Soc.* **1992**, *114*, 1895-1897. (d) Egholm, M.; Behrens, C.; Christensen, L.; Berg, R. H.; Nielsen, P. E.; Buchardt, O. Peptide nucleic acids containing adenine or guanine recognize thymine and cytosine in complementary DNA sequences. *J. Chem. Soc. Chem. Commun.* **1993**, 800-801.

29. Egholm, M.; Buchardt, O.; Christensen, L.; Behrens, C.; Freier, S. M.; Driver, D. A.; Berg, R. H.; Kim, S. K.; Norden, B.; Nielsen, P. E. PNA hybridizes to complementary oligonucleotides obeying the Watson-Crick hydrogen-bonding rules. *Nature*, **1993**, *365*, 566-568.

30. (a) Uhlmann, E.; Will, D. W.; Breipohl, G.; Langner, D.; Ryte, A. Synthesis and Properties of PNA/DNA Chimeras. *Angew. Chem. Int. Ed. Engl.* **1996**, *35*, 2632-2635.

31. Rose, D. J. Characterization of antisense binding properties of peptide nucleic acids by capillary gel electrophoresis. *Anal. Chem.* **1993**, *65*, 3545-3549.

32. Tomac, S.; Sarkar, M.; Ratilainen, T.; Wittung, P.; Nielsen, P. E.; Norden, B.; Graeslund, A. Ionic Effects on the Stability and Conformation of Peptide Nucleic Acid Complexes. *J. Am. Chem. Soc.* **1996**, *118*, 5544-5552.

33. Demidov, V. V.; Yavnilovich, M. V.; Belotserkovskii, B. P.; Frank-Kamenetskii, M. D.; Nielsen, P. E. Kinetics and mechanism of polyamide ("peptide") nucleic acid binding to duplex DNA. *Proc. Natl. Acad. Sci. USA*, **1995**, *92*, 2637- 2641.

34. (a) Nielsen, P. E.; Egholm, M.; Berg, R. H.; Buchardt, O. Sequence-selective recognition of DNA by strand displacement with a thymine-substituted polyamide. *Science*, **1991**, *254*, 1497-1501. (b) Nielsen, P. E.; Egholm, M.; Buchardt, O. Evidence for PNA_2-DNA triplex structure upon binding to dsDNA by strand displacement. *J Mol. Recogn*. **1994**, *7*, 165-170.

35. (a) Nielsen, P. E.; Egholm, M.; Berg, R. H.; Buchardt, O. Peptide nucleic acids (PNAs): Potential antisense and anti-gene agents. *Anti-Cancer Drug Design*. **1993**, *8*, 53 - 63. (b) J. C. Hanvey, N. J. Peffer, J. E. Bisi, S. A. Thomson, R. Cadilla, J. A. Josey, D. J. Ricca, C. F. Hassman, M. A. Bonham, K. G, Au, S. G. Carter, D. A. Bruckenstein, A. L. Boyd, S. A. Noble, L. E. Babiss, Antisense and antigene properties of peptide nucleic acids. *Science*, **1992**, *258*, 1481- 1485.

36. (a) Leijon, M.; Graeslund, A.; Nielsen, P. E.; Buchardt, O.; Norden, B.; Kristensen, S. M.; Eriksson, M. Structural characterization of PNA-DNA duplexes by NMR. Evidence for DNA in a B-like conformation. *Biochemistry*, **1994**, *22*, 9820-9825. (b) Eriksson, M.; Nielsen, P. E. Solution structure of a peptide nucleic acid-DNA duplex. *Nat. Struct. Biol*. **1996**, *3*, 410-413.

37. Egholm, M.; Buchardt, O.; Christensen, L.; Behrens, C.; Freier, S. M.; Driver, D. A.; Berg, R. H.; Kim, S. K.; Norden, B.; Nielsen, P. E. PNA hybridizes to complementary oligonucleotides obeying the Watson-Crick hydrogen-bonding rules. *Nature*, **1993**, *365*, 566-568.

38. Brown, S. C.; Thomson, S. A.; Veal, J. M.; Davis, D. G. NMR Solution structure of a peptide nucleic acid complexed with RNA. *Science*, **1994**, *265*, 777-780.

39. Bets, L.; Josey, J. A.; Veal, J. M.; Jordan, S. R. A nucleic acid triple helix formed by a peptide nucleic acid-DNA complex. *Science*, **1995**, *270*, 1838-1841.

40. Rasmussen, H.; Kastrup, J. S.; Nielsen, J. N.; Nielsen, J. M.; Nielsen, P. E. Crystal structure of peptide nucleic acid (PNA) duplex at 1.7 A resolution. *Nat. Struct. Biol*. **1997**, *4*, 98-101.

41. Knudsen, H.; Nielsen, P. E. Antisense properties of duplex- and triplex-forming PNAs. *Nucleic Acids Res.* **1996**, *24*, 494 - 500.

42. Nielsen, P. E.; Egholm, M.; Buchardt, O.; Sequence-specific transcription arrest by peptide nucleic acid bound to the DNA template strand. *Gene*, **1994**, *149*, 139- 145

43. Uhlmann, E.; Peyman, A.; Breipohl, G.; Will, D. W. PNA: Synthetic polyamide nucleic acids with unusual binding properties. *Angew. Chem. Int. Ed*. **1998**, *37*, 2796-2823.

44. Norton, J. C.; Piatyczek, M. A.; Wright, W. E.; Shay, J. W.; Corey, D. R. Inhibition of human telomerase activity by peptide nucleic acid. *Nature Biotechnol*. **1996**, *14*, 615-619.

45. Nielsen, P. E.; Egholm, M.; Berg, R. H.; Buchardt, O. Sequence specific inhibition of restriction enzyme cleavage by PNA. *Nucleic Acids Res*. **1993**, *21*, 197-200.

46. Demidov, V.; Frank-Kamenetskii, M. D.; Egholm, M.; Buchardt, O.; Nielsen, P. E. Sequence specific double strand DNA cleavage by peptide nucleic acid (PNA) targeting using nuclease S1. *Nucleic Acids Res.* **1993**, *21*, 2103–2107.

47. (a) Ganesh, K. N.; Nielsen, P. E. Peptide Nucleic Acids: analogs and derivatives. *Curr. Org. Chem.* **2000**, *4*, 931-943. (b) Kumar, V. A.; Ganesh, K. N. Conformationally constrained PNA analogues: Structural evolution toward DNA/RNA binding selectivity. *Acc. Chem. Res*. **2005**, *38*, 404-412. (c) Kumar, V. A. Structural preorganization of peptide nucleic acid: chiral cationic analogues with five-or six-membered ring structures. *Eur. J. Org. Chem.* **2002**, 2021-2032. (d)

Kumar, V. A.; Ganesh, K. N. Structure-editing of nucleic acids for selective targeting of RNA. *Curr. Med. Chem*. **2007**, *7*, 715-726.

48. Hyrup, B.; Egholm, M.; Nielsen, P. E.; Wittung, P.; Norden, B.; Buchardt, O. Structure-Activity Studies of the Binding of Modified Peptide Nucleic Acids (PNAs) to DNA. *J. Am. Chem. Soc.* **1994***, 116,* 7964-7970.

49. Hyrup, B.; Egholm, M.; Buchardt, O.; Nielsen, P. E.; Wittung, P. A flexible and positively charged PNA analogue with an ethylene-linker to the nucleobase: Synthesis and hybridization properties. *Bioorg. Med. Chem. Lett*. **1996**, *6*, 1083-1088.

50. (a) Dueholm, K. L.; Petersen, K. H.; Jensen, D. K.; Egholm, M.; Nielsen, P.E.; Buchardt O. Peptide nucleic acid (PNA) with a chiral backbone based on alanine. *Bioorg. Med. Chem. Lett*. **1994**, *4*, 1077-1080. (b) Haaima, G.; Lohse, A.; Buchardt, O. Nielsen, P.E. Peptide Nucleic Acids (PNAs) Containing Thymine Monomers Derived from Chiral Amino Acids : Hybridization and Solubility Properties of D-Lysine PNA. *Angew. Chem. Intl. Ed. Eng.* **1996**, *35*, 1939-1942. (c) Puschl, A.; Sforza, S.; Haaima, G.; Dahl, O.; Nielsen, P. E. Peptide nucleic acids (PNAs) with a functional backbone. *Tetrahedron Lett.* **1998**, *39*, 4707-4710.

51. (a) Lagriffoule, P.; Wittung, P.; Eriksson, M.; Jensen, K. K.; Norden, B.; Buchardt, O.; Nielsen, P. E. Peptide nucleic acids (PNAs) with conformationally constrained, chiral cyclohexyl derived backbone. *Chem. Eur. J.* **1997**, *3*, 912-919. (b) Govindaraju, T.; Gonnade, R. G.; Bhadbhade, M. M.; Kumar, V. A.; Ganesh, K. N. (1*S,*2*R*/1*R,*2*S*)-aminocyclohexyl glycyl thymine PNA: Synthesis, monomer crystal structures, and DNA/RNA hybridization studies. *Org. Lett*. **2003**, *5*, 3013-3016. (c) Govindaraju, T.; Kumar, V. A.; Ganesh, K. N.; Synthesis and evaluation of (1*S*,2*R*/1*R*,2*S*)- aminocyclohexyl-glycyl PNAs as conformationally pre-organized PNA analogues for DNA/RNA recognition. *J. Org. Chem*. **2004**, *69*, 1858-1865. (d) Govindaraju, T.; Kumar, V. A.; Ganesh, K. N. (SR/RS)-cyclohexanyl PNAs: conformationally preorganized PNA analogues with unprecedented preference for duplex formation with RNA. *J. Am. Chem. Soc.*, **2005**, *127*, 4144-4145. (e) Govindaraju, T.; Madhuri, V.; Kumar, V. A.; Ganesh. K. N. Cyclohexanyl Peptide Nucleic Acids (*ch*PNAs) for preferential RNA binding: effective tuning of dihedral angle β in PNAs for DNA/RNA discrimination. *J. Org. Chem.* **2006**, *71*, 14-21.

52. (a) Govindaraju, T.; Kumar, V. A.; Ganesh, K. N. *cis*-Cyclopentyl PNA (*cp*PNA) as constrained chiral PNA analogues: stereochemical dependence of DNA/RNA hybridization. *Chem. Commun.* **2004**, 860-861. (b) Govindaraju, T.; Kumar, V. A.; Ganesh, K. N. (1*S*,2*R*/1*R*,2*S*)-*cis*-Cyclopentyl PNAs (*cp*PNAs) as constrained PNA analogues: Synthesis and evaluation of *aeg*-*cp*PNA chimera and stereopreferences in hybridization with DNA/RNA. *J. Org. Chem.* **2004**, *69*, 5725-5734.

53. Maison, W.; Schlemminger, I.; Westerhoff, O.; Martens, J. Modified PNAs: A simple method for the synthesis of monomeric building blocks. *Bioorg. Med.Chem. Lett.* **1999**, *9*, 581-584.

54. (a) Krotz, A. H.; Buchardt, O.; Nielsen, P. E. Synthesis of 'retro-inverso' peptide nucleic acids: 1. Characterization of the monomers. *Tetrahedron Lett*. **1995**, *36*, 6937-6940. (b) krotz, A. H.; Buchardt, O.; Nielsen, P. E. Synthesis of 'retro-inverso' peptide nucleic acids: 2. Oligomerization and stability. *Tetrahedron Lett.* **1995**, *38*, 6941-6944. (c) Krotz, A. H.; Larsen, S.; Buchardt, O.; Nielsen, P. E. A 'Retro–Inverso' PNA: structural implications for DNA and RNA binding. *Bioorg. Med. Chem.* **1998**, *6*, 1983-1992.

55. (a) Kumar, V. A.; Ganesh, K. N. Conformationally constrained PNA analogues: Structural evolution toward DNA/RNA binding selectivity. *Acc. Chem. Res*. **2005**, *38*, 404-412. (b) Kumar, V. A. Structural preorganization of peptide nucleic acid: chiral cationic analogues with five-or six-membered ring structures. *Eur. J. Org. Chem.* **2002**, 2021-2032.

56. Gangamani, B. P.; Kumar, V. A.; Ganesh, K. N. Synthesis of (purinyl/pyrimidinyl acetyl)-4-aminoproline diastereomers with potential use in PNA synthesis. *Tetrahedron*, **1996**, *52*, 15017-15030.

57. D'Costa, M.; Kumar, V. A.; Ganesh, K. N. Aminoethylprolyl peptide nucleic acids (aepPNA): chiral PNA analogues that form highly stable DNA:aepPNA$_2$ triplexes. *Org. Lett.* **1999**, *1*, 1513-1516.

58. Sharma, N.; Ganesh, K. N. Regioselective oxidation of N-alkyl pyrrolidines to pyrrolidin-5-enes by $RuCl_3/NaIO_4$. *Tetrahedron Lett.* **2004**, *45*, 1403-1406.

59. Puschl, A.; Boesen, T.; Zuccarello, G.; Dahl, O.; Pitsch, S.; Nielsen, P. E. Synthesis of pyrrolidinone PNA: A novel conformationally restricted PNA analogue. *J. Org. Chem.* **2001**, *66*, 707-712.

60. D'Costa, M.; Kumar, V. A.; Ganesh, K. N. Synthesis of 4(S)-(N Boc-amino)-2(S/R)-(thymin-1-yl)-pyrrolidine-N-1-acetic acid: a novel cyclic PNA with constrained flexibility. *Tetrahedron. Lett.* **2002**, *43*, 883-886.

61. Shirude, P. S.; Kumar, V. A.; Ganesh, K. N. Chimeric peptide nucleic acids incorporating (2S,5R)-aminoethyl pipecolyl units: synthesis and binding studies. *Tetrahedron Lett.* **2004**, *45*, 3085-3088.

62. Puschl, A.; Boesen, T.; Tedeschr, T.; Dahl, O.; Nielsen, P. E. Synthesis of (3*R*,6*R*)- and (3*S*,6*R*)-piperidinone PNA. *J. Chem. Soc. Perkin 1*, **2001**, 2757-2763.

63. Haaima, G.; Hansen, H. F.; Christensen, L.; Dahl, O.; Nielsen, P. E. Increased DNA binding and sequence discrimination of PNA oligomers containing 2,6-diaminopurine. *Nucleic Acids Res.* **1997**, *25*, 4639-4643.

64. Egholm, M.; Christensen, L.; Deuholm, K. L.; Buchardt, O.; Coull, J.; Nielsen, P. E. Efficient pH-independent sequence-specific DNA binding by pseudoisocytosine-containing bis-PNA. *Nucleic Acids Res.* **1995**, *23*, 217-222.

65. (a) Gangamani, B. P.; Kumar V. A. 2-Aminopurine peptide nucleic acids (2-*ap*PNA): intrinsic fluorescent PNAanalogues for probing PNA-DNA interaction dynamics. *JCS Chem. Commun.* **1997***,* 1913-1914. (b) Gangamani, B. P.; Kumar, V. A.; Ganesh, K. N. Spermine conjugated peptide nucleic acids (spPNA): UV and fluorescence studies of PNA-DNA hybrids with improved stability. *Biochem. Biophys. Res. Commun.* **1997***, 240,* 778-782.

66. Eldrup, A. B.; Dahl, O.; Nielsen, P. E. A novel peptide nucleic acid monomer for recognition of thymine in triple-helix structures *J. Am. Chem. Soc.* **1997**, *119*, 11116-11117.

67. (a) Wojciechowski. F.; Hudson. R. H. E. Nucleobase modifications in peptide nucleic acids. *Cur. Top. Med. Chem.* 2007, *7,* 667-679. (b) Bajor, Z.; Sagi, G.; Tegyey, Z.; Kraicsovits, F. PNA-DNA Chimeras containing 5-alkynyl-pyrimidine PNA units. Synthesis, binding properties, and enzymatic stability. *Nucleosides & Nucleotides*, **2003**, *22*, 1963-1983. (d) Hudson, R. H. E.; Li, G.; Tse, J. The use of Sonogashira coupling for the synthesis of modified uracil peptide nucleic acid. *Tetrahedron Lett*. **2002**, *43*, 1381-1386.

68. (a) Rajeev, K. G.; Maier, M. A.; Lesnik, E. A.; Manoharan, M. High-Affinity Peptide Nucleic Acid Oligomers Containing Tricyclic Cytosine Analogues. *Org. Lett.* **2002**, *4*, 4395-4398. (b) Ausin, C.; Ortega, J. A.; Robles, J.; Grandas, A.; Pedroso, E. Synthesis of Amino- and Guanidino-G-Clamp PNA Monomers. *Org. Lett.* **2002**, *4*, 4073-4075. (b) Christensen, L.; Hansen, H. F.; Koch, T.; Nielsen, P. E. Inhibition of PNA triplex formation by N4-benzoylated cytosine. *Nucleic Acids Res.* **1998**, *26*, 2735-2739.

69. Challa, H.; Styers, M. L.; Woski, S. A. Nitroazole universal bases in peptide nucleic acids. *Org. Lett.* **1999**, *1*, 1639-1641.

70. Vysabhattar, R.; Ganesh, K. N. Cyanuryl peptide nucleic acid: Synthesis and DNA complexation properties. *Tetrahedron Lett*. **2008**, *49*, 1314-1318.

71. (a) Bonham, M. A.; Brown, S.; Boyd, A. L.; Brown, P. H.; Bruckenstein, D. A.; Hanvey, J. C.; Thomson, S. A.; Pipe, A.; Hassman, F.; Bisi, J. E.; Froehler, B. C.; Matteucci, M. D.; Wagner, R. W.; Noble, S. A.; Babiss, L. E. An assessment of the antisense properties of RNase H-competent and steric-blocking oligomers. *Nucleic Acids Res.* **1995**, *23*, 1197-1203. (b) Hanvey, J. C.; Peffer, N. J.; Bisi, J. E.; Thomson, S. A.; Cadilla, R.; Josey, J. A.; Ricca, D. J.; Hassman, C. F.; Bonham, M. A.; Au, K. G.; Carter, S. G.; Bruckenstein, D. A.; Boyd, A. L.; Noble, S. A.; Babiss, L. E. Antisense and antigene properties of peptide nucleic acids. *Science*, **1992**, *258*, 1481-1485.

72. Egholm, M.; Buchardt, O.; Nielsen, P. E.; Berg, R. H.; Peptide nucleic acids (PNA). Oligonucleotide analogs with an achiral peptide backbone. *J. Am. Chem. Soc.* **1992**, *114*, 1895 -1897.

73. (a) Petersen, K. H.; Jensen, D. K.; Egholm, M.; Nielsen, P. E.; Buchardt, O. A PNA-DNA linker synthesis of *N*-((4,4′-dimethoxytrityloxy)ethyl)-*N*-(thymin-1-ylacetyl)glycine. *Bioorg. Med. Chem. Lett.* **1995**, *11*, 1119-1124. (b) Petersen, K. H.; Buchardt, O.; Nielsen, P. E. Synthesis and oligomerization of N^{δ}-Boc-N^{α}-(thymin-1-ylacetyl)ornithine. *Bioorg. Med. Chem. Lett.* **1996**, *6*, 793-796. (c) Finn, P. J.; Gibson, N. J.; Fallon, R.; Hamilton, A.; Brown, T. Synthesis and properties of DNA-PNA chimeric oligomers. *Nucleic Acids Res.* **1996**, *24*, 3357-3363.

74. Bergmann, F.; Bannwarth, W. Tam, S. Solid phase synthesis of directly linked PNA-DNA-hybrids. *Tetrahedron Lett.* **1995**, *36*, 6823-6826.

75. Naguibneva, I.; Ameyar-Zazoua, M.; Nonne, N.; Polesskaya, A.; Ait-Si-Ali, S.; Groisman, R.; Souidi, M.; Pritchard, L. L.; Harel-Bellan, A. An LNA-based loss-of-function assay for micro- RNAs. *Biomed. Pharmacother.* **2006**, *60*, 633-638.

76. Ørom, U. A.; Kauppinen, S.; Lund, A. H. LNA-modified oligonucleotides mediate specific inhibition of microRNA function. *Gene*, **2006**, *372*, 137-141.

77. Abes, S.; Turner, J. J.; Ivanova, G.D.; Owen, D.; Williams, D.; Arzumanov, A.; Clair, P.; Gait, M. J.; Lebleu, B. Efficient splicing correction by PNA conjugation to an R_6-Penetratin delivery peptide. *Nucleic Acids Res.* **2007**, *35*, 4495-4502.

78. Kosch, T.; Naesby, M.; Wittung, P.; l Jørgensen, M.; Larsson, C.; Buchardt, O.; Stanley, C. J.; Norden, B.; Nielsen, P. E.; Ørum, H. PNA-peptide chimerae. *Tetrahedron Lett*. **1995**, *36*, 6933-6936.

79. Betts, L.; Joesy, S.A.; Veal, J. M.; Jorden, S. A Nucleic acid triple helix formed by a peptide nucleic acid-DNA complex. *Science*, **1995**, *270*, 1838-1841.

80. Griffith, M. C.; Risen, L. M.; Greig, M. J.; Lesnik, A.; Spankh, K. G.; Gritty, R. H.; Kiely, J. S.; Freier, S. M. Single and bis Peptide Nucleic Acids as triplexing agents: Binding and stoichiometry. *J. Am. Chem. Soc.* **1995**, *117*, 831-832.

81. Harrison, J. G.; Frier, C.; Laurant, R. Dennis, R.; Raney, K. D.; Balasubramanian, S. Inhibition of human telomerase by PNA-cationic peptide conjugates. *Bioorg. Med. Chem. Lett.* **1999**, *9*, 1273-1278.

Chapter 2

Design, synthesis and biophysical evaluation of backbone extended prolylPNA

2 Introduction

Since the beginning of the investigation of oligonucleotides as potential therapeutic agents that target nucleic acids, the search for modified nucleic acid mimics with improved properties has accelerated rapidly.[1] The properties comprise of enhanced binding-affinity to complementary nucleic acids, increased biological stability, and improved cellular uptake. Undoubtedly, one of the most interesting of the new derivatives are peptide nucleic acids (PNAs),[2] in which the entire sugar-phoshate backbone is replaced by an *N*-(2-aminoethyl) glycine polyamide structure (**II**, Figure 1). The nucleobases are attached to the backbone through a conformationally rigid tertiary acetamide linker.

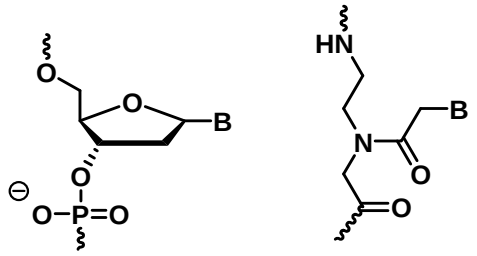

I, DNA **II, PNA**

Figure 1: Chemical structures of DNA and PNA

PNA binding to the target DNA/RNA sequences occurs with high sequence specificity and affinity.[3] Despite having several advantages like resistance to cellular enzyme (proteases and nucleases), the major limitations confounding its application are poor aqueous solubility, inefficient cellular uptake and ambiguity in DNA/RNA recognition arising from its equally facile binding in a parallel/antiparallel fashion with the complementary nucleic acid sequences.[4] The three dimensional structure of PNA:DNA and PNA:RNA duplex/triplexes[5] demonstrate that PNA does have the flexibility enabling the adaption to the A-form and B-form helices preferred by RNA or DNA, but the results also clearly show that the P-form structure preferred by PNA is much wider and more slowly winding helix. These results imply that PNA is not a perfect structural mimic of DNA or RNA, and therefore enough scope exists for chemical modifications for further improvement. Thus one should be able to design a peptide nucleic acid analogue as a better DNA mimic if one could construct a backbone which at its lowest energy state would adopt a B-form (or A-form) helix. To overcome

some of the drawbacks of PNA, attempts have been made to introduce asymmetry into PNA backbone in such a way that it becomes chiral as well induce certain conformational constraint towards unambiguous binding to complementary DNA/RNA.

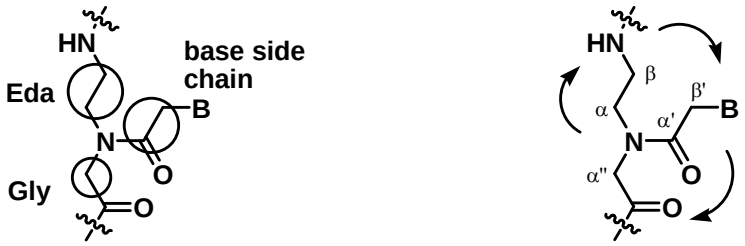

III IV

Figure 2: Building block of PNA oligomers. [Eda = ethylenediamine, Gly = glycine, B = nucleobase]

Reports till date,[6] suggest that the sterically allowed constrains of the PNA backbone may improve its tendency to hybridize with DNA/RNA, but this strongly depends on the stereochemistry of the residue. Introduction of chemical bridges in *aeg*PNA to get cyclic structures may help in constraining the backbone and thus achieving parallel/antiparallel orientation selective binding by virtue of chirality in the backbone.[6b-d] This structural preorganization of PNA may trigger a shift in the equilibrium towards the desired binding target (DNA/RNA) because of the reduced entropy loss upon complex formation, provided the enthalpic contributions remain unaffected. This may be achieved if the conformational freedom in *aeg*PNA (Figure 2) is curtailed by bridging the aminoethyl, glycyl or acetyl linker arms leading to cyclic analogues. These may have structures preorganized for efficient recognition of complementary DNA *via* hydrogen bonding.[6b-d] Conformational preorganization by introduction of structural constraints has been successful in DNA analogues such as locked nucleic acids (LNA)[7] in which the prelocked 3'-endo sugar conformation (like in DNA:RNA hybrids) favors binding with complementary DNA/RNA sequences. Other examples include conformationally frozen six-membered hexitol[8] and altritol[9] nucleic acids.

PNA oligomers where one of the repeating backbone unit is extended with a methylene group to *N*-(2-aminoethyl) segment (*apg*PNA, **VI**, Figure 3) was reported by

Nielsen et al.[10] The thermal stability of the hybrids between these PNA oligomers and complementary DNA oligonucleotides was significantly lower than that of the corresponding complexes involving unmodified PNA. Although the sequence selectivity was retained for the modified PNA oligomers corresponding to the *apg*PNA monomer (**VI**), it was not an effective structural modification.

It is well known that hybridization of complementary oligomers (DNA, RNA or PNA) is characterized by a large enthalpy gain and a significant entropy loss.[11] The decrease in entropy upon hybrid formation is naturally due to the formation of a highly ordered and fairly rigid duplex structure from two rather flexible and much less ordered single strands. Therefore constraining the single stranded PNA in a conformation identical or close to that found in the hybrid should greatly reduce the entropy loss and hence increase the free energy upon binding. Restricting the backbone flexibility, e.g. by introducing cyclic structures is thus an obvious strategy in the quest for oligomers with improved hybridization potency.

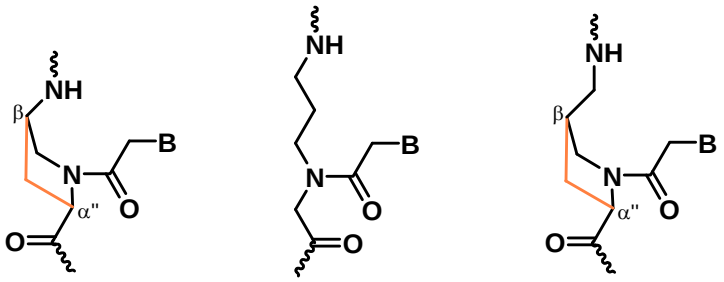

Figure 3: Structures of *aminoprolyl*PNA (*ap*PNA) monomer **V** and *aminopropylglycyl*PNA (*apg*PNA) monomer **VI** and targeted backbone extended *prolyl*PNA monomer **VII**

Introduction of a methylene bridge between the *β*-carbon atom of the aminoethyl segment and the *α*''-carbon of the glycine segment of *aeg*PNA for constraining the *aeg*PNA backbone resulted in 4-*aminoprolyl*PNA (**V**, Figure 3) having two chiral centers, was reported from our laboratory.[12] All four diastereomeric T monomers were synthesized from (2*S*,4*R*)-4-hydroxyproline and incorporated into PNA oligomers. None of the homochiral aminoprolyl thyminyl PNAs corresponding to any of the diastereomers bound to target DNA sequences, probably due to high rigidity in the backbone resulting in structural incompatibility. However, incorporation of single chiral D-*trans* or L-*trans* *ap*PNA monomer into *aeg*PNA at the N-terminus or within

the PNA sequence resulted in a higher binding to the target DNA with definite preference for a parallel or an antiparallel mode unlike the unmodified PNA. The efforts directed toward releasing the strain by replacing the backbone amide linker with carbamate linkage were not successful.[13] Therefore, keeping in view the above observations for *ap*PNA (**V**) and *apg*PNA (**VI**), it was planned to combine the two concepts to design the modified PNA monomer (**VII,** Figure 3) with controlled rigidity and flexibility.

2.1 Rationale and Objectives

The equal binding of PNA in parallel and antiparallel orientations to DNA/RNA reduces its target specificity by half and this may have significant implications for therapeutic applications depending on the other gene that gets affected.[14] This problem was addressed by introduction of chirality into achiral PNA backbones to affect orientational selectivity in complementary DNA/RNA binding. The ambiguity in DNA/RNA binding may lead to recognition of nonspecific target sequences, and achieving PNA specificity in binding is a desirable goal for successful therapeutic applications.

In the present work it was envisioned to incorporate chirality and controlled rigidity along with the extension of the ethylenediamine segment into the PNA backbone to modulate the biophysico-chemical properties. The introduction of a methylene bridge between the *β*- carbon atom of the aminopropyl segment and *α*''-carbon atom of the glycine segment of the *apg*PNA (**VI,** Figure 4) was envisaged to result the desired backbone extended prolyl PNA (**VIIa**, **VIIb**, Figure 4). This simultaneously leads to introduction of two chiral centres at *C*2 and *C*4 position.

The specific objectives of this chapter are

1. To develop methodologies for introduction of methylene group at *C*4 position of proline ring of (2*S,*4*S*)- and (2*S,*4*R*)- backbone extended *prolyl*PNA monomer.
2. Solid phase synthesis of oligomers incorporating (2*S,*4*S*)- and (2*S,*4*R*)- *prolyl*PNA monomer to *aeg*PNA backbone.
3. Cleavage from the solid support, purification and characterization of the oligomers.

4. Binding studies of modified PNA oligomers having (2*S*,4*S*)- and (2*S*,4*R*)- backbone extended *prolyl*PNA units and *aeg*PNA with complementary DNA using biophysical techniques UV, CD.

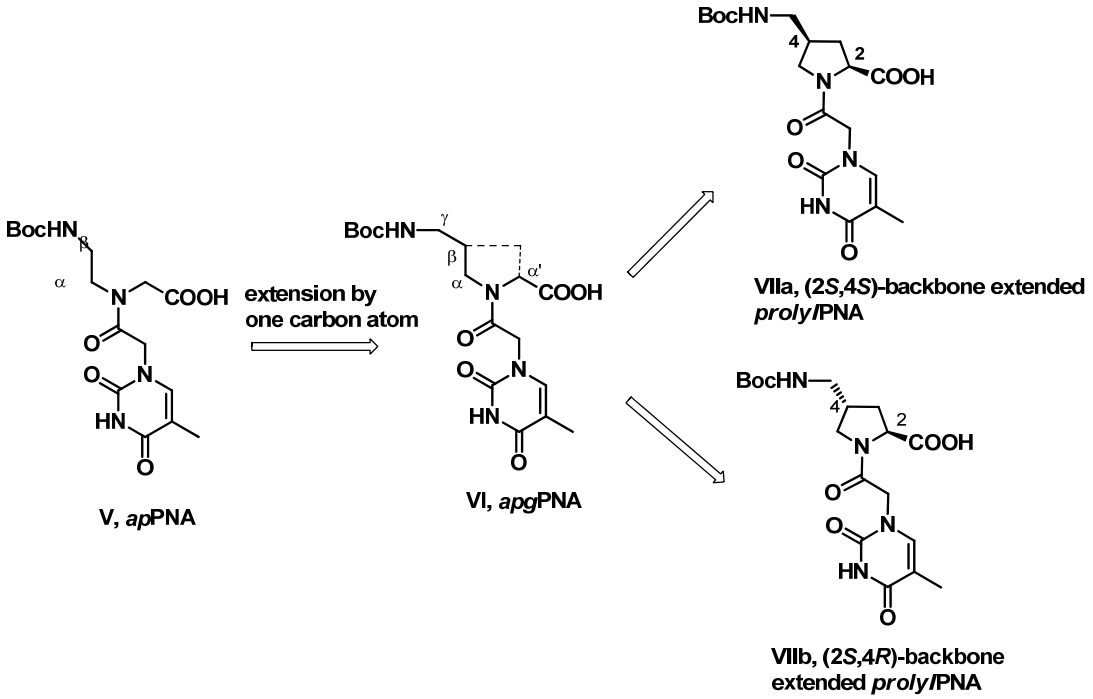

Figure 4: Schematic representation for the targeted modified PNA monomers

2.2 Results and Discussion

(2*S*,4*R*)-4-hydroxyproline is a versatile synthon.[15] It is the most abundant of the three naturally occurring diastereomers which is commercially available and is inexpensive. With its two chiral centers at *C*2 and *C*4, (2*S*,4*R*)-4-hydroxyproline is a material of choice to access multifunctionalized pyrrolidine rings. Thus, the synthesis of (2*S*,4*S*)-*prolyl*PNA monomer was achieved in nine steps starting from naturally occurring (2*S*,4*R*)-4-hydroxyproline.

2.2.1 Synthesis of (2*S*,4*S*)-backbone extended *prolyl*PNA monomer

Synthetic approach 1

In the first approach the synthesis was started with commercially available (2*S*,4*R*)-4-hydroxyproline **1** (Scheme 1). This was converted to its methyl ester hydrochloride derivative **2** by reacting with thionyl chloride and methanol. The hydrochloride salt **2** was then acylated with chloroacetyl choride in presence of triethyl

amine to achieve the acetylated product **3**. This was further alkylated with thymine nucleobase using K_2CO_3 as the base to obtain the product **4.** The 4*R*-hydroxyl group of compound **4** was converted to its 4*R*-*O*-tosyl derivative **5** by reacting with tosyl chloride in anhydrous pyridine. The conversion of 4*R*-*O*-tosylate **5** to 4*S*-cyanide derivative was attempted by nucleophilic substitution reaction using NaCN as the nucleophile. No product was observed and the starting material was recovered completely. This is perhaps due to the bulkiness of the group present in *N*1 position Therefore, an alternative approach (Scheme 2) was tried to achieve the synthesis of the targeted backbone-extended (2*S,*4*S*)-*prolyl*PNA monomer employing 4*S*-*O*-mesylate rather than tosylate and carrying displacement reaction before *N*1-substitution with thyminyl side chain.

Scheme 1: Synthesis of (2*S,*4*S*)-backbone extended *prolyl*PNA monomer

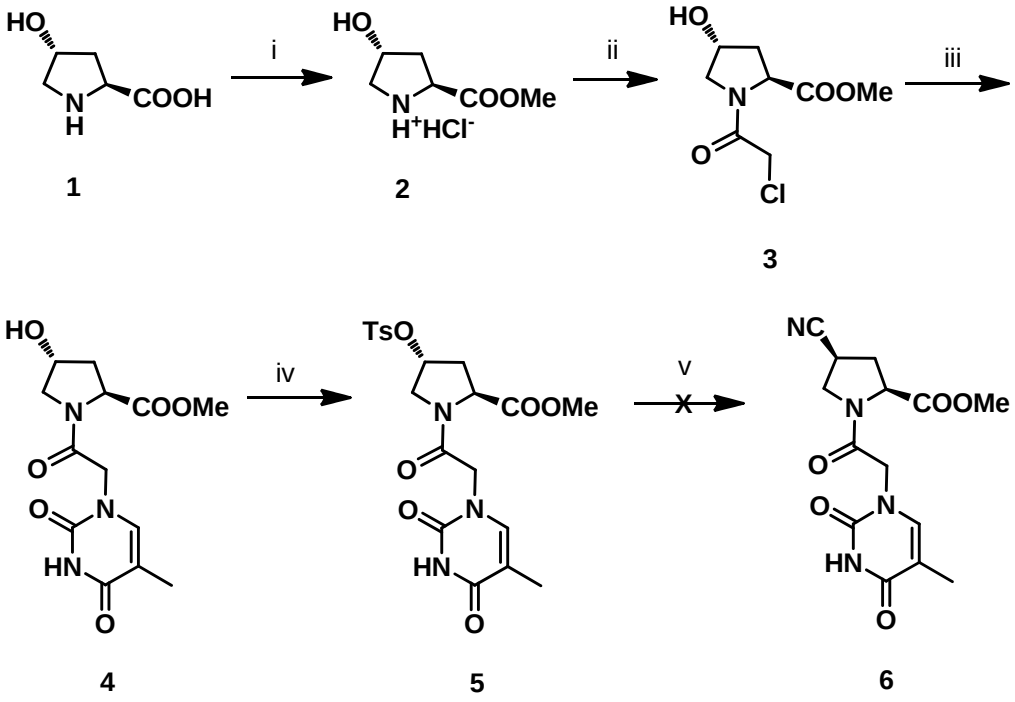

Reagents and conditions : (i) $SOCl_2$, MeOH, 0-60^oC (ii) $ClCH_2COCl$, Na_2CO_3, Dioxan:water 0^oC, 84% (iii) Thymine, K_2CO_3, DMF, 60^oC, 81% (iv) Tosyl chloride, Pyridine, 0^oC, 62% (v) NaCN, DMSO, 60^oC

Synthetic approach 2

(2*S,*4*R*)-4-hydroxyproline **1** was esterified with MeOH/$SOCl_2$ followed by the *N*1-protection with *t*-butylpyrocarbonate (*t*-Boc) in presence of Et_3N to obtain product

7.[12a] This was then 4-*O*-mesylated with mesyl chloride and pyridine to get an excellent yield of compound **8**.[12a,16] Hydroxyl functionality was also converted to its mesylate using triethyl amine as the base in dichloromethane solvent at ice cold temperature. In this case the conversion was slower and reaction was therefore incomplete to yield the (2*S,*4*R*)-mesylate **8**. Therefore pyridine was a better choice, which can fulfill the purpose of both solvent and the base for the above conversion. The conversion was confirmed by the appearance of ^{1}H NMR peak at δ 3.04 ppm for –CH_3 group present in the mesyatecompound **8**. The *N*1- protected 4*R*-*O*-mesylate **8** was subjected to S_N2 substitution reaction using NaCN as the source of nucleophile to yield the (2*S,*4*S*)-cyano compound **9** with inversion of configuration at the *C*4 position.[17]

Scheme 2: Synthesis of (2*S,*4*S*)-backbone extended *prolyl*PNA monomer

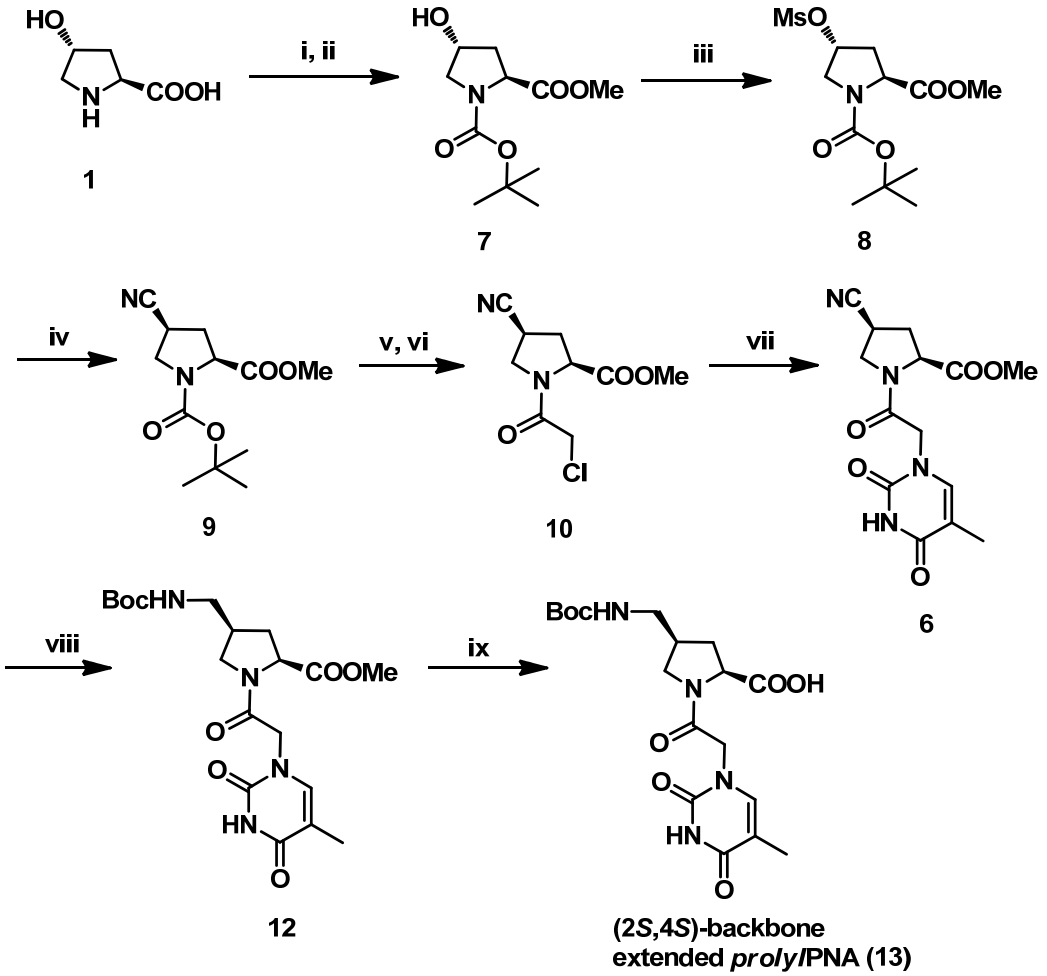

Reagents and condition: (i) $SOCl_2$, MeOH, 0-60^{o}C (ii) $(Boc)_2O$, Et_3N, ACN:H_2O, 85% (iii) Mesyl chloride, pyridine, 0^{o}C, 92% (iv) NaCN, DMSO, 60^{o}C, 35% (v) 50% TFA in DCM, 25% ammonia solution (vi) $ClCH_2COCl$, Et_3N, DCM, 0^{o}C, 72% (vii) Thymine, K_2CO_3, DMF, 60^{o}C, 81% viii) 10 mol% Pd/C, Et_3N, $(Boc)_2O$, MeOH, 87% (ix) 1N aq LiOH, THF, 80%.

Formation of cyano derivative **9** was confirmed by the disappearance of the ^{1}H NMR peak at δ 3.04 ppm for the –CH_3 group present in mesyl derivative **8** and was subjected to Boc deprotection using 50% TFA in DCM followed by neutralization and acylation with chloroacetyl chloride in presence of Et_3N to obtain the acylated derivative **10**. This compound was substituted with thymine nucleobase using K_2CO_3 as the base to achieve the product **6**. The nitrile was subjected to catalytic hydrogenation which gave the amine which was *in situ* Boc protected to give the protected amine **12**. The methyl ester was then hydrolyzed with 1N aq LiOH solution to get the final (2*S,*4*S*)-backbone extended *prolyl*PNA monomer **13.** The conversion was confirmed by the disappearance of the ^{1}H NMR peak at δ 3.61ppm for the ester –CH_3 group. All the unknown compounds synthesized were characterized by ^{1}H, ^{13}C and LCMS spectra and are included in the experimental section.

2.2.2 Synthesis of (2*S*,4*R*)-backbone extended *prolyl*PNA monomer

The synthesis of the (2*S,*4*R*)- diastereomer **19** (**VIIb,** Figure 4) was started from the (2*S,*4*R*)-4-hydroxyproline. Compound **7** (Scheme 3) with (2*S,*4*R*) stereochemistry was subjected to Mitsunobu reaction with *p*-toluene sulphonic acid in presence of PPh_3/DIAD to obtain the (2*S,*4*S*)-tosylated product **14** with inversion of configuration at *C*4 stereocenter. A second inversion at *C*4 stereocenter was done by converting the (2*S,*4*S*)-tosylate into (2*S,*4*R*)-cyano derivative **15** by S_N2 substitution reaction using NaCN as the nucleophile. This was confirmed by the disappearance of aromatic protons at δ 7.33-7.78 ppm in ^{1}H NMR and by ^{13}C NMR. In this case also the conversion yield was found to be very low, as seen for the other isomer. Product **15** was subjected to *N*-Boc deprotection followed by acetylation with chloroacetyl chloride to get product **16**. This was used for *N*-alkylation of thymine nucleobase using K_2CO_3 as the base to get compound **17**. Appearance of ^{1}H NMR peak at δ 7.28 ppm and 1.68 ppm shows the formation of desired product **17**, which appears due to the presence of thymine nucleobase. The reduction of nitrile group of compound **17** has been done using Pd/C as the catalyst and *in situ N*-Boc protection was done to obtain compound **18**. This was hydrolyzed to obtain the desired (2*S,*4*R*)-*prolyl*PNA monomer **19**. After completion of the synthesis of *N*-(thymin-1-yl)-(2*S,*4*S*)-4-Boc-methyl aminoproline **13** and *N*-(thymin-1-yl)-(2*S,*4*R*)-4-Boc-methyl aminoproline **19** monomers, were proposed for

use in solid phase synthesis. All the unknown compounds were characterized by ^{1}H NMR, ^{13}C NMR and LCMS experiment which were shown in the experimental section.

Scheme 3: Synthesis of (2*S*,4*R*)-backbone extended *prolyl*PNA monomer

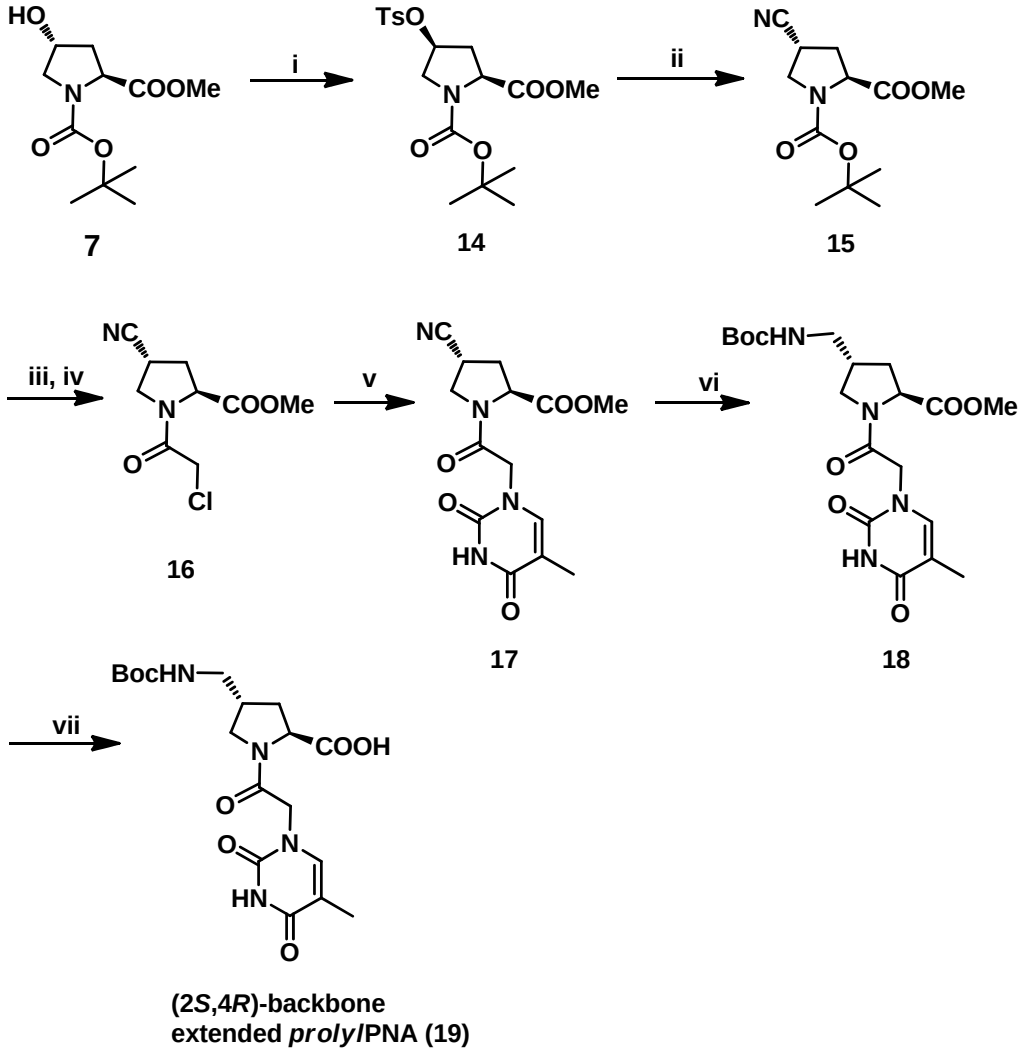

Reagents and condition: (i) *p*-toluene sulphonic acid, PPh_3, DIAD, THF, 54% (ii) NaCN, DMSO, 60°C, 28% (iii) 50% TFA in DCM, 25% ammonia solution (iv) $ClCH_2COCl$, Et_3N, DCM, 0°C, 73% (v) Thymine, K_2CO_3, DMF, 60°C, 81% (vi) 10 mol% Pd/C, MeOH, $(Boc)_2O$, Et_3N, 81% (vii) 1N aq LiOH, THF, 83%

2.2.3 Synthesis of aminoethylglycyl PNA monomers

The synthesis of unmodified *aeg*PNA monomers were carried out following the literature procedures.[18] The synthesis was started from the easily available 1,2-diaminoethane **20** (Scheme 4). This was treated with *t*-butyl pyrocarbonate to give the monoprotected derivative **21** and was obtained by using a large excess of 1,2-

diaminoethane over the *t*-butyl pyrocarbonate in high dilution conditions. The di-Boc derivative which was obtained as a minor product, being insoluble in water, could be removed by filtration through celite. The *N*1-Boc-1,2-diaminoethane **21** was then subjected to *N*-alkylation using ethylbromoacetate and triethyl amine in dry acetonitrile. The aminoethylglycine **22** was further treated with chloroacetyl chloride to yield the corresponding chloro derivative **23,** which is the common intermediate for the preparation of all the PNA monomers in good yield.

Scheme 4: Synthesis of aminoethylglycyl PNA monomers

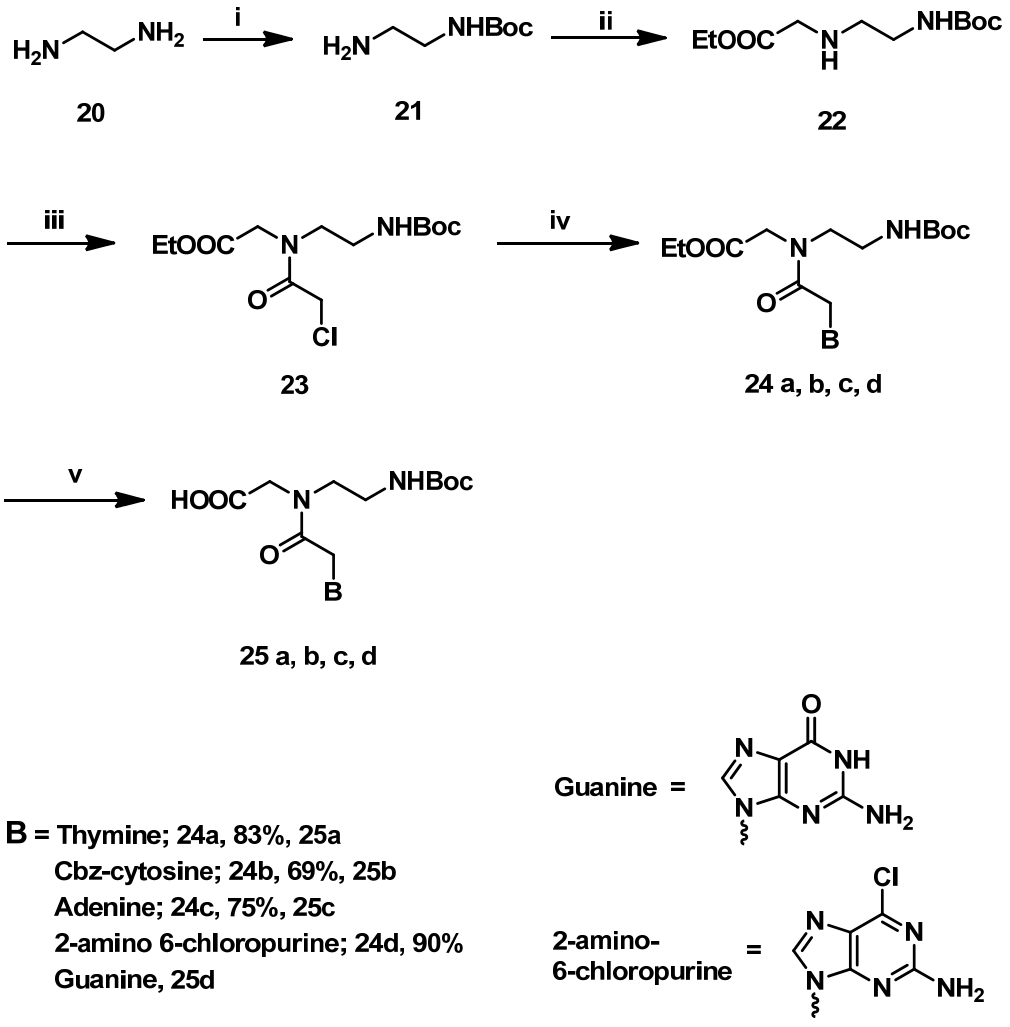

Reagents and condition: (i) $(Boc)_2O$, dioxane:H_2O, 63% (ii) ethyl bromoacetate, Et_3N, ACN, 83% (iii) $ClCH_2COCl$, Et_3N, DCM, 80% (iv) nucleobases (B), K_2CO_3, DMF, rt (v) 1N aq LiOH, THF

Thymine was reacted with ethyl *N*-(Boc-aminoethyl)-*N*-(chloroacetyl)-glycinate **23** using K_2CO_3 as a base to obtain the *N*-(Boc-aminoethylglycyl)-thymine ethyl ester **24a** in high yield. In the case of cytosine, the *N*4-amino group was protected as its benzyloxycarbonyl derivative, and used for alkylation employing K_2CO_3 as the base to provide the *N*1 substituted product **24b**. Although adenine is known to undergo both *N*7- and *N*9- substitution, *N*7-alkylation was not observed when K_2CO_3 was used as the base to get the product **24c**. The *N*-alkylation of 2-amino-6-chloropurine with ethyl *N*-(Boc-aminoethyl)-*N*-(chloroacetyl)-glycinate was facile with K_2CO_3 as the base and yielded the corresponding *N*-(Boc-aminoethylglycyl)-(2-amino-6-chloropurine)-ethyl ester **24d** in excellent yield. All compounds exhibited ^{1}H and ^{13}C NMR spectra consistent with the reported data.[18] The ethyl esters were hydrolyzed in the presence of LiOH to give the corresponding acids **(25a-d)**, which were further used for solid phase synthesis. The need for the exocyclic amino groups of adenine and guanine to be protected was eliminated, as these have been found to be unreactive under the conditions used for peptide coupling.

2.3 General principle of Solid Phase Peptide Synthesis (SPPS)

The solid phase peptide synthesis method introduced by Merrifield,[19] offers great advantages in contrast to solution phase method. The fundamental promise of this technique involves the incorporation of *N*-α-amino acids into a peptide of any desired sequence with one end of the sequence remaining attached to a solid support matrix. After the desired sequence of amino acids has been obtained, the peptide can be removed from the polymeric support (Figure 5). The solid support is a synthetic polymer that bears reactive groups such as $-NH_2$. These groups are made so that they can react easily with the carboxyl group of an *N*-α-protected amino acid, thereby covalently binding it to the polymer. The amino protecting group can then be removed and a second *N*-α-protected amino acid can be coupled to the attached amino acid. These steps are repeated until the desired sequence is obtained. At the end of the synthesis, a different reagent is applied to cleave the bond between the C-terminal amino acid and the polymer support; the peptide is then released into solution and can be obtained from the solution.

The advantage of the solid phase synthesis over the solution phase are (i) all the reactions are performed in a single vessel minimizing the loss due to transfer (ii) large excess of monomer carboxylic acid component can be used resulting in high coupling efficiency (iii) the excess soluble reagents can be removed from the peptide-solid support matrix by filtration and washed away at the end of each coupling step (iv) the method is amenable to automation and semi micro manipulation.

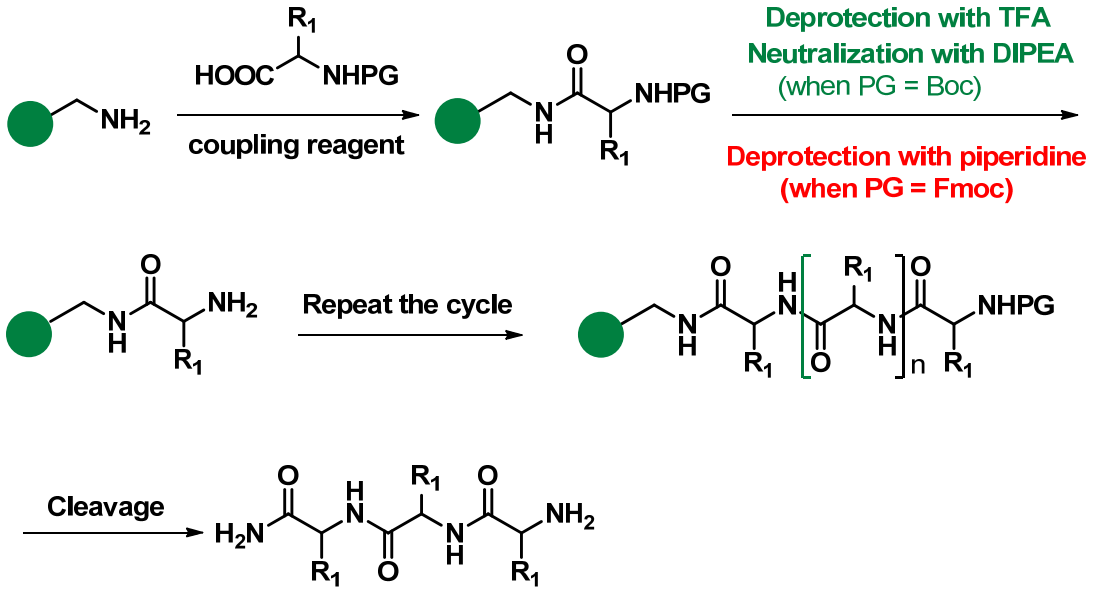

Figure 5: General protocol for solid phase peptide synthesis

Currently, two protocols are available for the routine synthesis of peptides by solid phase method (Figure 5).[20] First method involves the use of *t*-butyloxycarbonyl (*t*-Boc)[18,21] group as *N*-α-protection that is removed by acidic conditions such as 50% TFA in DCM. The reactive side chains of amino acids are protected with groups that are stable at *t*-Boc deprotection conditions and removable under strongly acidic conditions using HF in dimethyl sulfide or TFMSA in TFA. Alternatively a base labile protecting group strategy is used involving 9-fluorenylmethyloxycarbonyl (Fmoc)[22] group for *N*-α-protection, which is stable to acidic conditions but can be cleaved efficiently with a secondary base such as piperidine. In both protocols, the linker group that joins the peptide to the resin is chosen such that the side chain protecting groups and the linker are cleaved in one step at the end of the peptide synthesis.

2.3.1 General protocols for PNA synthesis

As in the case of solid phase peptide synthesis, PNA synthesis is also done conveniently from the C- terminus to the N- terminus. For this, the monomeric units must have their amino functions suitably protected, with their carboxylic acid functions free. Out of the two commonly used strategy *t*-butyloxycarbonyl (*t*-Boc) and the 9 flurorenylmethoxycarbonyl (Fmoc), the Boc- strategy was selected for the present work as Fmoc protection strategy is associated with acyl migration from the tertiary amide to the free amine formed during deprotection under basic (piperidine) conditions.[22,23]

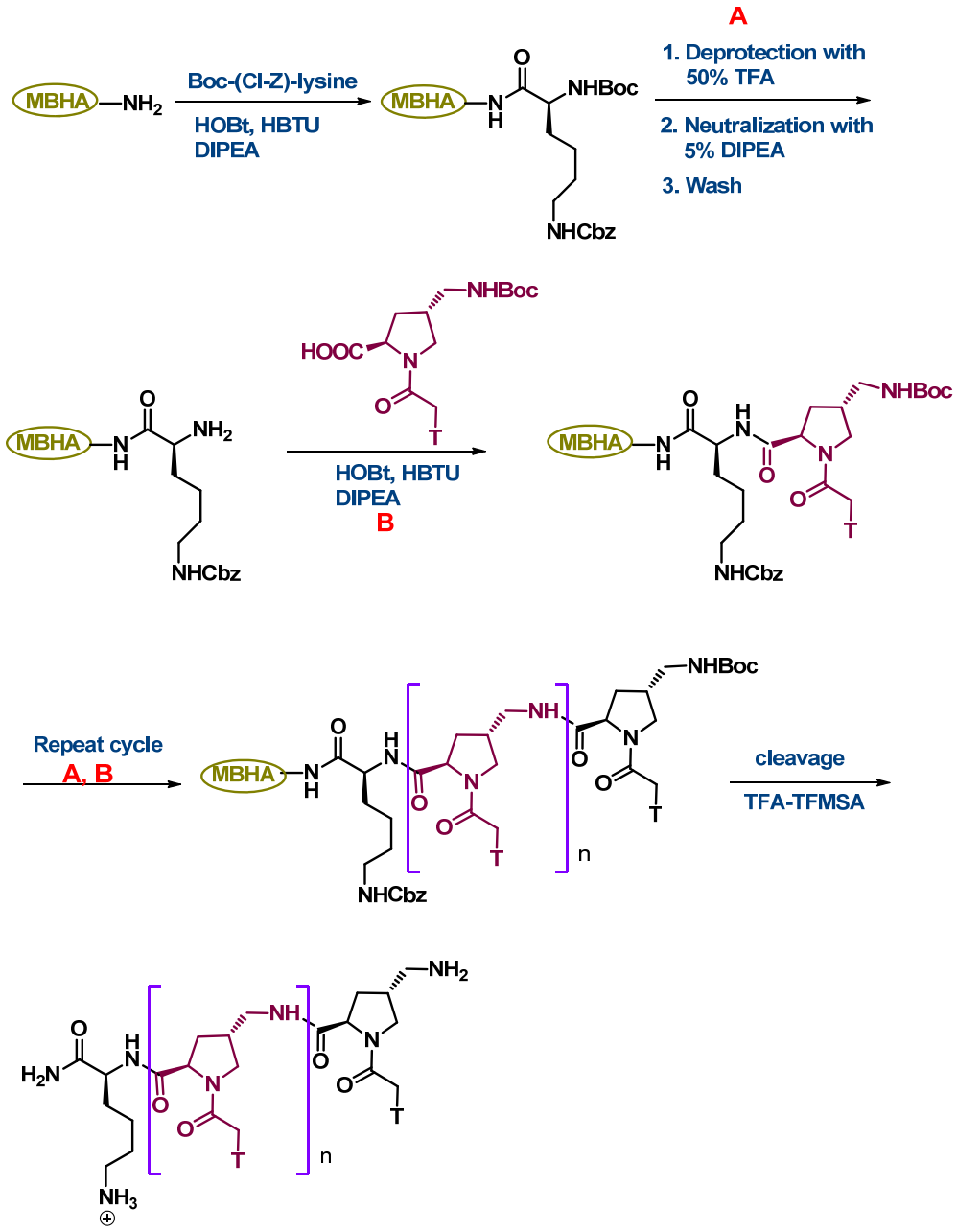

Figure 6: Protocol for PNA synthesis by *t*-Boc strategy

The amino function of the monomers was protected as the corresponding Boc-derivative and the carboxylic acid function was free to enable coupling with the resin-linked monomer. MBHA resin (4-methyl-benzhydryl amine resin) was used as the solid support on which the oligomers were built and the monomers were coupled by *in situ* activation with HBTU/HOBt (Figure 6). In the synthesis of all oligomers, orthogonally protected (Boc/Cl-Cbz) L-lysine was selected as the *C*-terminal spacer-amino acid and it is linked to the resin through amide bond. The introduction of charged groups, for instance a C-terminal lysine amide greatly improves the water solubility of the resulting oligomers. The amine content on the resin was determined by the picrate assay[24] and found to be 2.00 mmol/g and loading was suitably lowered to approximately 0.35 mmol/g by partial acetylation of amine content using calculated amount of acetic anhydride. Free $-NH_2$ on the resin available for coupling was again estimated before starting synthesis.

The PNA oligomers were synthesized using repetitive cycles, each comprising the following steps

Step 1: Deprotection of the *N*-Boc group using 50% TFA in CH_2Cl_2.

Step 2: Neutralization of the TFA salt formed with 5% DIPEA in DCM to liberate the free amine.

Step 3: Coupling of the free amine on the resin with the free carboxylic acid group of the added monomer using HBTU and HOBt as the coupling reagent.

2.3.2 Cleavage of the PNA oligomers from the solid support

The oligomers were cleaved from the solid support (L-lysine derivatized MBHA resin), using trifluoromethanesulphonic acid (TFMSA) in the presence of trifluoroacetic acid (TFA) (Low, High TFMSA-TFA method),[20] which yields oligomer having L-lysine-amide at their C-termini (Table 1). A cleavage time of 1.5-2 hrs at room temperature was found to be optimum. The side chain protecting groups were also cleaved during this cleavage process. After cleavage reaction, the oligomer was precipitated out by diethyl ether. Various oligomers synthesized in the present study are shown in Table 1.

Table 1: PNA sequences synthesized for the present study

S. No	Entry	PNA sequence
1	**PNA1**	H.TTTTTTTT-LysNH$_2$
2	**PNA2**	H.**t$_{SS}$** TTTTTTT-LysNH$_2$
3	**PNA3**	H.TTT **t$_{SS}$** TTTT-LysNH$_2$
4	**PNA4**	H.TTT **t$_{SS}$** TTT **t$_{SS}$**-LysNH$_2$
5	**PNA5**	H.TTTTTTT **t$_{SS}$**-LysNH$_2$
6	**PNA6**	H.**t$_{SR}$** TTTTTTT-LysNH$_2$
7	**PNA7**	H.TTT **t$_{SR}$** TTTT-LysNH$_2$
8	**PNA8**	H.TTT **t$_{SR}$** TTT **t$_{SR}$**-LysNH$_2$
9	**PNA9**	H.TTTTTTT **t$_{SR}$**-LysNH$_2$
		Mixed sequences
10	**PNA10**	H.T ATT ATT ATT-LysNH$_2$
11	**PNA11**	H.**t$_{SS}$** ATT ATT ATT-LysNH$_2$
12	**PNA12**	H.T ATT A**t$_{SS}$**T ATT-LysNH$_2$
13	**PNA13**	H.**t$_{SS}$** ATT A**t$_{SS}$**T ATT-LysNH$_2$
14	**PNA14**	H.T ATT ATT AT**t$_{SS}$**-LysNH$_2$
15	**PNA15**	H.**t$_{SR}$** ATT ATT ATT-LysNH$_2$
16	**PNA16**	H.T ATT A**t$_{SR}$**T ATT-LysNH$_2$
17	**PNA17**	H.**t$_{SR}$** ATT A**t$_{SR}$**T ATT-LysNH$_2$
18	**PNA18**	H.T ATT ATT AT**t$_{SR}$**-LysNH$_2$

A/T = *aeg*PNA Adenine/Thymine monomers,

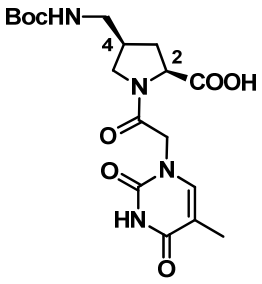

t_{SS} = (2*S*,4*S*)-backbone extended *proly*lPNA monomer

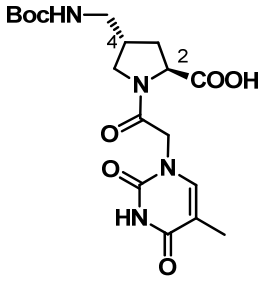

t_{SR} = (2*S*,4*R*)-backbone extended *proly*lPNA monomer

The synthesis of the oligomers incorporating the conformationally constrained chiral modified units **13** and **19** at specific positions in the *aeg*PNA oligomer was done on the solid support using the procedures described above. Polypyrimidine (thymine) octamers (**PNA1-PNA9**) are synthesized to study the effect of the two prolyl isomers (2*S*,4*S*) and (2*S*,4*R*), for their triplex forming ability. The mixed purine-pyrimidine oligomers (**PNA11-PNA18)** were synthesized for comparative studies with mixed *aeg*PNA (**PNA10**) oligomer.

2.3.3 Purification of the PNA oligomers

All the cleaved oligomers were subjected to initial gel filtration. The purity of the so obtained oligomers was checked by analytical HPLC (C18 column, CH_3CN-H_2O system), which shows more than 70-80% purity. These were subsequently purified by reverse phase HPLC on a semi preparative C18 column. The purity of the oligomers

was again ascertained by analytical RP-HPLC and their integrity was confirmed by MALDI-TOF mass spectrometric analysis (Figure 7-10).

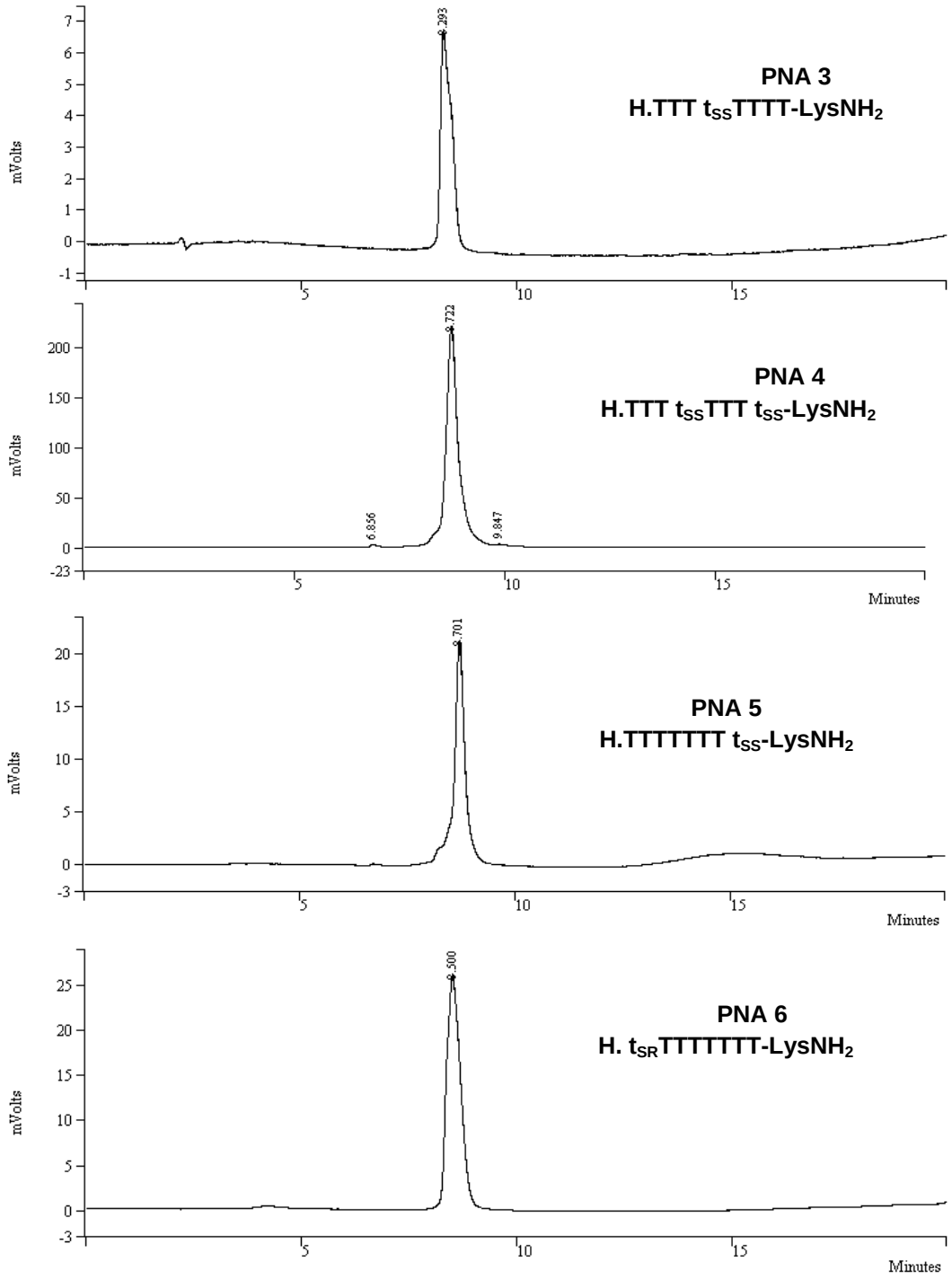

Figure 7: HPLC profile for **PNA3-PNA6**

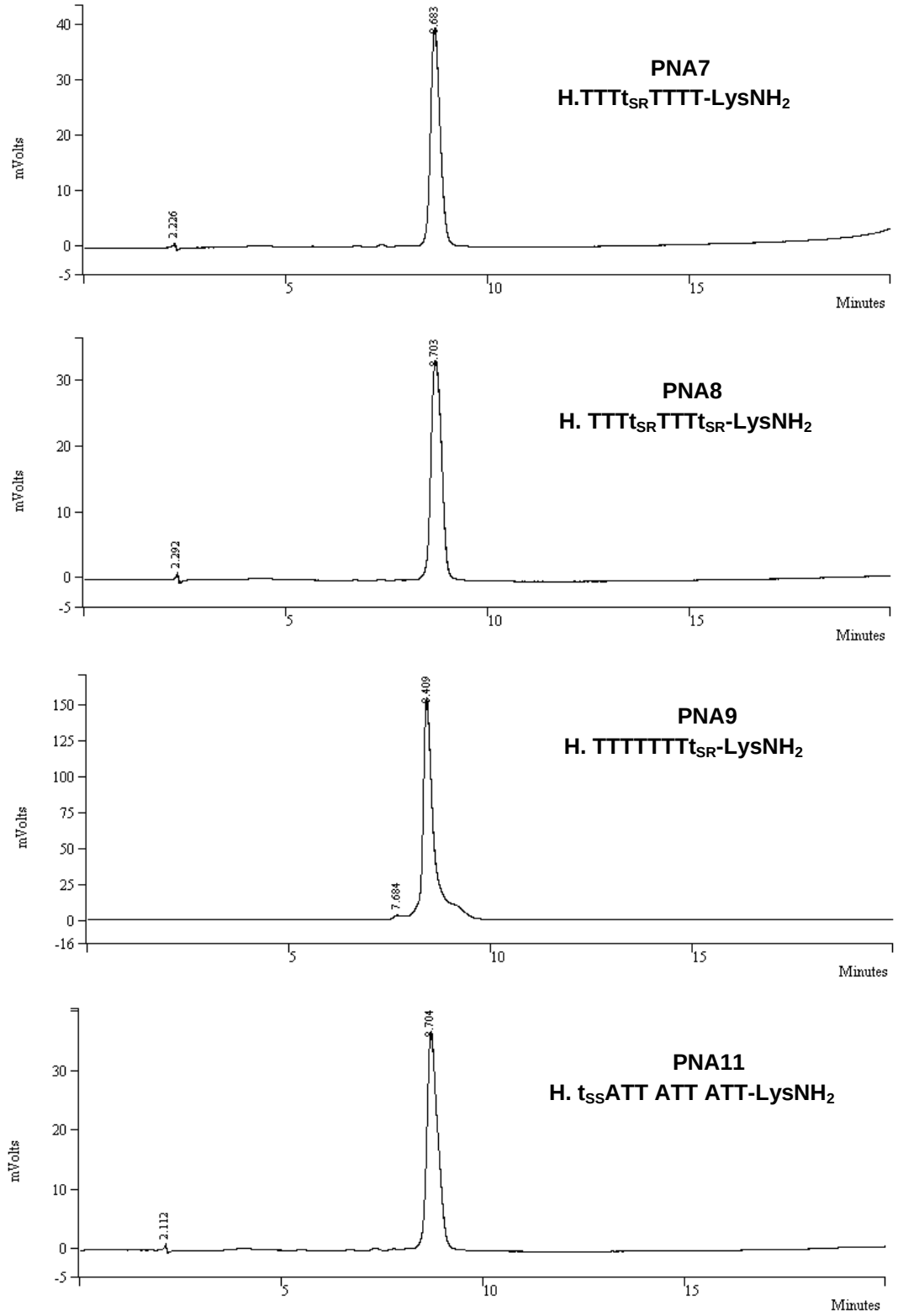

Figure 8: HPLC profile for **PNA7-PNA11**

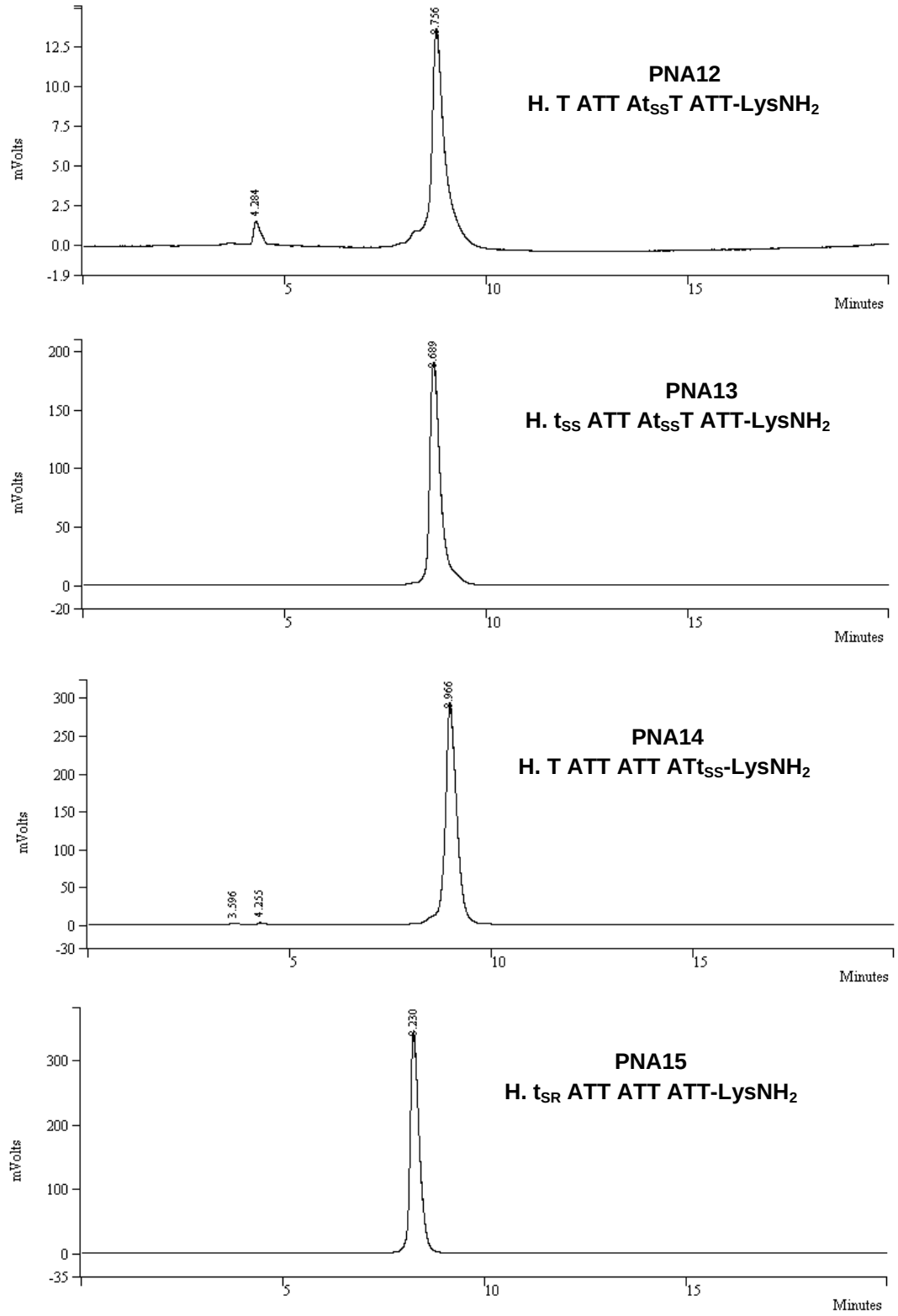

Figure 9: HPLC profile for **PNA12-PNA15**

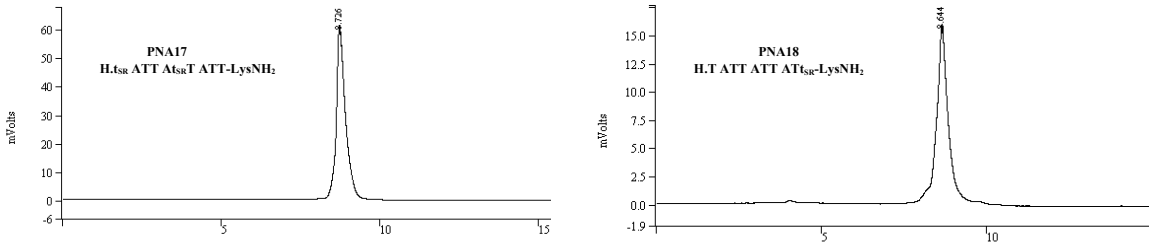

Figure 10: HPLC profile for **PNA17** and **PNA18**

The HPLC retention time of the synthesized oligomers is shown in Table 2. The observed molecular weight has been mentioned in the same Table along with the molecular formula of all the oligomers. The MALDI-TOF data for confirmation of the oligomers are shown later in the experimental section.

Table 2: HPLC and MALDI-TOF mass spectral analysis of modified PNAs.

S. No	PNA	HPLC R.T(min)	Mol. Formula	Calc. MW*	Obs. MW
1	**PNA1**	8.17	$C_{97}H_{130}N_{32}O_{33}$	2272.31	2296.67
2	**PNA2**	8.36	$C_{98}H_{131}N_{33}O_{33}$	2299.34	2300.90
3	**PNA3**	8.29	$C_{98}H_{131}N_{33}O_{33}$	2299.34	2298.37
4	**PNA4**	8.72	$C_{100}H_{133}N_{33}O_{33}$	2325.38	2326.89
5	**PNA5**	8.70	$C_{98}H_{131}N_{33}O_{33}$	2299.34	2297.32
6	**PNA6**	8.50	$C_{98}H_{131}N_{33}O_{33}$	2299.34	2300.46
7	**PNA7**	8.68	$C_{98}H_{131}N_{33}O_{33}$	2299.34	2323.19
8	**PNA8**	8.70	$C_{100}H_{133}N_{33}O_{33}$	2325.38	2324.11
9	**PNA9**	8.40	$C_{98}H_{131}N_{33}O_{33}$	2299.34	2300.30
10	**PNA10**	8.65	$C_{119}H_{155}H_{49}O_{35}$	2831.87	2830.87
11	**PNA11**	8.70	$C_{121}H_{157}N_{49}O_{35}$	2857.91	2859.66
12	**PNA12**	8.75	$C_{121}H_{157}N_{49}O_{35}$	2857.91	2857.96
13	**PNA13**	8.68	$C_{123}H_{159}N_{49}O_{35}$	2883.95	2886.51
14	**PNA14**	8.96	$C_{121}H_{157}N_{49}O_{35}$	2857.91	2859.90
15	**PNA15**	8.43	$C_{121}H_{157}N_{49}O_{35}$	2857.91	2860.05
16	**PNA16**	8.30	$C_{121}H_{157}N_{49}O_{35}$	2857.91	2861.99
17	**PNA17**	8.72	$C_{123}H_{159}N_{49}O_{35}$	2883.95	2884.71
18	**PNA18**	8.64	$C_{121}H_{157}N_{49}O_{35}$	2857.91	2862.59

*All the MW has been calculated by Chem Draw Ultra 8.0

2.3.4 Synthesis of complementary oligonucleotides

The DNA oligonucleotides **DNA1-DNA3** (Table 3) were synthesized on ABI 3900 High Throughput DNA Synthesizer using standard β-cyanoethyl phosphoramidite chemistry.[25] The oligomers were synthesized in the 3' to 5' direction on polystyrene

solid support, followed by ammonia treatment. The oligonucleotides were desalted by gel filtration, their purity ascertained by RP-HPLC on a C18 column to be more than 95% and were used for the biophysical studies of PNAs without further purification.

Table 3: DNA oligonucleotides used in the present work

S. No.	DNA	Sequence	Type
		Sequence 5' to 3'	
1	**DNA1**	CG AAAAAAAA GC	Match
2	**DNA2**	A TAA TAA TAA	Parallel
3	**DNA3**	AAT AAT AAT A	Antiparallel

2.4 Biophysical studies of PNA:DNA complexes

For the study of binding selectivity, specificity and discrimination of the modified PNA towards complementary DNA, the stoichiometry of the (2*S*,4*S*)- and (2*S*,4*R*)-PNA:DNA was first determined using Job's method.[26] The UV-melting studies were then carried out with all the synthesized oligomers and the T_m data was compared with the control *aeg*PNA. The stability of the (2*S*,4*S*)- and (2*S*,4*R*)-PNA duplexes with DNA was also studied. The CD spectra of single strands and corresponding complexes with complementary DNA were recorded.

2.4.1 CD Spectroscopy of (2*S*,4*S*)- and (2*S*,4*R*)-PNA:DNA complexes

The (2*S*,4*S*) and (2*S*,4*R*)-PNA single strand oligomers exhibited very low induced CD signals. The CD for single stranded (2*S*,4*S*) and (2*S*,4*R*)-PNA oligomers and their complex with complementary DNA (Figure 11) was recorded. The homopyrimidine PNA oligomers (**PNA2-PNA9**) when complexed with complementary **DNA1** show a very low induced CD with positive maxima at 257 and 285 nm, a negative minimum at 244 nm, and cross-over points at 235 and 247 nm. A positive band in the region of 255 to 260 nm as seen in the CD spectra of the complexes is characteristic of the *poly*(dA) [PNA-T_8]$_2$ complex[27] and confirms that homopyrimidine PNA oligomers (**PNA2-PNA9**) bind to **DNA1** in 2:1 stoichiometry i.e. PNA_2:DNA, which was further confirmed by Job's method. Similarly CD spectra have been recorded for the single stranded mixed purine/pyrimidine sequences (**PNA11-PNA18)** and for the complexes with complementary **DNA3** for the antiparallel binding mode.

These spectra show a positive maxima in between 260 to 270 nm and a negative maxima at 242 to 250 nm with cross-over points at 238 and 255 nm. The binding stoichiometry for these complexes will further be confirmed by Job's plot.

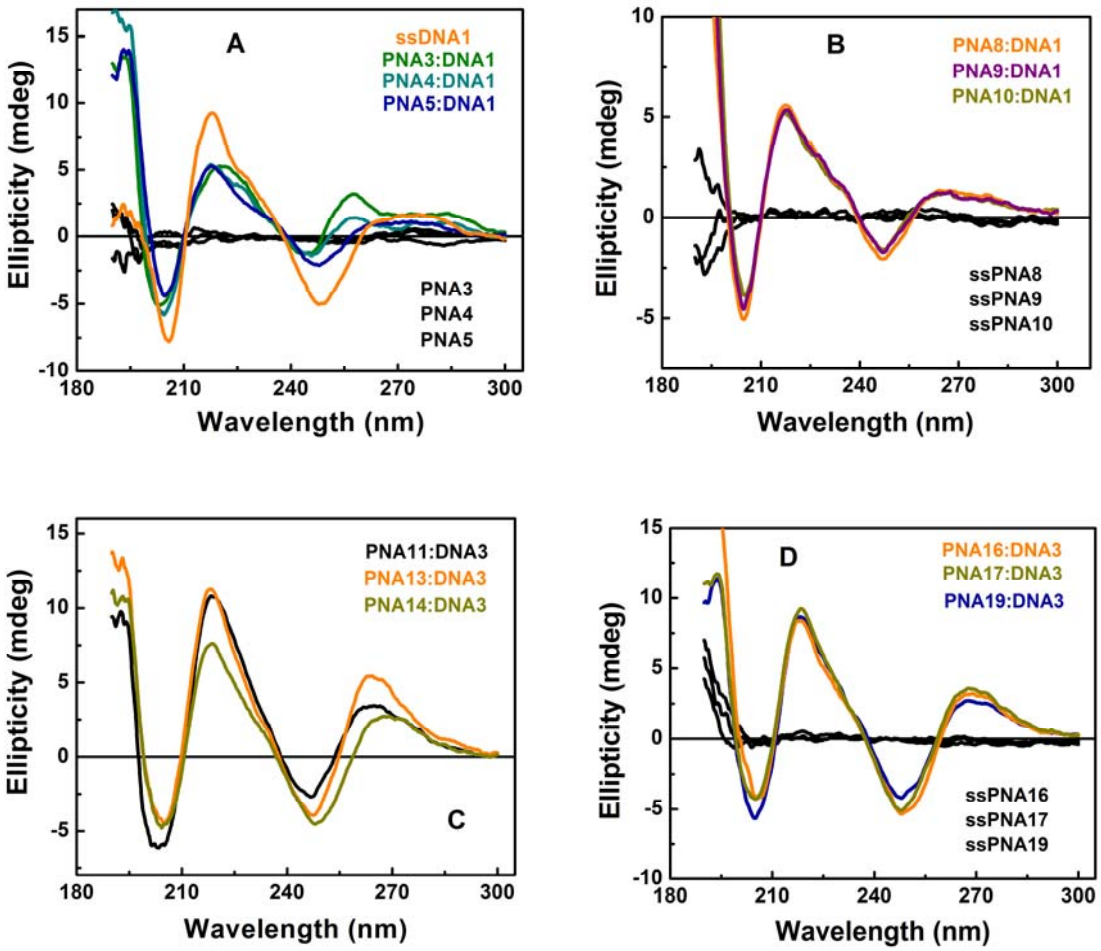

Figure 11: CD patterns for single stranded and hybridized **PNA2-PNA18** with complementary DNAs

2.4.2 Binding stoichiometry: CD-mixing curves

Circular dichroism (CD) measurement is useful to determine the stoichiometry of duplexes and triplexes. The stoichiometry of the paired strands may be obtained from the isodichroic point of mixing curves (Figure 12), in which the optical property at a given wavelength is plotted as a function of the mole fractions of each stand (Job's plot).[26] CD-Job's plot was performed to determine the binding stoichiometry of PNA:DNA. Similarly the binding stoichiometry can be determined by UV spectroscopy measurement at a particular wavelength by plotting absorbance vs mole fractions. In

both the cases the discontinuation point is known as the binding stoichiometry of DNA:PNA.

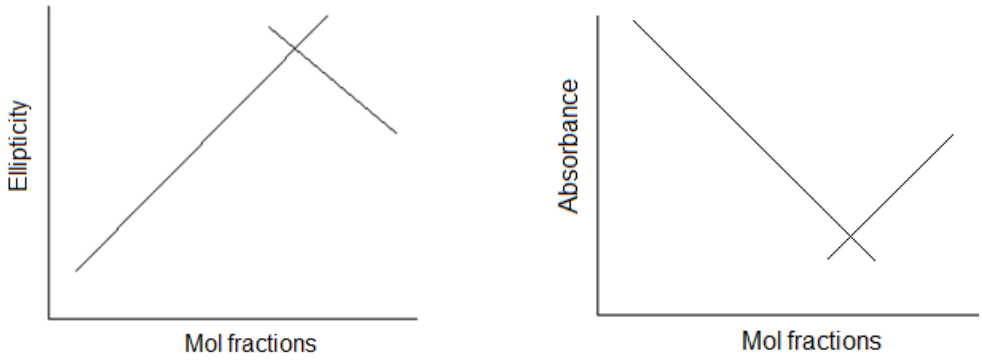

Figure 12: CD and UV mixing showing PNA:DNA binding stoichiometry

The CD mixing experiments were carried out by mixing the appropriate oligomers in different molar ratios keeping the total concentration constant. In this experiment, the ellipticity of different molar ratios (100:0, 90:10, 80:20, 70:30, 60:40, 50:50 to 0:100) of **PNA4:DNA1, PNA8:DNA1** and **PNA13:DNA3** complexes were recorded at 256 nm by maintaining the total concentration constant (Figure 13 and Figure 14).

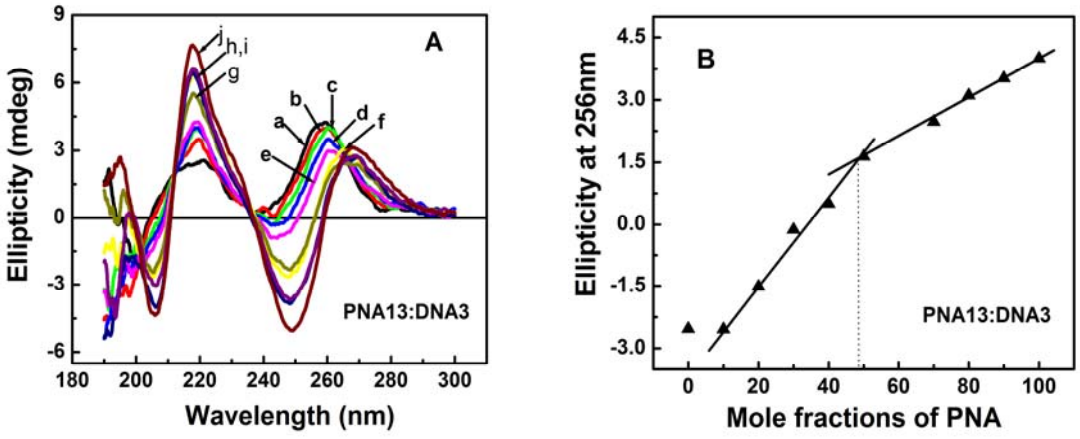

Figure 13: (A) CD-curves for (2*S*,4*S*)-**PNA13** and the complementary **DNA3** in molar ratios of (a)100:0 (b) 90:10 (c) 80:20 (d) 70:30 (e) 60:40 (f) 50:50 (g) 40:60 (h) 30:70 (i) 20:80 (j) 10:90 (k) 0:100 (Buffer, 10 mM Sodium phosphate pH 7.4, 100 mM NaCl) (B) CD-Job's plot corresponding to 256 nm for (2*S*,4*S*)-**PNA13**

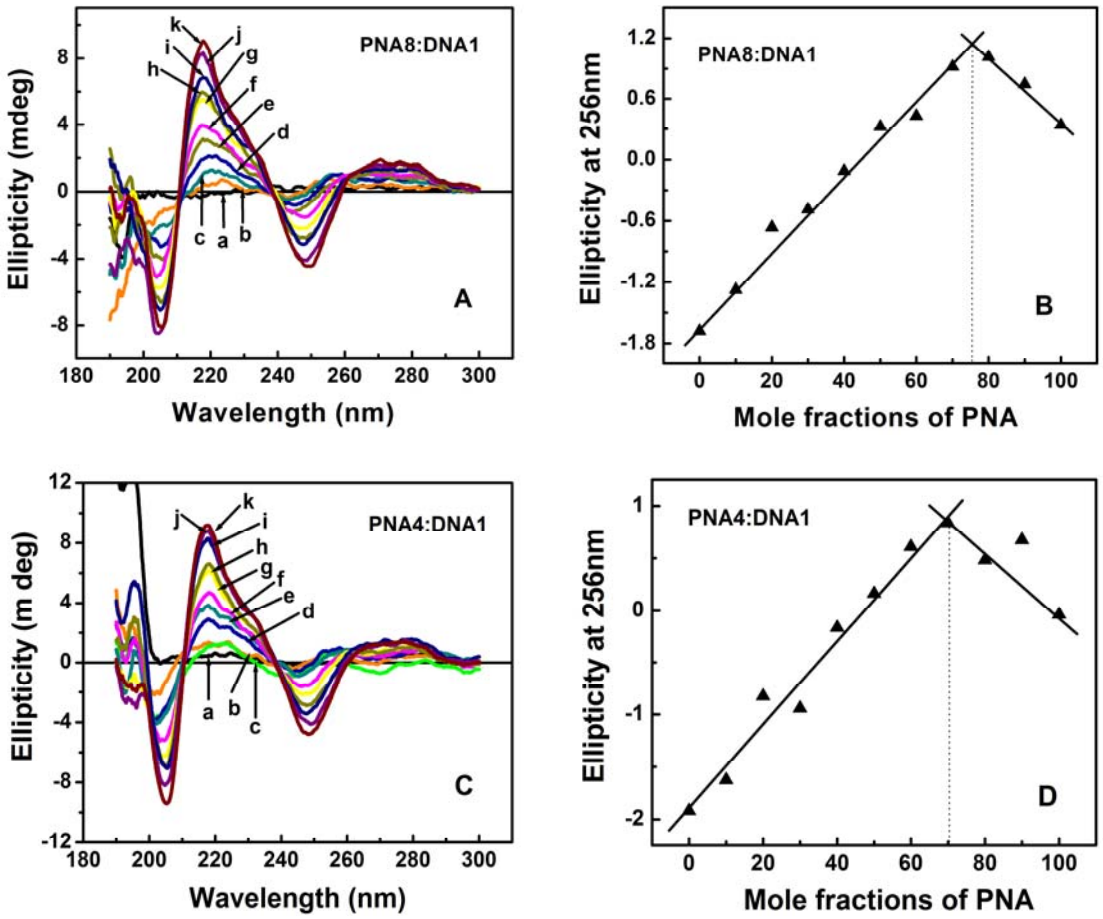

Figure 14: CD curves for (A) (2*S*,4*R*)-**PNA8** and (C) (2*S*,4*S*)-**PNA4** with complementary **DNA1,** d(CGA$_8$GC) in molar ratios of (a)100:0 (b) 90:10 (c) 80:20 (d) 70:30 (e) 60:40 (f) 50:50 (g) 40:60 (h) 30:70 (i) 20:80 (j) 10:90 (k) 0:100 (Buffer, 10 mM Sodium phosphate pH 7.4, 100 mM NaCl); (B) and (D) are CD-Job's plot at 256 nm for corresponding (2*S*,4*R*)-**PNA8** and (2*S*,4*S*)-**PNA4** respectively

The profile showed a breakpoint around 2:1 stoichiometry for homopyrimidine **PNA4:DNA1** and **PNA8:DNA1** complexes at wavelength 256 nm, confirming the formation of PNA$_2$:DNA triplex (Figure 14) and 1:1 stoichiometry was observed for purine-pyrimidine mixed base **PNA13:DNA3** complex which confirms the formation of a PNA:DNA duplex (Figure 13).

2.4.3 UV-Spectroscopy

Monitoring the UV absorption at 260 nm as a function of temperature has been extensively used to study the thermal stability of nucleic acid system and consequently, PNA:DNA/RNA hybrids as well. Increasing temperature perturbs this system, inducing

a structural transition by causing disruption of hydrogen bonds between the base pairs, diminished stacking between adjacent nucleobases and larger torsional motions in the backbone leading to a loss of secondary and tertiary structure. This is evidenced by an increase in the UV absorption at 260 nm, termed as hyperchromicity. The DNA melting is readily monitored by measuring its absorbance at a wavelength of 260 nm. A plot of absorbance vs temperature gives a sigmoidal curve in case of duplexes/triplexes and midpoint of transition gives the T_m (Figure 15).

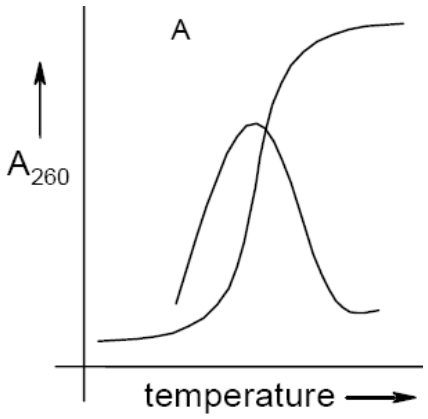

Figure 15: Melting curve of PNA/DNA

In case of triplexes, the first dissociation leads to the duplex (Watson-Crick duplex) and the third strand (Hoogsteen strand) followed by duplex dissociation at higher temperature into two single strands.[28] The DNA triplex melting shows a characteristic double sigmoidal transition with separate melting temperature for each transition. A non-sigmoidal (e.g. linear) transition with low hyperchromicity is a consequence of non-duplexation (non-complementation). In many cases, the transitions are broad and the exact T_ms are obtained from the peak in the first derivative plots. This technique has provided valuable information regarding complementary interactions in nucleic acid hybrids involving DNA, RNA and PNA.

Results and Discussion

The hybridization studies of modified PNAs with complementary **DNA1** were done by temperature dependent UV-absorbance experiments. The stoichiometry of PNA:DNA complexation as established by CD mixing data at 256 nm (Job's plot), for homopyrimidine was 2:1 ratio and for purine-pyrmidine mixed bases was 1:1 ratio

(Figure 13 and 14). The thermal stabilities (T_m) of PNA_2:DNA triplexes were obtained for different PNA modifications with complementary **DNA1** (Figure 16, Table 4) and PNA: DNA duplexes with complementary **DNA2** and **DNA3** (Figure 17, Table 5).

Thermal stability of triplexes: Unlike DNA triplexes, which show two distinct transitions corresponding to triplex to duplex melting and later duplex to single strands melting, (2*S*,4*S*)- and (2*S*,4*R*)-PNA_2:DNA triplexes show single transition similar to *aeg*PNA_2:DNA triplex melting.

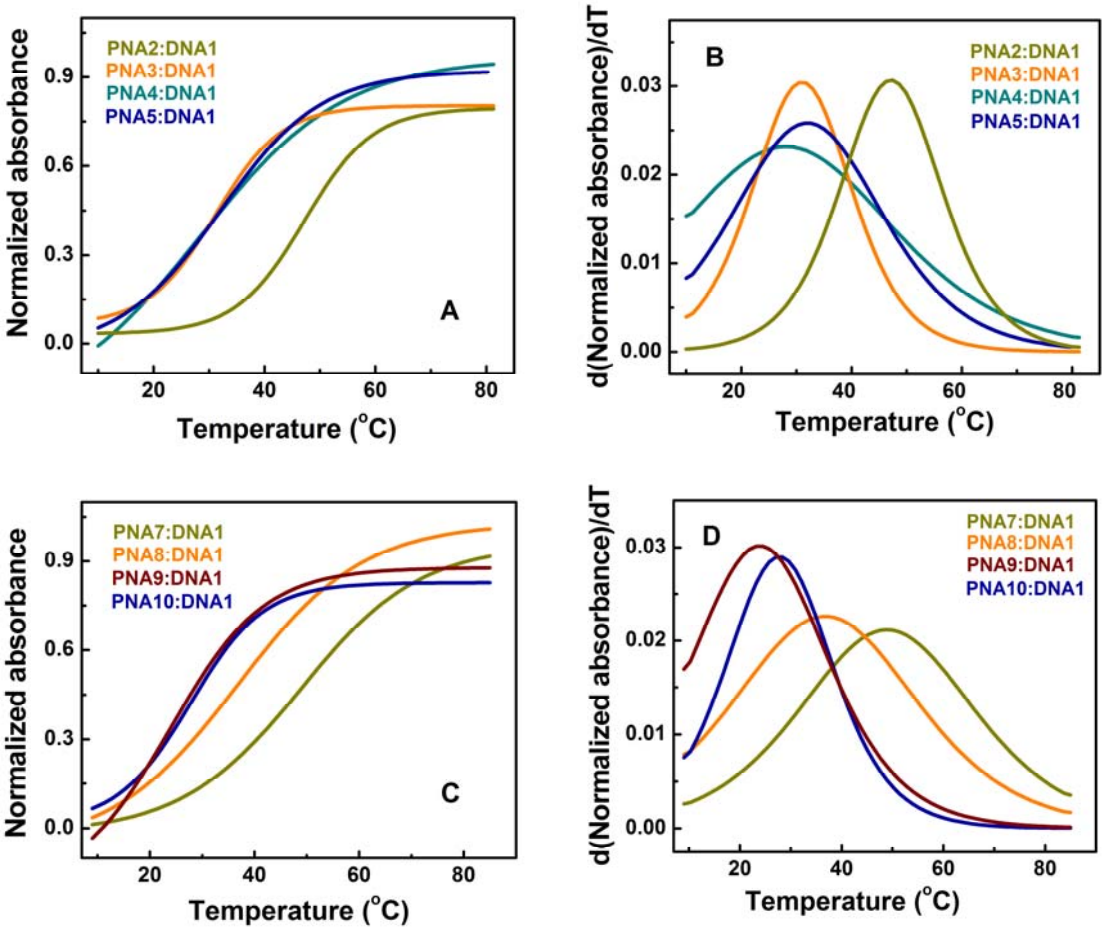

Figure 16: Melting curves for homopyrimidine PNAs (**PNA2-PNA10**) complexed with **DNA1** (CGA_8GC) (10 mM sodium phosphate buffer, pH=7.4, 100 mM NaCl)

Table 4: UV-T_m values for homopyrimidine oligomers

S. No.	Entry	Triplex (PNA_2:DNA)	UV-T_m(°C) PNA_2:cDNA	ΔT_m (°C)
1	**PNA1** **DNA1** **PNA1**	H_2NLys-TTTTTTTT.H 5'CGAAAAAAAA3' H.TTTTTTTT-LysNH_2	45.0	--
2	**PNA2** **DNA1** **PNA2**	H_2NLys-TTTTTTT**t**$_{SS}$.H 5'CGAAAAAAAA3' H.**t**$_{SS}$TTTTTTT-LysNH_2	47.4	+2.4
3	**PNA3** **DNA1** **PNA3**	H_2NLys-TTTT**t**$_{SS}$TTT.H 5' CGAAAAAAAAGC 3' H.TTT**t**$_{SS}$TTTT-LysNH_2	30.5	-14.5
4	**PNA4** **DNA1** **PNA4**	H_2NLys-**t**$_{SS}$TTT**t**$_{SS}$TTT.H 5' CGAAAAAAAAGC 3' H.TTT**t**$_{SS}$TTT**t**$_{SS}$-LysNH_2	28.1	-16.9
5	**PNA5** **DNA1** **PNA5**	H_2NLys-**t**$_{SS}$TTTTTTTH 5' CGAAAAAAAAGC 3' H.TTTTTTT**t**$_{SS}$-LysNH_2	31.4	-13.6
6	**PNA6** **DNA1** **PNA6**	H_2NLys-TTTTTTT**t**$_{SR}$.H 5' CGAAAAAAAAGC 3' H.**t**$_{SR}$TTTTTTT-LysNH_2	48.9	+3.9
7	**PNA7** **DNA1** **PNA7**	H_2NLys-TTTT**t**$_{SR}$TTT.H 5' CGAAAAAAAAGC 3' H.TTT**t**$_{SR}$TTTT-LysNH_2	37.3	-7.7
8	**PNA8** **DNA1** **PNA8**	H_2NLys-**t**$_{SR}$TTT**t**$_{SR}$TTT.H 5' CGAAAAAAAAGC 3' H.TTT**t**$_{SR}$TTT**t**$_{SR}$-LysNH_2	24.4	-20.6
9	**PNA9** **DNA1** **PNA9**	H_2NLys-**t**$_{SR}$TTTTTTT.H 5' CGAAAAAAAAGC 3' H.TTTTTTT**t**$_{SR}$-LysNH_2	28.3	-16.7

All values are an average of at least 3 experiments and accurate within ± 0.5°C, Buffer: Sodium phosphate (10 mM), and 100 mM NaCl, pH 7.4

The stabilities of PNA:DNA complexes differed depending upon the stereochemistry, position and the number of the modified units introduced in *aeg*PNA (**PNA1**, entry1). UV-melting profiles of all the homopyrimidine sequences (**PNA2-PNA9**, entry 2-9) are shown in Figure 16. The T_m data observed for the homopyrimidine (2*S*,4*S*) and (2*S*,4*R*)-PNA:DNA complexes is summarized in Table 4. The N-terminus modification in homopyrimidine *aeg*PNA with (2*S*,4*S*)- and (2*S*,4*R*)-

modified PNA (**PNA2** and **PNA6,** entry 2 and 6) unit shows stabilization towards DNA binding by 2.4°C and 3.9°C respectively compared to unmodified *aeg*PNA. The middle modification in *aeg*PNA oligomers with both (2*S,*4*S*)- and (2*S,*4*R*)- isomer (**PNA3** and **PNA7**, entry 3 and 7) separately decreases the UV melting temperature (T_m) by 14.5°C and 7.7°C respectively, indicating destabilization towards DNA binding. Similarly C-terminus single modification of the oligomer shows destabilization in complementary DNA binding by 13.6°C and 16.7°C for (2*S,*4*S*)- and (2*S,*4*R*)- isomers (**PNA5** and **PNA9**, entry 5 and 9) respectively.

Incorporation of two modified units, one at C-terminus and the other at the middle of the *aeg*PNA oligomer destabilizes for both the isomer (2*S,*4*S*)- and (2*S,*4*R*)- more than all other single modifications (**PNA4** and **PNA8**, entry 4 and 8). The decrease in stability for the backbone modified PNA:DNA hybrids, compared to that of the unmodified hybrids, is ascribed to geometric constraints in the PNA or a larger loss in entropy upon complex formation. In the case of middle modification the destabilization of PNA:DNA binding is pronounced in (2*S,*4*S*)- isomer compared to (2*S,*4*R*)- isomer.

Thermal stability of duplexes: To study the effect of modified PNA monomers on corresponding duplexes, the mixed sequence decamer PNAs (Table 5, **PNA10-18)** incorporating thymine monomer of either the (2*S,*4*S*)-backbone extended *prolyl*PNA or (2*S,*4*R*)-backbone extended *prolyl*PNA unit at different positions of *aeg***PNA10** decamer were synthesized.

The T_m values of various PNAs hybridized with complementary DNA for parallel and antiparallel bindings were determined from temperature dependent UV absorbance summarized in Table 5 (Figure 17) and the binding stoichiometry was determined by CD Job's plot (Figure 13). This showed 1:1 binding as expected for a duplex. In the case of (2*S,*4*S*)- isomer the N-terminus modification (**PNA11,** entry 3) for mixed purine-pyrimidine PNA oligomer shows 10°C stabilization in antiparallel binding to the complementary DNA. Interestingly the same oligomer does not bind to the complementary DNA in parallel mode (Table 5, entry 4). Similarly N-terminus modification of (2*S,*4*R*)- isomer (**PNA15,** entry 11) stabilizes the cDNA binding by 4.5°C in antiparallel orientation and does not bind in parallel mode.

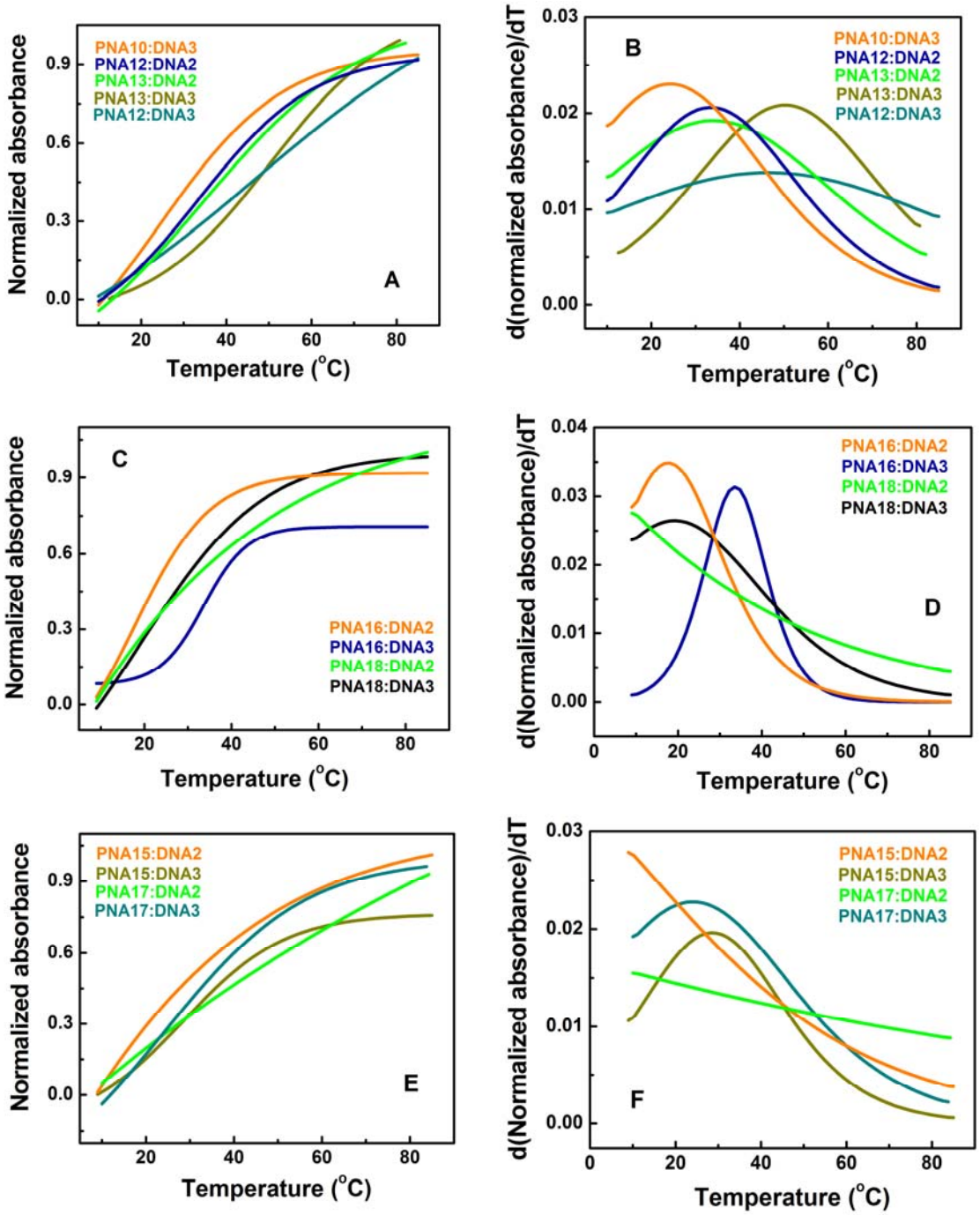

Figure 17: Melting curves for purine-pyrimidine mixed PNAs (**PNA10-PNA18**) complexed with **DNA2 (**5' ATAATAATAA 3') and **DNA3** (5' AATAATAATA 3') and the corresponding first derivative curves. (10mM sodium phosphate buffer, pH=7.4, 100 mM NaCl)

Table 5: UV-T_m values for mixed purine-pyrimidine oligomers

S. No	Entry	PNA:DNA duplex	Binding orientation	UV- Tm	ΔTm
1	**PNA10** **DNA3**	H. T ATT ATT ATT-LysNH$_2$ 5’ AAT AAT AAT A 3’	antiparallel	23.9	----
2	**PNA10** **DNA2**	H. T ATT ATT ATT-LysNH$_2$ 5’ A TAA TAA TAA 3’	parallel	10.2	----
3	**PNA11** **DNA3**	H. **t$_{SS}$** ATT ATT ATT-LysNH$_2$ 5’ AAT AAT AAT A 3’	antiparallel	33.9	+10.0
4	**PNA11** **DNA2**	H. **t$_{SS}$** ATT ATT ATT-LysNH$_2$ 5’ A TAA TAA TAA 3’	parallel	NB[a]	NA[b]
5	**PNA12** **DNA3**	H.T ATT A**t$_{SS}$**T ATT-LysNH$_2$ 5’ AAT AAT AAT A 3’	antiparallel	48.1	+25.2
6	**PNA12** **DNA2**	H.T ATT A**t$_{SS}$**T ATT-LysNH$_2$ 5’ A TAA TAA TAA 3’	parallel	34.1	+23.9
7	**PNA13** **DNA3**	H. **t$_{SS}$** ATT A**t$_{SS}$**T ATT-LysNH$_2$ 5’ AAT AAT AAT A 3’	antiparallel	50.6	+26.7
8	**PNA13** **DNA2**	H. **t$_{SS}$** ATT A**t$_{SS}$**T ATT-LysNH$_2$ 5’ A TAA TAA TAA 3’	parallel	34.4	+24.2
9	**PNA14** **DNA3**	H.T ATT ATT AT**t$_{SS}$**-LysNH$_2$ 5’ AAT AAT AAT A 3’	antiparallel	NB	NA
10	**PNA14** **DNA2**	H.T ATT ATT AT**t$_{SS}$**-LysNH$_2$ 5’ A TAA TAA TAA 3’	parallel	NB	NA
11	**PNA15** **DNA3**	H. **t$_{SR}$** ATT ATT ATT-LysNH$_2$ 5’ AAT AAT AAT A 3’	antiparallel	28.4	+4.5
12	**PNA15** **DNA2**	H. **t$_{SR}$** ATT ATT ATT-LysNH$_2$ 5’ A TAA TAA TAA 3’	parallel	NB	NA
13	**PNA16** **DNA3**	H.T ATT A**t$_{SR}$**T ATT-LysNH$_2$ 5’ AAT AAT AAT A 3’	antiparallel	33.4	+9.5
14	**PNA16** **DNA2**	H.T ATT A**t$_{SR}$**T ATT-LysNH$_2$ 5’ A TAA TAA TAA 3’	parallel	18.0	+7.8
15	**PNA17** **DNA3**	H. **t$_{SR}$** ATT A**t$_{SR}$**T ATT-LysNH$_2$ 5’ AAT AAT AAT A 3’	antiparallel	23.7	-0.2
16	**PNA17** **DNA2**	H. **t$_{SR}$** ATT A**t$_{SR}$**T ATT-LysNH$_2$ 5’ A TAA TAA TAA 3’	parallel	NB	NA
17	**PNA18** **DNA3**	H. T ATT ATT AT**t$_{SR}$**-LysNH$_2$ 5’ AAT AAT AAT A 3’	antiparallel	19.3	-4.6
18	**PNA18** **DNA2**	H. T ATT ATT AT**t$_{SR}$**-LysNH$_2$ 5’ A TAA TAA TAA 3’	parallel	NB	NA

[a]NB indicates non-binding to complementary DNA and [b]NA indicates not-applicable

Middle modification for (2*S*,4*S*) isomer (**PNA12,** entry 5, 6) shows stabilization of 25.2°C in antiparallel and 23.9°C in parallel mode. For (2*S*,4*R*) isomer stabilization is 9.5°C and 7.8°C for antiparallel and parallel binding respectively (Table 5, entry 13, 14), for middle modification (**PNA16)** as compared to the *aeg*PNA (**PNA10**). The C-terminus modification of (2*S*,4*S*) isomer (**PNA14,** entry 9, 10) does not bind to the complementary DNA both in parallel and antiparallel orientation. Although (2*S*,4*R*) isomer shows destabilization of 4.6°C towards antiparallel (**PNA18,** entry 17) binding, it does not bind to the complementary DNA in parallel mode (**PNA18**, entry 18). Incorporation of two units of (2*S*,4*S*)- isomer (**PNA13,** entry 7, 8) to *aeg***PNA10** shows a considerable increase of T_m values than the control *aeg*PNA. This double modification shows 26.7°C and 24.2°C increase in T_m for antiparallel and parallel binding respectively. But in case of (2*S*,4*R*)-isomer double modification of the PNA oligomer (**PNA17**, entry 15, 16) binds to complementary DNA by equal affinity as in *aeg*PNA in antiparallel mode and does not bind in parallel mode.

In the following section all the melting data have been compared for modified homopyrimidine and mixed purine-pyrimidine oligomers with unmodified *aeg*PNA oligomer (Figure 18, 19).

2.5 Comparison of (2*S*,4*S*)- and (2*S*,4*R*)- backbone extended *prolyl*PNA with *aeg*PNA oligomers

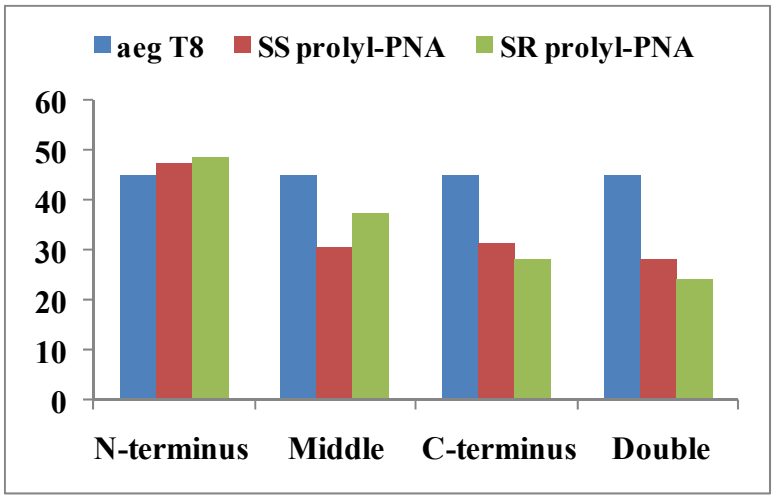

Figure 18: Bar diagram for comparison of homopyrimidine (2*S*,4*S*)- and (2*S*,4*R*)- modified *prolyl*PNA oligomers with unmodified homothymine octameric *aeg*PNA oligomer.

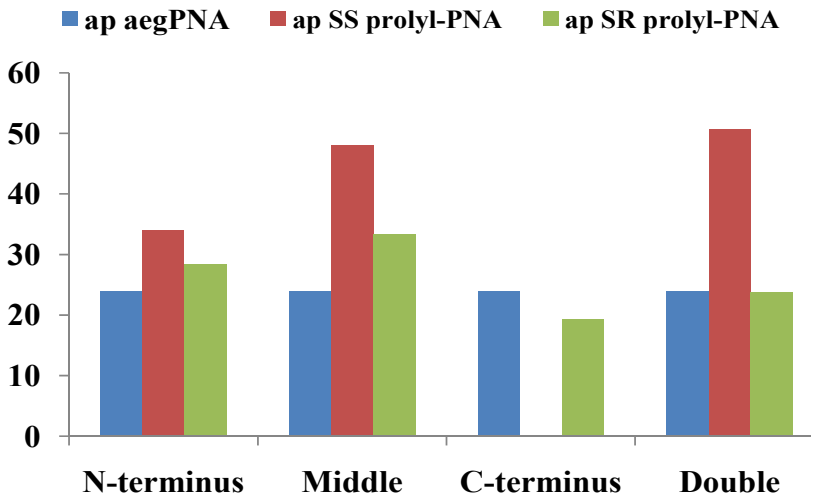

Figure 19: Bar diagram for comparison of mixed purine-pyrimidine (2*S*,4*S*) and (2*S*,4*R*) modified *prolyl*PNA oligomers with unmodified mixed *aeg*PNA oligomer.(ap indicates antiparallel)

2.6 Comparison of UV-T_m of backbone extended *prolyl* PNAs wth *ap*PNA and *apg*PNA

Introduction of a single unit of *apg*T (**VI**, Figure 4) which was reported earlier by Nielsen et al. with extended backbone was placed in the middle of a homopyrimidine PNA decamer. It caused a decrease in T_m by 11°C, relative to the corresponding unmodified PNA:DNA hybrids. It was now observed that the middle modification in *aeg*PNA T_8 oligomer independently with (2*S*,4*S*) and (2*S*,4*R*)-isomer decreases the UV melting temperature (T_m) by 14.5°C and 7.7°C respectively, indicating destabilization towards DNA binding, destabilization being more in case of (2*S*,4*S*)-isomer than the (2*S*,4*R*)-isomer. Hence it can be concluded that the (2*S*,4*R*)-isomer is better stabilizing than the *apg*PNA monomer and conversely (2*S*,4*S*)-isomer is having a lower binding ability towards complementary DNA compared to *apg*PNA oligomer. The N-terminus modification of *ap*PNA (**V,** Figure 4) in mixed purine pyrimidine sequence stabilize the complementary DNA binding by 10-15°C. The (2*S*,4*S*) isomer the *N*-terminus modification in mixed purine-pyrimidine PNA oligomer shows 10°C stabilization in antiparallel binding mode to the complementary DNA binding, which is found to be equal as the *ap*PNA mixed oligomer. Although the N-

terminus modification of (2*S*,4*R*) isomer stabilizes (ΔT_m= + 4.5°C) the complementary DNA binding, it is lower than the *ap*PNA as well as for the (2*S*,4*S*)-*prolyl* isomer.

2.7 Conclusions

A method was developed successfully for the synthesis of (2*S*,4*S*)- and (2*S*,4*R*)-backbone extended *prolyl*PNA monomer. The modified oligomers corresponding to both *prolyl*PNA monomers were synthesized by SPPS method using HOBt/HBTU/DIEA as the coupling reagent. Pure oligomers obtained after cleavage from solid support were purified by RP-HPLC and subjected for temperature dependent UV and CD spectroscopic studies. The binding stoichiometry was determined from Job's plot which was found to be 2:1 and 1:1 for homopyrimidine and mixed purine-pyrimidine sequences respectively.

The temperature dependent UV experiment shows a stabilization of 3.9°C and 2.4°C towards complementary DNA binding for N-terminal homopyrimidine oligomer synthesized from (2*S*,4*R*)-backbone extended *prolyl*PNA (**PNA6**) and (2*S*,4*S*)-backbone extended *prolyl*PNA (**PNA2**) monomer respectively. All the other homopyrimidine sequences (**PNA3-PNA5** and **PNA7-PNA9**) synthesized from both the isomers destabilize the complementary DNA binding showing a maximum destabilization for double modified (**PNA4** and **PNA8**) oligomers.

The N-terminus (**PNA11**), middle (**PNA12**) and bi modification (**PNA13**) for mixed purine-pyrimidine oligomers derived from (2*S*,4*S*)-isomer stabilizes the complementary DNA binding by 10°C, 25°C and 26°C respectively for antiparallel binding orientation. But C-terminus modification for (2*S*,4*S*)-isomer (**PNA14**) for the same isomer does not bind to complementary antiparallel DNA oligomer.

Mixed oligomers containing (2*S*,4*R*)-isomer at the *N*-terminus (**PNA15**) and middle modification (**PNA16**) show a stabilization by 4.5°C and 9.5°C respectively in antiparallel mode. Double modification for (2*S*,4*R*)- isomer (**PNA17**) shows an equal binding affinity as the unmodified PNA oligomer and the C-terminus modification (**PNA18**) destabilizes by 4.6°C towards the complementary antiparallel DNA binding.

2.8 Experimental

General remarks: ^{1}H and ^{13}C NMR spectra were recorded on 200 MHz and 50 MHz respectively. Chemical shifts are given in δ (ppm) scale. Mass spectra were obtained by LCMS techniques. Melting points of samples were determined in open capillary tubes and are uncorrected. TLC was performed using TLC aluminium sheets precoated with silicagel $60F_{254}$ (Merck). Silica gel 60-120 and 100-200 mesh was used for column chromatography using ethyl acetate/petroleum ether and dichloromethane/methanol mixture as elution solvent depending upon the compound polarity and chemical nature. Commercial reagents were generally used as received. Solvents used in organic reactions were distilled under an inert atmosphere. Unless otherwise noted, all reactions were carried out at room temperature. Oligomers were characterized by RP HPLC, using C18 column and MALDI-TOF mass spectrometry. For all the MALDI-TOF spectra α-cyano-4-hydroxy cinnamic acid was used as the matrix for PNA oligomers. All CD spectra shown are the average of at least 5 scans, recorded at 10°C with wavelength scanned from 190-300 nm. The cells had optical path length of 1cm and all samples were constituted in 10 mM sodium phosphate buffer (pH = 7.4) containing 100 mM NaCl.

(2*S*,4*R*)-4-hydroxyproline methyl ester hydrochloride (2)

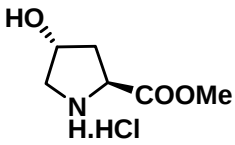

A suspension of (2*S*,4*R*)-4-hydroxyproline **1** (4.0 g, 30.5 mmol) in anhydrous methanol (40 mL) was stirred at 0^{o}C. Thionyl chloride (2.6 mL, 36.6 mmol) was added dropwise to the reaction mixture. The stirring was continued at 0^{o}C during the addition of thionyl chloride. After completing the addition it was allowed to come to room temperature. The reaction mixture was refluxed for another 6 hrs. Methanol was removed under vacuum till the white solid obtained. The precipitate was washed with EtOAc and followed by diethyl ether. The residue was dried under vacuum over phosphorus pentoxide yielded methyl ester hydrochloride **2** as a white solid. This solid was used for the next reaction without further purification.

***N*-(2-chloroacetyl)-(2*S*,4*R*)-4-hydroxyproline methyl ester (3)**

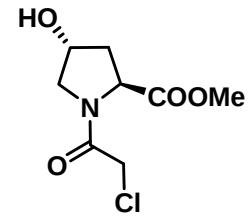

A mixture of compound **2** (4.7 g, 30.5 mmol) and Na_2CO_3 (22.6 g, 213.4 mmol) was dissolved in 100 mL dioxan:water (1:1). Reaction mixture was allowed to attain 0^oC. Chloroacetyl chloride (12.1 mL, 152.5 mmol) diluted with 20 mL of dioxan was added slowly to the reaction mixture at 0^oC over a period of 15 min. Then it was allowed to stir for another 0.5 hr at 0^oC. After completion of the reaction, dioxan was removed under vacuum and the aqueous layer was extracted with ethyl acetate (50 mL x 3). The organic layer was washed with saturated $NaHCO_3$ solution and followed by brine and dried over Na_2SO_4. The reaction mixture was purified by column chromatography to yield the product **3** as a white crystalline solid (5.4 g, 84%).

^{1}H NMR (200 MHz, $CDCl_3$) δ_H 1.99-2.06 (m, 1H), 2.29-2.41 (m, 1H), 3.74 (s, 3H), 3.74-3.83 (m, 2H), 4.09 (s, 2H), 4.55-4.59 (m, 2H); **^{13}C NMR** (50 MHz, $CDCl_3$) δ_C 37.5, 41.9, 52.6, 55.2, 58.2, 70.2, 165.8, 172.4; **DEPT NMR** (50 MHz, $CDCl_3$) δ_C 37.5, 41.9, 52.6, 55.2, 58.2, 70.2; **LCMS (EI)** *m/z* 222.3, Found 245.4 [M+Na^+].

***N*-(thymin-1-yl)-(2*S*,4*R*)-4-hydroxyproline methyl ester (4)**

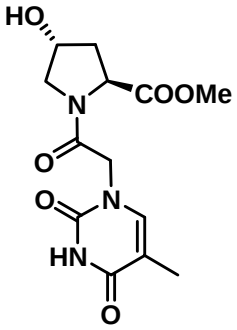

A mixture of chloro compound **3** (5.0 g, 23.6 mmol), thymine (3.0 g, 23.6 mmol) and anhydrous K_2CO_3 (3.9 g, 28.3 mmol) in dry DMF (30 mL) under inert atmosphere was heated with stirring at 60°C for 6 hrs. After cooling, the solvent was removed under reduced pressure to leave a residue, which was extracted in ethyl acetate (50 mL x 5) and dried over anhydrous Na_2SO_4. The organic layer was evaporated and the crude compound was purified by column chromatography to afford a white solid of thymine monomer ethyl ester **4** (5.6 g, 81%).

^{1}H NMR (200 MHz, $CDCl_3$+DMSO-d_6) δ_H 1.87 (d, 3H), 1.94-2.07 (m, 1H), 2.25-2.36 (m, 1H), 3.66-2.81 (m, 5H), 4.38-4.69 (m, 4H), 7.08-7.09 (d, 1H); **^{13}C NMR** (50 MHz, $CDCl_3$+DMSO-d_6) δ_C 17.0, 42.2, 53.3, 57.0, 57.7, 59.1, 62.8, 74.3, 114.4, 146.2, 156.1, 169.7, 170.6, 177.1; **DEPT NMR** (50 MHz, $CDCl_3$+DMSO-d_6) δ_C 17.1, 42.2, 53.3, 57.0, 59.1, 62.8, 74.3, 146.2; **MS (EI)** *m/z* 311.2, Found 334.8 [M+Na^+].

***N*-(thymin-1-yl)-(2*S*,4*R*)-4*O*-tosylproline methyl ester (5)**

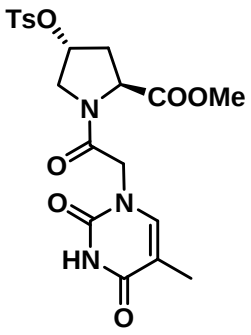

To a solution of compound **4** (3.5 g, 20.3 mmol) in dry pyridine (35 mL) at 0°C tosyl chloride (4.6 g, 24.4 mmol) was added slowly in small portions with constant stirring. After the completion of addition, the ice bath was removed and stirring was continued at ambient temperature for 2 hrs. Pyridine was removed under reduced pressure and the residue was taken in water and extracted with ethyl acetate (50 mL x 3). The combined organic layer was washed with saturated $NaHCO_3$ solution followed by brine and dried over anhydrous Na_2SO_4. The organic layer was evaporated to yield a colorless crystalline solid which was purified by column chromatography to get the product **5** (3.2 g, 62%) in pure form.

^{1}H NMR (200 MHz, $CDCl_3$) δ_H 1.90 (s, 3H), 2.08-2.22 (m, 1H), 2.48 (m, 4H), 3.72 (s, 3H), 3.82-3.91 (m, 2H), 4.44-4.56 (m, 2H), 7.00 (d, 1H), 7.38-7.42 (d, 2H), 7.79-7.63 (d, 2H), 9.27 (s, 1H); **^{13}C NMR** (50 MHz, $CDCl_3$) δ_C 12.3, 21.7, 35.0, 48.3, 52.0, 52.8, 57.6, 77.6, 110.7, 127.8, 130.2, 132.9, 140.8, 145.7, 151.1, 164.4, 165.4, 171.4; **DEPT NMR** (50 MHz, $CDCl_3$) δ_C 12.3, 21.7, 35.0, 46.3, 52.0, 53.4, 57.6, 78.6, 127.8, 130.2, 140.8; **MS (EI**) *m/z* 465.4 , Found 466.0 [M+H], 488.0 [M+Na^+].

***N*-Boc-(2*S*,4*R*)-4-hydroxyproline methyl ester (7)**[12a]

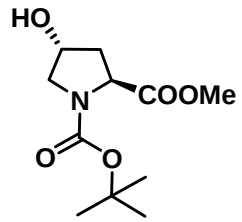

(2*S*,4*R*)-4-hydroxyproline (5.2 g, 39.6 mmol) was suspended in dry methanol and cooled in an ice bath. Thionyl chloride (3.2 mL, 43.6 mmol) was added slowly with vigorous stirring and the resulting solution was refluxed for 8 hrs. The solvent was removed under reduced pressure using KOH trap and the solid obtained was further dried under high vacuum to obtain the methyl ester hydrochloride as white crystalline solid, which was dissolved in 70 mL of dioxan:water (1:1) and TEA (8.4 mL, 59.5 mmol) followed by the slow addition of Boc anhydride (10.9 mL, 47.5 mmol). The mixture was stirred at ambient temperature for 16 hrs. The resulting reaction mixture was concentrated to half its volume, extracted with ethyl acetate (50 mL x 4), the organic layer was washed with brine and as evaporated to yield compound **7** (8.26 g, 85%).

^{1}H NMR (200 MHz, $CDCl_3$) δ_H 1.41-1.46 (d, 9H), 2.0-2.13 (m, 1H), 2.2-2.33 (m, 1H), 3.58-3.62 (m, 2H), 3.73 (s, 3H), 4.35-4.49 (m, 2H); **^{13}C NMR** (50 MHz, $CDCl_3$) δ_C 28.1, 38.3 (min), 38.9 (maj), 52.0 (maj), 52.1 (min) 54.5, 57.5 (min), 57.9 (maj), 69.0 (maj), 69.7 (min), 80.4, 154.0 (maj), 154.6 (min), 173.5 (min), 173.7 (maj); **DEPT NMR** (50 MHz, $CDCl_3$) δ_C 28.1, 32.3 (min), 38.9 (maj), 52.0 (maj), 52.2 (min), 54.5, 57.5 (min), 57.9 (maj), 69.0 (maj), 69.7 (min). **MS (EI)** *m/z* 245.2, Found 268.7 [M+Na$^+$]

***N*-Boc-(2*S*,4*R*)-4*O*-mesyl-proline methyl ester (8)**[12a,16]

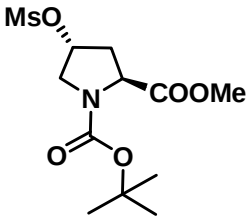

To a solution of hydroxyl compound **7** (5.0 g, 20.3 mmol) in dry pyridine (35 mL) at 0^{o}C mesyl chloride (1.9 mL, 24.4 mmol) was added dropwise with constant stirring. After the addition was complete, the ice bath was removed and stirring continued at ambient temperature for 2 hrs. Pyridine was removed under reduced pressure and the residue was taken in water and extracted with ethyl acetate (50 mL x 3). The organic layer was washed with saturated $NaHCO_3$ solution and followed by brine (50 mL) and dried over anhydrous Na_2SO_4. The organic layer was evaporated to yield a colorless crystalline solid which on purification gave the product **8** (6.06 g, 92 %).

^{1}H NMR (200 MHz, $CDCl_3$) δ_H 1.42-1.47 (d, 9H), 2.17-2.30 (m, 1H), 2.5-2.71 (m, 1H), 3.04 (s, 3H), 3.71-3.87 (m, 5H), 4.32-4.48 (m, 1H), 5.24-5.3 (m, 1H); **^{13}C NMR** (50 MHz, $CDCl_3$) δ_C 27.7 (min), 28.1 (maj), 36.2 (min), 37.4 (maj), 38.6, 52.1, 52.2, 57.0 (min), 57.4 (maj), 77.9 (maj), 78.2 (min), 80.8, 153.3 (maj), 153.9 (min), 172.7; **DEPT NMR** (50 MHz, $CDCl_3$) δ_C 27.7 (min), 28.1 (maj), 32.2 (min), 37.4 (maj), 38.6, 52.1, 52.2, 57.0 (min), 57.4 (maj), 77.9 (maj), 78.2 (min); **MS (EI)** *m/z* 323.36, Found 346.2 [M+Na$^+$]

***N*-Boc-(2*S*,4*S*)-4-Cyanoproline methyl ester (9)**[16]

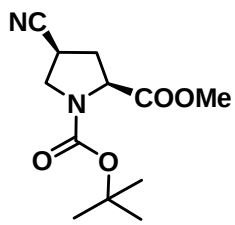

The mesylate **8** (5.0 g, 15.4 mmol) was taken in dry DMSO (20 mL) to which NaCN (6.03 g, 123.2 mmol) was added and the mixture was stirred at 60^{o}C for 48 hrs. After completion of the reaction, the reaction mixture was diluted with (60 mL) water

and was extracted with ethyl acetate (75 mL x 4). The combined organic layer was washed with brine and evaporated to dryness to obtain oily residue which was further purified by silica gel column chromatography. Colorless solid was obtained as the pure product **9** (1.36 g, 35%).

^{1}H NMR (200 MHz, $CDCl_3$) δ_H 1.40-1.45 (d, 9H), 2.2-2.4 (m, 1H), 2.58-2.75 (m, 1H), 3.05-3.20 (m, 1H), 3.2-3.66 (m, 1H), 3.77 (s, 3H), 3.85-4.05 (m, 1H), 4.25-4.5 (m, 1H); **^{13}C NMR** (50 MHz, $CDCl_3$) δ_C 26.3 (maj), 27.1 (min), 28.0, 33.3 (min), 34.2 (maj), 49.0, 52.3, 57.8 (min), 58.1 (maj), 80.9, 118.9, 152.8 (maj), 153.3 (min), 171.8; **DEPT NMR** (50 MHz, $CDCl_3$) δ_C 26.3 (maj), 27.1 (min), 28.0, 33.3 (min), 34.2 (maj), 49.0, 52.3, 57.8 (min), 58.1(min); **MS (EI)** *m/z* 254.2, Found 277.1 [M+Na^+]; $[\alpha]_D$ = -26.31^o (c 1.0, $CHCl_3$)

***N*-(2-chloroacetyl)-(2*S*,4*S*)-4-Cyanoproline methyl ester (10)**

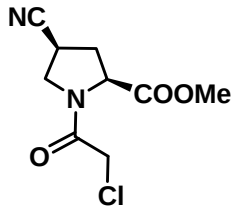

The compound **9** (1.2 g, 4.7 mmol) was dissolved in minimum volume of DCM and 50% TFA in DCM was added slowly at 0^{o}C. Reaction mixture was allowed to stir for 1hr from 0^{o}C to rt. 10% aqueous ammonia solution was added to the reaction mixure for neutralization and then the aqueous layer was extracted repeatedly with DCM. The combined organic layer was dried over anhydrous Na_2SO_4 and the solvent removed to obtain the free amine which was dried under high vacuum. This free amine was dissolved in dry DCM (10 mL) and TEA (0.98 mL, 7.05 mmol). Chloroacetyl chloride (0.5 mL, 5.64 mmol) diluted with 5 mL of DCM was added slowly to the reaction mixture at 0^{o}C over a period of 15 min. It was then allowed to stir for another 0.5 hr at 0^{o}C. Water was added to the reaction mixture and then extracted with DCM (30 mL x 3). The organic layer was washed with saturated $NaHCO_3$ solution, followed by brine and dried over anhydrous Na_2SO_4. The reaction mixture was purified by column chromatography to yield the product as a yellow liquid **10** (0.78 g, 72%).

^{1}H NMR (200 MHz, $CDCl_3$) δ_H 2.29-2.39 (m, 1H), 2.60-2.81 (m, 1H), 3.21-3.3 (m, 1H), 3.76 (s, 3H), 3.82-4.25 (m, 4H), 4.52-4.62 (m, 1H); **^{13}C NMR** (50 MHz, $CDCl_3$) δ_C 25.5 (min), 27.7 (maj), 32.4 (maj), 34.4 (min), 41.7, 49.5 (maj), 49.8 (min), 52.7 (maj), 53.3 (min), 58.4, 118.6 (maj), 119.5 (min), 164.9, 170.6; **DEPT NMR** (50 MHz,

$CDCl_3$) δ_C 25.5 (min), 27.7 (maj), 32.4 (maj), 34.4 (min), 41.7, 49.5 (maj), 49.8 (min), 52.7 (maj), 53.3 (min), 58.4; **MS (EI)** *m/z* 230.6, Found 253.1 [M+Na^+]; $[\alpha]_D$ = -32.25^o (c 1.0, $CHCl_3$).

***N*-(thymin-1-yl)-(2*S*,4*S*)-4-Cyanoproline methyl ester (6)**

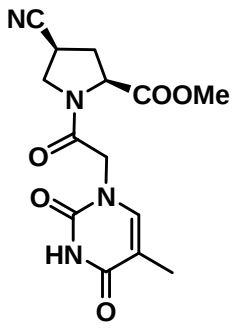

A mixture of chloro- compound **10** (1.5 g, 6.5 mmol), thymine (0.82 g, 6.5mmol) and anhydrous K_2CO_3 (1.07 g, 7.8 mmol) in dry DMF (10 mL) under nitrogen was heated with stirring at 60°C for 6 hrs. After cooling, the solvent was removed under reduced pressure to leave a residue, which was extracted in ethyl acetate (50 mL x 5) and dried over anhydrous Na_2SO_4. The solvent was evaporated and the crude compound was purified by column chromatography to afford a white solid of thymine monomer methyl ester **6** (1.67 g, 81%)**.**

^{1}H NMR (200 MHz, DMSO-d_6) δ_H 1.66 (s, 3H), 1.99-2.12 (m, 1H), 2.60-2.64 (m, 1H), 3.55 (s, 3H), 3.65-3.73 (m, 2H), 3.90-3.99 (m, 1H), 4.25-4.49 (m, 3H), 7.23 (s, 1H), 11.24 (s, 1H) **^{13}C NMR** (50 MHz, DMSO-d_6) δ_C 12.3, 25.5 (min), 27.6 (maj), 32.3 (maj), 34.3 (min), 48.7 (maj), 50.0 (min), 52.6 (maj), 53.2 (min), 57.8 (min), 58.4 (maj), 108.8, 120.5 (maj), 121.2 (min), 142.3, 151.4, 164.8, 166.0 (maj), 166.7 (min), 171.3; **DEPT NMR** (50 MHz, DMSO-d_6) δ_C 12.3, 25.5 (min), 27.6 (maj), 32.3 (maj), 34.3 (min), 48.7 (maj), 50.0 (min), 52.6 (maj), 53.2 (min), 57.8 (maj), 58.4 (maj), 142.3; **MS (EI)** *m/z* 320.3, Found 343.1 [M+Na^+]; $[\alpha]_D$ = -40.0^o (c 1.0, DMSO).

***N*-(thymin-1-yl)-(2*S*,4*S*)-4-Boc-methyl aminoproline methyl ester (12)**

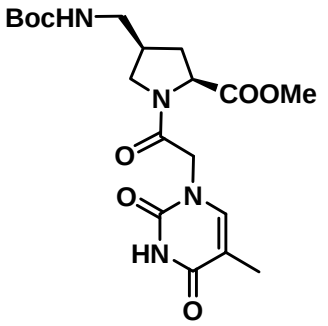

To a solution of the above compound **6** (0.5 g, 1.5 mmol) in anhydrous methanol (10 mL) placed in a hydrogenation flask was added di-*t*-butyl dicarbonate (0.41 mL, 1.8 mmol) and Pd/C (10 mol%). The mixture was hydrogenated in Parr apparatus (rt, 50 psi, 5 h). The catalyst was filtered, the filtrate was evaporated under reduced pressure and the residue was purified by column chromatography to obtain a white solid **12** (0.57 g. 87%)

^{1}H NMR (200 MHz, DMSO-d_6) δ_H 1.15-1.18 (d, 9H), 1.53 (s, 3H), 2.08-2.21 (m, 1H), 2.79-2.81 (m, 1H), 2.98-3.02 (m, 1H), 3.39 (s, 3H), 3.52-3.56 (m, 2H), 3.99-4.07 (m, 1H), 4.25-4.37 (m, 2H), 6.79 (m, 1H), 7.11 (s, 1H); **^{13}C NMR** (50 MHz, DMSO-d_6) δ_C 12.3, 28.7, 32.5, 42.0, 48.8, 49.6, 52.3, 59.2, 78.3, 108.6, 142.5, 151.4, 156.3, 164.9, 165.9, 172.6; **DEPT NMR** (50 MHz, DMSO-d_6) δ_C 12.3, 28.7, 32.5, 39.6, 42.0, 48.8, 49.6, 52.3, 59.1, 142.5; **MS (EI)** *m/z* 424.4, Found 425.4 [M + H], 447.3 [M+Na$^+$]; $[\alpha]_D$ = -36.6^o (c 1.0, DMSO)

***N*-(thymin-1-yl)-(2*S*,4*S*)-4-Boc-methyl aminoproline (13)**

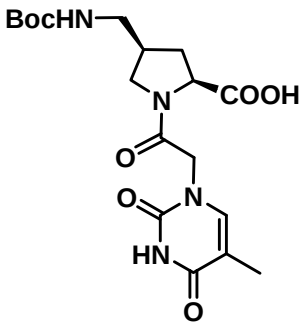

To a solution of **12** (0.72 g, 1.7 mmol) in THF (4 mL) was added 1M aq. LiOH (5 mL). The reaction was stirred at room temperature for 0.5hrs. The excess of alkali was neutralized by Dowex H^+ resin, which was then filtered off. The filtrate was then evaporated to get the product **13** as white foam with good yield (0.55 g, 80%).

^{1}H NMR (200 MHz, DMSO-d_6) δ_H 1.37 (s, 9H), 1.74 (s, 3H), 2.10-2.51 (m, 2H), 2.89-2.93 (m, 2H), 4.07-4.09 (t, 2H), 4.26-4.43 (m, 2H), 6.97 (m, 1H), 7.33 (s, 1H), 11.23 (b s, 1H); **^{13}C NMR** (50 MHz, DMSO-d_6) δ_C 12.3, 28.6, 34.4, 37.0, 43.0, 48.5, 49.7 (min), 50.6 (maj), 60.7 (min), 61.4 (maj), 77.9, 108.3, 142.9, 151.5, 156.1, 164.9, 166.2, 174.2; **MS (EI)** *m/z* 410.1, Found 433.5 [M+Na$^+$].

***N*-Boc-(2*S*,4*S*)-4*O*-tosyl-proline methyl ester (14)**

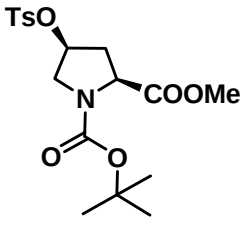

The mixture of compound **7** (5.5 g, 22.4 mmol), PPh_3 (9.4 g, 35.8 mmol) and *p*-toluene sulfonic acid (6.1 g, 35.8 mmol) dissolved in dry THF (100 mL) was cooled to 0^{o}C on ice bath, under argon atmosphere. The mixture was stirred for 30 min at 0^{o}C. Diisopropyl azodicarboxylate (7.04 mL, 35.8 mmol) was added slowly and allowed to stir at room temperature for another 8 hrs. THF was removed under vacuo and the resulting orange colored thick oil was dissolved in 150 mL petroleum ether, by triturating with spatula and resulting solution was kept overnight at room temperature. The white powder settled was filtered and the residue was washed with petroleum ether followed by diethylether, afforded compound **14** as white crystalline solid (4.83 g, 54%).

^{1}H NMR (200 MHz, $CDCl_3$) δ_H 1.40-1.44 (d, 9H), 2.33-2.45 (m, 2H), 2.45 (s, 3H), 3.62 (m, 2H), 3.69 (s, 3H), 4.30-4.47 (m, 1H), 5.03-5.05 (m, 1H), 7.33-7.37 (dd, 2H), 7.70-7.79 (dd, 2H); **^{13}C NMR** (50 MHz, $CDCl_3$) δ_C 21.6 (maj), 21.9 (min), 28.1, 35.9 (maj), 35.9 (min), 51.5 (maj), 52.2 (min), 56.9 (min), 57.3 (maj), 69.8, 78.9, 80.5, 127.7, 129.9, 133.4, 145.1, 153.3 (maj), 153.7 (min), 171.6 (min), 171.9 (maj); **DEPT NMR** (50 MHz, $CDCl_3$) δ_C 21.6 (maj), 21.9 (min), 28.1, 35.97 (min), 36.9 (maj), 51.5 (maj), 52.0 (min), 52.2, 56.9 (min), 57.3 (maj), 69.8, 77.7, 78.9, 127.7, 129.9; **MS (EI)** *m/z* 399.4, Found 422.4 [M+Na^+].

***N*-Boc-(2*S*,4*R*)-4-Cyanoproline methyl ester (15)**

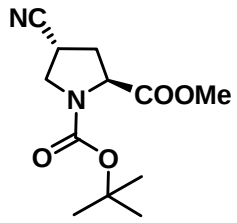

Compound **15** (0.98 g, 28%) was synthesized from the tosylate **14** as mentioned earlier for compound **9**.

^{1}H NMR (200 MHz, $CDCl_3$) δ_H 1.41-1.46 (d, 9H), 2.32-2.6 (m, 2H) 3.1-3.3 (m, 1H), 3.58-3.7 (m, 1H), 3.75 (s, 3H), 3.85-4.05 (m, 1H) 4.36-4.51 (m, 1H); **^{13}C NMR** (50 MHz, $CDCl_3$) δ_C 26.3 (maj), 26.4 (min), 28.0, 33.5 (min), 34.4 (maj), 49.0, 52.3, 57.8, 80.9, 119.0, 152.8 (maj), 153.4 (min), 172.2; **DEPT NMR** (50 MHz, $CDCl_3$) δ_C 26.3 (maj), 26.4 (min), 28.0, 33.5 (min), 34.4 (maj), 49.0, 52.3, 57.8; **MS (EI)** *m/z* 254.2, Found 277.2 [M+Na^+]; $[\alpha]_D$ = +24.15^o (c 1.0, $CHCl_3$).

***N*-(2-chloroacetyl)-(2*S*,4*R*)-4-Cyanoproline methyl ester (16)**

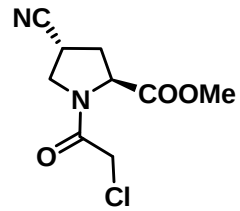

The compound (2*S,*4*R*)-**16** was prepared from the Boc deprotected free amine using the similar procedure as the one described for the compound (2*S,*4*S*)-**10** with yield (0.73 g, 73%).

^{1}H NMR (200 MHz, $CDCl_3$) δ_H 2.42-2.67 (m, 2H), 3.3-3.5 (m, 1H), 3.76 (s, 3H), 3.81-4.14 (m, 4H), 4.64-4.75 (m, 1H); **^{13}C NMR** (50 MHz, $CDCl_3$) δ_C 25.4 (min), 27.78 (maj), 32.6 (maj), 34.7 (min), 41.6, 52.8 (maj), 53.3 (min), 58.2, 118.4, 165.0, 170.9; **DEPT NMR** (50 MHz, $CDCl_3$) δ_C 25.4(min), 27.7 (maj), 32.6 (maj), 34.7 (min), 41.6, 49.4, 52.8 (maj), 53.3 (min), 58.2; **MS (EI)** *m/z* 230.6, Found 253.2 [M+Na^+]; $[\alpha]_D$ = +31.01^o (c 1.0, $CHCl_3$)

***N*-(thymin-1-yl)-(2*S*,4*R*)-4-Cyanoproline methyl ester (17)**

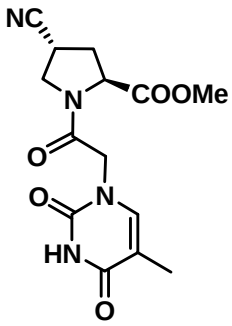

The procedure described for compound (2*S,* 4*S*)-**6** was used to prepare (2*S,*4*R*)-**17** (1.12 g, 81%) from compound **16** (1.0 g, 4.3 mmol).

^{1}H NMR (200 MHz, DMSO-d_6) δ_H 1.77 (s, 3H), 2.25-2.52 (m, 2H), 3.56 (s, 3H), 3.66-4.03 (m, 3H), 4.35-4.39 (m, 1H), 4.52 (s, 2H), 7.37 (s, 1H), 11.35 (s, 1H); **^{13}C NMR** (50 MHz, DMSO-d_6) δ_C 11.8, 27.3 (maj), 31.8 (maj), 33.9 (min), 48.0, 48.3, 52.1, 57.7, 108.2, 119.7, 141.8, 150.9, 164.3, 165.6, 170.7; **DEPT NMR** (50 MHz, DMSO-d_6) δ_C 11.8, 24.2 (min), 27.3 (maj), 31.8 (maj), 33.9 (min), 48.0, 48.3, 52.2 (maj), 52.8 (min), 57.1 (min), 57.7 (maj), 141.8; **MS (EI)** *m/z* 320.3, Found 343.3 [M+Na^+]; $[\alpha]_D$ = +38.03^o (c 1.0, DMSO).

***N*-(thymin-1-yl)-(2*S*,4*R*)-4-Boc-methyl aminoproline methyl ester (18)**

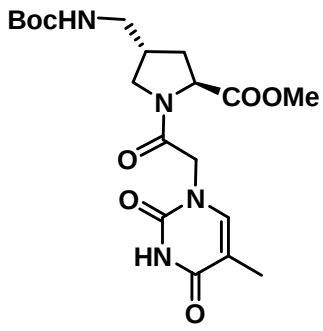

The Boc protected amine (2*S,*4*R*)-**18** (0.75 g, 81%) was obtained on hydrogenation of the cyanide (2*S,*4*R*)-**17** (0.7 g, 2.2 mmol) following the procedure described for the synthesis of the Boc-protected amine (2*S,*4*S*)-**12**.

^{1}H NMR (200 MHz, DMSO-d_6) δ_H 1.32 (s, 9H), 1.68 (s, 3H), 1.86 (m, 1H), 2.44 (m, 1H), 2.80-3.01 (m, 1H), 3.55-3.66 (m, 4H), 4.30-4.49 (m, 3H), 6.98 (t, 1H), 7.28 (m, 1H), 11.25 (s, 1H); **^{13}C NMR** (50 MHz, DMSO-d_6) δ_C 11.8, 28.1, 31.7, 48.2, 48.7, 51.8 (maj), 52.5 (min), 58.1, 77.7, 108,1, 141.9, 150.9, 155.8, 164.3, 165.4, 171.9; **DEPT NMR** (50 MHz, DMSO-d_6) δ_C 11.8, 28.1, 31.7, 38.3, 41.3, 48.2, 48.7, 51.8 (maj), 52.5 (min), 58.1, 141.9; **MS (EI)** *m/z* 424.4, Found 447.5 [M+Na^+]; $[\alpha]_D$ = +36.1^o (c 1.0, DMSO).

***N*-(thymin-1-yl)-(2*S*,4*R*)-4-Boc-methyl aminoproline (19)**

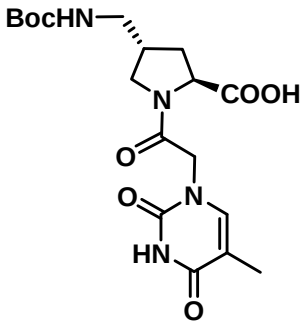

The compound (2*S*,4*R*)-**19** (0.41 g, 83%) was synthesized from starting material (2*S*,4*R*)-**18** (0.70 g, 3.3 mmol) following the same procedure described for acid (2*S*,4*S*)-**13.**

^{1}H NMR (200 MHz, MeOH-d_4) δ_H 1.44-1.47 (d, 9H), 1.86 (s, 3H), 1.99-2.11 (m, 1H), 3.29-3.43 (m, 2H), 3.79-3.82 (m, 1H), 4.47-4.73 (m, 3H), 7.33 (s, 1H); **MS (EI)** *m/z* 410.1, Found 433.5 [M+Na^+].

***N*1-(*t*-Boc)-1,2-diaminoethane (21)**

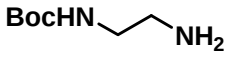

1,2-diaminoethane (20 g, 0.33 mol) was taken in dioxane: water (1:1, 500 mL) and cooled in an ice-bath. Boc anhydride (8.1 ml, 35 mmol) in dioxane (50 mL) was slowly added with stirring. The mixture was stirred for 8 hrs and the resulting solution was concentrated to 100 mL. The *N*1, *N*2-di-Boc derivative not being soluble in water, precipitated, and it was removed by filtration. The corresponding *N*1-mono-Boc derivative was obtained by repeated extraction from the filtrate in ethyl acetate. Removal of solvents yielded the mono-Boc diaminoethane (3.45 g, 63%)

^{1}H NMR (200 MHz, $CDCl_3$) δ_H 5.21 (br s, 1H), 3.32 (t, 2H), 2.54 (t, 2H,), 1.42 (s, 9H).

Ethyl *N*-(2-Boc-aminoethyl)-glycinate (22)

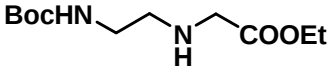

The *N*1-Boc-1,2-diaminoethane **21** (3.2 g, 20 mmol) was treated with ethylbromoacetate (2.25 mL, 20 mmol) in acetonitrile (100 mL) in the presence of K_2CO_3 (2.4 g, 20 mmol) and the mixture was stirred at ambient temperature for 5 hrs. Acetonitrile was removed from the reaction mixture and the residue was extracted with ethyl acetate and further purification by column chromatography yield the ethyl *N*-(2-Boc-aminoethyl)-glycinate **22** (4.3 g, 83%) as a colourless oil.

^{1}H NMR (200 MHz, $CDCl_3$) δ_H 5.02 (br s, 1H), 4.22 (q, 2H), 3.35 (s, 2H), 3.20 (t, 2H,) 2.76 (t, 2H), 1.46 (s, 9H), 1.28 (t, 3H).

Ethyl *N*-(Boc-aminoethyl)-*N*-(chloroacetyl)-glycinate (23)

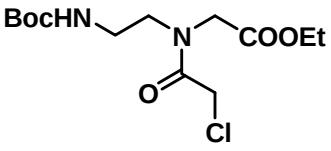

The ethyl *N*-(2-Bocaminoethyl) glycinate **22** (4.0 g, 14 mmol) was taken in 10% aqueous Na_2CO_3 (75 mL) and dioxane (60 mL). Chloroacetyl chloride (6.5 mL, 0.75 mmol) was added in two portions with vigorous stirring. The reaction was complete within 15 min. The reaction mixture was brought to pH 8.0 by addition of 10% aqueous Na_2CO_3 and concentrated to remove the dioxane. The product was extracted from the aqueous layer with dichloromethane and was purified by column chromatography to obtain the ethyl *N* (Boc-aminoethyl)- *N*-(chloroacetyl)-glycinate **23** as a colourless oil in good yield (4.2 g, 80%).

^{1}H NMR (200 MHz, $CDCl_3$) δ_H 5.45 (br s, 1H), 4.1- 4.9 (s, 2H), 4.00 (s, 2H), 3.53 (t, 2H), 3.28 (q, 2H), 1.46 (s, 9H), 1.23 (t, 3H).

***N*-(Boc-aminoethylglycyl)-thymine ethyl ester (24a)**

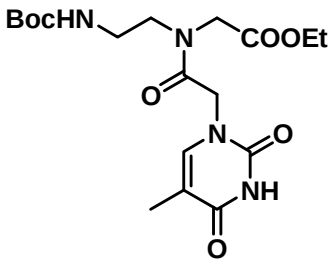

Ethyl *N*-(Boc-aminoethyl)- *N* (chloroacetyl)-glycinate **23** (1.0 g, 3.1 mmol) was stirred with anhydrous K_2CO_3 (0.47 g, 3.4 mmol) in DMF with thymine (0.41 g, 3.25 mmol) to obtain the desired compound **24a** in good yield. DMF was removed under reduced pressure and the oil obtained was purified by column chromatography to afford **24a**. (1.0 g, 83%).

^{1}H NMR (200 MHz, $CDCl_3$) δ_H 9.00 (br s, 1H), 7.05 (min) & 6.98 (maj) (s, 1H), 5.65 (maj) & 5.05 (min) (br s, 1H), 4.58 (maj) & 4.44 (min) (s, 1H), 4.25 (m, 2H), 3.55 (m, 2H), 3.36 (m, 2H), 1.95 (s, 3H), 1.48 (s, 9H), 1.28 (m, 3H); **^{13}C NMR** (50 MHz, $CDCl_3$) δ_C 170.8, 169.3, 167.4, 164.3, 156.2, 151.2, 141.1, 110.2, 79.3, 61.8, 61.2, 48.5, 48.1, 47.7, 38.4, 28.1, 13.8, 12.2.

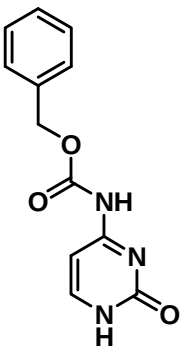

***N*4-Benzyloxycarbonyl cytosine**

Over a period of about 15 min, 50% solution of bezyloxycarbonyl chloride in toluene (12.3 mL, 36 mmol) was added dropwise to a suspension of cytosine (2.0 g, 18 mmol) in dry pyridine (100 mL) at 0^{o}C under anhydrous conditions. The reaction mixture was stirred vigorously for 20 hrs, after which the pyridine suspension

was evaporated to dryness, under vacuum. To the residue, an ice cold water (20 mL) was added followed by acidification by 2 N HCl to pH ~2.0. The resulting white precipitate was filtered off, washed with water and partially dried by air suction. The still wet precipitate was boiled with absolute ethanol (50 mL) for 10 min, cooled to 0^{o}C, filtered, washed thoroughly with ether and vacuum dried to obtain the product (2.9 g, 65%).

^{1}H NMR (200 MHz, DMSO-d_6) δ_H 7.71-7.67 (d, 1H, *J* = 7.32 Hz), 7.28 (s, 5H), 6.84-6.6 (d, 1H, *J* = 7.32), 5.02 (s, 2H).

***N*-(Boc-aminoethylglycyl)-(*N*4-benzyloxycarbonyl cytosine)ethyl ester (24b)**

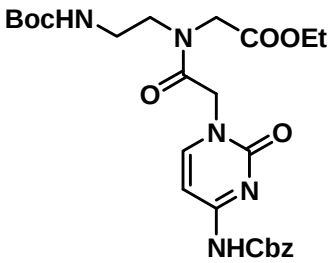

The compound **24b** was synthesized starting from compound **23** following the similar procedure for the synthesis of **24a**.

^{1}H NMR (200 MHz, $CDCl_3$) δ_H 7.65 (d, 1H), 7.35 (s, 5H), 7.25 (d, 1H), 5.70 (br s, 1H), 5.20 (s, 2H), 4.71 (maj) & 4.22 (min) (br s, 2H), 4.15 (q, 2H), 4.05 (s, 2H), 3.56 (m, 2H), 3.32 (m, 2H), 1.48 (s, 9H), 1.25 (t, 3H).

***N*-(Boc-aminoethylglycyl)-adenine ethyl ester (24c)**

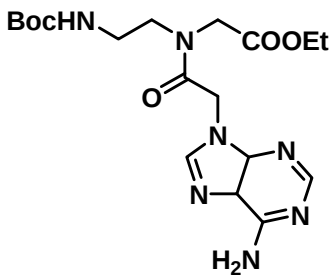

Compound **24c** was obtained from compound **23** using the same reaction procedure as for the synthesis of **24a**.

^{1}H NMR (200 MHz, $CDCl_3$) δ_H 8.32 (s, 1H), 7.95 (min) & 7.90 (maj) (s, 1H), 5.93 (maj) & 5.80 (min) (br, 2H), 5.13 (maj) & 4.95 (min), 4.22 (min) & 4.05 (maj) (s, 2H), 4.20 (m, 2H), 3.65 (maj) & 3.55 (min) (m, 2H), 3.40 (maj) & 3.50 (min) (m, 2H), 1.42 (s, 9H), 1.25 (m, 3H).

***N*-(Boc-aminoethylglycyl)-2-amino-6-chloropurine ethyl ester (24d)**

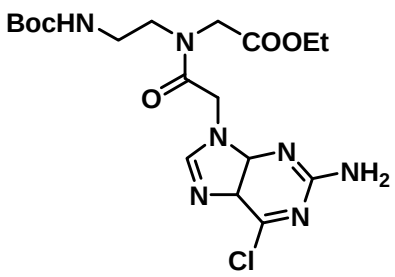

A mixture of 2-amino-6 chloropurine (1.14 g, 6.8 mmol), K_2CO_3 (0.93 g, 7.0 mmol) and ethyl *N*-(Boc-aminoethyl)-*N*-(chloroacetyl)-glycinate 15 (2.4 g, 7.0 mmol) were taken in dry DMF (20 mL) and stirred at room temperature for 4 hrs. K_2CO_3 was

removed by filtration, and DMF was evaporated under reduced pressure. The resulting residue was purified by column chromatography to obtain the *N*-(Boc-aminoethylglycyl)-2-amino-6-chloropurine ethyl ester **24d** in excellent yield (2.55 g, 90%).

^{1}H NMR (200 MHz, $CDCl_3$) δ_H 7.89 (min) & 7.85 (maj) (s, 1H), 7.30 (s, 1H), 5.80 (br s, 1H, NH), 5.18 (br, 2H), 5.02 (maj) & 4.85 (min) (s, 2H), 4.18 (min) & 4.05 (maj) (s, 2H), 3.65 (maj) & 3.16 (min) (m, 2H), 3.42 (maj) and 3.28 (min) (m, 2H), 1.50 (s, 9H), 1.26 (m, 3H).

2.8.1 Hydrolysis of the ethyl ester functions of PNA monomers (25a-25d) (General method)

The ethyl esters were hydrolyzed using 1N aqueous NaOH (5 mL) in THF (5 mL) and the resulting acid was neutralized with activated Dowex-H^+ till the pH of the solution becomes slightly acidic. The resin was removed by filtration and the filtrate was concentrated to obtain the resulting Boc protected acids **(25a-25d)** in excellent yield (>80%). In case of cytosine monomer ethyl ester, mild base 0.5 M LiOH was used to avoid deprotection of the exocyclic amine-protecting group by strong bases.

2.8.2 Solid phase peptide synthesis

Picric acid estimation of resin functionalization

The typical procedure for estimation of the loading value of the resin was carried out with 5 mg of the resin which comprises the following steps:

The resin was swollen in dry CH_2Cl_2 for 2 hrs. After soaking with CH_2Cl_2, it was drained off and a 50% solution of TFA in CH_2Cl_2 was added (1 mL x 3), 15 min each. After washing thoroughly with CH_2Cl_2, the TFA salt was neutralized with 5% solution of DIPEA in CH_2Cl_2 (1 mL x 5min each). The free amine was treated with a 0.1M picric acid solution in CH_2Cl_2 (1 mL x 2 min each). The excess picric acid was removed by extensively washing the resin with CH_2Cl_2. The adsorbed picric acid was displaced form the resin by adding a solution of 5% DIPEA in CH_2Cl_2. The eluant was collected and the volume was made up to 10 mL with CH_2Cl_2 in a volumetric flask. The absorbance was recorded at 358nm in ethanol and the concentration of the amine groups on the resin was calculated using the molar extinction coefficient of picric acid as 14,500 $cm^{-1}M^{-1}$ at 358nm.

Kaiser's Test

Kaiser's test was used to monitor the Boc-deprotection and amide coupling steps in the solid phase peptide synthesis. Three solutions were used, *viz.* (1) Ninhydrin (5.0 g) dissolved in ethanol (100 mL) (2) Phenol (80 g dissolved in ethanol (20 mL) and (3) KCN (0.001M aqueous solution of KCN in 98 mL pyridine). To a few beads of the resin taken in a test tube, was added 3-4 drops of each of the three solutions desribed above. The tube was heated for 5 min, and the colour of the beads was noted. A blue colour on the beads and in the solution indicated successful deprotection, while colourless beads were observed upon completion of the amide coupling reaction.

Cleavage of the PNA oligomers from the solid support

The resin bound PNA oligomer (5 mg) was kept in an ice-bath with thioanisole (10 μL) and 1,2-ethanedithiol (4 μL) for 10min, TFA (60 μL) was added and shaken manually and kept for another 10 min. TFMSA (8 μL) was added and stirring continued for 1.5 hrs. The reaction mixture was filtered through a sintered funnel. The residue was washed with TFA (3 x 2 mL) and the combined filtrate and washings were evaporated under vacuum and co-evaporated with diethyl ether, avoiding heating during this process. The residue was precipitated using dry diethyl ether and centrifuged. The diethyl ether layer was decanted and the solid part was redissolved in water.

Gel Filtration

The crude PNA oligomer obtained after ether precipitation was dissolved in water (~0.2 mL) and loaded on a gel filtration column. This column consisted of G25 Sephadex and had a void volume of 1 mL. The oligomer was eluted with water and ten fractions of 1 mL volume each were collected. The presence of the PNA oligomer was detected by measuring the absorbance at 260 nm.

RP-HPLC

The purity of the so obtained PNA oligomers was checked by analytical RP-HPLC on C18 column using a gradient of 0 to 100% CH_3CN in water containing 0.1% TFA at a flow rate of 1.5 mL/min. These were subsequently purified by RP-HPLC on a

semi preparative C18 column. The purity of the oligomers was again ascertained by analytical RP-HPLC.

MALDI-TOF Mass Spectrometry

Literature reports the analysis of PNA purity by MALDI-TOF mass spectrometry in which several matrices have been explored, *viz*. sinapinic acid (3,5-dimethoxy-4-hydroxycinnamic acid),[29] CHCA (α-cyano-4-hydroxycinnamic acid)[30] and DHB (2,5-dihydroxybenzoic acid). Out of these, CHCA (α-cyano-4-hydroxycinnamic acid) was found to give the best signal to noise ratio. For all the MALDI-TOF spectra recorded for the *prolyl*PNAs reported in this chapter, CHCA (α-cyano-4-hydroxycinnamic acid) was used as the matrix and was found to give satisfactory results.

2.8.3 UV-T_m experiments

UV melting experiments were performed on Lambda-35 UV Spectrometer (Perkin- Elmer) equipped with a thermal melt system, PTP-6 Peltier Temperature Programmer with water circulator Thermoshake K20. The sample for T_m measurement was prepared by mixing calculated amount of stock oligonucleotide and PNA solutions together in 2 mL of 10 mM sodium phosphate buffer, 100 mM NaCl (pH 7.4). The samples 2 mL were transferred to quartz cell, sealed with Teflon stopper after degassing with nitrogen gas for 15 min, and equilibrated at the starting temperature for at least 15 min. The OD at 260 nm was recorded in steps from 10-85^oC with temperature increment of 0.5^oC/min. The data were processed using Microcal Origin 6.0 and T_m values derived from the first derivative curve.

2.8.4 CD-Jobs plot

CD spectra were recorded on a JASCO J-715 spectropolarimeter. The CD spectra of the PNA:DNA complexes and the relevant single strands were recorded in 10 mM sodium phosphate buffer, 100 mM NaCl, pH 7.4. The temperature of the circulating water was kept below the melting temperature of the PNA:DNA complexes, i.e., at 10^oC. The CD spectra of the homothymine T single strands, mixed base PNA single strand and the derived PNA:DNA duplexes were recorded as an accumulation of 5 scans from 300 to 190 nm using a 1 cm cell path length. For the binding

stoichiometry determination a solution of **DNA1**, were added with the complementary **PNA4** and **PNA8** separately to make 11 different fractions with molar ratios from 0-100% with fixed concentration of 2 μM. The samples were annealed by keeping the samples at 90^{o}C for 2 min followed by slow cooling to room temperature. Then the samples were cooled by keeping at 4^{o}C for overnight. The spectra were recorded at the range of 190-300 nm. The ellipticity value was plotted as a function of the PNA mole fraction at 256nm.

2.9 References

1. Uhlmann, E.; Peyman, A. Antisense oligonucleotides: A new therapeutic principle. *Chem. Rev.* **1990**, *90*, 543-584.
2. (a) Nielsen, P. E.; Egholm, M.; Berg, R. H.; Buchardt, O. Sequence-selective recognition of DNA by strand displacement with a thymine-substituted polyamide. *Science,* **1991**, *254*, 1497-1500. (b) Hyrup, B.; Nielsen, P. E. Peptide Nucleic Acids (PNA): Synthesis, properties and potential applications. *Bioorg. Med. Chem. Lett.* **1996**, *4*, 5-23. (c) Goodchild, J. Conjugate of oligonucleotides and modified oligonucleotides: A review of their synthesis and properties. *Bioconjugate Chem.* **1990**, *1*, 165-177.
3. (a) Nielsen, P. E.; Haaima, G. Peptide Nucleic Acid (PNA). A DNA mimic with a pseudopeptide backbone. *Chem. Soc. Rev.* **1997**, 73-78 (b) Nielsen, P. E.; Egholm, M.; Berg, R. H.; Buchardt, O. Sequence-selective recognition of DNA by strand displacement with a thymine-substituted polyamide. *Science,* **1991**, *254*, 1497-1500.
4. (a) Hyrup, B.; Nielsen, P. E. Peptide Nucleic Acids (PNA): Synthesis, properties and potential applications. *Bioorg. Med. Chem.* **1996**, *4*, 5-23. (b) Uhlmann, E.; Peyman, A.; Breipohl, G.; Will, D. W. PNA: Synthetic polyamide nucleic acids with unusual binding properties. *Angew. Chem. Int. Ed.* **1998**, *37*, 2796-2823. (c) Uhlmann, E.; Will, D. W.; Breipohl, G.; Langer, D. Synthesis and properties of PNA/DNA chimeras. *Angew. Chem. Int. Ed. Engl.* **1996**, *35*, 2632-2635.
5. (a) Betts, L.; Josey, J. A.; Veal, J. M.; Jordan, S. R. A Nucleic acid triple helix formed by a Peptide Nucleic Acid-DNA Complex. *Science*, **1995**, *270*, 1838-1841. (b) Leijon, M.; Graslund, A.; Nielsen, P. E.; Buchardt, O.; Norden, B.; Kristensen, S. M.; Eriksson, M. Structural characterization of PNA-DNA duplexes by NMR. Evidence for DNA in a B-like conformation. *Biochemistry,* **1994**, *33,* 9820-9825. (c) Brown, S. C.; Thomson, S. A.; Veal, J. M.; Davis, D. G. Structural characterization of PNA-DNA duplexes by NMR. Evidence for DNA in a B-like conformation. *Science,* **1994**, *265,* 777-780.
6. (a) Ganesh, K. N.; Nielsen, P. E. Peptide Nucleic Acids: analogs and derivatives. *Curr. Org. Chem.* **2000**, *4*, 931-943. (b) Kumar, V. A.; Ganesh, K. N. Conformationally constrained PNA analogues: Structural evolution toward DNA/RNA binding selectivity. *Acc. Chem. Res*. **2005**, *38*, 404-412. (c) Kumar, V. A. Structural preorganization of peptide nucleic acid: chiral cationic analogues with five-or six-membered ring structures. *Eur. J. Org. Chem.* **2002**, 2021-2032. (d) Kumar, V. A.; Ganesh, K. N. Structure-editing of nucleic acids for selective targeting of RNA. *Curr. Med. Chem*. **2007**, *7*, 715-726.
7. Wengel, J. Synthesis of 3'-C- and 4'-C-branched oligodeoxynucleotides and the development of Locked Nucleic Acid (LNA). *Acc. Chem. Res*. **1999**, *32*, 301-310**.**
8. Lescrinier, E.; Esnouf, R.; Schraml, J.; Busson, R.; Heus, H. A.; Hilbers, C. W.; Herdewijn, P. Solution structure of a HNA-RNA hybrid. *Chem. Biol*. **2000**, *7*, 719-731.

9. Allart, B.; Khan, K.; Rosemeyer, H.; Schepers, G.; Hendrix, C.; Rothenbacher, K.; Seela, F.; Aerschot, A. V.; Herdewijn, P. D-alritol nucleic acids (ANA): Hybridization properties, stability and initial structural analysis. *Chem. Eur. J.* **1999**, *5*, 2424-2431.

10. Hyrup, B.; Egholm, M.; Nielsen, P. E.; Wittung, P.; Norden, B.; Buchardt O. Structure-activity studies of the binding of modified peptide nucleic acids (PNAs) to DNA. *J. Am. Chem. Soc.* **1994***, 116,* 7964-7970.

11. (a) Egholm, M.; Buchardt, O.; Christensen, L.; Beherens, C.; Frier, S. M.; Driver, D. A.; Berg, R. H.; Kim, S. K.; Norden, B.; Nielsen, P. E. PNA hybridizes to complementary oligonucleotides obeying the Watson-Crick hydrogen bonding rules. *Nature*, **1993**, *365*, 566-568. (b) Tomac, S.; Sarkar, M.; Ratilainen, T.; Wittung, P.; Nielsen, P. E.; Norden, B.; Graslund, A. Ionic effects on the stability and conformation of peptide nucleic acid complexes. *J Am. Chem. Soc.* **1996**, *118*, 5544-5549.

12. (a) Gangamani, B. P.; Kumar, V. A.; Ganesh, K. N. Synthesis of N^{α}-(purinyl/pyrimidinylacetyl)-4-aminoproline diastereomers with potential use in PNA synthesis. *Tetrahedron*, **1996**, *52*, 15017-15030. (b) Gangamani, B. P.; Kumar, V. A.; Ganesh, K. N. Chiral analogues of peptide nucleic acids: Synthesis of 4-aminoprolyl nucleic acids and DNA complementation studies using UV/CD spectroscopy. *Tetrahedron*, **1999**, *55*, 177-192. (c) Gangamani, B. P.; D'Costa, M.; Kumar, V. A.; Ganesh, K. N. *Nucleoside & Nucleotides.* **1999**, *18*, 1409-1011**.**

13. Meena; Kumar, V. A. Pyrrolidine carbamate nucleic acids: Synthesis and DNA binding studies. *Bioorg. Med. Chem. Lett.* **2003**, *16*, 3393-3399.

14. (a) Egholm, M.; Buchardt, O.; Christensen, L.; Beherens, C.; Frier, S. M.; Driver D. A.; Berg, R. H.; Kim, S. K.; Norden, B.; Nielsen, P. E. *Nature*, **1993**, *365*, 566-568. (b) Uhlmann, E.; Will, D. W.; Breipohl, G. Langer, D. Synthesis and Properties of PNA/DNA Chimeras. *Angew. Chem. Int. Ed. Engl.* **1996**, *35*, 2632-2635.

15. Remuzon, P. Trans-4-Hydroxy-L-Proline, a useful and versatile chiral starting block. *Tetrahedron,* **1996**, *52*, 13803-13835.

16. (a)Abraham, D. J.; Mokotoff, M.; Sheh, L.; Simmons, J. E. Design, synthesis, and testing of antisickling agents. Proline derivatives designed for the donor site. *J. Med. Chem.* **1983**, *26*, 549-554.

17. Webb, T. R.; Eigenbrot, C. Conformationally restricted arginine analogues. *J. Org. Chem*. **1991**, *56*, 3009-3016.

18. Dueholm, K. L.; Egholm, M.; Behrens, C.; Christensen, L.; Hansen, H. F.; Vulpius, T.; Petersen, K. H.; Berg, R. H.; Nielsen, P. E.; Buchardt, O. Synthesis of peptide nucleic acid monomers containing the four natural bases: Thymine, cytosine, adenine, and guanine and their oligomerization. *J. Org. Chem*. **1994**, *59*, 5767-5773.

19. Merrifield, R. B. Solid phase synthesis I. The synthesis of a tetrapeptide. *J. Am. Chem. Soc*. **1963**, *85*, 2149-2154.

20. Christensen, L.; Fitzpatrick, R.; Gildea, B.; Petersen, K.; Hansen, H. F.; Koch, C.; Egholm, M.; Buchardt, O.; Nielsen, P. E.; Coull, J.; Berg, R. H. Solid-phase synthesis of peptide nucleic acids. *J. Peptide Sci.* **1995**, *3*, 175-183.

21. Anderson, G. W.; McGreoger, A. C. *t*-Butyloxycarbonyl aminoacids and their use in peptide synthesis. *J. Am. Chem. Soc*. **1957**, *79*, 6180-6183.

22. (a) Thomson, S. A.; Josey, J. A.; Cadilla, R.; Gaul, M. D.; Hassman, C. F.; Luzzio, M. J. Fmoc mediated synthesis of peptide nucleic acids. *Tetrahedron*, **1995**, *51*, 6179-6194. (b) Goodnow, R. A.; Jr. Richou, A-R.; Tam, S. Synthesis of thymine, cytosine, adenine, and guanine containing *N*-Fmoc protected amino acids: building blocks for construction of novel oligonucleotide backbone analogs. *Tetrahedron Lett.* **1997**, *38*, 3195 -3198.

23. Erickson, B. W.; Merrifield, R. B. Solid phase Peptide Synthesis. In the proteins Vol. II, 3rd ed.; Neurath, H. and Hill, R. L. eds.; Academic Press, New York, **1976**, pp 255.

24. (a) Kaiser, E.; Colescott, R. L.; Bossinger, C. D.; Cook, P. I. Color test for the detection of free terminal amino groups in the solid phase synthesis of peptides. *Anal. Biochem*. **1970**, *34*, 595-598. (b) Kaiser, E.; Bossinger, C. D.; Cplescott, R. L.; Olsen, D. B. Color test for terminal prolyl residues in the solid phase synthesis of peptides. *Anal. Chim. Acta*. **1980**, *118*, 149-151.

25. (a) Gait, J. M; Oligonucleotide synthesis: A practical approach. *IRL Press Oxford*, Uk, **1984**, *217.* (b) Agrawal, S. in Protocols for oligonucleotides and analogs: Synthesis and properties. *Methods in Molecular Biology*. Agrawal, S. (ed), vol 20, Totowa, NJ. Humana Press, Inc., **1993**.

26. (a) Job, P. *Ann. Chim*. **1928**, *9*, 113-203. (b) Cantor, C. R.; Schimmel, P. R.; *Biophys. Chem.Part III*, **1980**, *624.*

27. Kim, S. K.; Nielsen, P. E.; Egholm, M.; Buchardt, O.; Berg, R. H.; Norden, B. Right-handed triplex formed between peptide nucleic acid PNA-T8 and poly(dA) shown by linear and circular dichroism spectroscopy. *J. Am. Chem. Soc.* **1993**, *115*, 6477-6481.

28. Soyfer, V. N.; Potaman, V. N. Triple Helical Nucleic Acids, Eds **1996**, *Springler-Verlag, New York.*

29. Beavis R. C.; Chait B. T. Matrix-assisted laser-desorption mass spectrometry using 355 nm radiation. *Rapid Commun. Mass Spectrom.* **1989**, *3*, 436-439.

30. Beavis, R. C. α-Cyano-4-hydroxycinnamic acid as a matrix for matrix-assisted laser desorption mass spectrometry. *Org. Mass Spectrom.* **1992**, *27*, 156-158.

2.10 Appendix

Compound **Page No.**

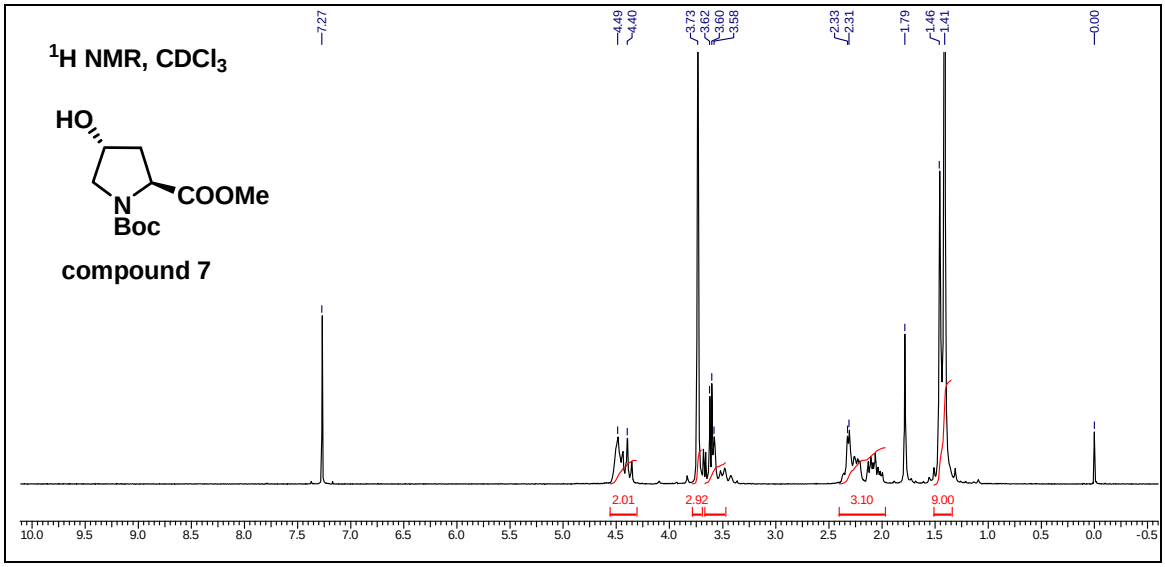
^{1}H NMR, CDCl$_3$
HO
N
Boc
COOMe
compound 7
7.27
4.49
4.40
3.73
3.62
3.60
3.58
2.33
2.31
1.79
1.46
1.41
0.00
2.01
2.92
3.10
9.00

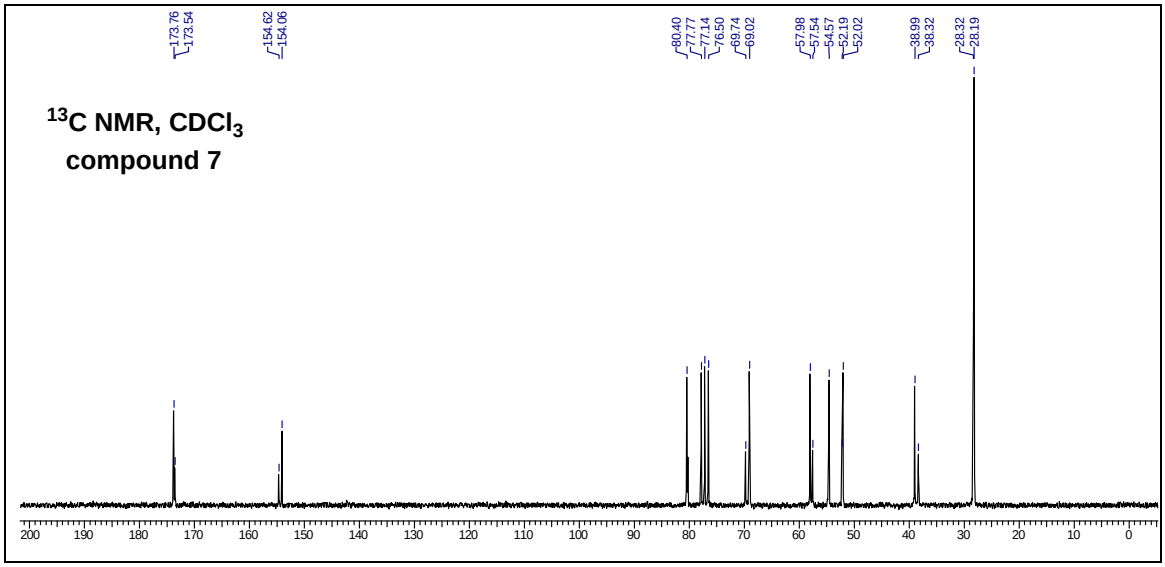
^{13}C NMR, CDCl$_3$
compound 7
173.76
173.54
154.62
154.06
80.40
77.77
77.14
76.50
69.74
69.02
57.98
57.54
54.57
52.19
52.02
38.99
38.32
28.32
28.19

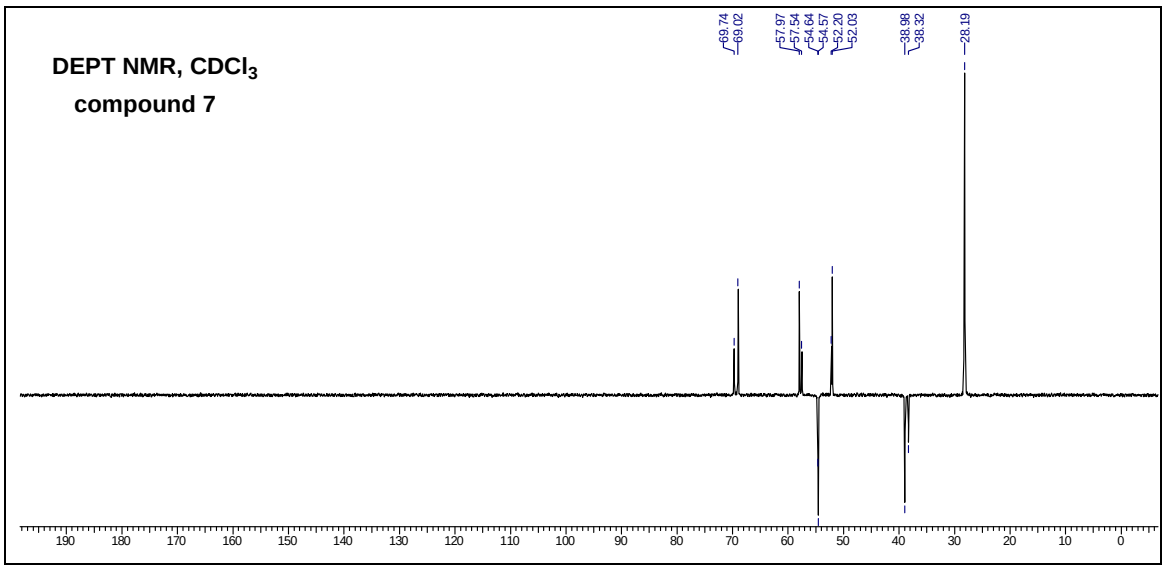
DEPT NMR, CDCl$_3$
compound 7
69.74
69.02
57.97
57.54
54.64
54.57
52.20
52.03
38.98
38.32
28.19

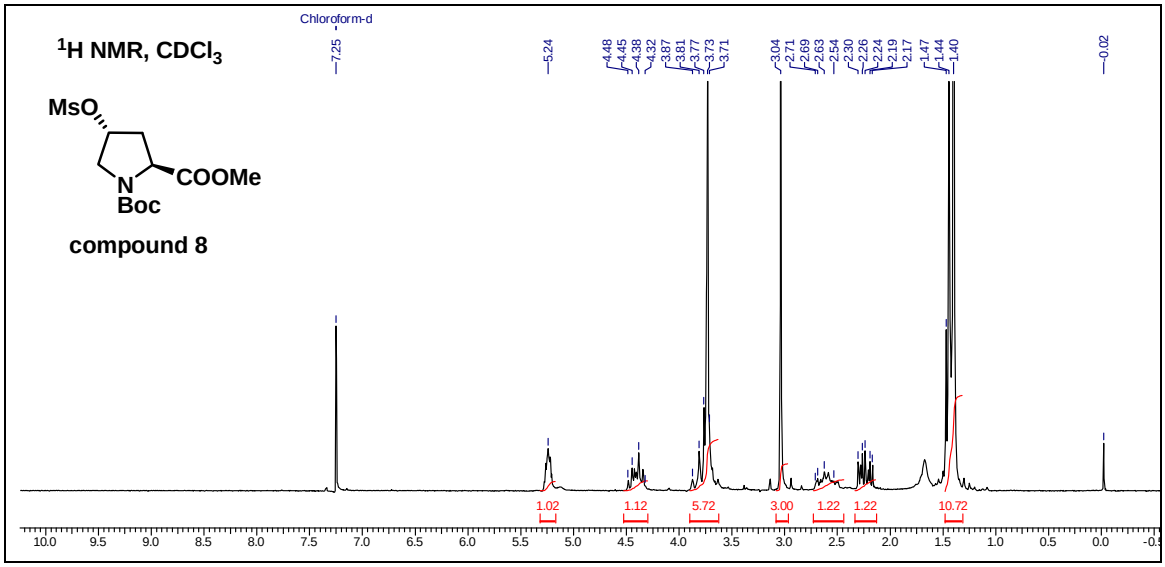
^{1}H NMR, CDCl$_3$
MsO
N
Boc
COOMe
compound 8
Chloroform-d
7.25
5.24
4.48
4.45
4.38
4.32
3.87
3.81
3.77
3.73
3.71
3.04
2.71
2.69
2.63
2.54
2.30
2.26
2.24
2.19
2.17
1.47
1.44
1.40
0.02
1.02
1.12
5.72
3.00
1.22
1.22
10.72

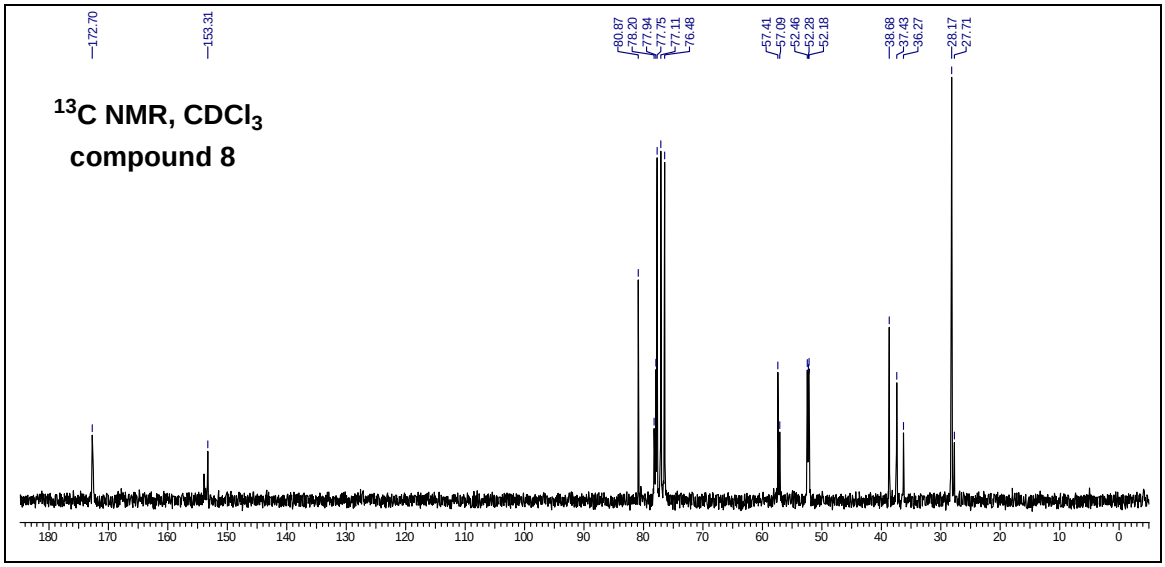
^{13}C NMR, CDCl$_3$
compound 8
172.70
153.31
80.87
78.20
77.94
77.75
77.11
76.48
57.41
57.09
52.46
52.28
52.18
38.68
37.43
36.27
28.17
27.71

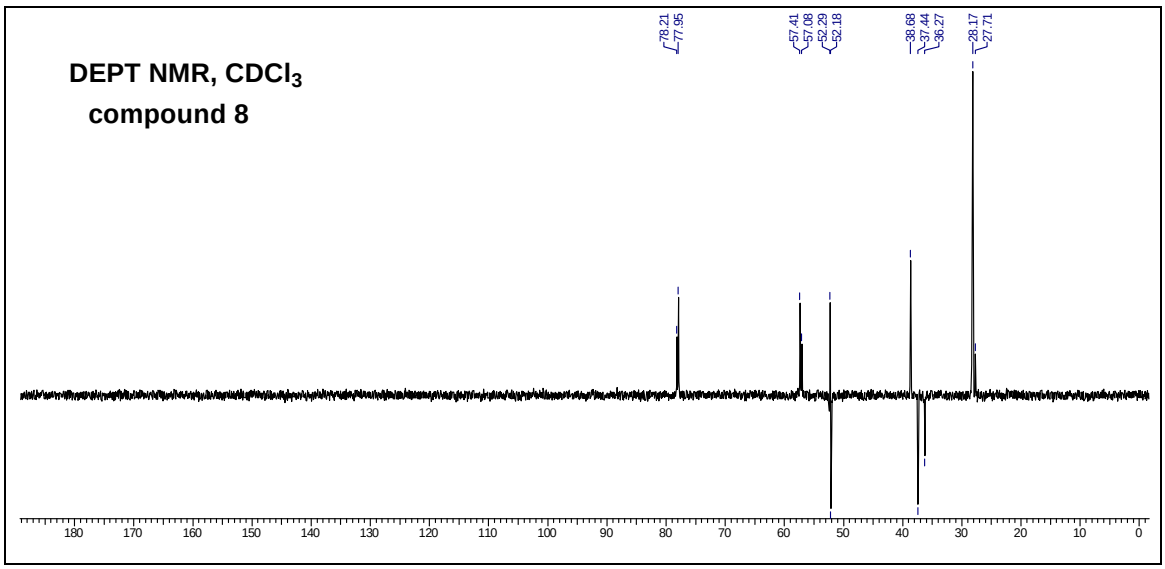
DEPT NMR, CDCl$_3$
compound 8
78.21
77.95
57.41
57.08
52.29
52.18
38.68
37.44
36.27
28.17
27.71

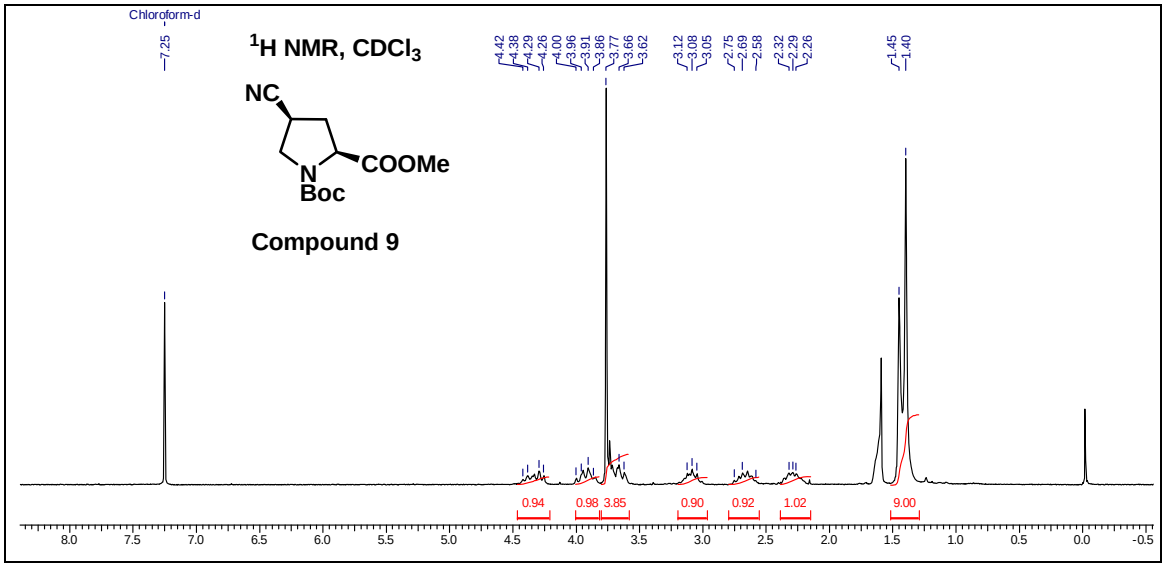
Chloroform-d
7.25
^{1}H NMR, CDCl$_3$
4.42
4.38
4.29
4.26
4.00
3.96
3.91
3.86
3.77
3.66
3.62
3.12
3.08
3.05
2.75
2.69
2.58
2.32
2.29
2.26
1.45
1.40
NC
COOMe
N
Boc
Compound 9
0.94
0.98
3.85
0.90
0.92
1.02
9.00

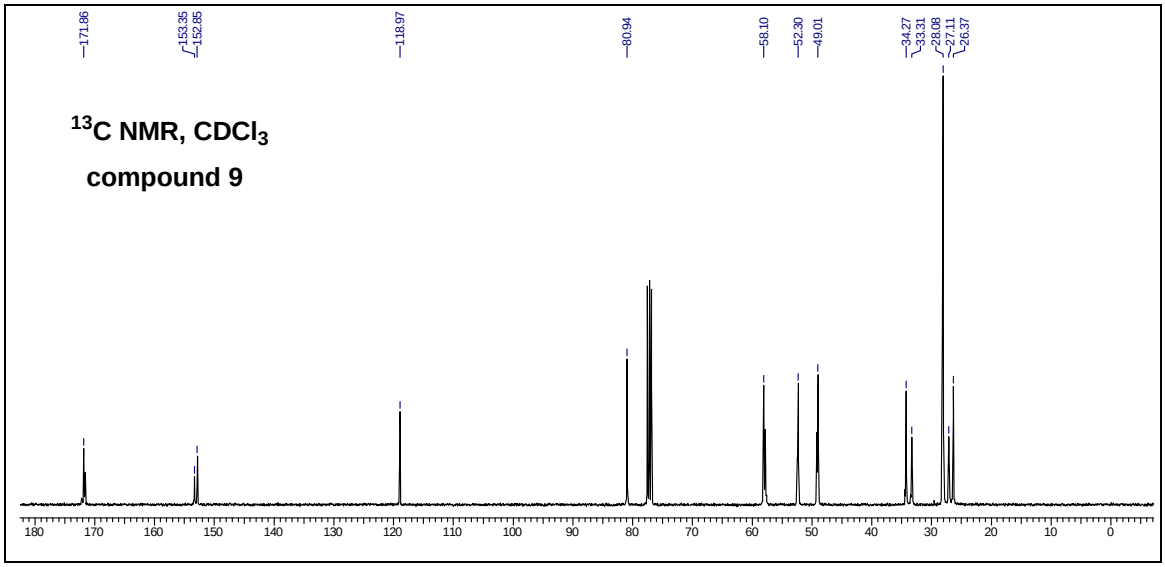
171.86
153.35
152.85
118.97
80.94
58.10
52.30
49.01
34.27
33.31
28.08
27.11
26.37
^{13}C NMR, CDCl$_3$
compound 9

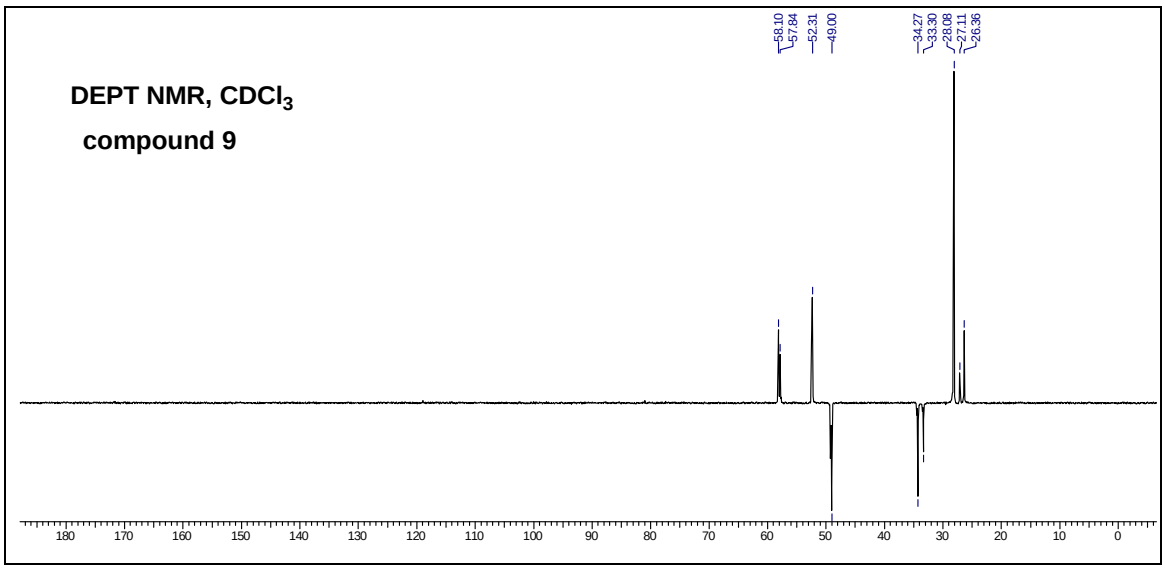
58.10
57.84
52.31
49.00
34.27
33.30
28.08
27.11
26.36
DEPT NMR, CDCl$_3$
compound 9

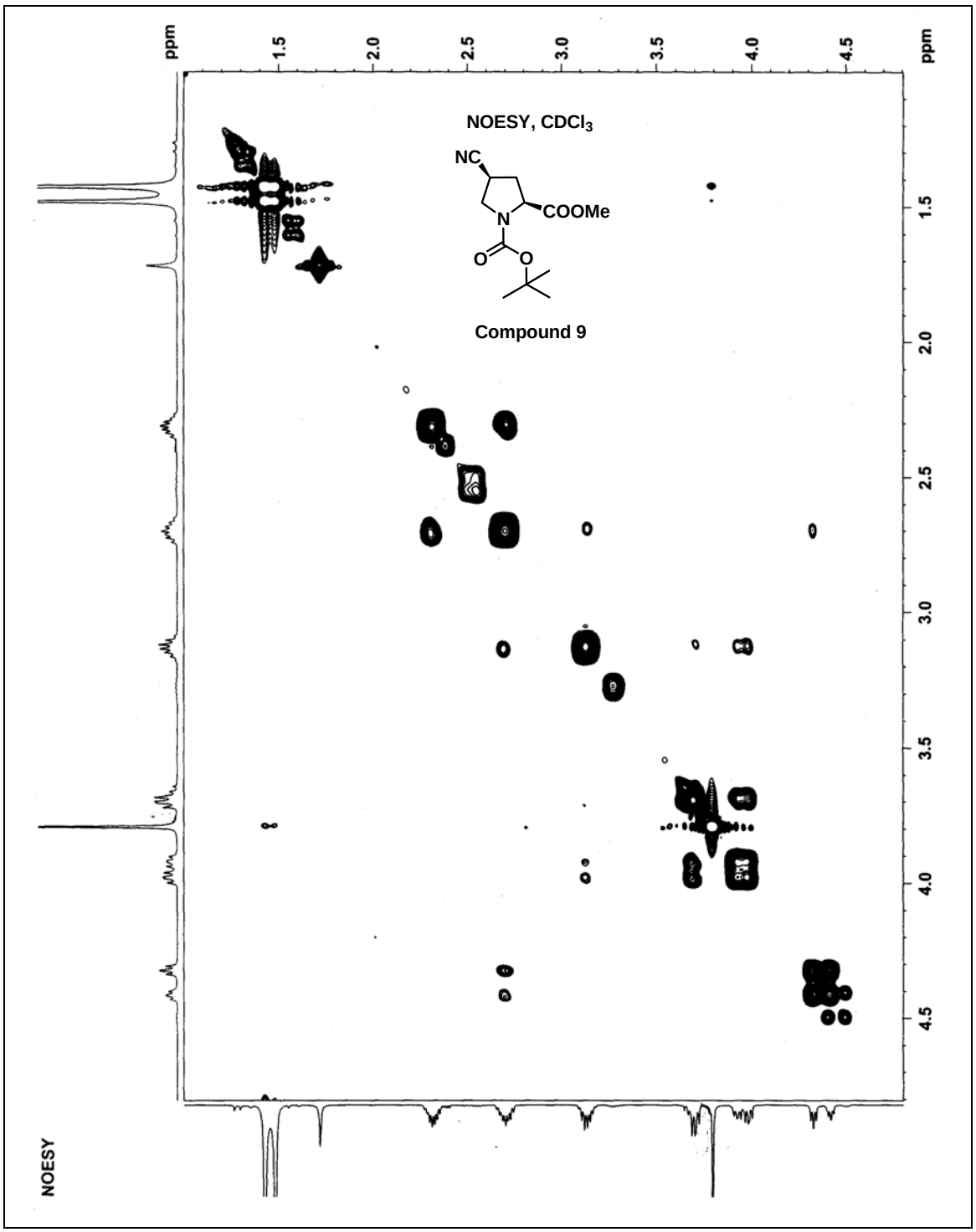
NOESY, CDCl3
NC
COOMe
N
O
O
Compound 9
ppm
1.5
2.0
2.5
3.0
3.5
4.0
4.5
NOESY

COSY, $CDCl_3$

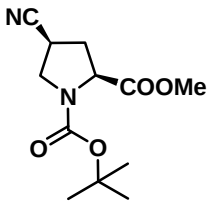

Compound 9

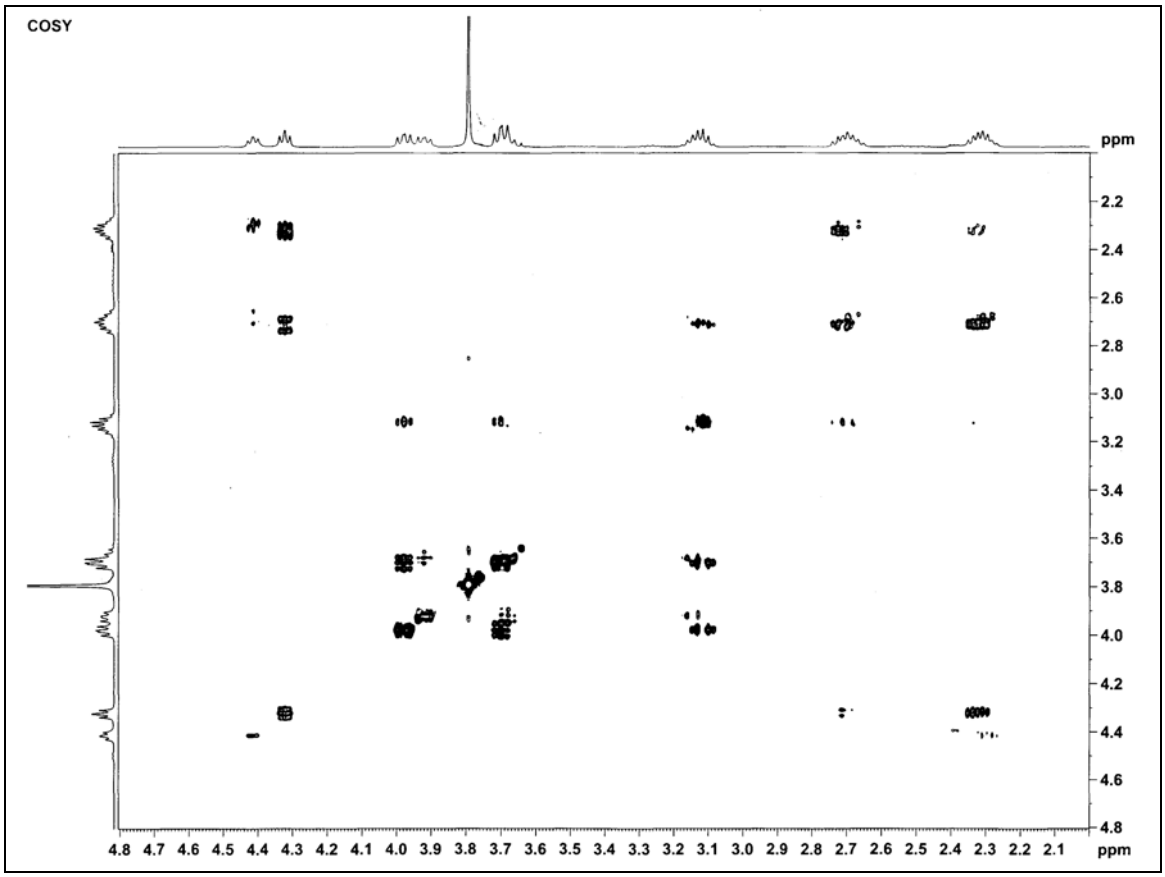

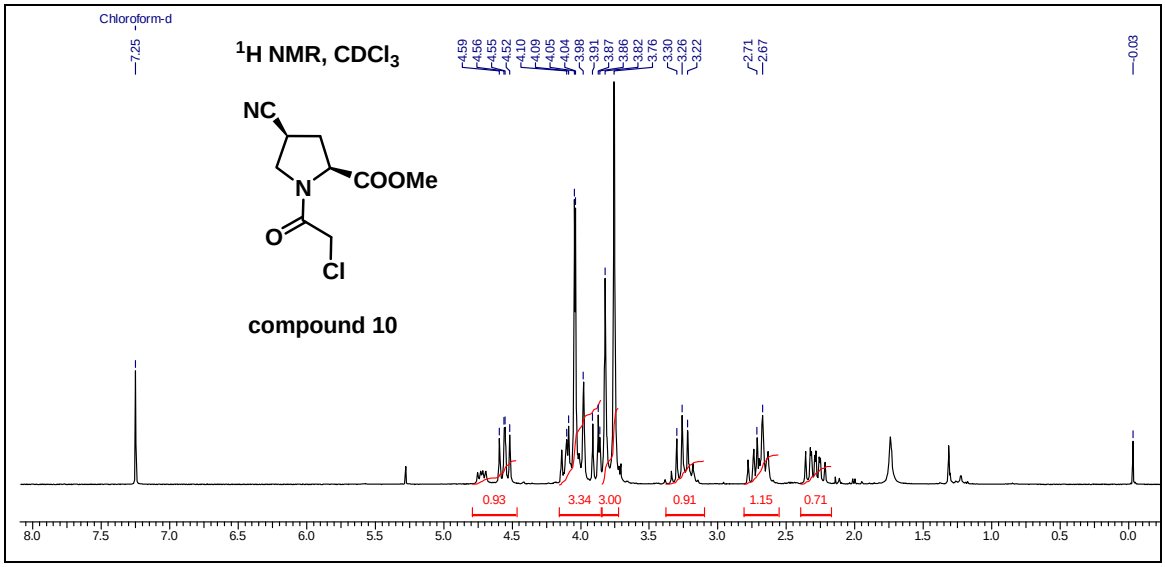
Chloroform-d
7.25
^{1}H NMR, CDCl$_3$
NC
COOMe
N
O
Cl
compound 10
4.59
4.56
4.55
4.52
4.10
4.09
4.05
4.04
3.98
3.91
3.87
3.86
3.82
3.76
3.30
3.26
3.22
2.71
2.67
0.03
0.93
3.34
3.00
0.91
1.15
0.71

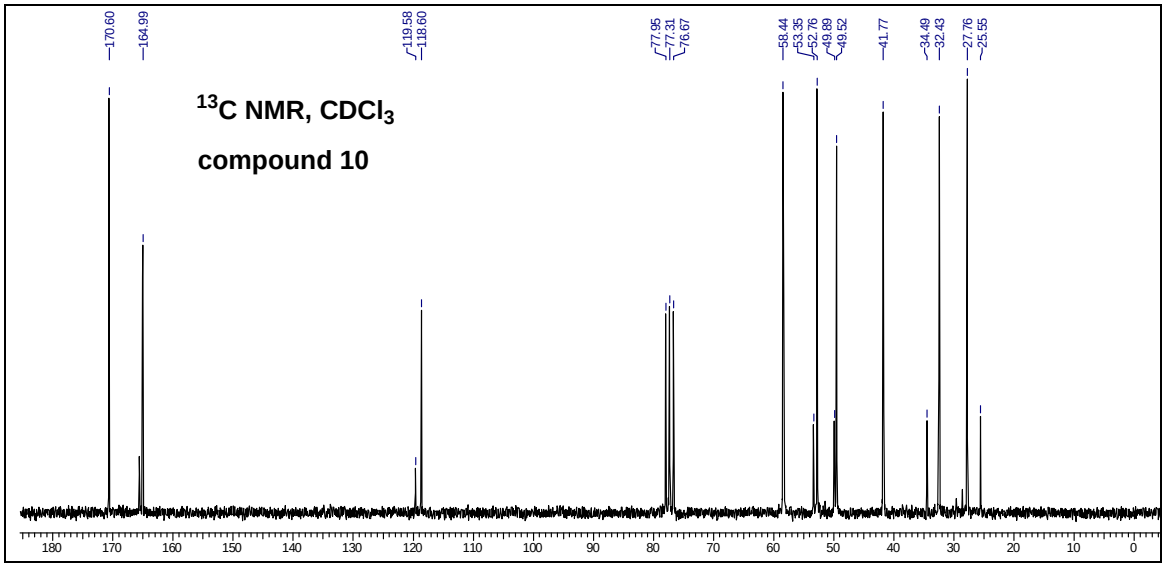
170.60
164.99
119.58
118.60
77.95
77.31
76.67
58.44
53.35
52.76
49.99
49.52
41.77
34.49
32.43
27.76
25.55
^{13}C NMR, CDCl$_3$
compound 10

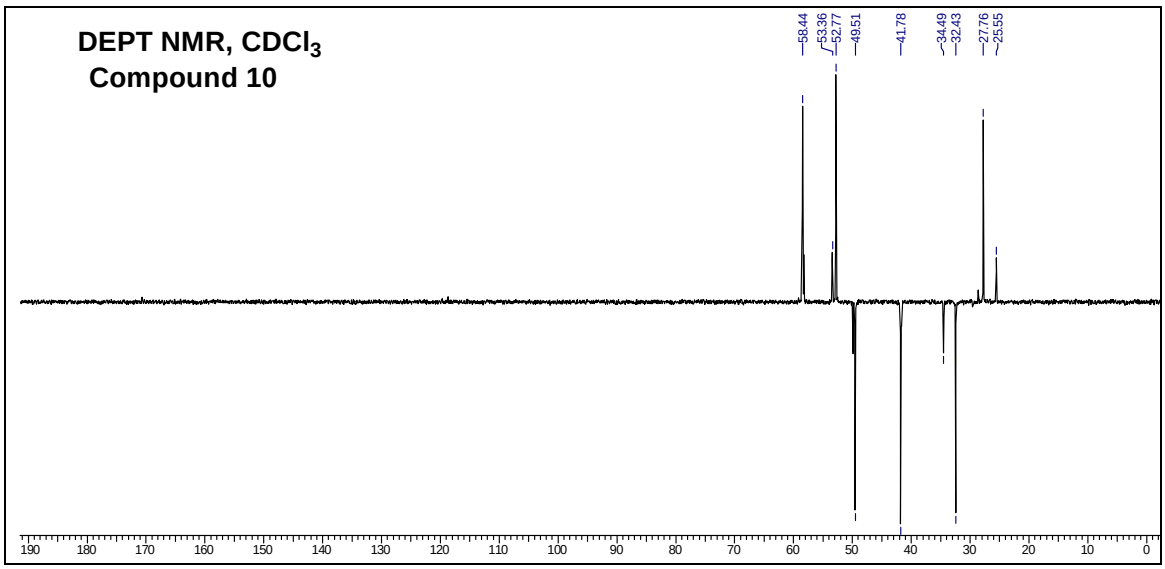
DEPT NMR, CDCl$_3$
Compound 10
58.44
53.36
52.77
49.51
41.78
34.49
32.43
27.76
25.55

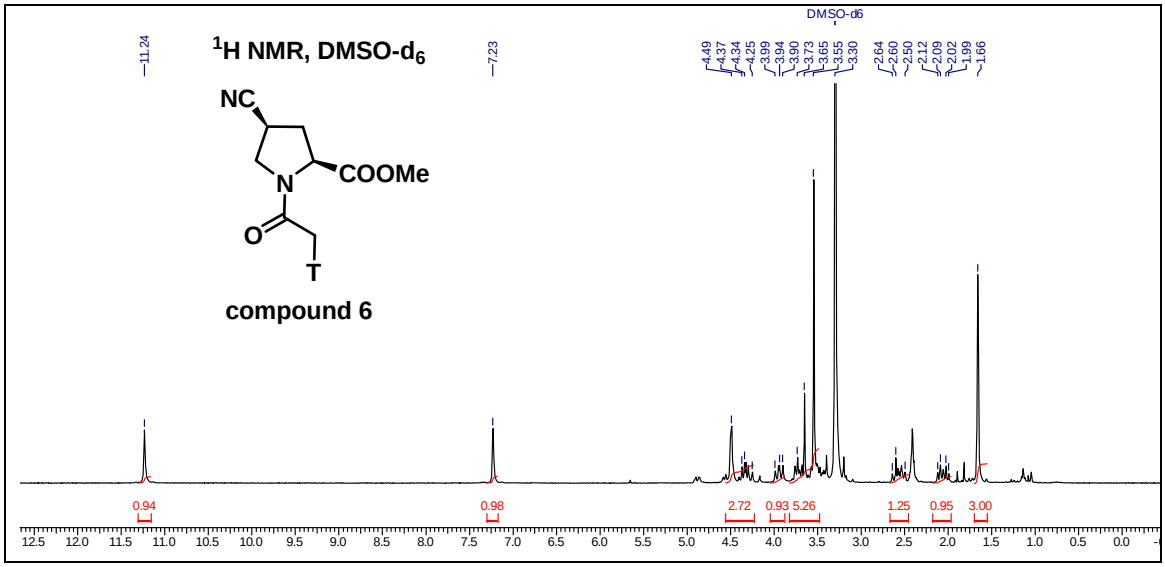
^{1}H NMR, DMSO-d$_6$
NC
COOMe
N
O
T
compound 6
DMSO-d6

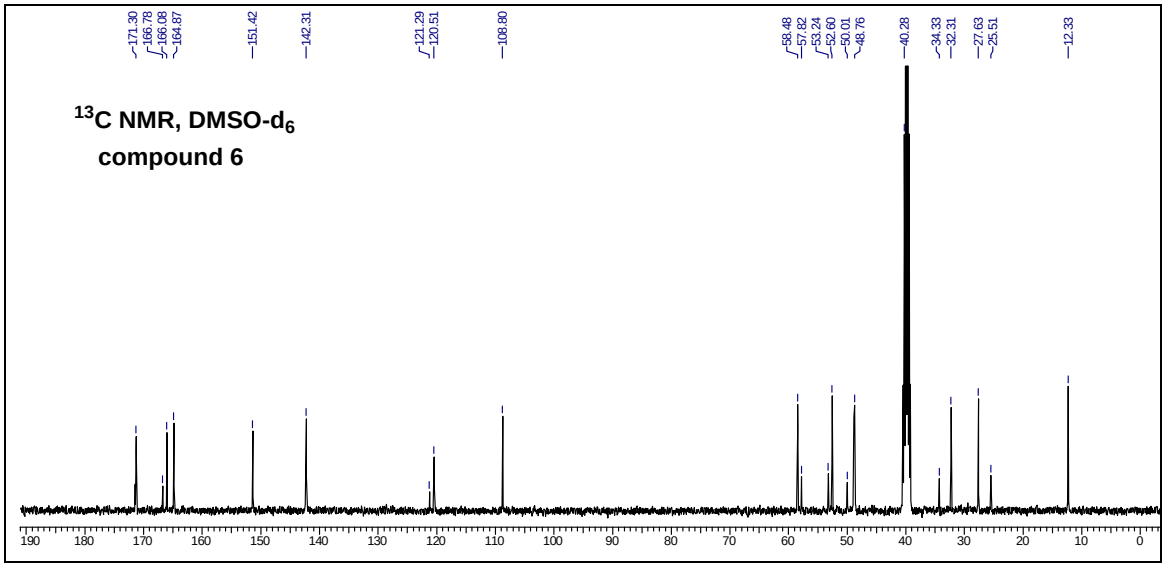
^{13}C NMR, DMSO-d$_6$
compound 6

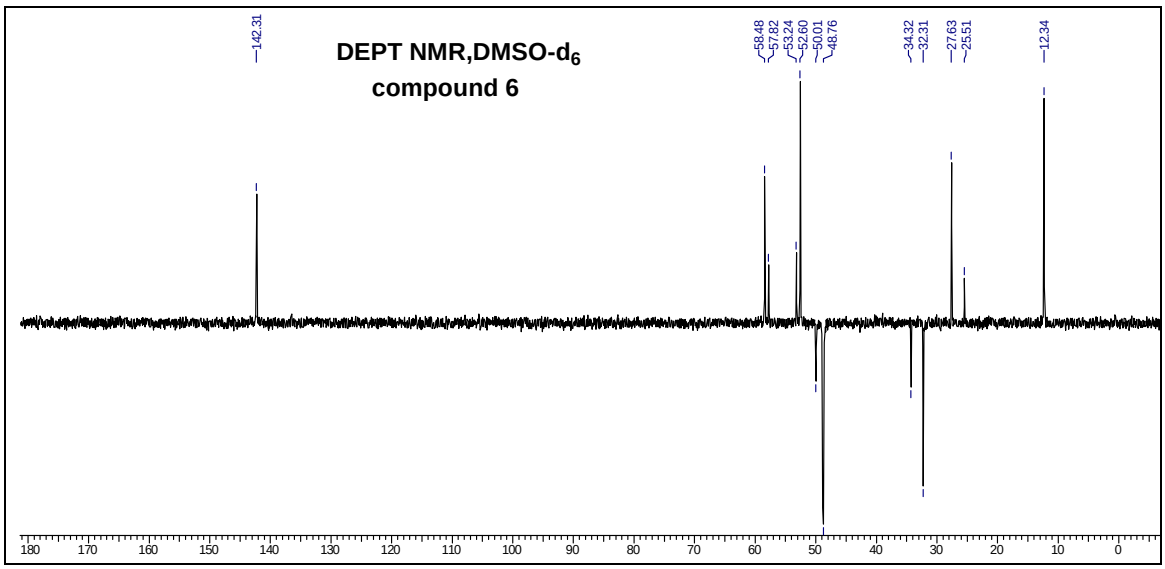
DEPT NMR,DMSO-d$_6$
compound 6

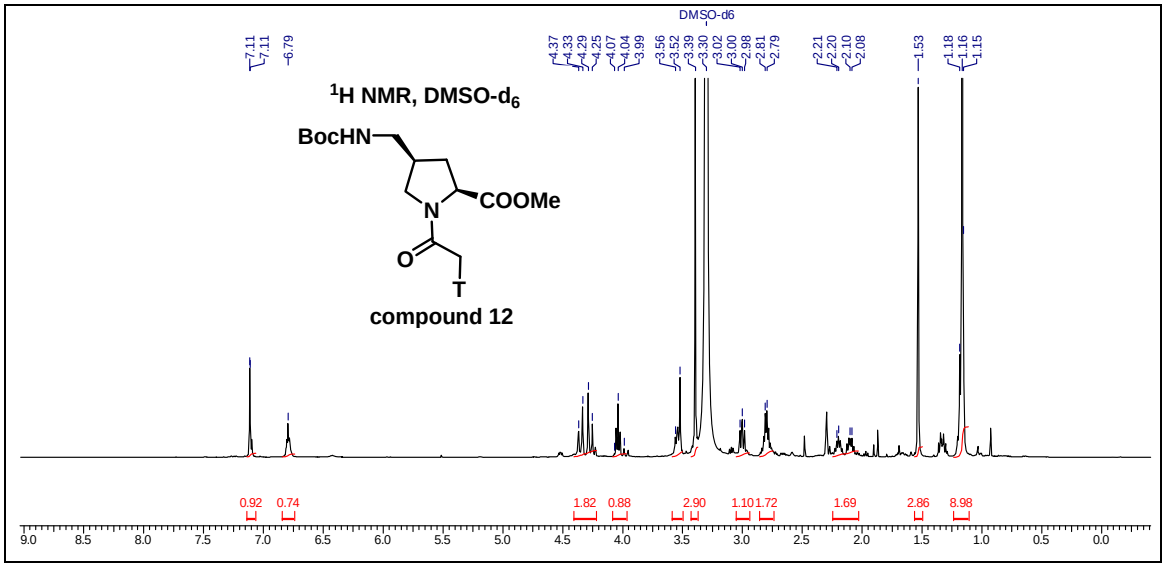
DMSO-d6
^{1}H NMR, DMSO-d$_6$
BocHN
COOMe
N
O
T
compound 12

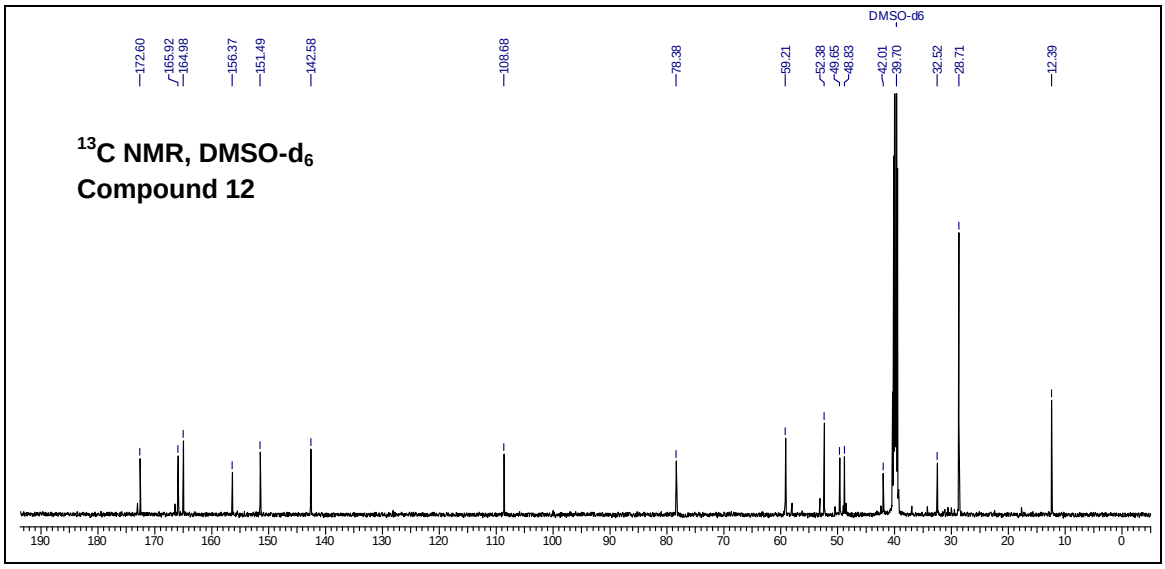
DMSO-d6
^{13}C NMR, DMSO-d$_6$
Compound 12

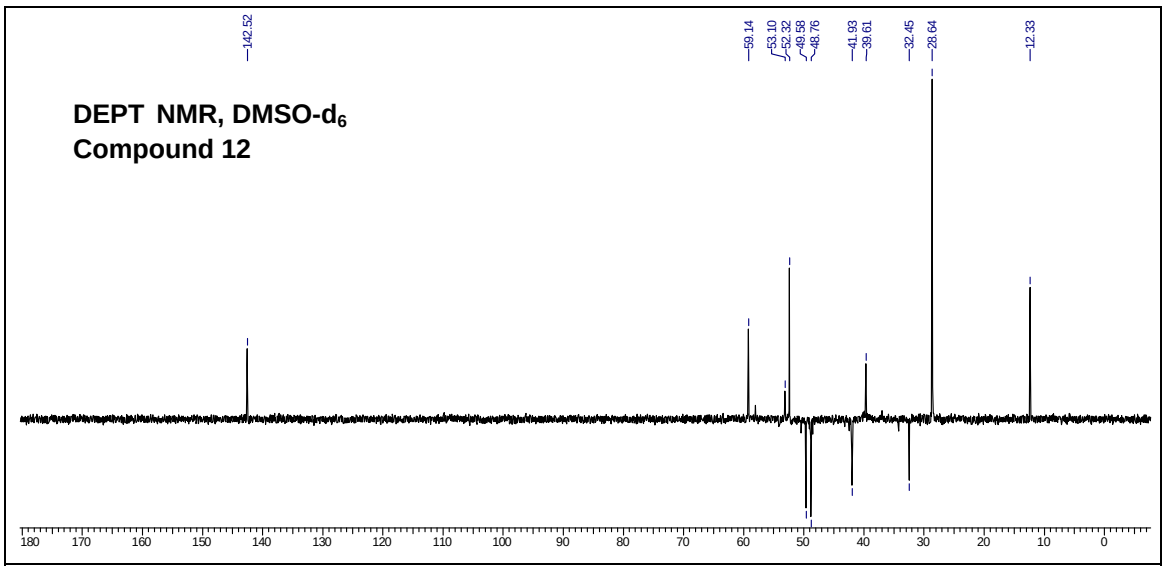
DEPT NMR, DMSO-d$_6$
Compound 12

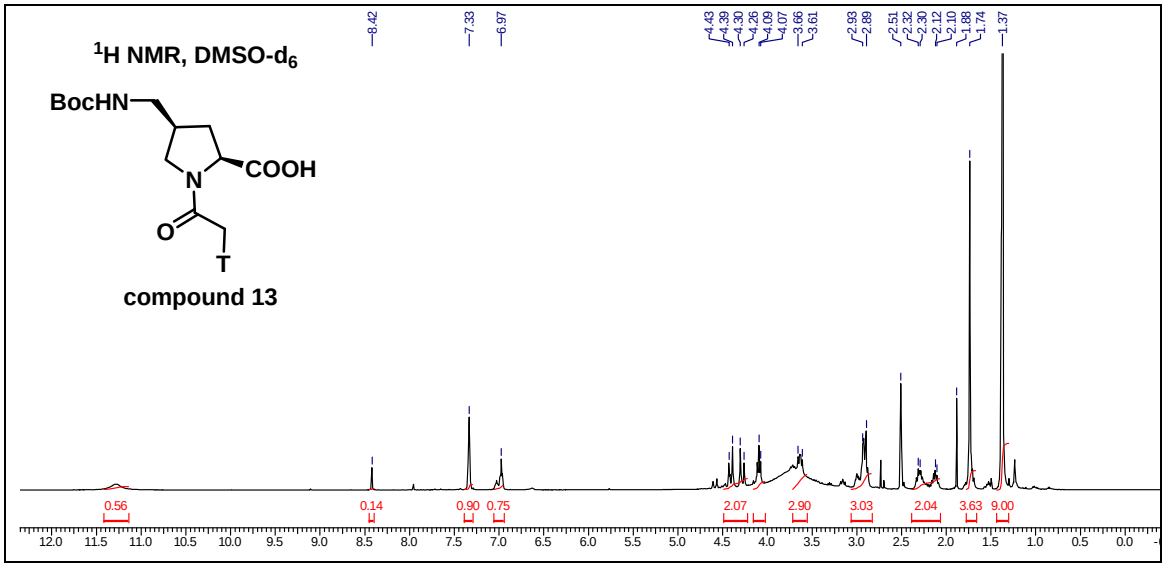
^{1}H NMR, DMSO-d$_6$
BocHN
COOH
N
O
T
compound 13

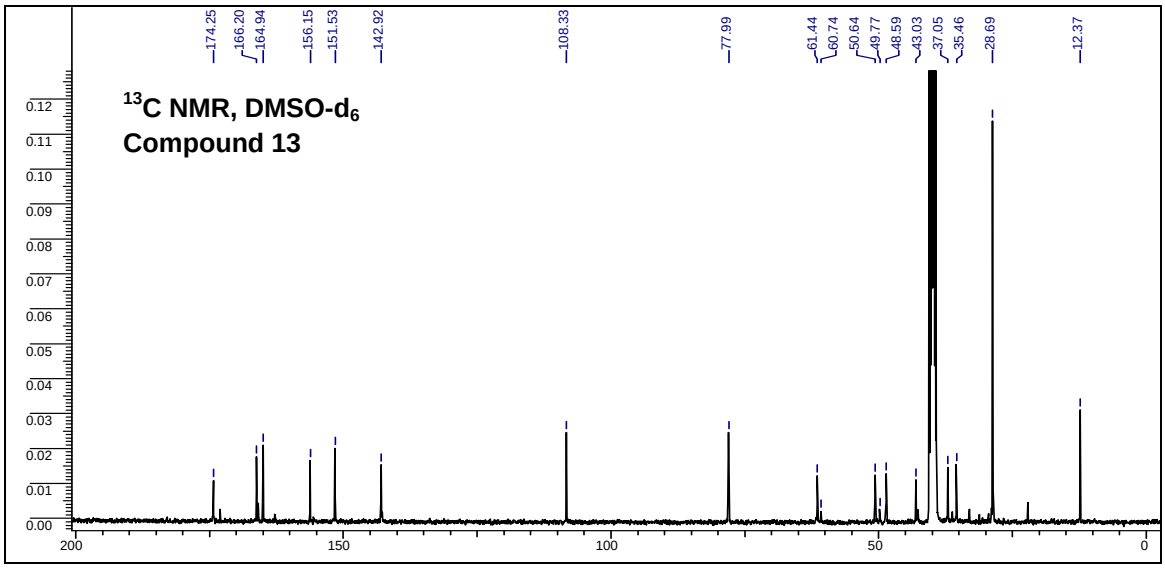
^{13}C NMR, DMSO-d$_6$
Compound 13

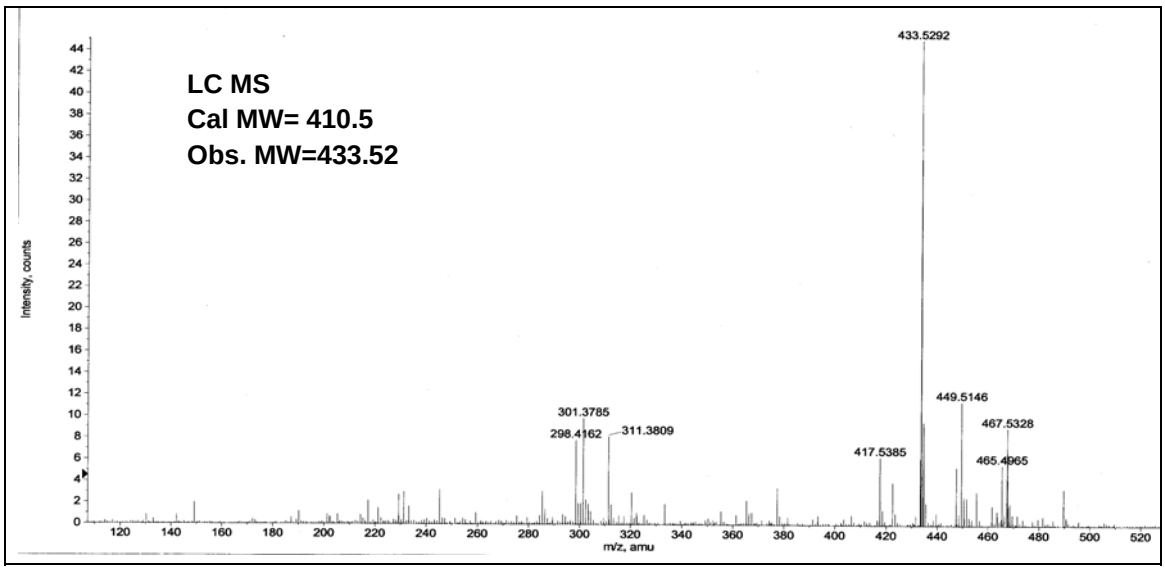
LC MS
Cal MW= 410.5
Obs. MW=433.52
Intensity, counts
m/z, amu

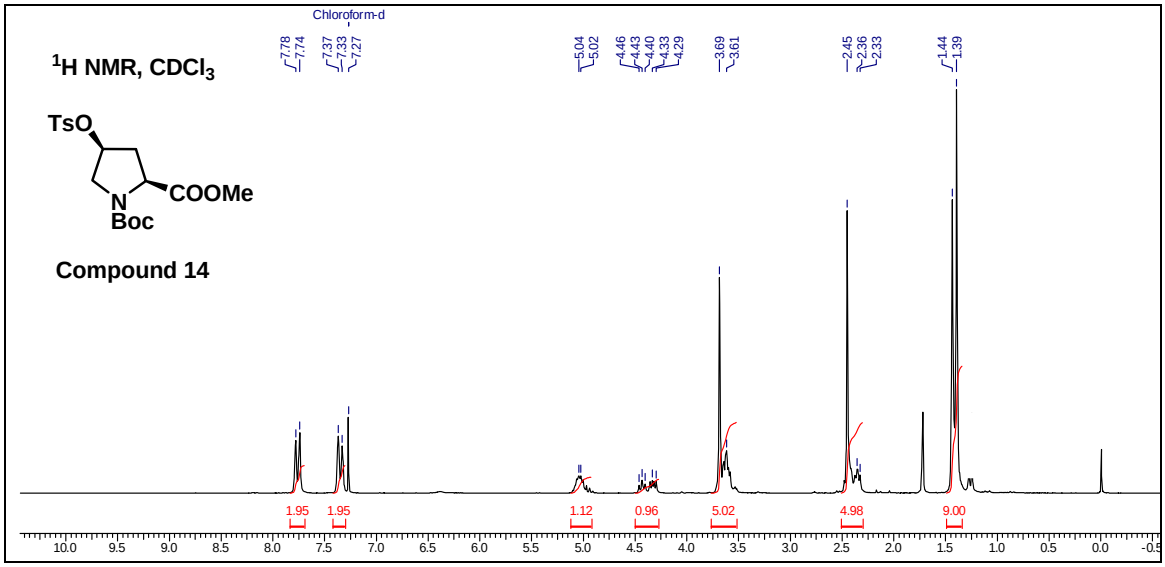
Chloroform-d
^{1}H NMR, CDCl$_3$
TsO
COOMe
N
Boc
Compound 14
7.78
7.74
7.37
7.33
7.27
5.04
5.02
4.46
4.43
4.40
4.33
4.29
3.69
3.61
2.45
2.36
2.33
1.44
1.39
1.95
1.95
1.12
0.96
5.02
4.98
9.00

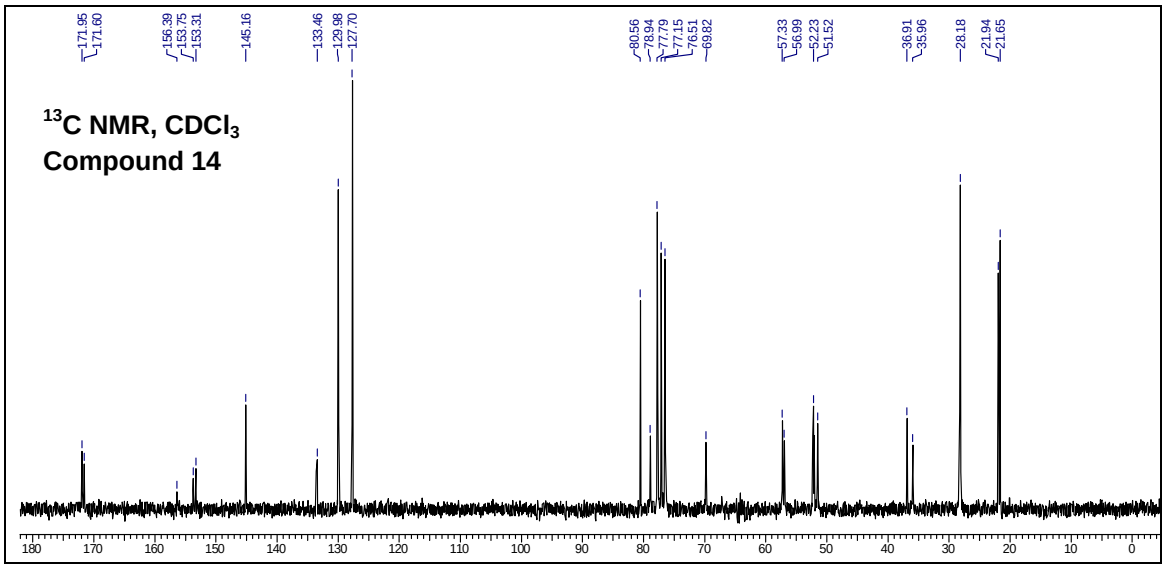
^{13}C NMR, CDCl$_3$
Compound 14
171.95
171.60
156.39
153.75
153.31
145.16
133.46
129.98
127.70
80.56
78.94
77.79
77.15
76.51
69.82
57.33
56.99
52.23
51.52
36.91
35.96
28.18
21.94
21.65

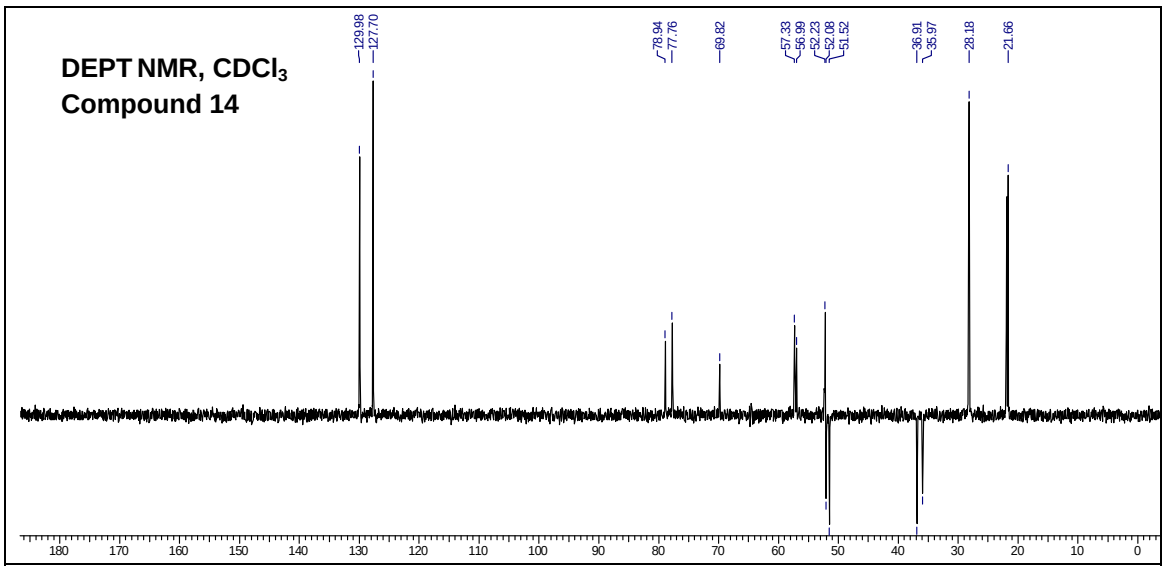
DEPT NMR, CDCl$_3$
Compound 14
129.98
127.70
78.94
77.76
69.82
57.33
56.99
52.23
52.08
51.52
36.91
35.97
28.18
21.66

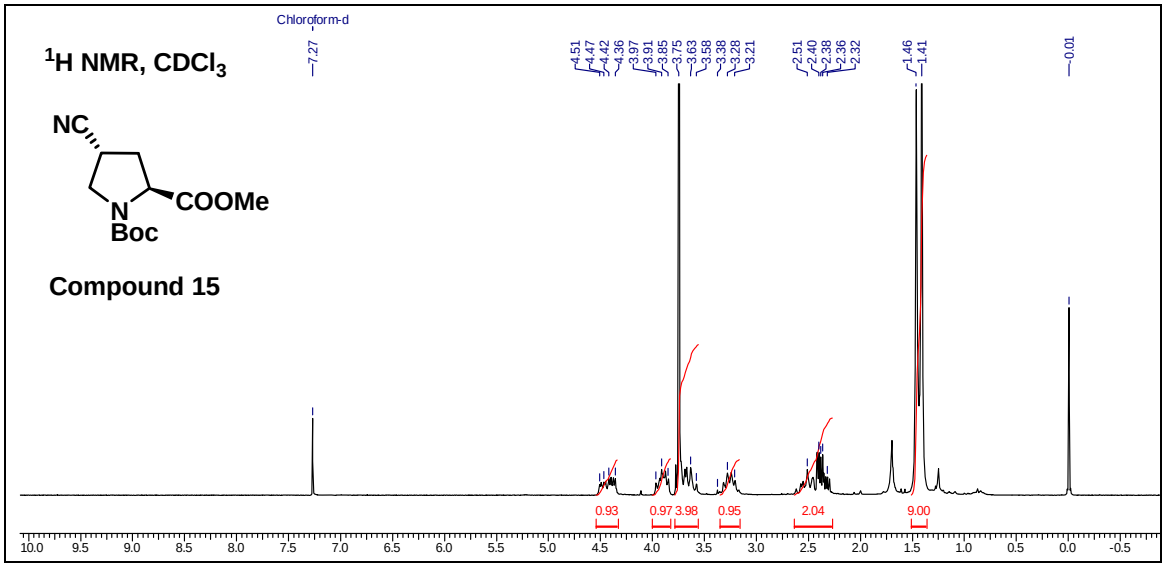

^{1}H NMR, $CDCl_3$

Compound 15

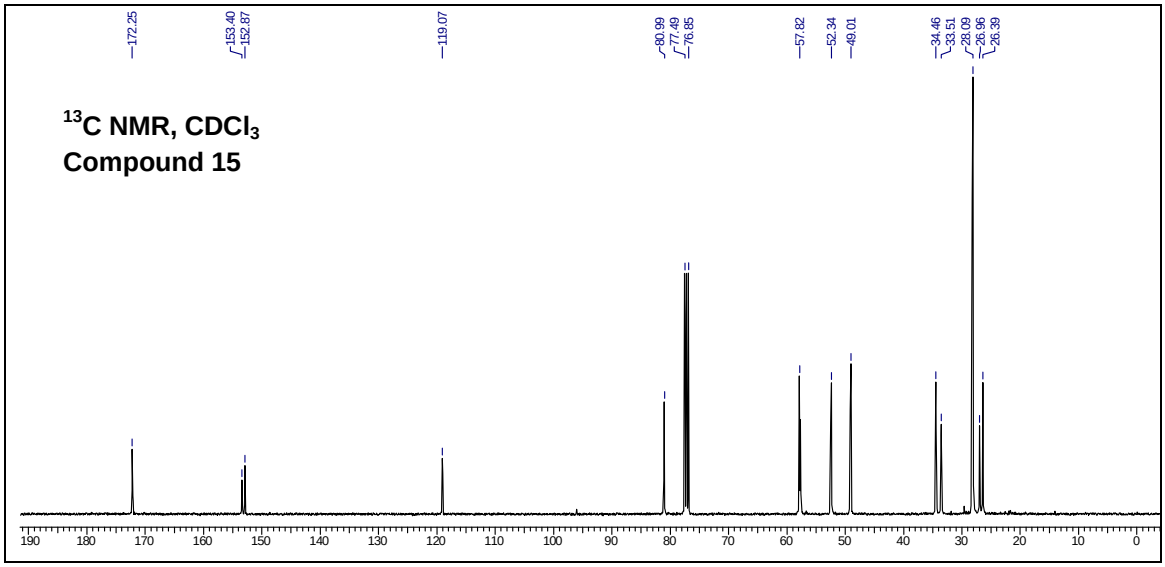

^{13}C NMR, $CDCl_3$
Compound 15

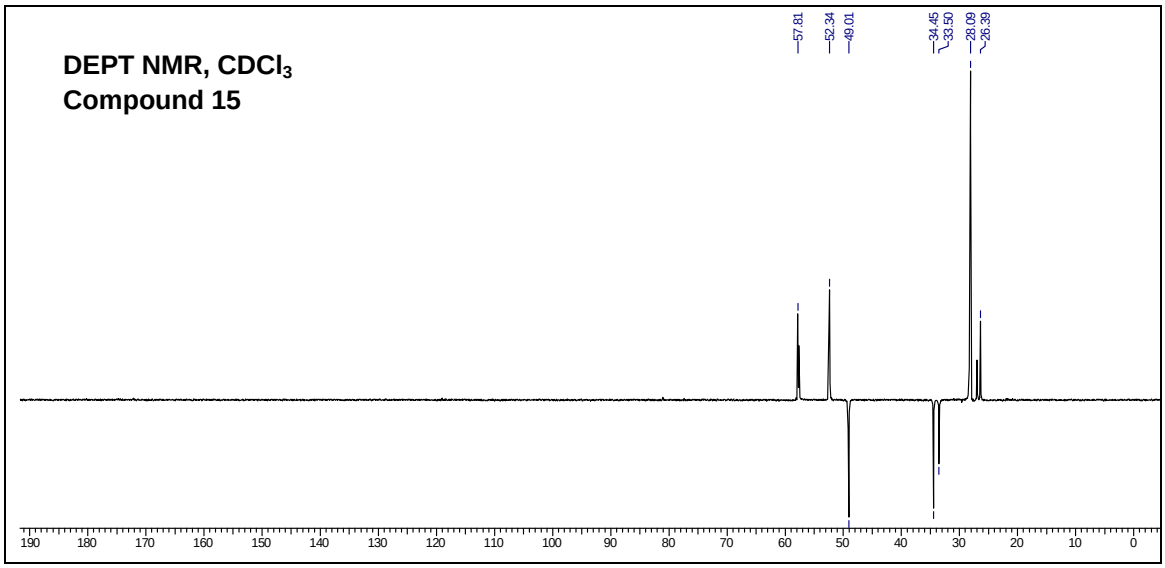

DEPT NMR, $CDCl_3$
Compound 15

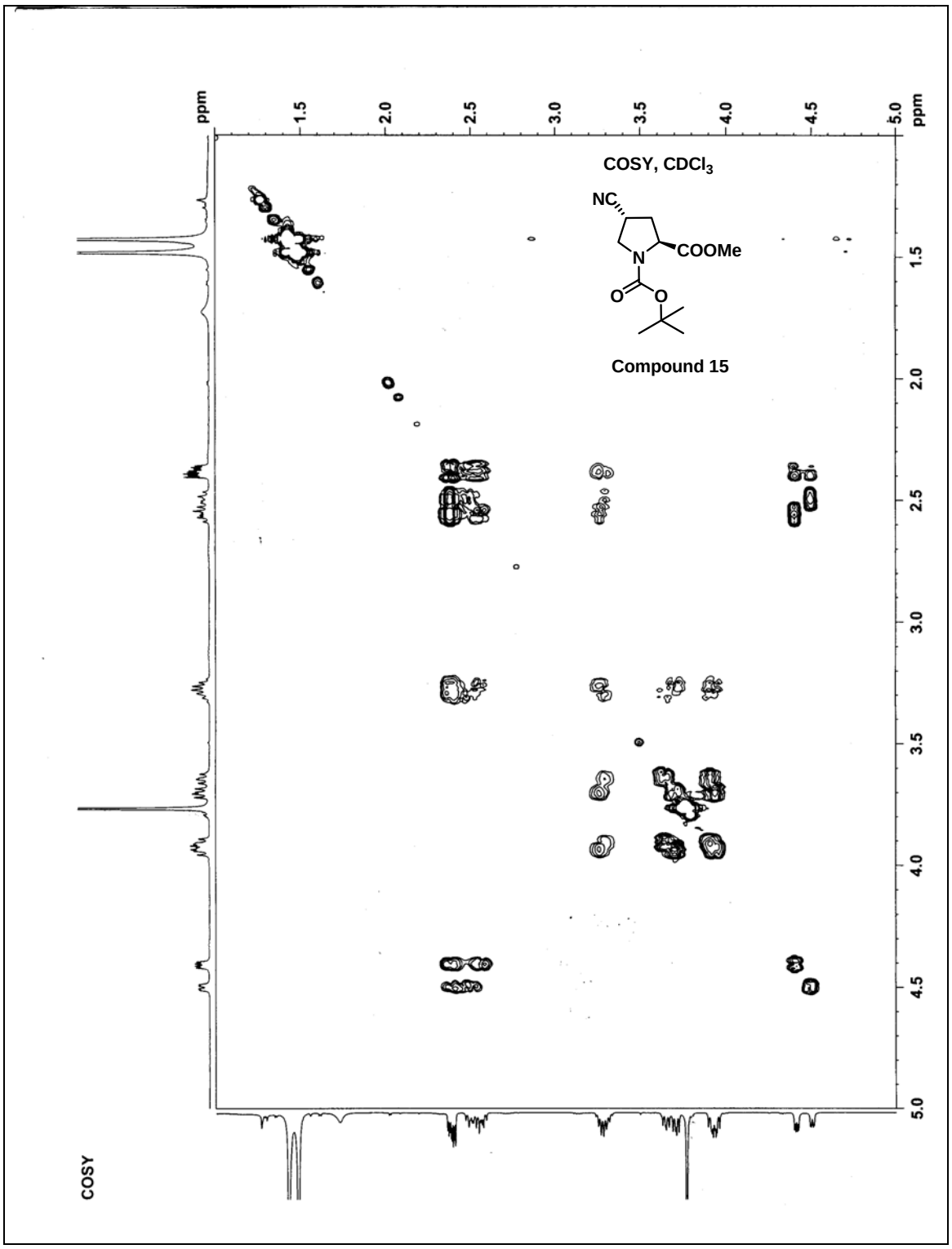
COSY, CDCl3
NC
COOMe
N
O
O
Compound 15
ppm
1.5
2.0
2.5
3.0
3.5
4.0
4.5
5.0
COSY

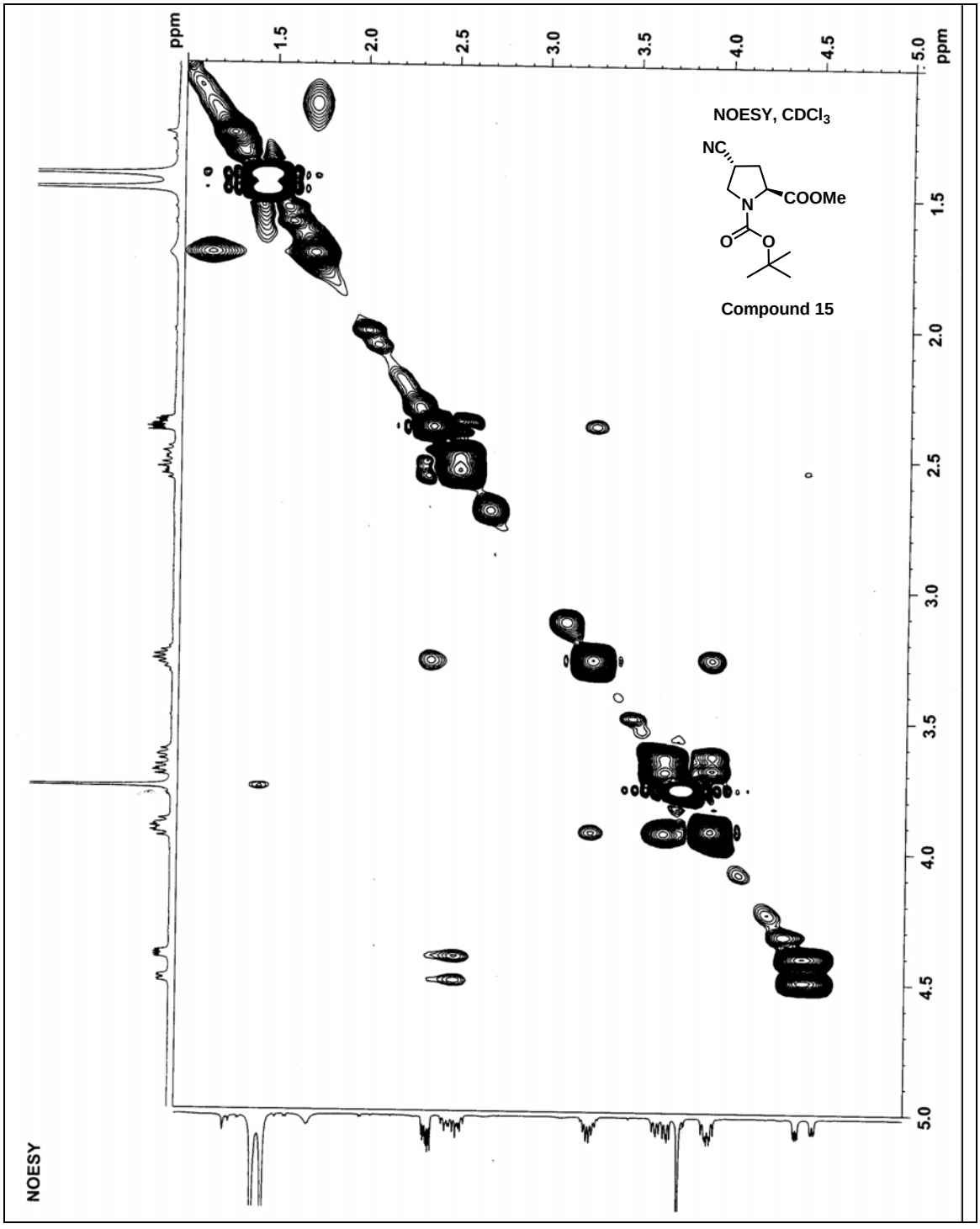
NOESY, CDCl3
NC
COOMe
N
O
O
Compound 15
NOESY
ppm
1.5
2.0
2.5
3.0
3.5
4.0
4.5
5.0

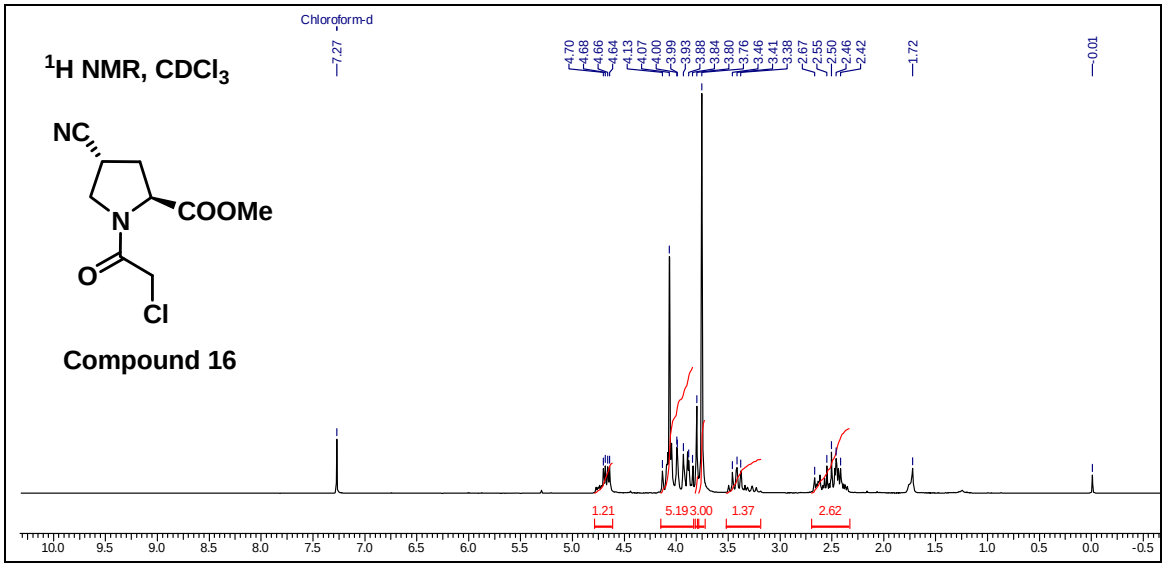

^{1}H NMR, $CDCl_3$

Compound 16

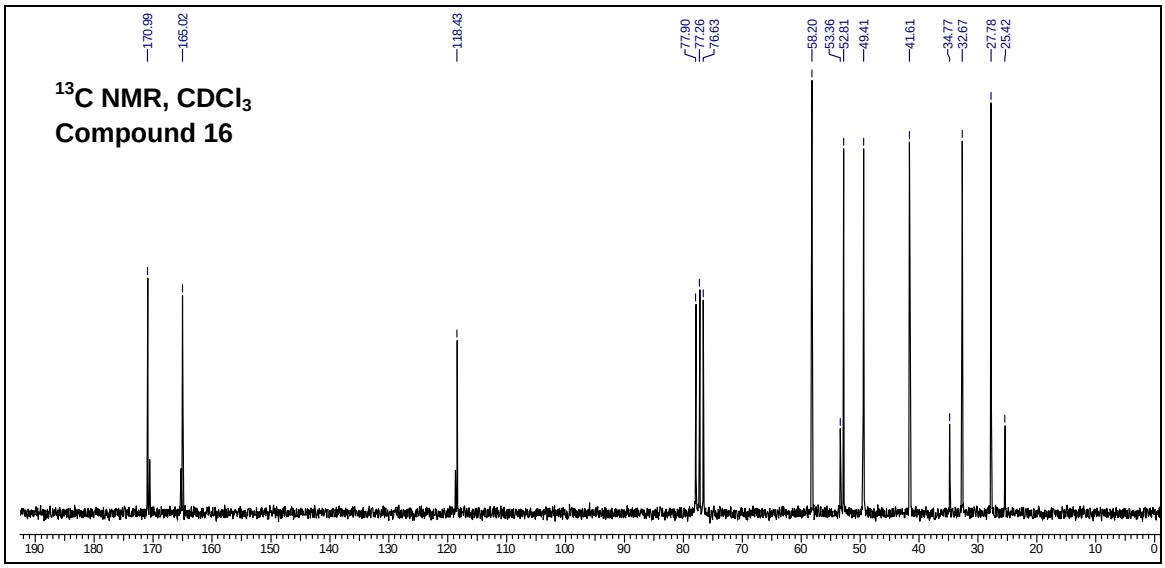

^{13}C NMR, $CDCl_3$
Compound 16

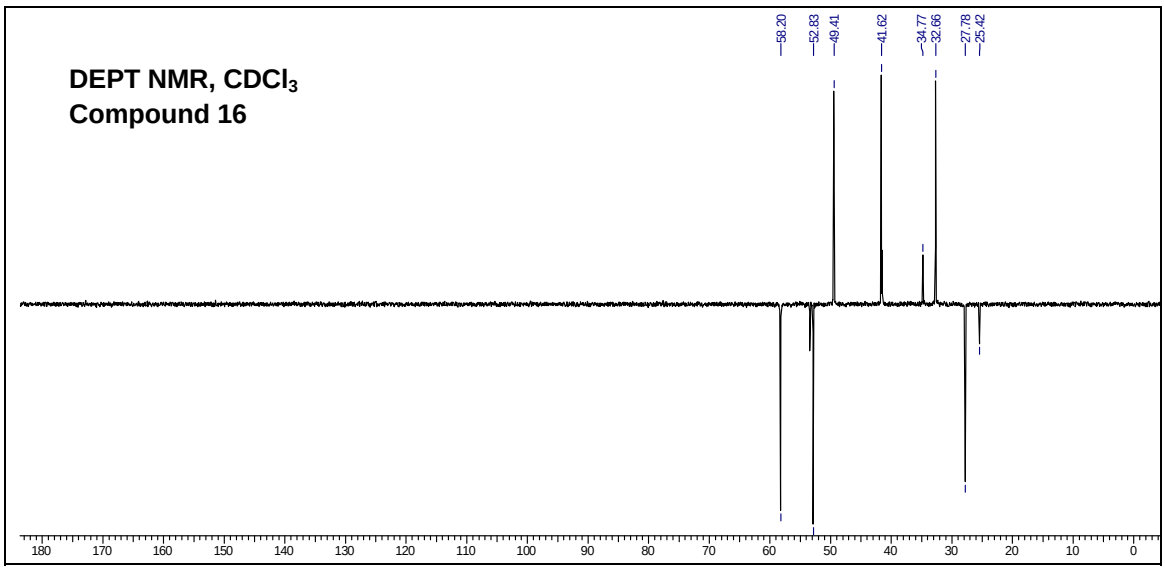

DEPT NMR, $CDCl_3$
Compound 16

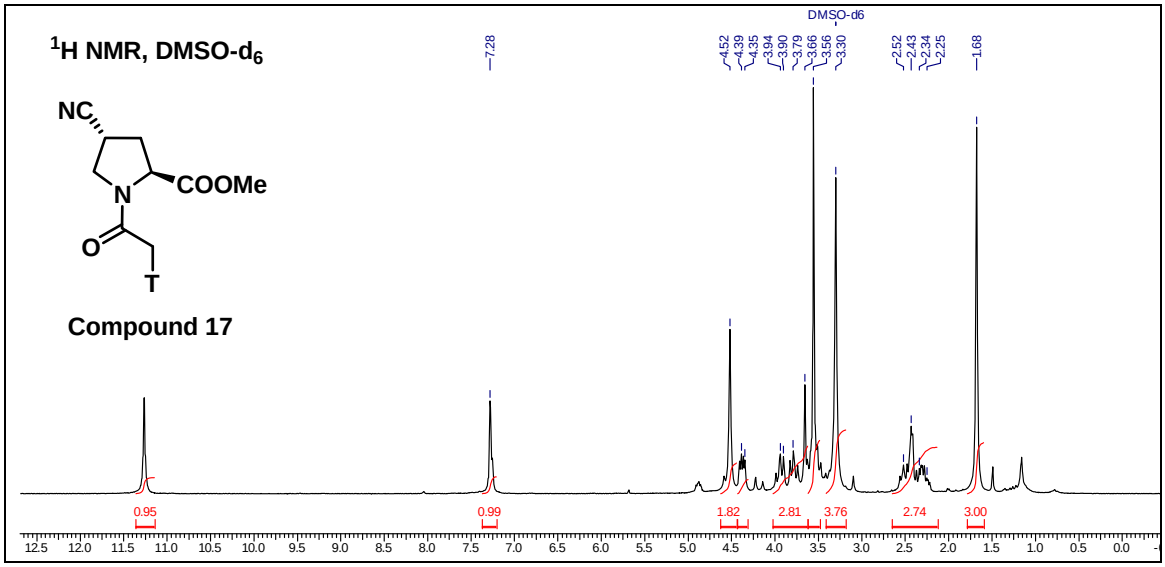
^{1}H NMR, DMSO-d$_6$
NC
COOMe
N
O
T
Compound 17
DMSO-d6
7.28
4.52
4.39
4.35
3.94
3.90
3.79
3.66
3.56
3.30
2.52
2.43
2.34
2.25
1.68
0.95
0.99
1.82
2.81
3.76
2.74
3.00

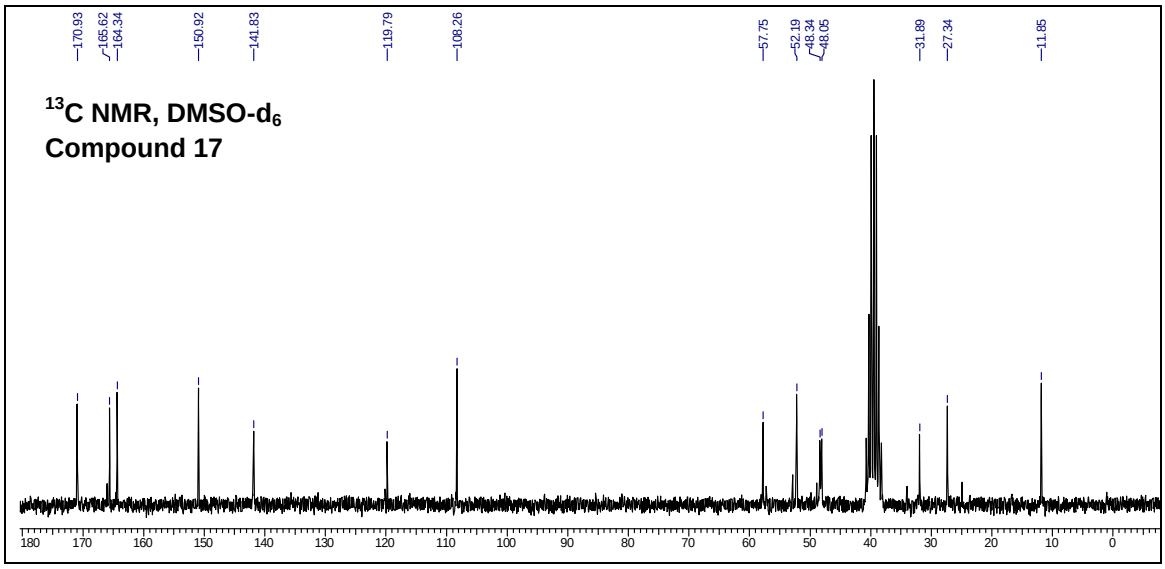
^{13}C NMR, DMSO-d$_6$
Compound 17
170.93
165.62
164.34
150.92
141.83
119.79
108.26
57.75
52.19
48.34
48.05
31.89
27.34
11.85

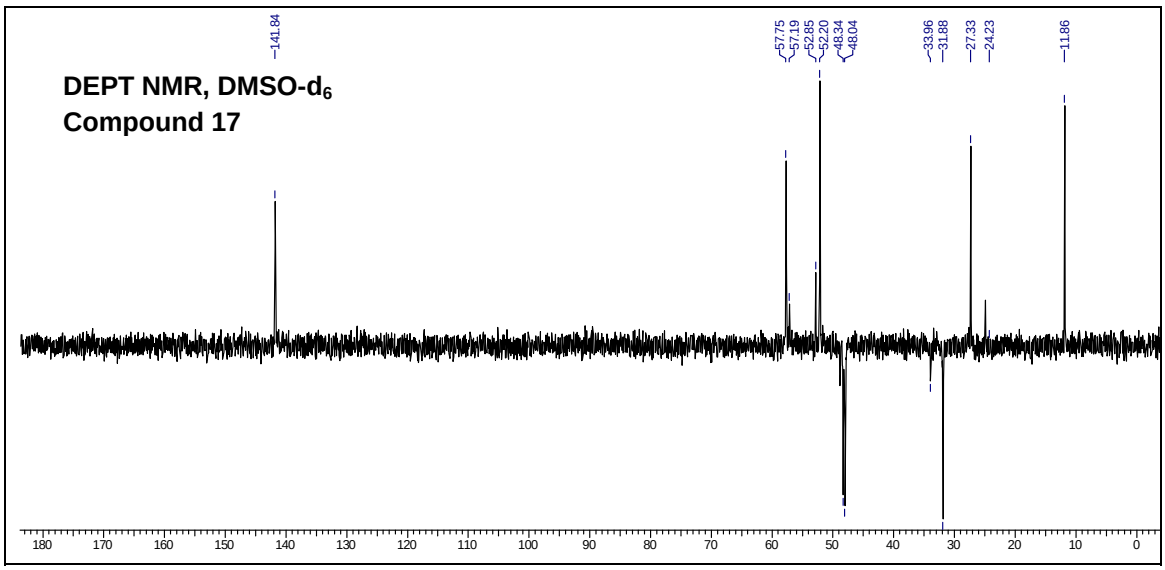
DEPT NMR, DMSO-d$_6$
Compound 17
141.84
57.75
57.19
52.85
52.20
48.34
48.04
33.96
31.88
27.33
24.23
11.86

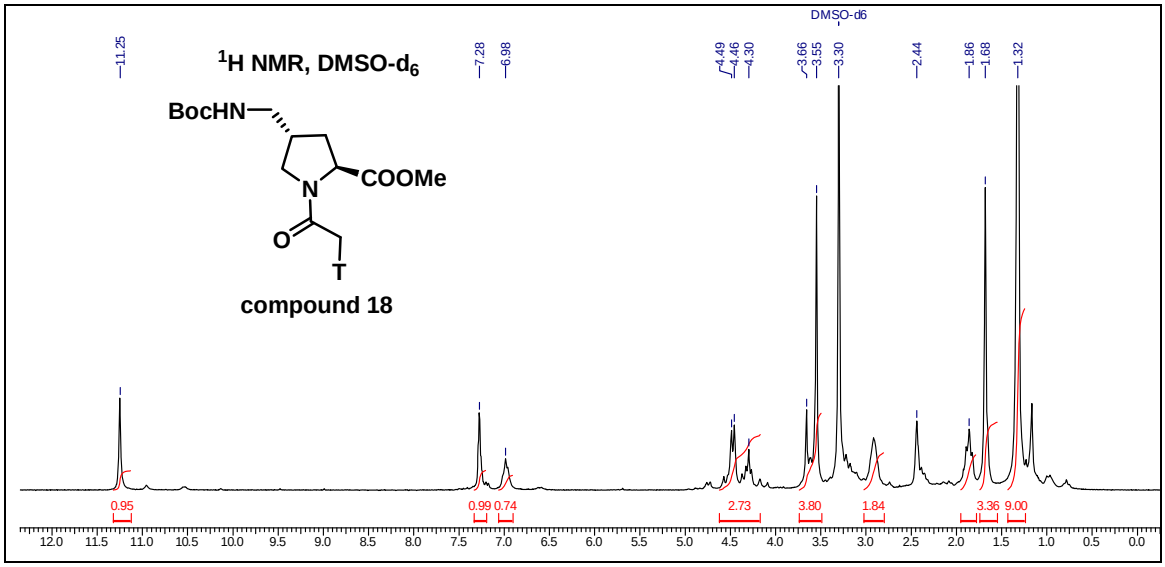

^{1}H NMR, DMSO-d_6

compound 18

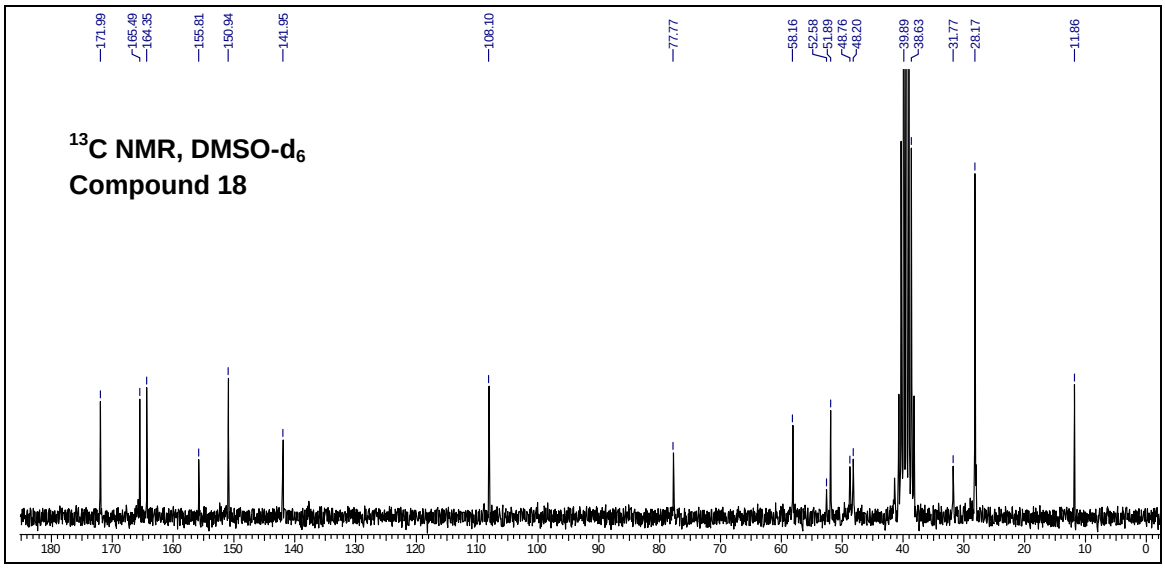

^{13}C NMR, DMSO-d_6
Compound 18

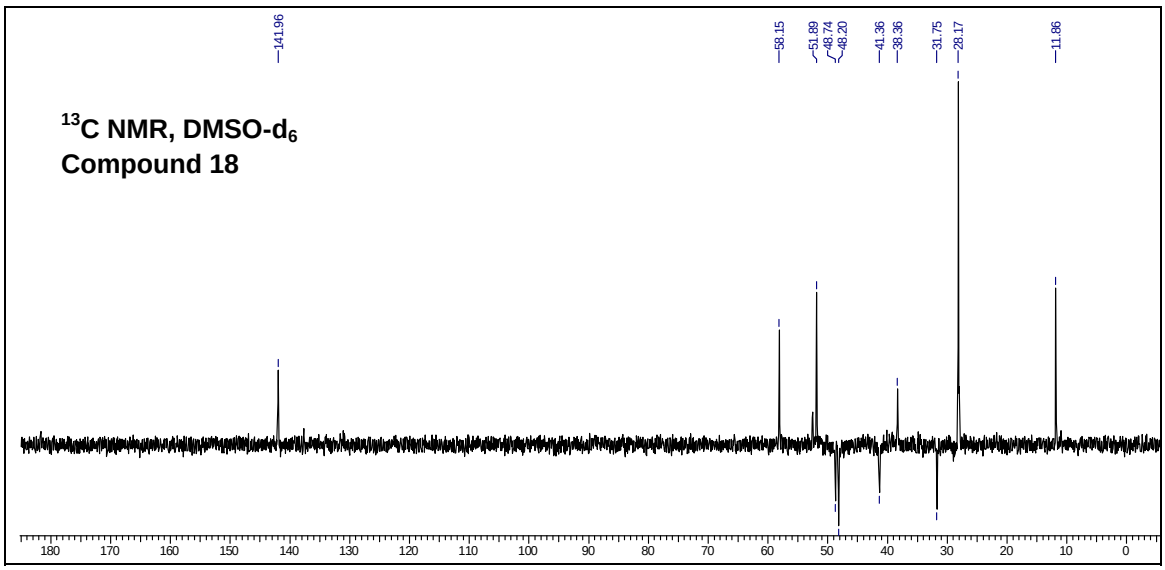

^{13}C NMR, DMSO-d_6
Compound 18

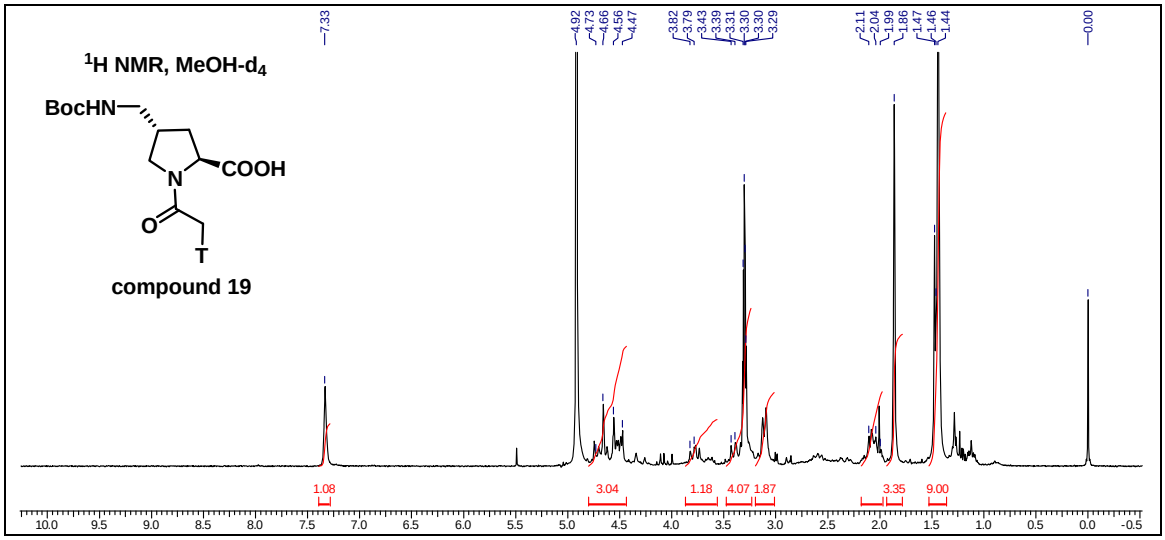
^{1}H NMR, MeOH-d$_4$
BocHN
COOH
N
O
T
compound 19
7.33
4.92
4.73
4.66
4.56
4.47
3.82
3.79
3.43
3.39
3.31
3.30
3.30
3.29
2.11
2.04
1.99
1.86
1.47
1.46
1.44
0.00
1.08
3.04
1.18
4.07
1.87
3.35
9.00

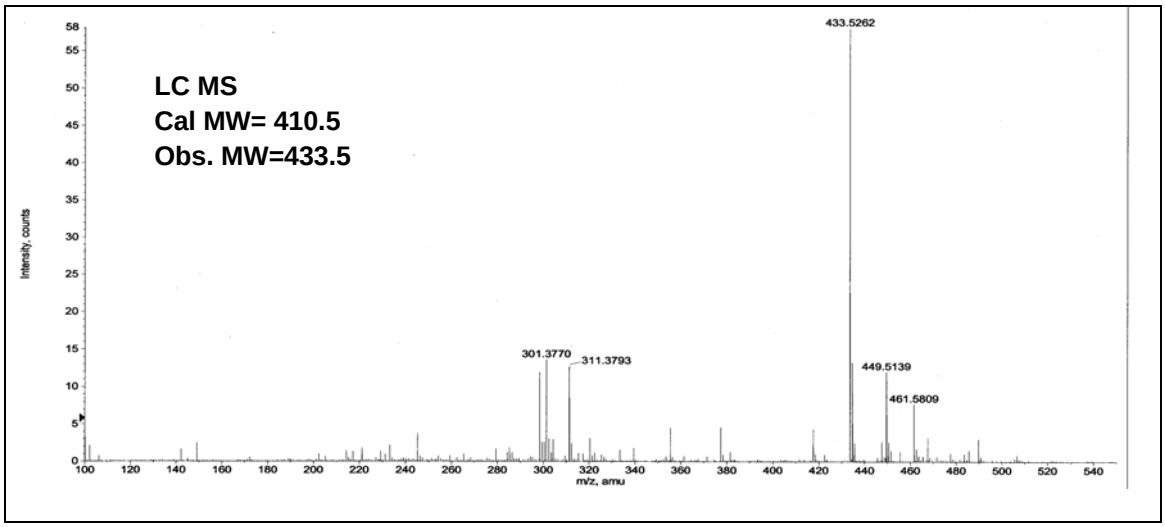
LC MS
Cal MW= 410.5
Obs. MW=433.5
Intensity, counts
m/z, amu
433.5262
301.3770
311.3793
449.5139
461.5809

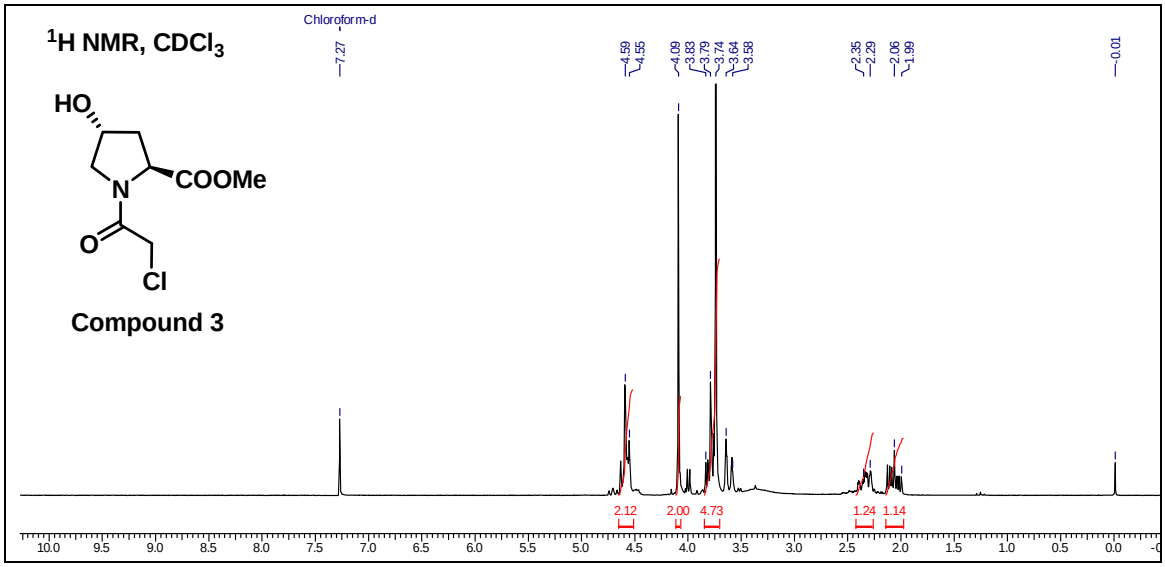
^{1}H NMR, CDCl$_3$
Chloroform-d
7.27
4.59
4.55
4.09
3.83
3.79
3.74
3.64
3.58
2.35
2.29
2.06
1.99
0.01
HO
COOMe
N
O
Cl
Compound 3
2.12
2.00
4.73
1.24
1.14

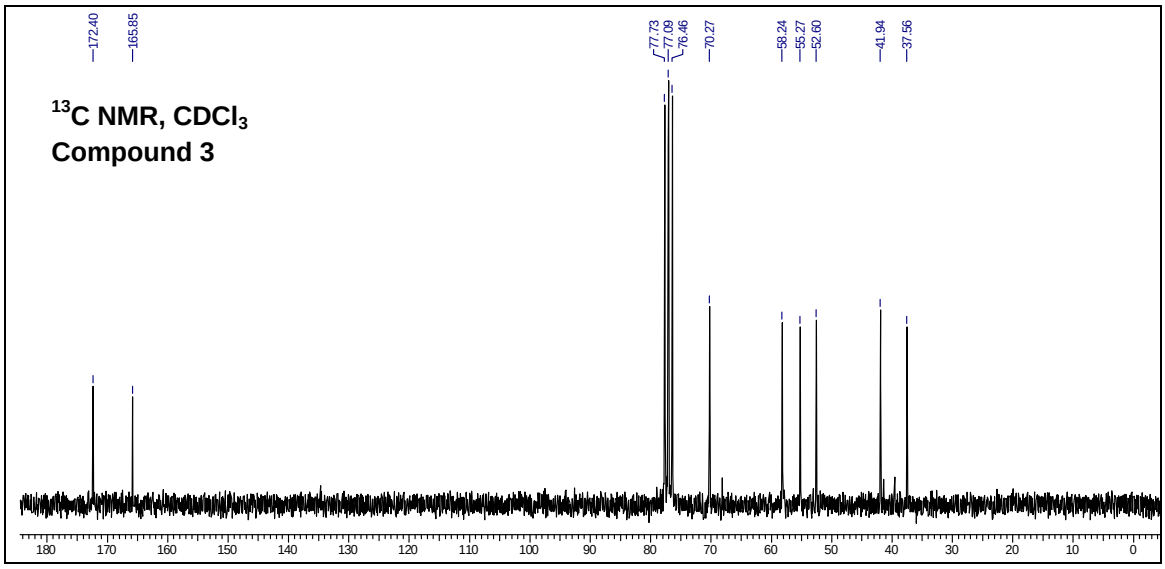
^{13}C NMR, CDCl$_3$
Compound 3
172.40
165.85
77.73
77.09
76.46
70.27
58.24
55.27
52.60
41.94
37.56

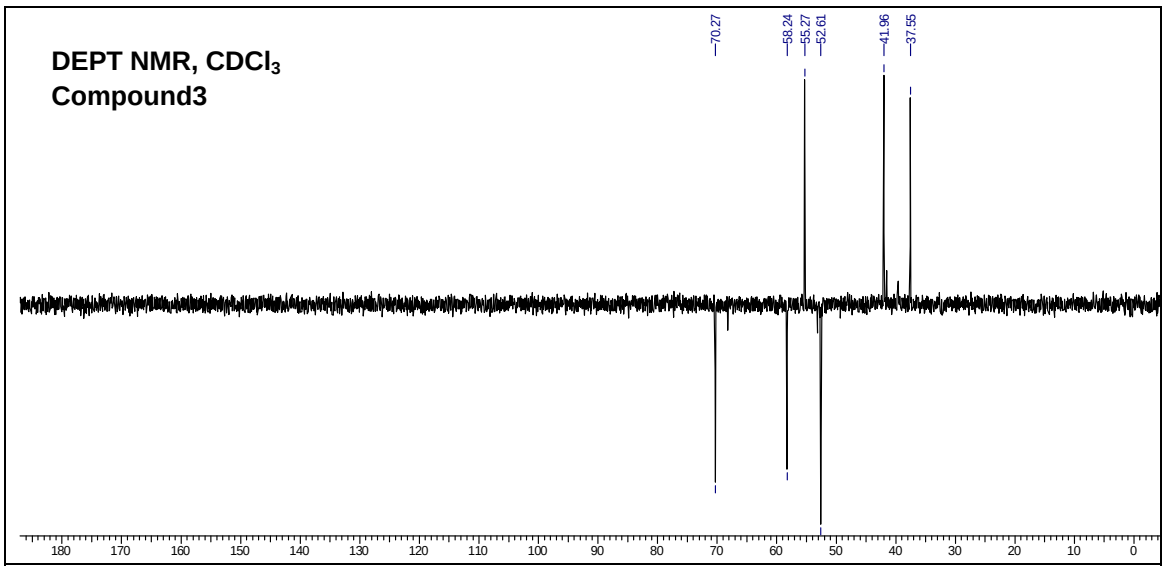
DEPT NMR, CDCl$_3$
Compound3
70.27
58.24
55.27
52.61
41.96
37.55

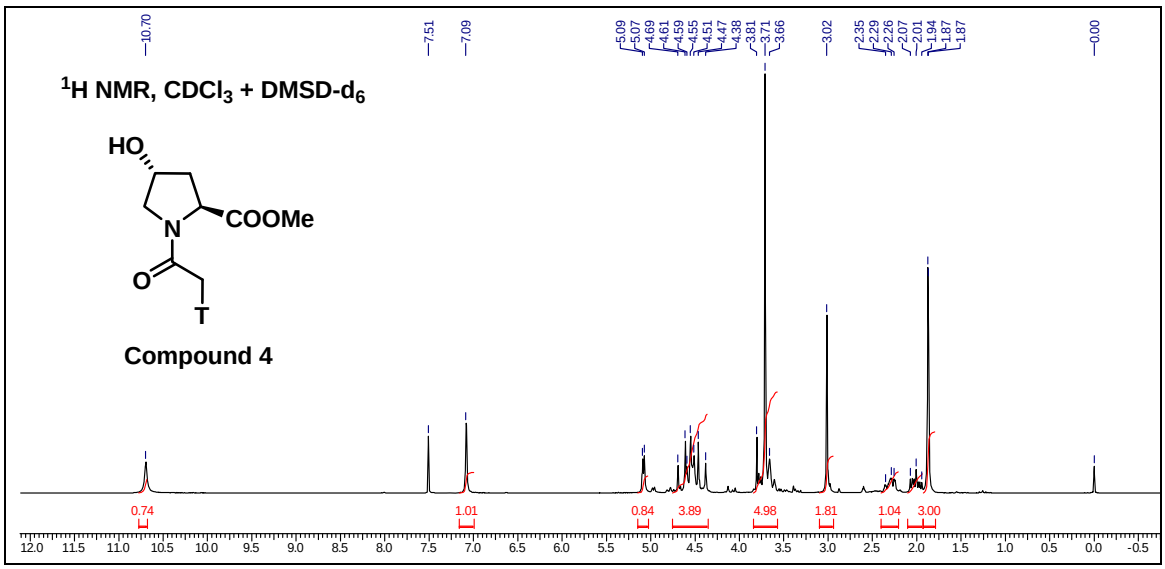
10.70
7.51
7.09
5.09
5.07
4.69
4.61
4.59
4.55
4.51
4.47
4.38
3.81
3.71
3.66
3.02
2.35
2.29
2.26
2.07
2.01
1.94
1.87
1.87
0.00
1H NMR, CDCl3 + DMSD-d6
HO
N
COOMe
O
T
Compound 4
0.74
1.01
0.84
3.89
4.98
1.81
1.04
3.00

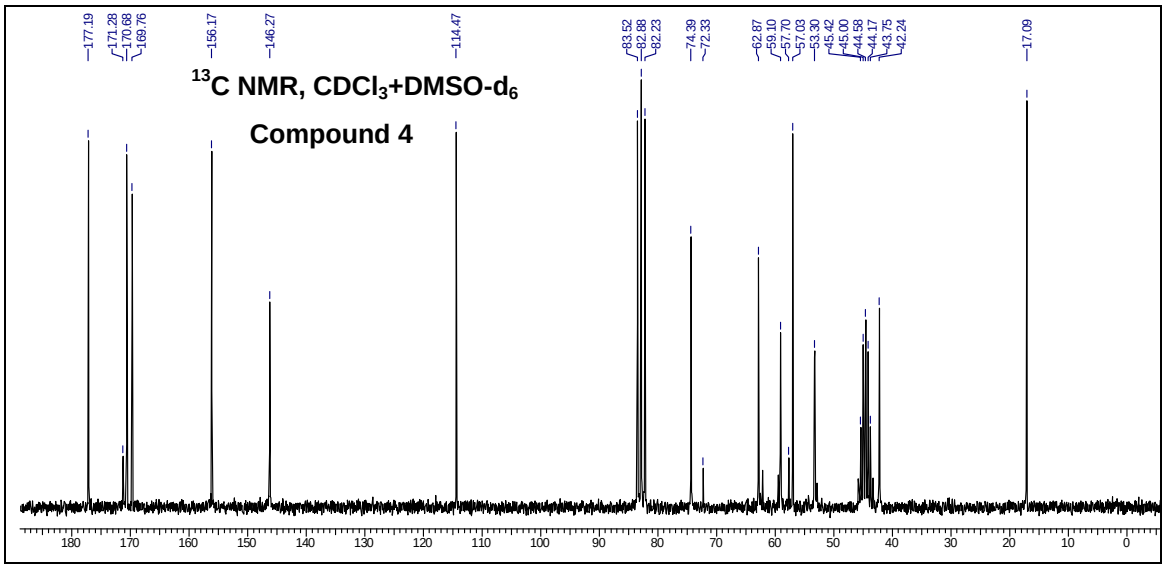
177.19
171.28
170.68
169.76
156.17
146.27
114.47
83.52
82.88
82.23
74.39
72.33
62.87
59.10
57.70
57.03
53.30
45.42
45.00
44.58
44.17
43.75
42.24
17.09
13C NMR, CDCl3+DMSO-d6
Compound 4

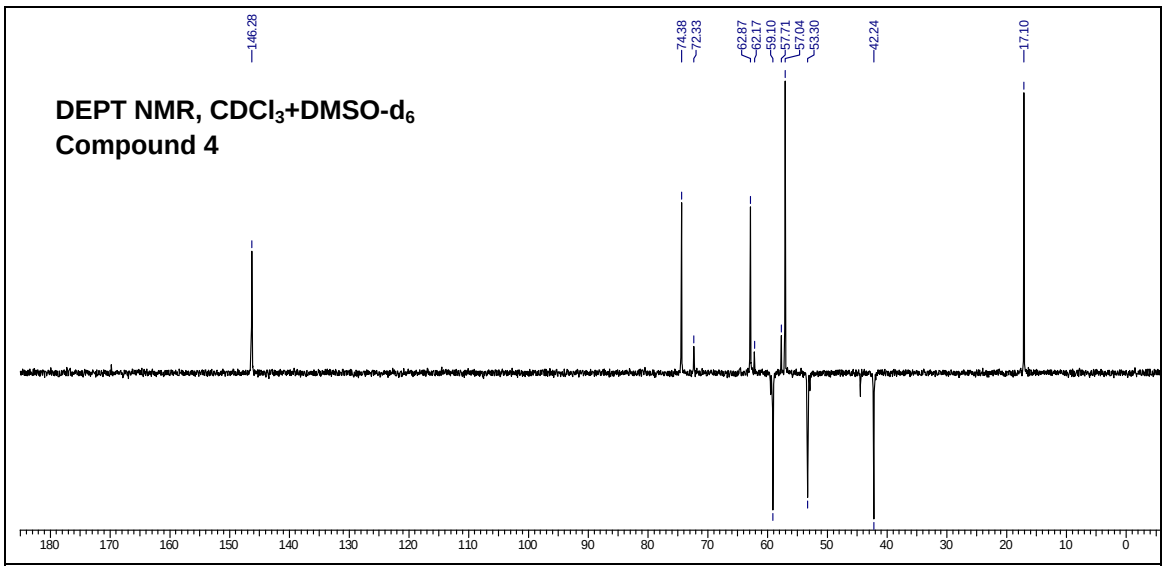
146.28
74.38
72.33
62.87
62.17
59.10
57.71
57.04
53.30
42.24
17.10
DEPT NMR, CDCl3+DMSO-d6
Compound 4

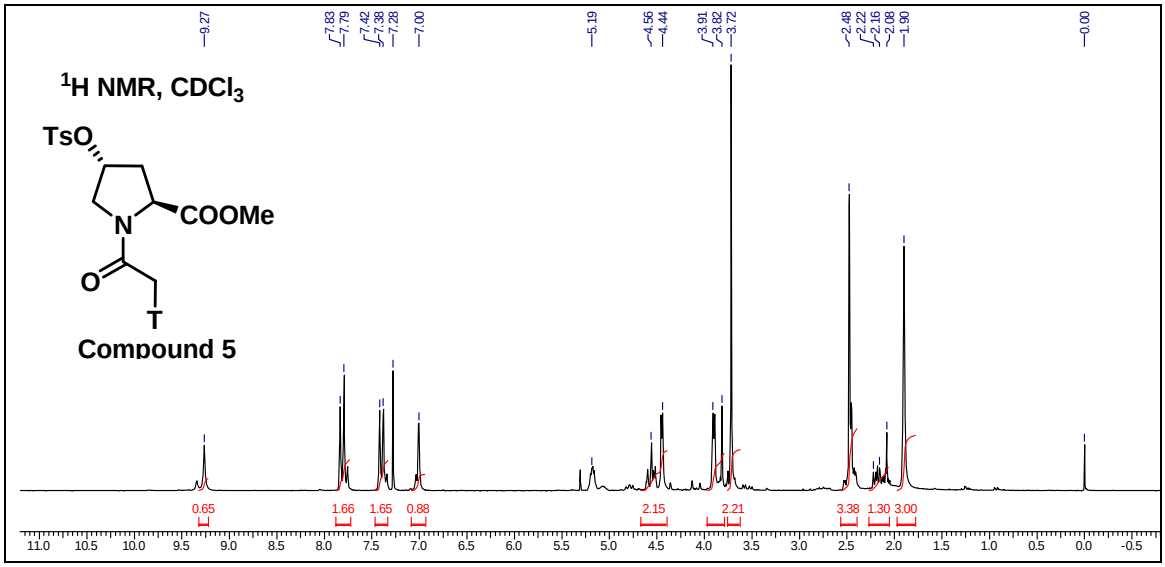
9.27
7.83
7.79
7.42
7.38
7.28
7.00
5.19
4.56
4.44
3.91
3.82
3.72
2.48
2.22
2.16
2.08
1.90
0.00
^{1}H NMR, CDCl$_3$
TsO
N
COOMe
O
T
Compound 5
0.65
1.66
1.65
0.88
2.15
2.21
3.38
1.30
3.00

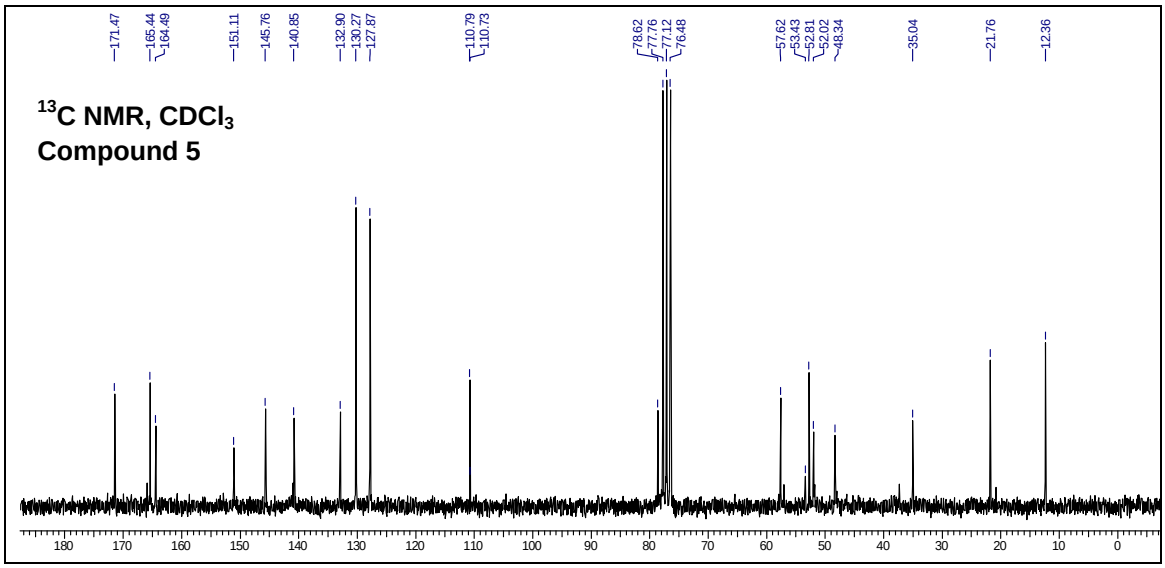
171.47
165.44
164.49
151.11
145.76
140.85
132.90
130.27
127.87
110.79
110.73
78.62
77.76
77.12
76.48
57.62
53.43
52.81
52.02
48.34
35.04
21.76
12.36
^{13}C NMR, CDCl$_3$
Compound 5

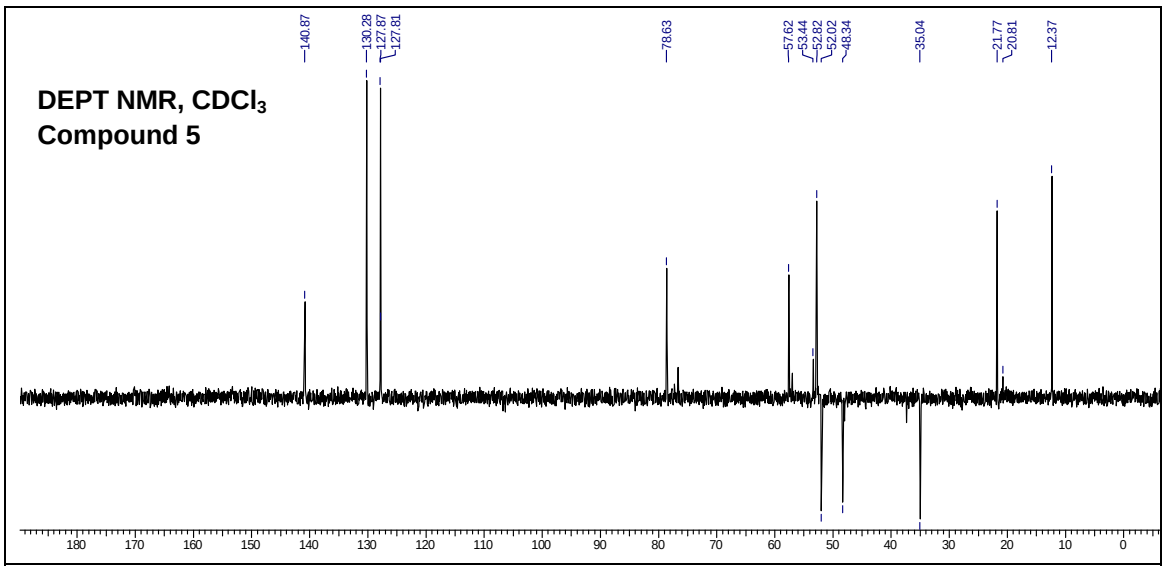
140.87
130.28
127.87
127.81
78.63
57.62
53.44
52.82
52.02
48.34
35.04
21.77
20.81
12.37
DEPT NMR, CDCl$_3$
Compound 5

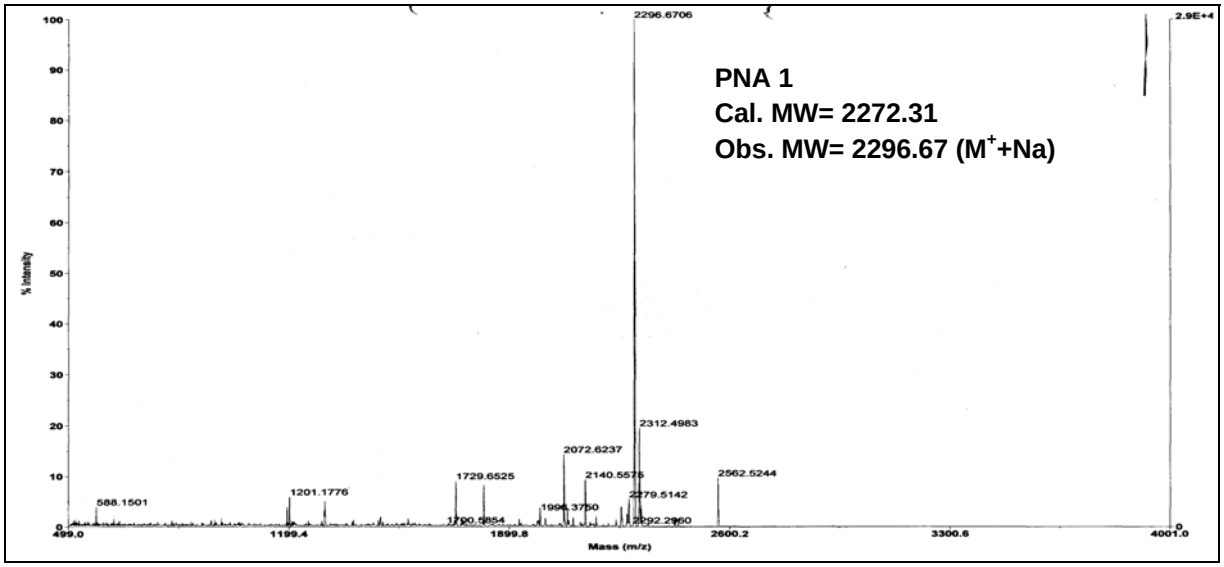
PNA 1
Cal. MW= 2272.31
Obs. MW= 2296.67 (M+ +Na)
2296.6706
2312.4983
2072.6237
1729.6525
2140.5576
2562.5244
2279.5142
588.1501
1201.1776
% Intensity
Mass (m/z)

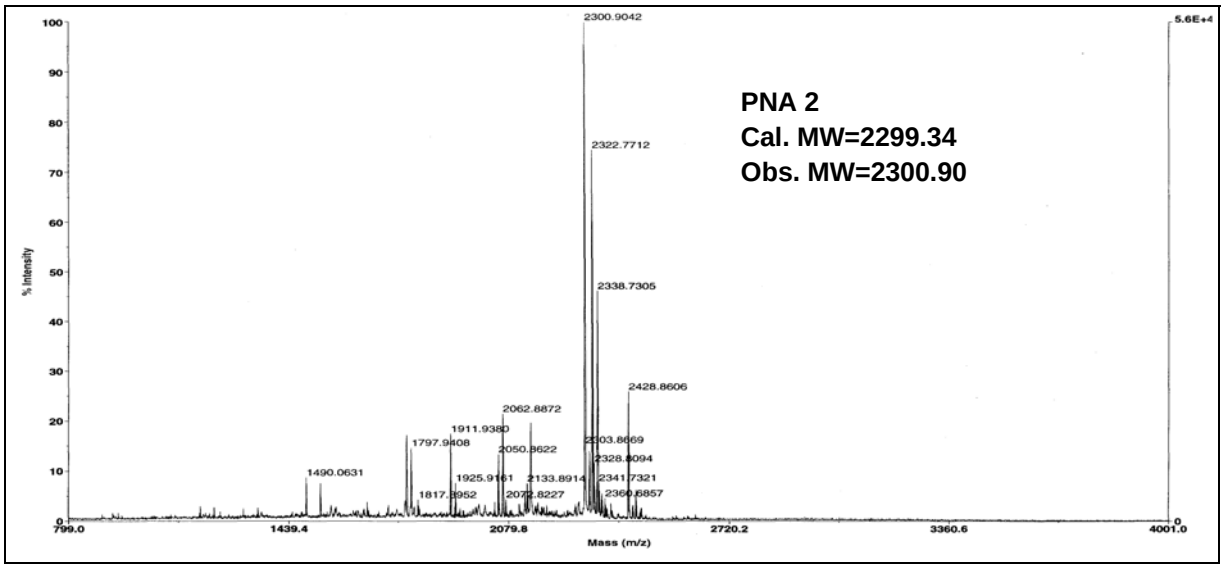
PNA 2
Cal. MW=2299.34
Obs. MW=2300.90
2300.9042
2322.7712
2338.7305
2428.8606
2062.8872
1911.9380
1797.9408
2050.3622
1490.0631
% Intensity
Mass (m/z)

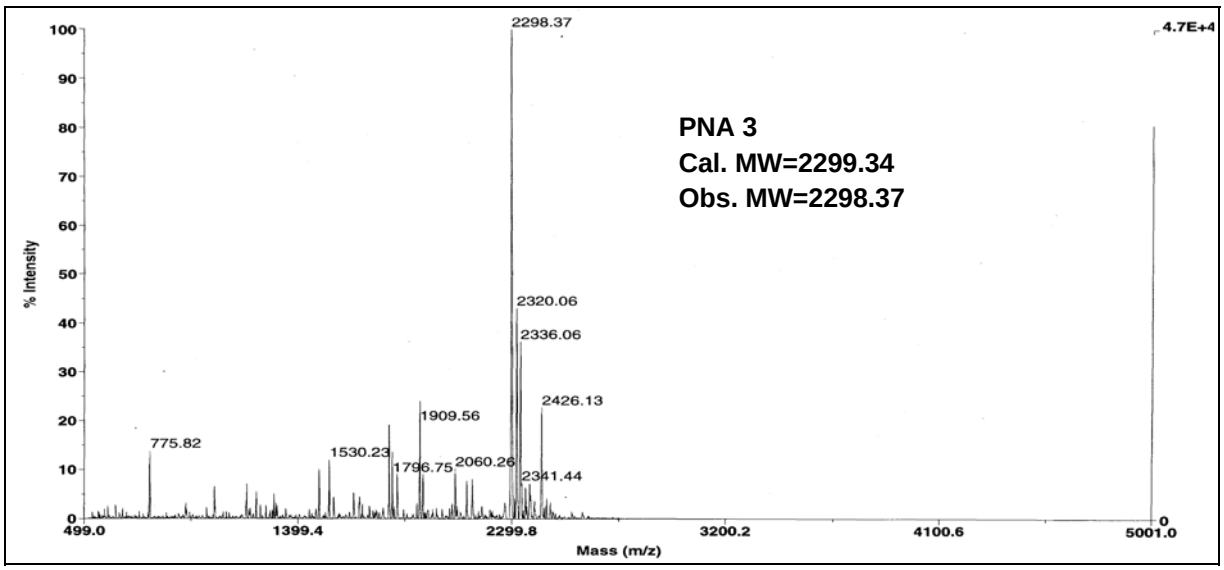
PNA 3
Cal. MW=2299.34
Obs. MW=2298.37
2298.37
2320.06
2336.06
2426.13
1909.56
775.82
1530.23
1796.75
2060.26
2341.44
% Intensity
Mass (m/z)

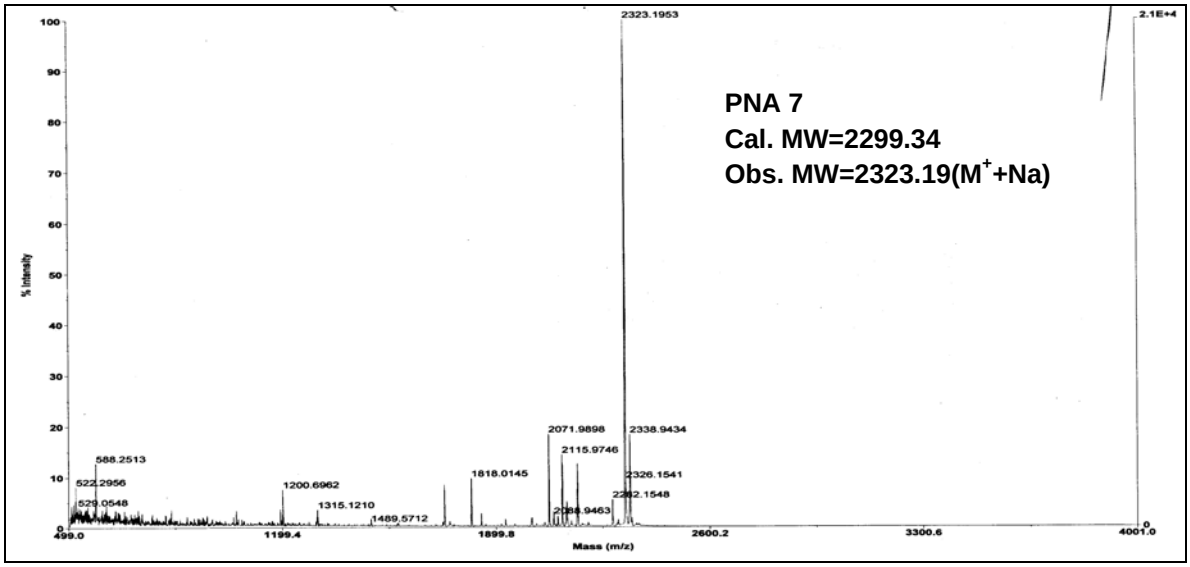
PNA 7
Cal. MW=2299.34
Obs. MW=2323.19(M+ +Na)
% Intensity
Mass (m/z)

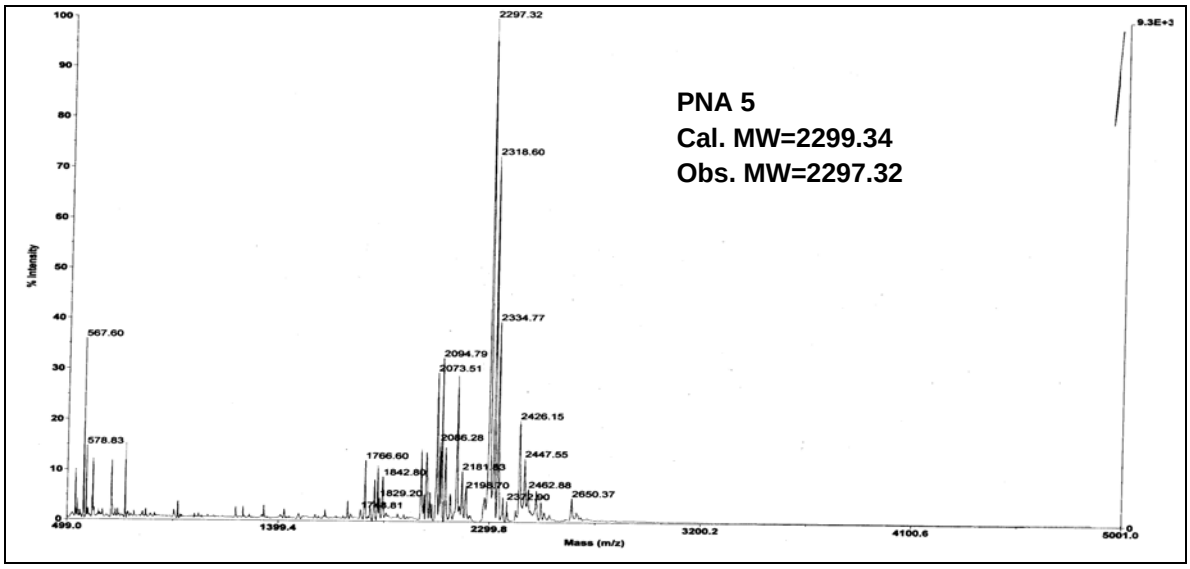
PNA 5
Cal. MW=2299.34
Obs. MW=2297.32
% Intensity
Mass (m/z)

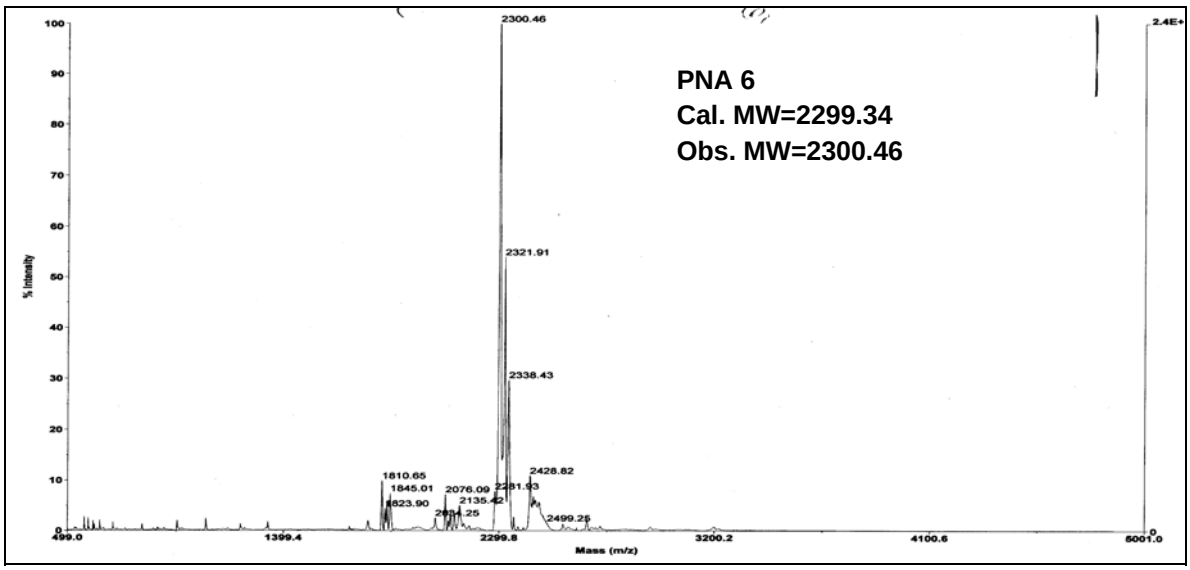
PNA 6
Cal. MW=2299.34
Obs. MW=2300.46
% Intensity
Mass (m/z)

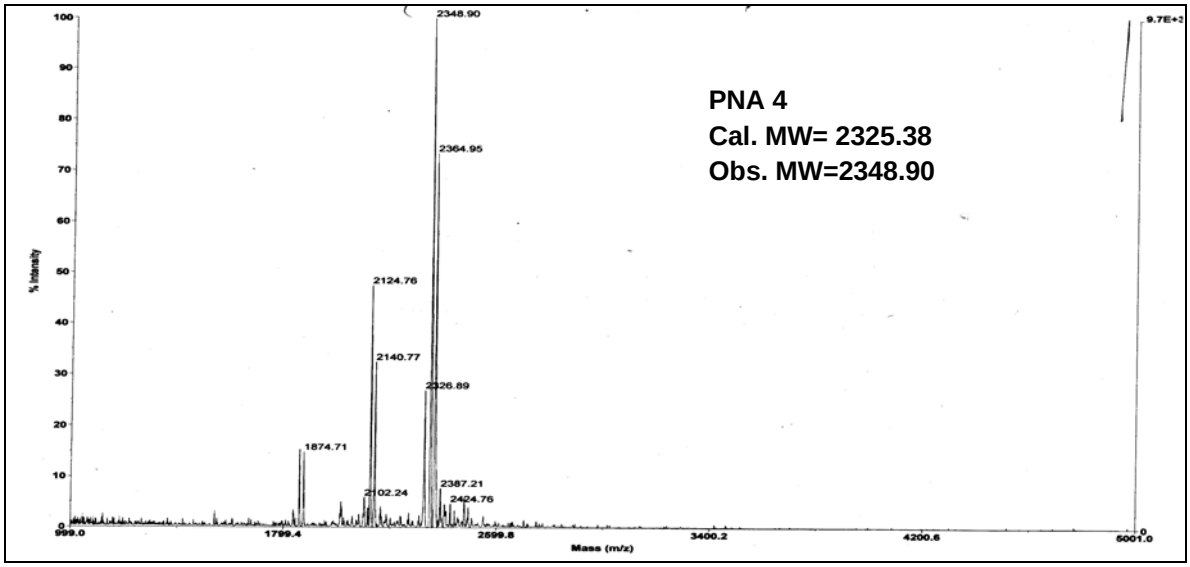
PNA 4
Cal. MW= 2325.38
Obs. MW=2348.90
2348.90
2364.95
2124.76
2140.77
2326.89
1874.71
2102.24
2387.21
2424.76
% Intensity
Mass (m/z)

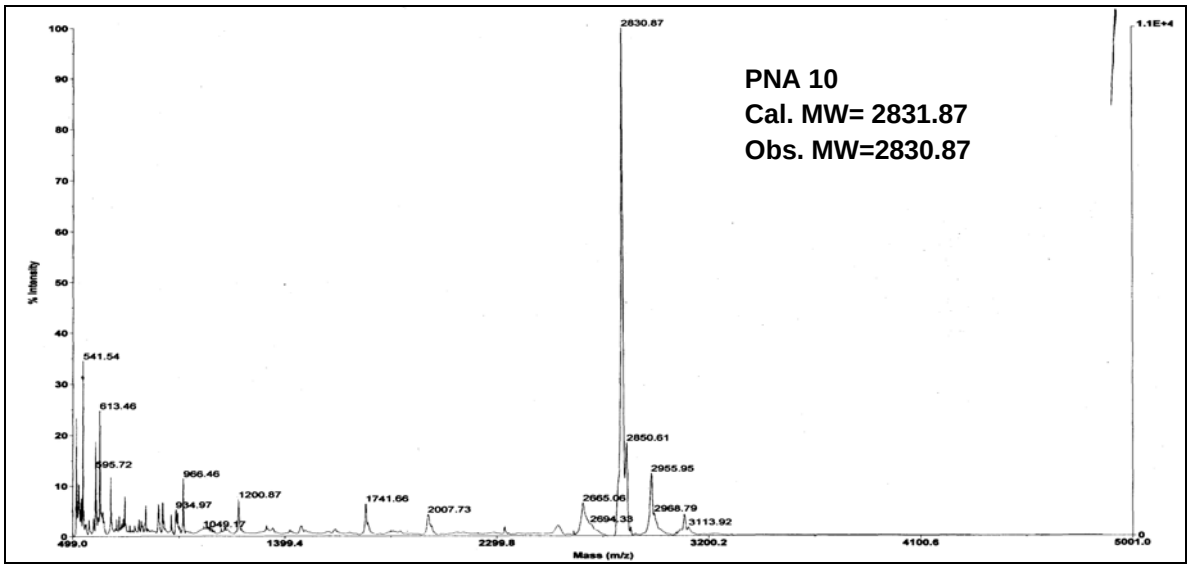
PNA 10
Cal. MW= 2831.87
Obs. MW=2830.87
2830.87
541.54
613.46
695.72
966.46
1200.87
1741.66
2007.73
2850.61
2955.95
2968.79
3113.92
% Intensity
Mass (m/z)

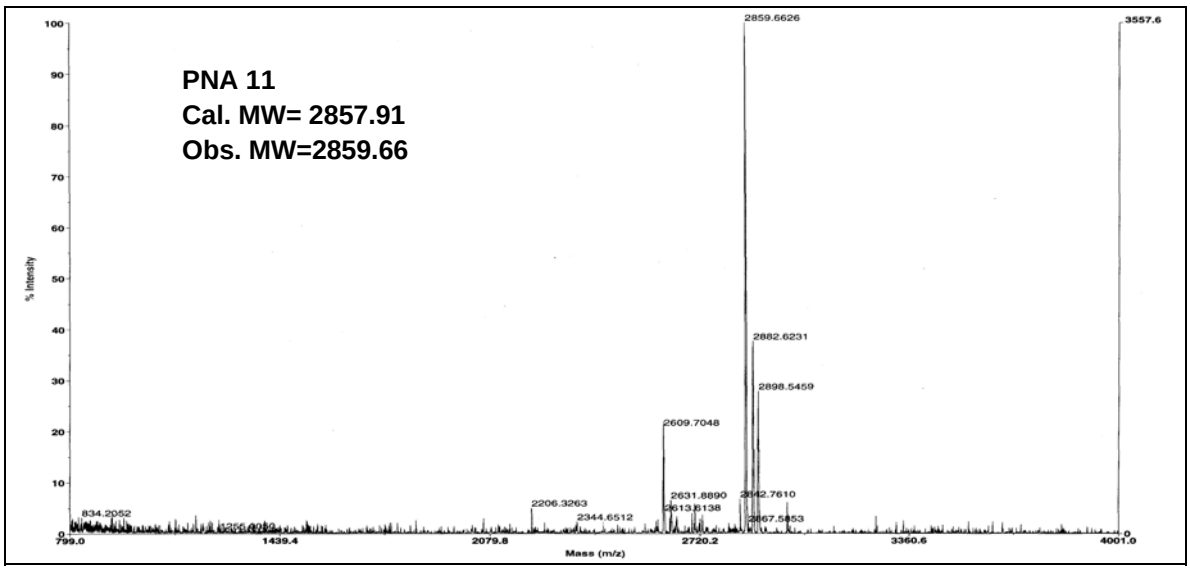
PNA 11
Cal. MW= 2857.91
Obs. MW=2859.66
2859.6626
3557.6
2882.6231
2898.5459
2609.7048
834.2052
2206.3263
2344.6512
2631.8890
2642.7610
% Intensity
Mass (m/z)

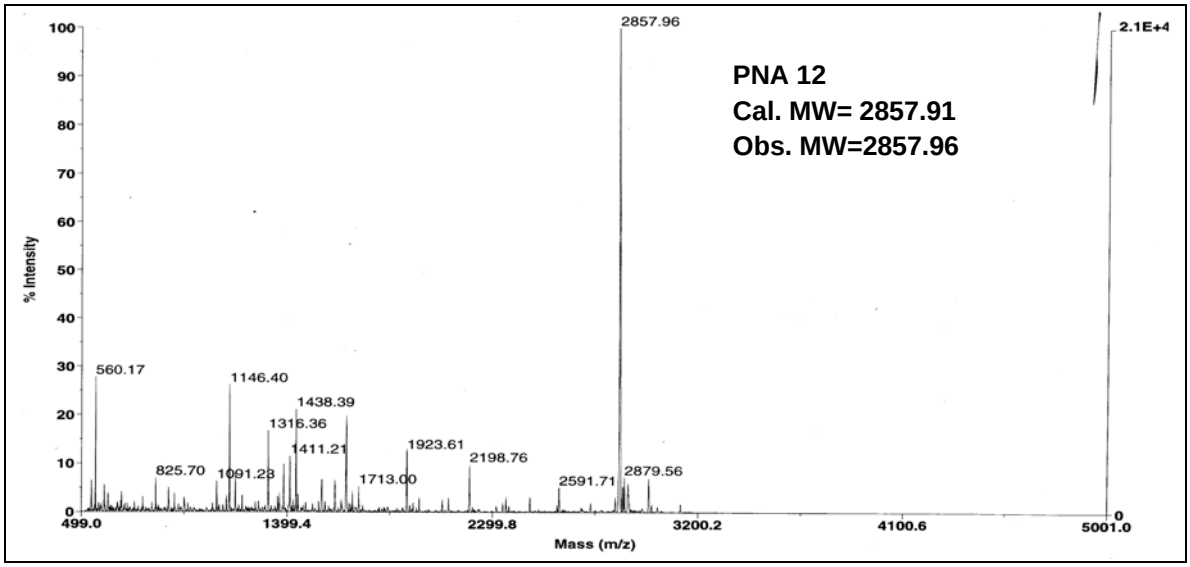
PNA 12
Cal. MW= 2857.91
Obs. MW=2857.96
% Intensity
Mass (m/z)
2857.96
2.1E+4
560.17
1146.40
1438.39
1316.36
1411.21
1923.61
2198.76
825.70
1091.23
1713.00
2591.71
2879.56

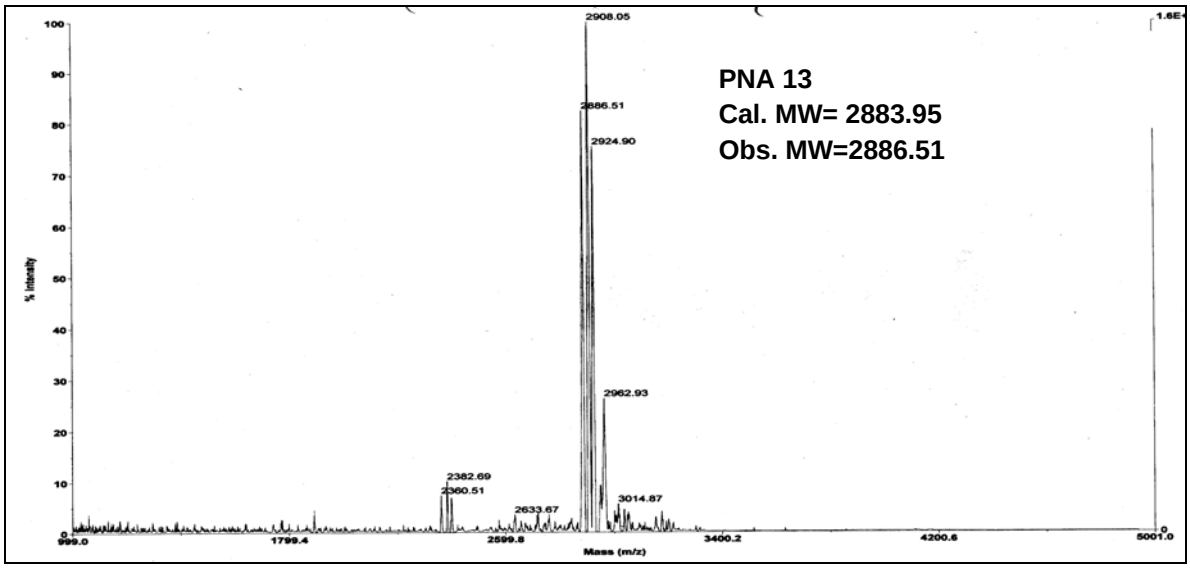
PNA 13
Cal. MW= 2883.95
Obs. MW=2886.51
% Intensity
Mass (m/z)
2908.05
2886.51
2924.90
2962.93
2382.69
2360.51
2633.67
3014.87

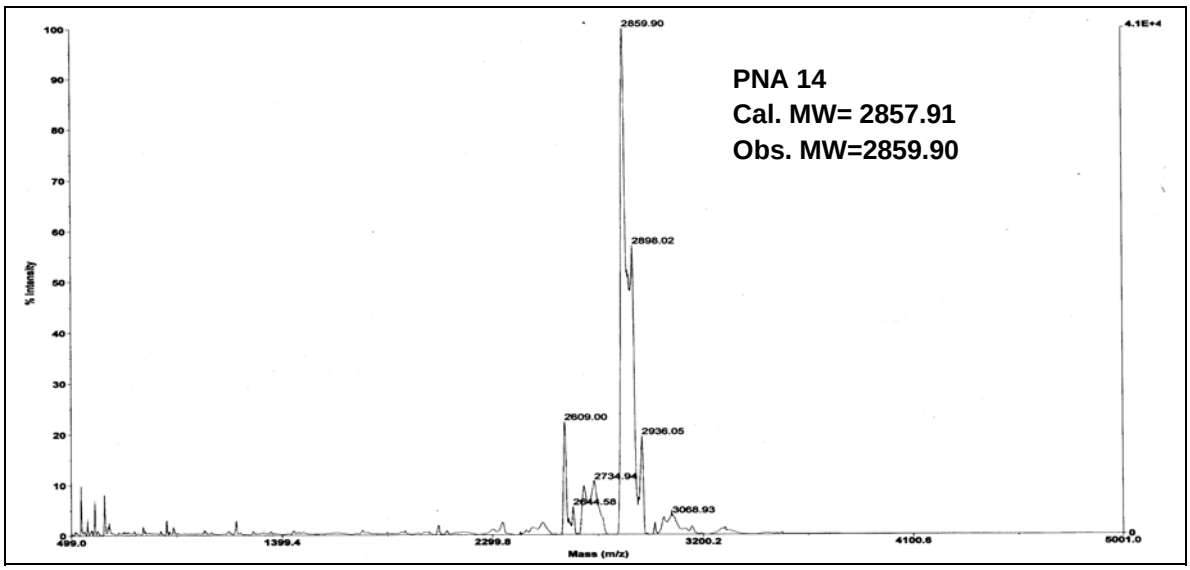
PNA 14
Cal. MW= 2857.91
Obs. MW=2859.90
% Intensity
Mass (m/z)
2859.90
4.1E+4
2898.02
2609.00
2936.05
2734.94
2644.58
3068.93

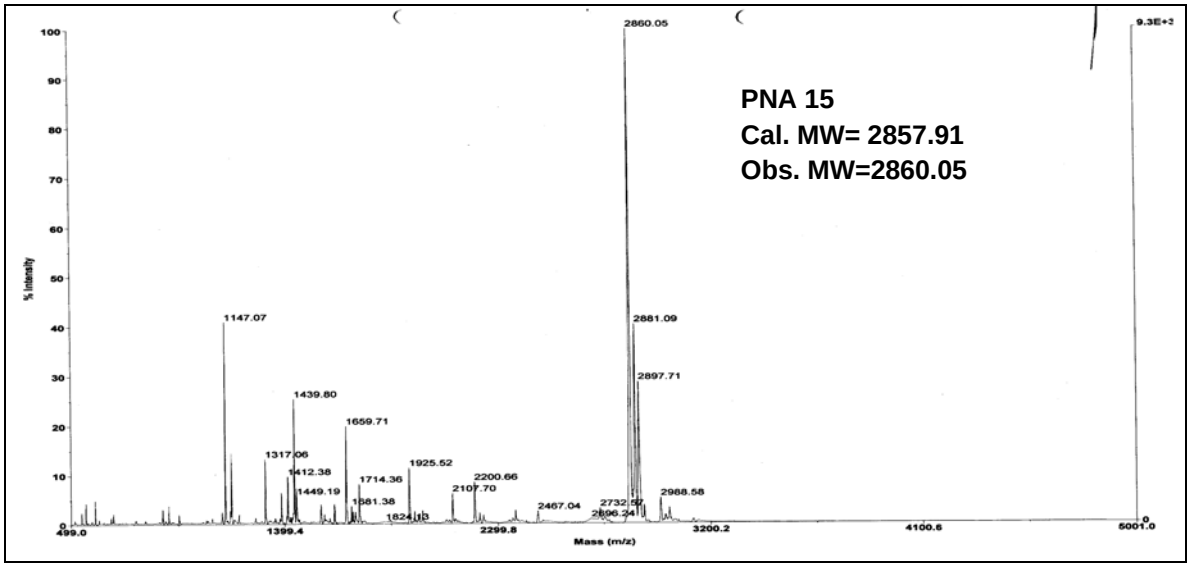
PNA 15
Cal. MW= 2857.91
Obs. MW=2860.05
% Intensity
Mass (m/z)
2860.05
2881.09
2897.71
1147.07
1439.80
1659.71
1317.06
1412.38
1449.19
1714.36
1925.52
2200.66
2107.70
2467.04
2988.58
499.0
1399.4
2299.8
3200.2
4100.6
5001.0

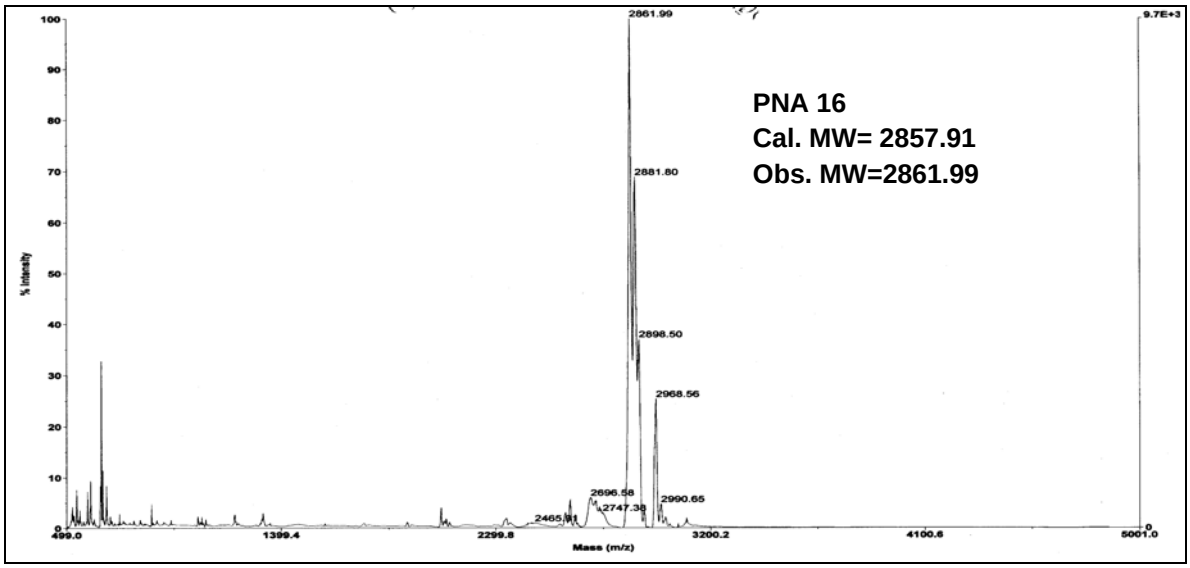
PNA 16
Cal. MW= 2857.91
Obs. MW=2861.99
% Intensity
Mass (m/z)
2861.99
2881.80
2898.50
2968.56
2696.58
2747.38
2990.65
499.0
1399.4
2299.8
3200.2
4100.6
5001.0

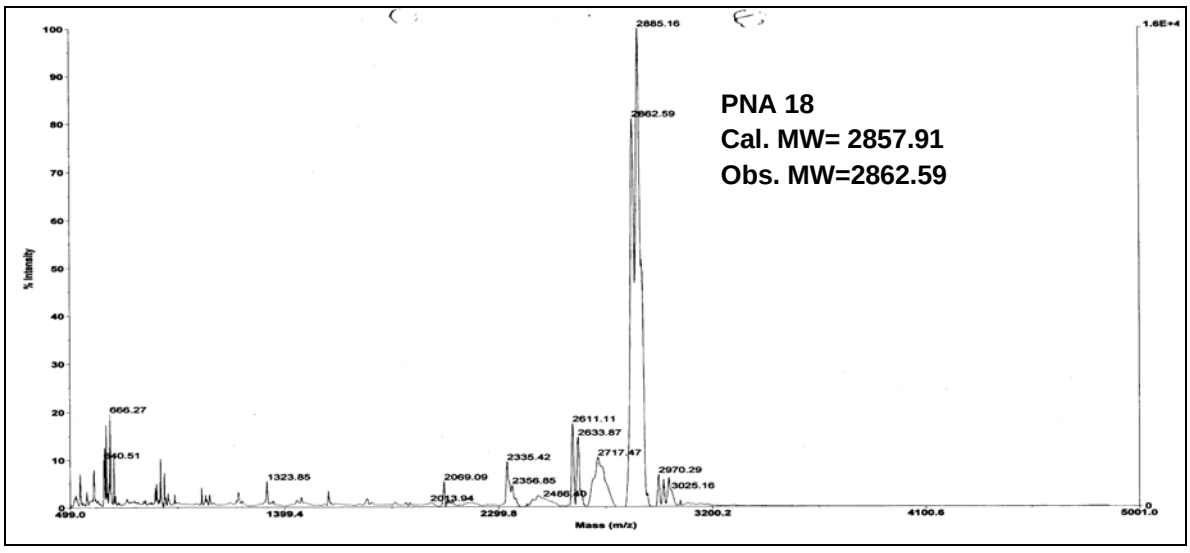
PNA 18
Cal. MW= 2857.91
Obs. MW=2862.59
% Intensity
Mass (m/z)
2885.16
2862.59
666.27
2611.11
2633.87
2717.47
2335.42
2970.29
3025.16
2069.09
2356.85
1323.85
499.0
1399.4
2299.8
3200.2
4100.6
5001.0

Chapter 3

Synthesis of 1,2,3-triazole des-peptdic analogues of PNA and its biophysical studies

3 Introduction

Peptide Nucleic acid (PNA) is one of the most successful examples of nucleic acid analogues that exhibit strong hybridization with cDNA/RNA.[1] As mentioned in the Chapter 1, there have been several modifications of PNA backbone aimed at enhancing the selectivity of hybridization (e.g. parallel/antiparallel, DNA/RNA hybridization preferences) and improving solubility, but most of them have retained the polyamide backbone.[2] There has been a long-standing interest in non-peptidic links that adopt well-defined conformations as alternative to peptide bond in design of peptidomimetic drugs.[3] Replacement of amide bonds by cyclic rings incorporating 1,2,3-triazole or 1,2,3,4-tetrazole moieties have been reported recently. These azole structures can be easily accessed synthetically by Huisgen [3+2] cycloaddition reaction between azides and alkynes.[4] This cycloaddition reaction of alkynes and organic azide has the advantage of high chemoselectivity since, only a few functional groups react with azides and alkynes in the absence of other reagents. In fact, this kinetic stability of alkynes and azides is directly responsible for their slow cycloaddition, which generally requires elevated temperatures and long reaction times. Good regioselectivity in the uncatalyzed Huisgen type cycloaddition is observed for coupling reactions involving highly electron-deficient terminal alkynes, but reactions with other alkynes usually afford mixtures of the 1,4- **(1)** and 1,5-**(2)** regioisomers (Figure 1).

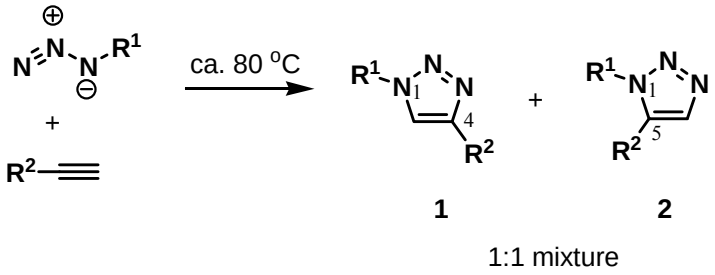

Figure 1: Products of thermal Huisgen 1,3-cycloaddition.

Efforts to control the 1,4-versus 1,5-regioselectivity problem has met with varying success till date.[5] Sharpless et al.[6] have identified a number of reactions that meet the criteria for click chemistry, arguably the most powerful of which discovered to date is the copper(I)-catalyzed variant of the Huisgen 1,3-dipolar cycloaddition of azides and alkynes to afford 1,2,3-triazoles. Cu^{I}-catalyzed reaction sequence which

regiospecifically unites azides and terminal alkynes to give only 1,4-disubstituted 1,2,3-triazoles (Figure 2) are abundantly present as part of small molecule drugs. The reaction is also compatible with the side chains of all the amino acids in protected form and is experimentally simple. It also has enormous scope as it tolerates most organic functional groups and shows a wide scope with respect to varying substituents on both alkyne and azide reactants. The reaction proceeds in a variety of solvents, tolerates a wide range of pH values, and performs well over a broad range of temperature.[6]

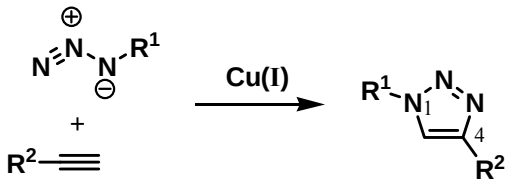

Figure 2: Copper (I)-catalyzed Huisgen 1,3-dipolar cycloaddition

3.1 Proposed mechanism for Cu(I) catalyzed 1,3 dipolar cycloaddition

Although thermal dipolar cycloaddition of azides and alkynes is believed to occur through a concerted mechanism, DFT calculations on monomeric copper acetylide complexes indicate that the concerted mechanism is strongly disfavored relative to a stepwise mechanism.[7] Stepwise cycloaddition catalyzed by a monomeric Cu^{I} species lowers the activation barrier relative to the uncatalyzed process by 11kcal/mol, which explains the rate enhancement observed under Cu^{I} catalysis.

The sequence begins with the coordination of the alkyne **2** to the Cu(I) species **1**, displacing one of the ligands. Conversion of the alkyne **2** to the acetylide **4** is well known to be involved in many C-C bond forming reactions in which Cu acetylide species are formed as intermediate. The initial coordination of acetylene to form π-complex **3** lowers the p*K*a of alkyne**.** In the next step the azide **5** replaces one of the ligands and binds to the copper atom via the nitrogen proximal to carbon, forming intermediate **6**. This is effectively a starting point for the stepwise sequence. After that, the distal nitrogen of the azide in **6** attacks the C-2 carbon of the acetylide, forming the unusual six-membered copper(III) metallacycle **7**. This metallocycle positions the

bound azide properly for subsequent ring contraction by a transannular association. Protonation of triazole-copper derivative **8** followed by dissociation of the product ends the reaction and regenerates the catalyst.

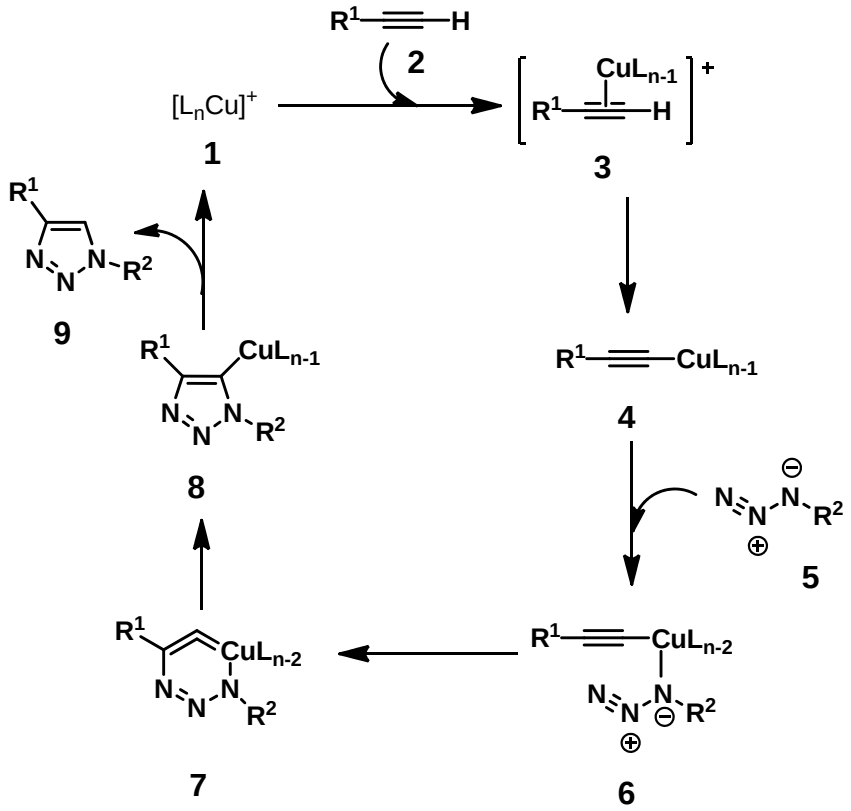

Figure 3: Proposed outline of species involved in the catalytic cycle.[7]

3.2 Biological properties and application of triazole based peptidomimetics

3.2.1 1,2,3-triazole cyclotetrapeptide mimetics

The use of 1,2,3-triazoles in peptidomimetics[8] has been widely reported following the discovery of regioselective Cu^{I}-catalyzed click chemistry in 2002. To assess the biological effects of 1,2,3-triazole units a series of three triazole analogues of the naturally occurring cyclotetrapeptide cyclo-[Pro-Tyr-Pro-Val] **10**, a potent tyrosinase inhibitor isolated from *L. helveticus* has been synthesized. The failure to obtain the cyclotetrapeptide **10** due to the problematic ring closure step, Bock et al.[9] synthesized the cyclotetrapeptide analogues **11**, **12** and **13** (Figure 4), where amides were replaced by 1,2,3-triazole units.

The inhibitory effects of cyclotetrapeptide analogues **11–13** on mushroom tyrosinase indicate that the triazole analogues not only retain inhibition activity, but in fact, cyclotetrapeptide analogues **11** and **12** both show an approximately threefold increase in activity relative to the natural product.

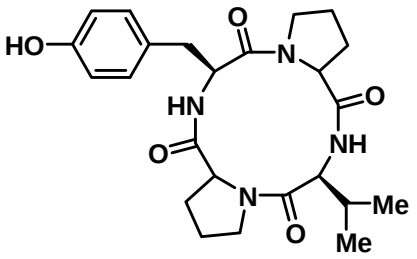

cyclo-[Pro-tyr-pro-val] 10

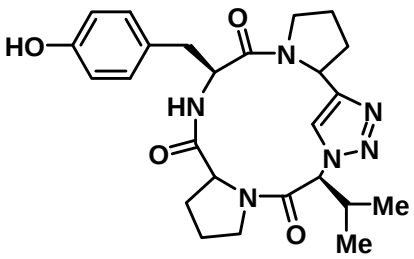

11

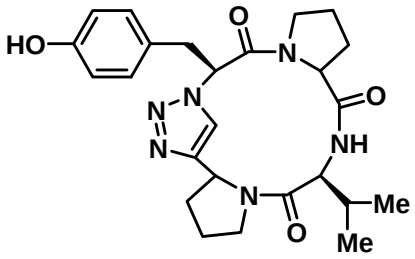

12

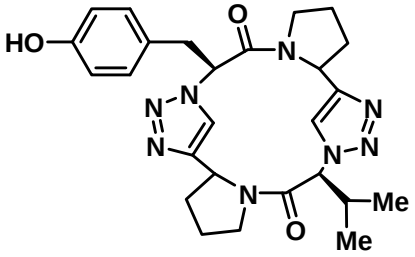

13

Figure 4: Structures of different triazole based cyclotetrapeptide

3.2.2 Nonpeptidic foldamers

Arora et al.[10] reported a new class of distinctly folded nonpeptidic oligomers in which the amide bond is substituted with heteroaromatic rings to generate peptidomimetics, yet maintaining the chiral main chain and amino acid side chains (Figure 5A). These molecules potentially afford specific conformations featuring a diverse set of side chains without the limitations imposed by the secondary amide bond. The 1,4-substituted oligomers were prepared through Cu^{I}-catalyzed azide-alkyne [3+2] cycloaddition with suitable amino alkyne and azide. Solution NMR studies on trimers and tetramers suggest that these oligomers adopt zigzag conformations reminiscent of peptide β-strand conformation.

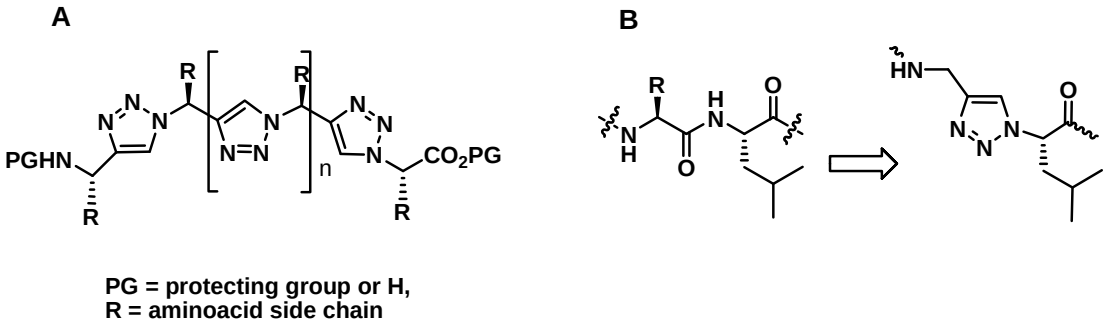

Figure 5: (A) Structure 1,3-substituted triazolamer, (B) Native dipeptide and the L-leucine derived triazole ε^2-amino acid incorporated as a replacement

Triazole ε^2-amino acid[11] (Figure 5B) can be used as a dipeptide surrogate in α-helical coiled coils. These are potentially useful in the context of peptide and protein secondary structures. Dipeptides K_8L_9, $K_{15}L_{16}$ and $E_{22}L_{23}$ were replaced with L-leucine derived triazole ε-amino acid in pLI mutant α-helical coiled coil GCN4 sequence (Figure 5B), separately in different sequences. The modified peptides retain much of the native α-helical character, but the position of the ε^2-amino acid substitution differently influences the thermodynamic stability. Notably, the ε-residue in each chain fully participates in α-helical backbone hydrogen bonding.

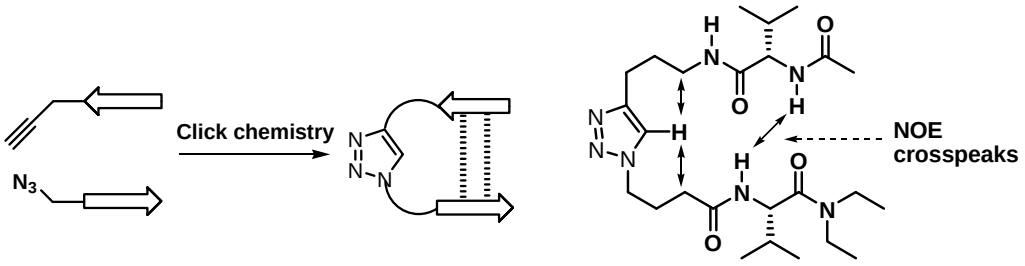

Figure 6: Construction of β-sheet mimetics

Click chemistry was used to combine azido- and alkyne functionalized peptides to give putative β-turn mimics[12] (Figure 6). Molecular modeling indicates that the propensity to form intramolecular amide-amide hydrogen bonding depends on the length of the spacers that connect the two amides to the triazole ring. The secondary structures of these compounds were examined by ^{1}H NMR in chloroform, which showed NOE crosspeaks and temperature/concentration variations of NH chemical shifts, and the FTIR data that are consistent with a small sheet-like structure. Since,

hydrogen-bonding effects are emphasized in non-protic media, it remains to be established that these constructs are secondary structure mimics in aqueous solutions.

3.2.3 Turn formation of peptoids

Peptoids[13] are a class of synthetic oligomers (Figure 7B) that consist of repeating N-substituted glycine units and are capable of folding into discrete structures. Incorporation of 1,5-substituted triazole amino acid (Figure 7A) into peptoid oligomers induce turn formation in a peptide backbone.[14] The triazole induces a constraint that is geometrically similar to a *cis*-double bond, while acting as an amide isostere with respect to polarity. This triazole monomer induces hairpin formation when it is incorporated into a peptoid backbone in aqueous solution.

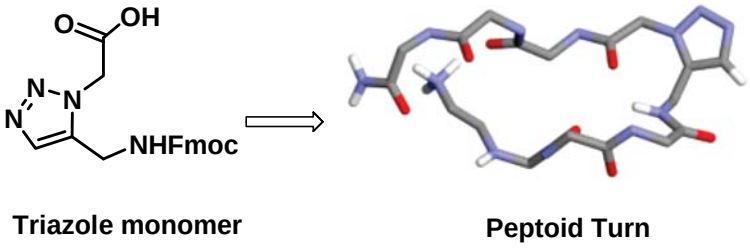

A

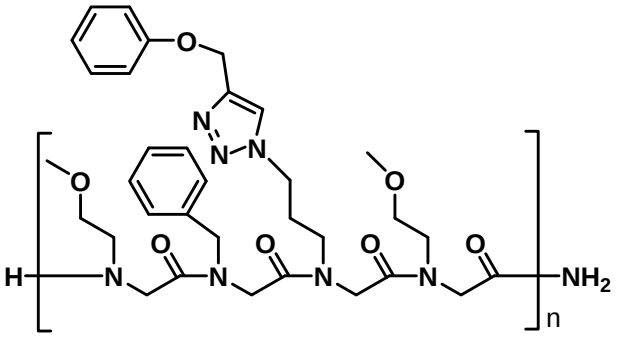

B

Figure 7: **(A)** Structure of 1,5 substituted triazole monomer and **(B)** triazole based peptoid oligomer

3.2.4 Triazole-Linked dumbbell oligonucleotides

Triazole-crosslinked dumbbell oligodeoxynucleotide[15] (Figure 8) were synthesized with use of the Cu(I) catalyzed alkyne-azide cycloaddition (CuAAC) with oligodeoxynucleotides possessing *N*-3-(azidoethyl)thymidine and *N*-3(propargyl)

thymidine at the 3'- and 5'-termini. These oligodeoxynucleotides act as decoy molecules[15] to achieve biological responses leading to alteration of gene expression and show excellent stability against snake venom phosphodiesterase (3'-exonuclease). Moreover, the dumbbell oligodeoxynucleotides have the ability to bind to NF-κB p50 homodimer within a similar range of affinity to that of a control double stranded decoy oligodeoxynucleotide. The greater the number of the thymidine residues constituting the loop region, the higher the binding affinity of the dumbbell oligodeoxynucleotides to the NF-κB. The protein binding ability of the dumbbell oligodeoxynucleotides can be modulated by altering the loop size. Therefore the crosslinking by the triazole structure does not prevent the dumbbell oligodeoxynucleotides from binding to the NF-κB transcription factor and could be proposed as powerful decoy molecules.

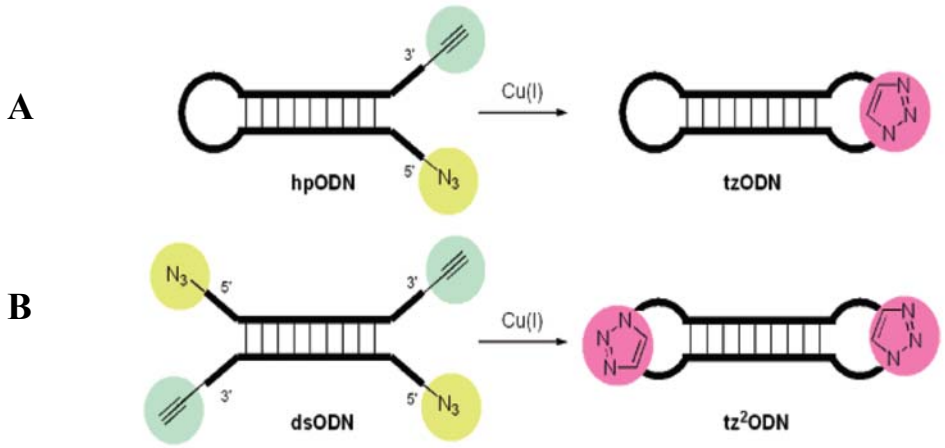

Figure 8: Formation of triazole cross-linked dumbbell-like ODNs (tzODN and tz^2ODN) by the copper catalyzed azide-alkyne cycloaddition: (A) cross-linking of hairpin ODN (hpODN) at a single site and (B) cross-linking of double-stranded ODNs (dsODN) at both termini.

3.2.5 Triazole linked DNA and organometallic PNA

Analogues of 1,2,3-triazole DNA (Figure 9A) that can be polymerized by copper-catalysed Huisgen [3+2] cycloaddition reaction on solid support has been reported recently.[16] This triazole DNA formed a stable double strand with a natural DNA strand in a 1:1 stoichiometric ratio. The melting temperature was found to be higher in case of

triazole DNA than the unmodified control DNA. As click chemistry tolerates a wide range of functionalities, the method provides a powerful strategy for synthesizing artificial oligonucleotides.

PNA monomers and oligomers were labeled with reversible redox active moiety ferrocene using click chemistry, which are particularly useful for electrochemical biosensing.[17] The advantage of this methodology is its possible use on the solid support and is attractive as it allows the use of an excess, cheaper and easier to make reagents to yield useful bioconjugates quantitatively and with minimal purification problems.

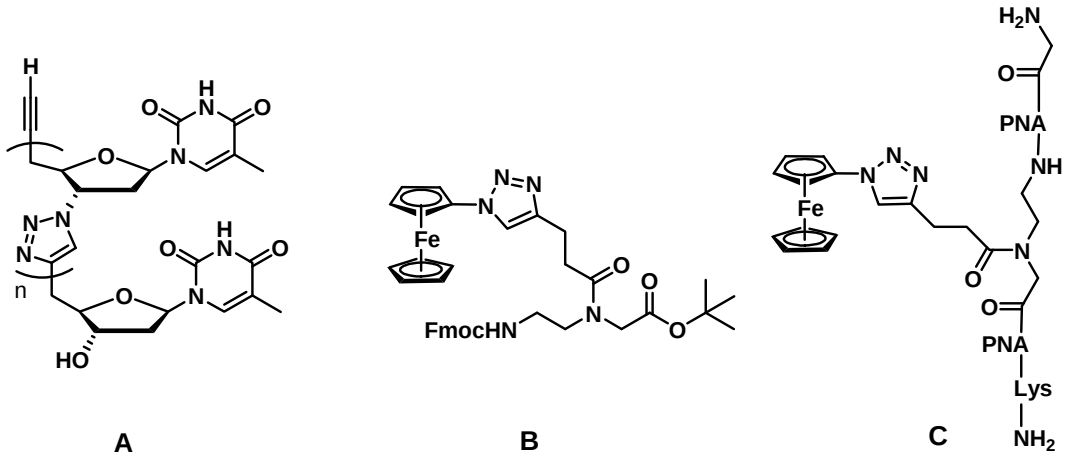

Figure 9: Structures of **(A)** triazole-linked DNA analogue **(B)** ferrocenyl-PNA monomer **(C)** oligomeric ferrocene-PNA conjugate

3.3 Rationale and objectives of present work

The interest in this reaction stems from the useful biological activity of 1,2,3-triazoles. These heterocycles function as rigid linking units that can mimic the atom placement and electronic properties of a peptide bond without the same susceptibility to hydrolytic cleavage. Some structural differences between triazoles and amide bonds of course exist; most notably, the extra atom in the triazole backbone leads to a calculated increase in distance of 1.1 Å over the typical amide bond and quite similar in terms of planarity[8] (Figure 10). Triazoles also possess a much stronger dipole moment than an amide bond, but this may actually enhance peptide bond mimicry by increasing the hydrogen bond donor and acceptor properties of the triazole.

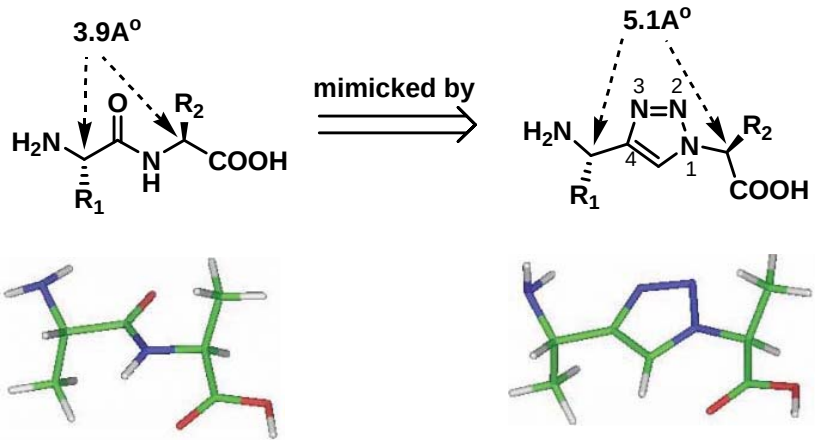

Figure 10: Topological and electronic similarities of amides and 1,2,3-triazoles[8]

In addition to the possibility of both the N(2) and N(3) triazole atoms acting as hydrogen bond acceptors, the strong dipole may polarize the C(5) proton to such a degree that it can function as a hydrogen-bond donor, like the amide proton. Therefore triazoles are versatile in replacing the amide links with fair retention of conformational properties. The unique attribute of triazole ring is a large dipole moment (~5D) causing favorable dipole-dipole interactions and torsional effects, leading to defined conformations.[18] In this context, we have explored the replacement of the amide functions in polyamide backbone of PNA with the triazole rings (Figure 11) to examine its effect on PNA hybridization properties.

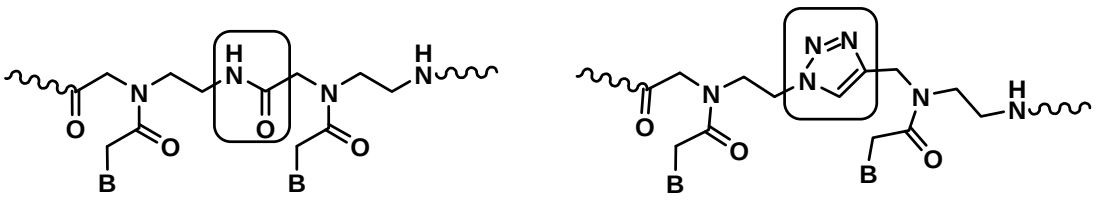

I, *aeg*PNA **II, 1,2,3-*triazolyl*lPNA**

Figure 11: Structures of *aeg*PNA and 1,2,3-*triazolyl*PNA oligomers

Our main objectives for the incorporation of 1,2,3-triazole unit to the PNA backbone comprises,

i) Synthesis of *aeg*PNA monomer **III** containing azide and alkyne functionalities (Figure 12). Further this monomer can be incorporated to solid support for the systematic deprotection and click reaction to obtain triazole based PNA oligomers.

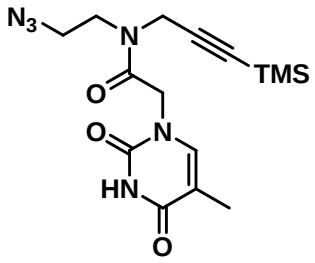

III

Figure 12: structure of azide and alkyne functionalized monomer

ii) Synthesis of 1,2,3-triazole PNA dimer **IV** for block coupling in solid support. The dimer can be synthesized from the azide functionalized monomer **V** and the acetylene functionalized monomer **VI** (Figure13).

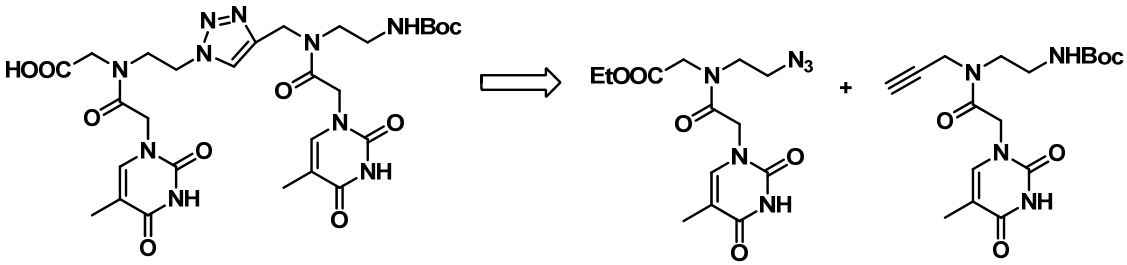

IV **V** **VI**

Figure 13: Retrosynthetic pathway of triazole dimer

iii) Generation of triazole link in **VII** from click reaction of the polymer supported azido component **VII** with the acetylenic component **VI** synthesized in solution (Figure14).

iv) Characterization and the biophysical studies of the *triazolyl* PNA oligomers

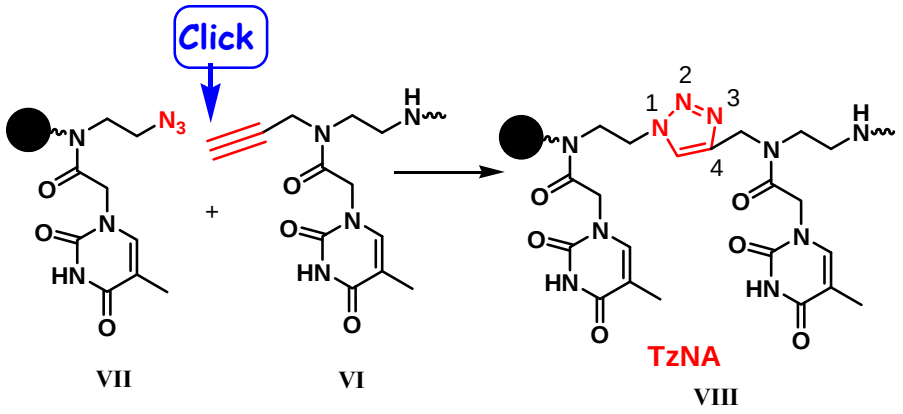

Figure 14: Schematic representation of click chemistry on solid support

3.4 Results and Discussion

The varoius methods attempted for the incorporation of 1,2,3-triazole unit to the PNA backbone have been described in the following sections.

3.4.1 Synthesis of azide and alkyne functionalized monomer (III, 22)

The synthesis of azide and alkyne functionalized monomeric unit **III** or **22** (Scheme 1), was started from the commercially available glycine **14** which was esterified with methanol and thionyl chloride to obtain methyl ester hydrochloride salt **15**, which upon alkylation with propargyl bromide in presence of K_2CO_3 gave the mono alkylated product **16** (Scheme 1) under dilution conditions. In acetonitrile-K_2CO_3 reaction condition the amount of di-alkylated product obtained was negligible.

The mono alkylated product **16** was then treated with chloroacetyl chloride to obtain the acetyl derivative **17** in good yield. Condensation of **17** with thymine nucleobase gave the product **18**. To avoid the probability of intramolecular coupling reaction leading to polymerization in molecules such as **22** possessing azide and free acetylene groups, one of the functional groups needs to be protected. Hence, the alkyne functionality of compound **18** was protected with TMS using trimethylsilyl chloride in presence of *t*-BuLi to get the product **19**, so that during oligomerization TMS can be deprotected before click reaction. But the yield for the above conversion was very low (ca 12%). Efforts were made to increase the yield by varying the reaction conditions, but there was no desired success. Due to this difficulty, further synthesis of the azide and alkyne functionalized targeted monomer **22** was discontinued.

Scheme1: Synthesis of azide and alkyne functionalized monomer

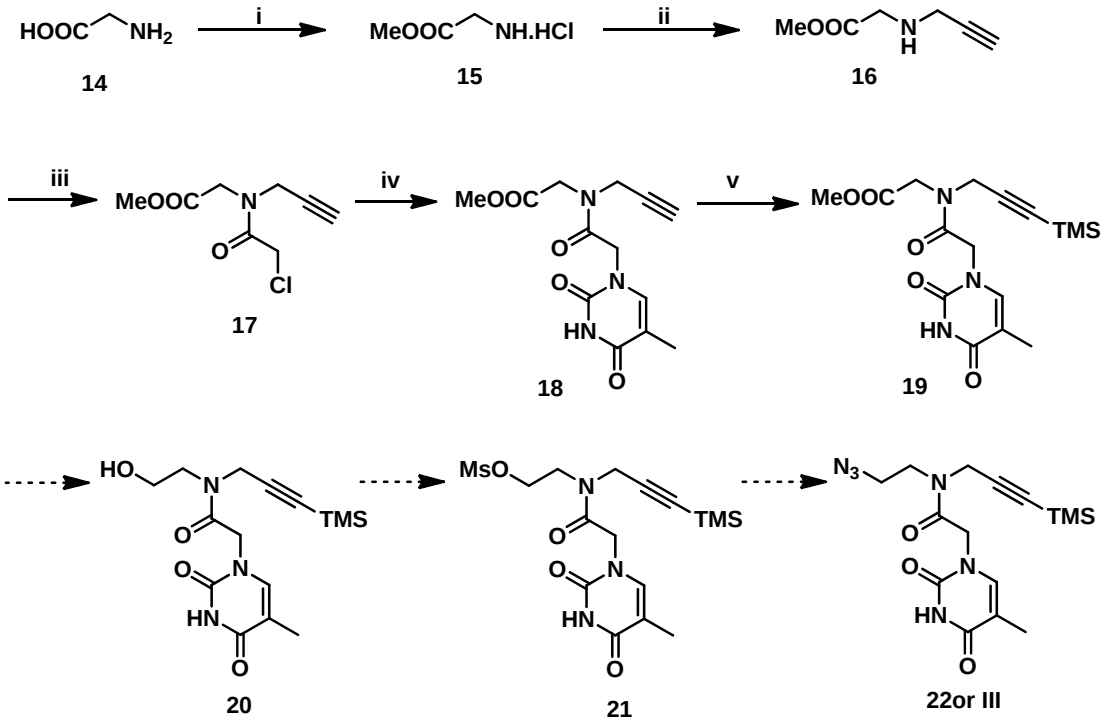

Reagents and conditions: i) $SOCl_2$, MeOH ii) propargyl bromide, K_2CO_3, ACN, 45% iii) CH_2COCH_2Cl, Et_3N, DCM, 64% iv) Thymine, K_2CO_3, DMF, 72% v) TMSCl, *t*-BuLi, THF, -78^oC, 12%.

Alternatively the synthesis of 1,2,3-triazole dimer **IV** (Figure 13) was proposed for incorporation of triazole unit in PNA backbone. For the synthesis of 1,2,3-triazole dimer **IV** the azide functionalized monomer **V** and the alkyne functionalized monomer **VI** needed to be synthesized and this was done as shown in Scheme 2 and Scheme 3 respectively.

3.4.2 Synthesis of azide functionalized monomer (V, 30)

2-Aminoethanol **23** was alkylated with ethyl bromoacetate to get the alkylated product **24**. This alkylation step leads to two nonseparable products having very low R_f difference, one of which may be the *O*-alkyled product. The compound **24** was found to be unstable. Therefore, it was taken to the next step without isolation. The hydroxyl group of compound **24** was protected with TBDPS using TBDPSCl to obtain **25**, which was confirmed by the appearance of aromatic protons at δ 7.38-7.70 ppm in ^1H NMR spectra. The free secondary amine in the compound **25** was converted to its acyl

derivative **26** using chloroacetyl chloride in presence of triethylamine, which was subsequently used for N-alkylation of thymine nucleobase to get the product **27**. The appearance of peaks at δ 6.65 ppm and 1.83 ppm in ^{1}H NMR showed the formation of the product. The TBDPS group was deprotected by using 1M TBAF in THF to get the free alcohol **28,** which was polar due to the presence of the free hydroxyl group as well as the thymine nucleobase making it difficult for isolation. Therefore, it was directly converted to its mesyl derivative **29** which was also found to be unstable perhaps due to the formation of stable six membered ring. The mesyl reaction mixture was subjected to substitution reaction with NaN_3 to get the azide functionalized monomer **30** or **V** (Scheme 2) in an overall 10-15% yield, which has been characterized by ^{1}H NMR and LCMS experiment. All the unknown compounds synthesized were characterized by ^{1}H NMR, ^{13}C NMR and LCMS spectra and are given in the experimental section.

Scheme 2: Synthesis of azide functionalized fragment

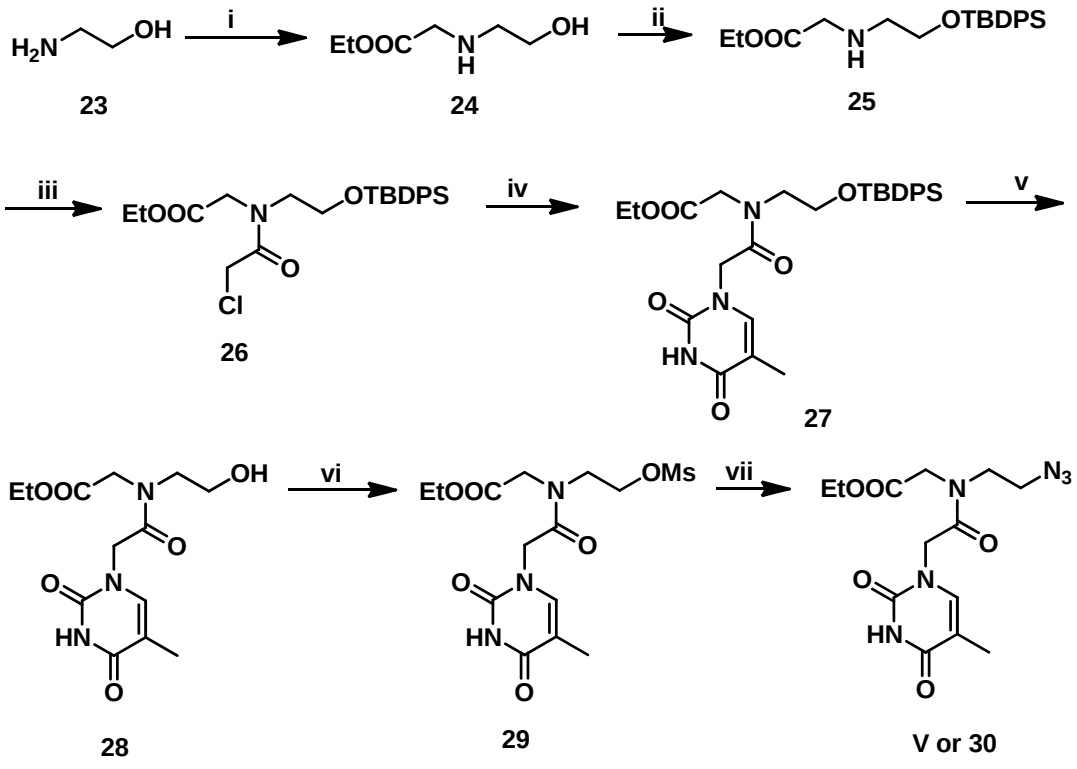

Reagents and conditions: i. Ethyl bromoacetate, Et_3N, ACN ii. TBDPSCl, imidazole, DMF, 60% iii. $ClCH_2COCl$, Et_3N, DCM, 75% iv. Thymine, K_2CO_3, DMF, 63% v. 1M TBAF, THF vi. MsCl, pyridine vii. NaN_3, DMF, 15%

3.4.3 Synthesis alkyne functionalized monomer (VI, 35).

The synthesis of the *N*-alkyne functionalized title compound **VI** or **35** was accomplished starting from the commercially available 1,2-diaminoethane **31**. Mono N-Boc protection of the compound **31** was selectively done by using *tert*-butyl pyrocarbonate following reported procedure[1] to obtain the product **32**. This upon N-monoalkylation with propargyl bromide gave the *N*-*tert*-butyl-2-(prop-2-ynylamino)ethylcarbamate **33**. This conversion was confirmed by the appearance of a triplet at δ 2.3-2.3 ppm in ^{1}H NMR, which was further confirmed by ^{13}C NMR and LCMS spectra. Compound 13 was acylated with chloroacetyl chloride in presence of triethylamine to afford the product *N*1-*tert*-butyl-N2-[2-chloro acetamido-N^{2}-*N*-(prop-2-ynyl)]ethylcarbamate **34**. This was condensed with thymine in the presence of K_2CO_3 in DMF yielding the desired product **35** (Scheme 3). Characterization of the unknown compounds has been done by ^{1}H NMR, ^{13}C NMR and LCMS spectra which are given in the experimental section.

Scheme 3: Synthesis of alkyne functionalized fragment

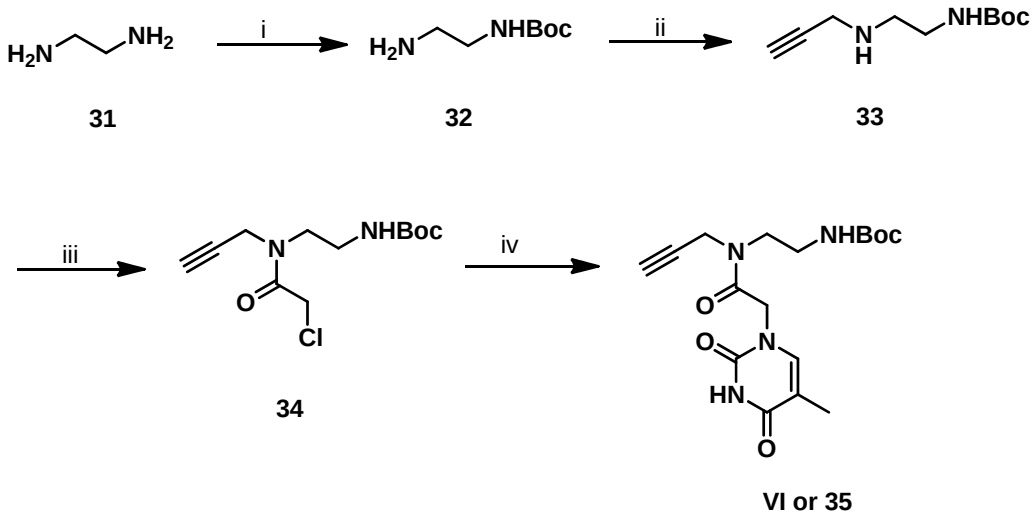

Reagents and conditions: i. $(Boc)_2O$, THF, 60% ii. Propargyl bromide, K_2CO_3, CH_3CN, 56% iii. $ClCH_2COCl$, Et_3N, DCM, 81% iv. Thymine, K_2CO_3, DMF, 83%

Synthesis of dimer

Due to low yields and synthetic difficulties experienced for the synthesis of the azide component **V**, approach using the synthesis of the dimer was also discontinued.

3.5 Synthesis of triazole based PNA oligomers on solid support

After various failed attempts to obtain the desired triazole PNA monomers (**22, 30**) in solution phase as described in the above section, it was thought to design a synthetic protocol wherein the conversion of amine to azide can be done on solid support itself. The acetylene monomer **V,** synthesized in the solution phase with high yield can be used as the other component for the 1,2,3-triazole formation reaction on solid support.[19] Here the replacement of the amide link in *aeg*PNA backbone by 1,2,3-triazole unit was done by solid phase click reaction between the polymer supported azido component **VII** with the acetylenic component **VI** synthesized in solution (Figure 14). The aminoethylglycyl (*aeg*) thymine monomer for initial coupling was synthesized by reported procedure.[1, 20] All new compounds were characterized by ^{1}H, ^{13}C NMR, IR and mass spectral data.

3.5.1 Results and Discussion

The amide bond replacement by 1,2,3-triazole unit was achieved in *aeg*PNA oligomers by using the Huisgen 1,3-dipolar cycloaddition reaction. The first *aeg*-thymine monomer was incorporated into solid support using Boc chemistry on L-lysine derivatized(4-methylbenzhydryl) amine (MBHA) resin as reported before,[21] using HBTU/HOBt/DIEA in DMF as the coupling reagent (Scheme 5).

In the second step, Boc was deprotected with 50% of TFA in DCM and followed by the conversion of the free amine to azide using freshly prepared triflyl azide[22] and copper sulphate in DCM. The alkyne functionalized monomer **35** was reacted with the azide, bound to the solid support using copper(I) iodide/ascorbic acid/DIEA to introduce the 1,2,3-triazole moiety by click reaction in the desired position of the PNA backbone (Scheme 5). The same cycle was repeated to obtain the oligomers of different lengths. For the initial coupling, the completion of the reaction was monitored by Kaiser test. After synthesizing the dimer/trimer, the resin beads become colored due to the use of CuI. Hence, it is difficult to monitor the reaction progress by Kaiser test, irrespective of triazole formation reaction and the conversion of the free amine to its corresponding azide. To overcome this problem, after every coupling reaction some of the resin beads were removed from the reaction mixture. It

was then subjected to TFA-TFMSA cleavage to get the oligomer in solution, which was characterized by RP-HPLC and confirmed by MALDI-TOF.

Scheme 5: Synthetic protocol for the synthesis of 1,2,3-triazole PNA oligomers on solid support

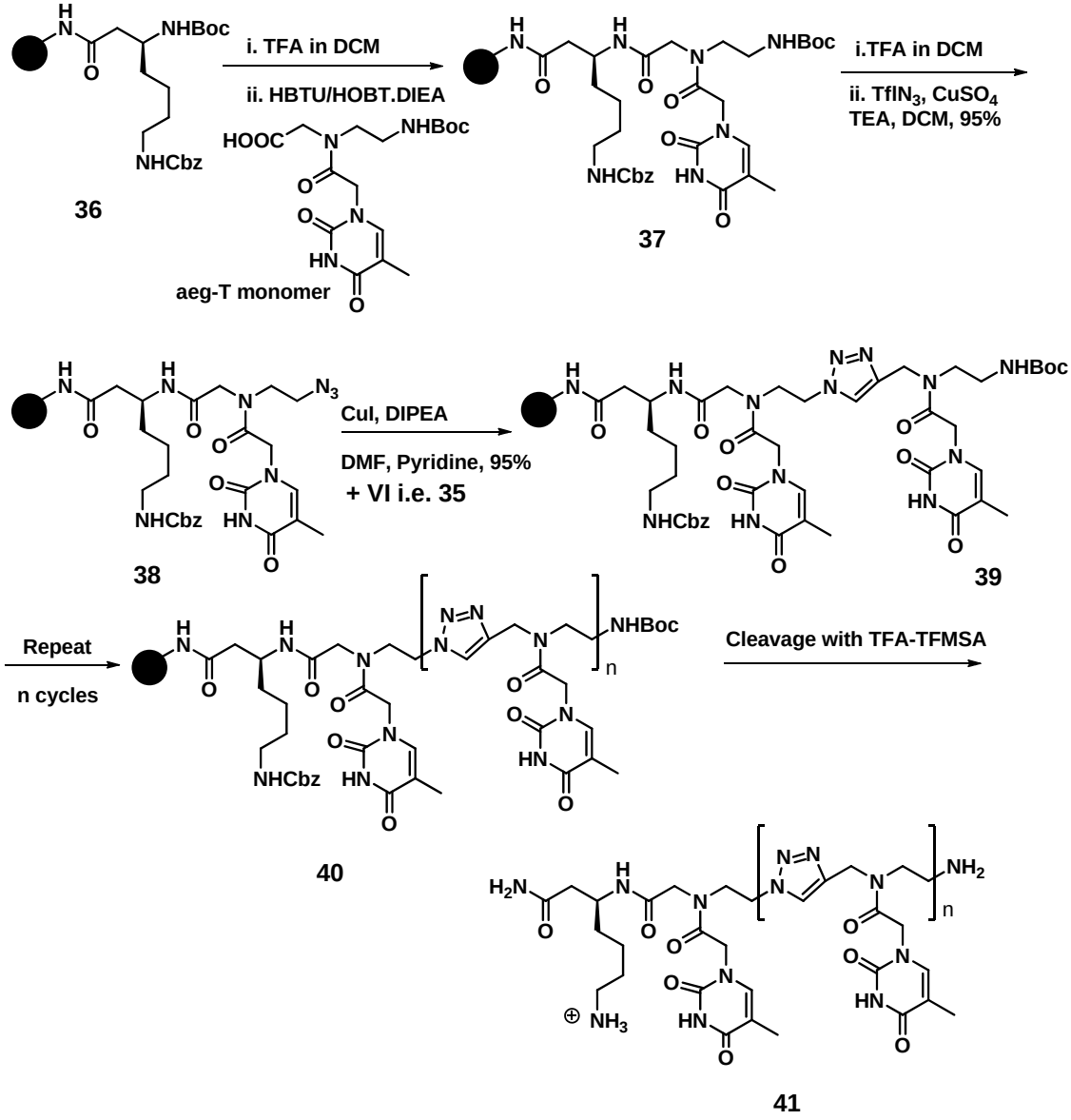

3.5.2 Cleavage of the PNA Oligomers from the Solid Support

During the synthesis of tetramer **PNA22** (Table1) where all the amide bonds were replaced by 1,2,3-triazole, the conversion of amine to azide as well as the triazole formation reaction shows more than 90% HPLC purity. Crude RP-HPLC profiles are shown for dimer, trimer and tetramer of **PNA22** which represent the successful 1,2,3-

triazole synthesis on solid support. These oligomers were further confirmed by MALDI-TOF (Figure 15, 16) data. Along with the synthesis of **PNA22** the oligomers **PNA19-PNA21** (Table1) were also synthesized for confirmation of the synthesis. Once the conversion of amine to azide and the synthesis of 1,2,3-triazole unit on solid support was confirmed, Boc deprotection-condensation (with T or T*) cycle was repeated to obtain the target mixed backbone PNA oligomers having 1,2,3-triazole unit in shown positions. After the completion of synthesis, the oligomers were cleaved from the resin using "low-high TFA-TFMSA" procedure[23] followed by RP-HPLC (Figure 17) purification on Merck C18 column and characterized by mass spectrometry (MALDI-TOF). The corresponding MALDI-TOF spectra have shown in the experimental section.

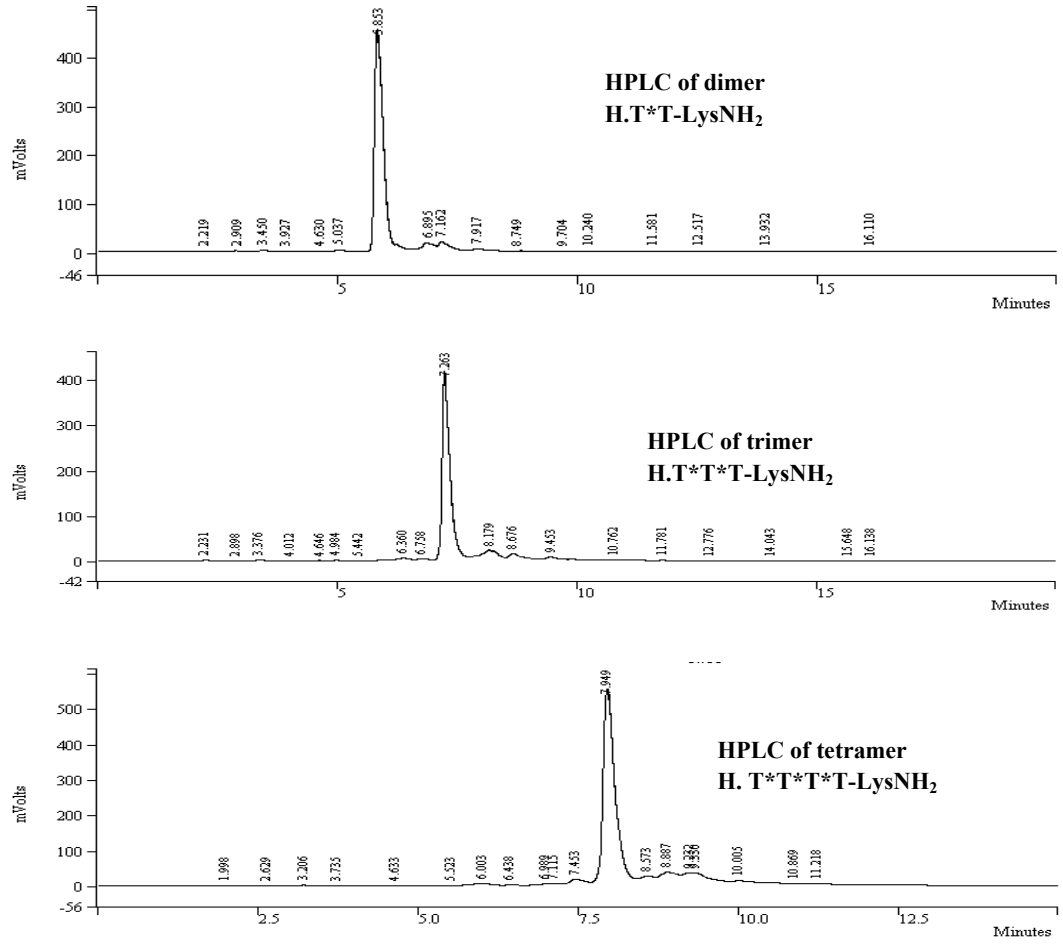

Figure 15: RP-HPLC profile of crude dimer and trimer and tetramer

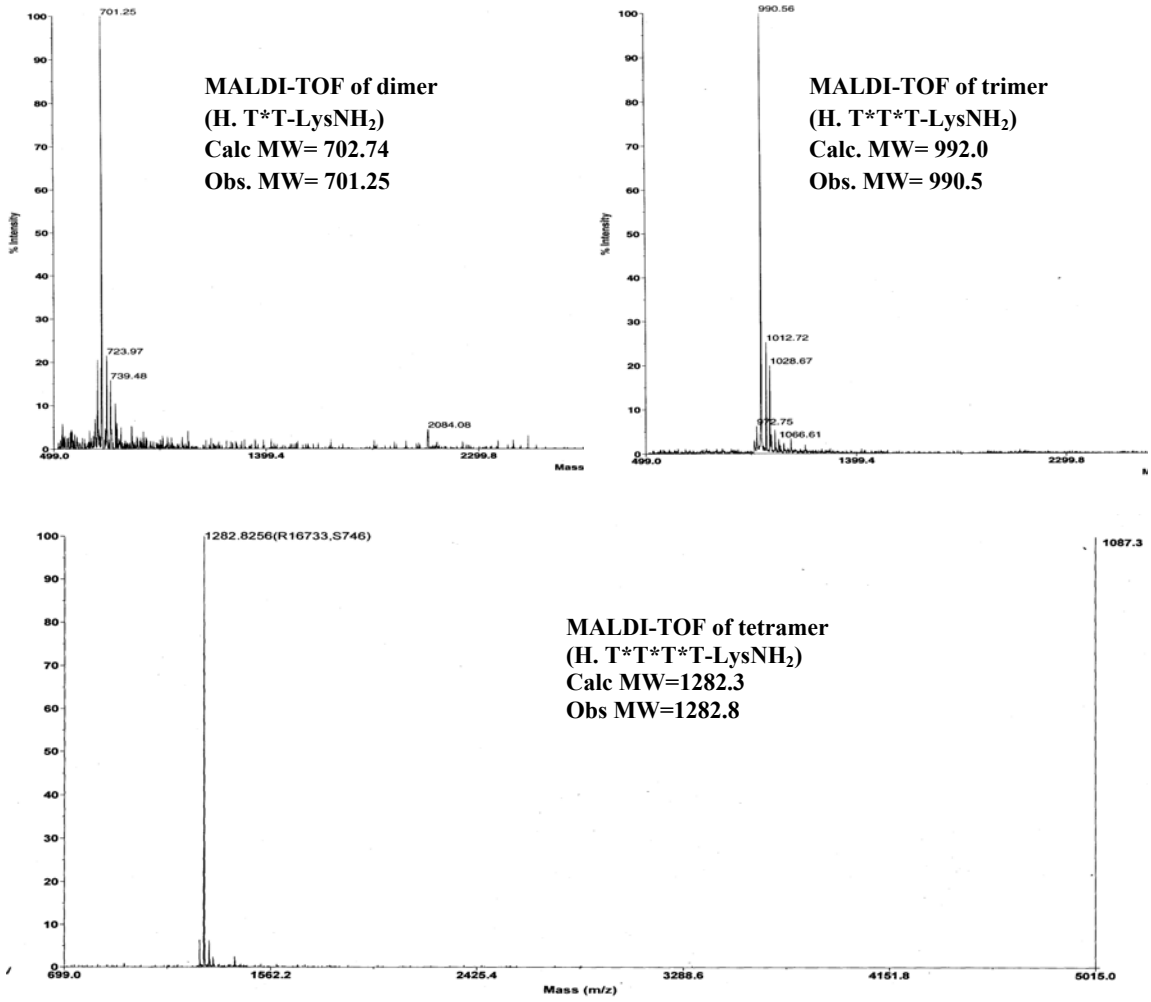

Figure 16: MALDI-TOF of crude dimer, trimer and tetramer PNA**22**

Table 1: Oligomers synthesized for biophysical studies

Entry	PNA composition	Mol.formula	RP-HPLC RT	Calc. MW	Obs. MW
PNA19	H-T T T*T- Lys NH_2	$C_{51}H_{71}N_{21}O_{16}$	7.4	1234.2	1234.8
PNA20	H-T*T T*T- Lys NH_2	$C_{52}H_{71}N_{23}O_{15}$	7.8	1258.2	1258.8
PNA21	H-T T*T T- Lys NH_2	$C_{51}H_{71}N_{21}O_{16}$	7.4	1234.2	1235.8
PNA22	H-T*T*T*T- Lys NH_2	$C_{53}H_{71}N_{25}O_{14}$	8.0	1282.3	1282.8
PNA24	H-T T T T T T- Lys NH_2	$C_{72}H_{99}N_{27}O_{25}$	7.7	1742.7	1742.4
PNA25	H-T T T T T*T- Lys NH_2	$C_{73}H_{99}N_{29}O_{24}$	8.1	1766.7	1767.0
PNA26	H-T* T T T T T- Lys NH_2	$C_{73}H_{99}N_{29}O_{24}$	8.1	1766.7	1767.1
PNA27	H-T T*T T*T T- Lys NH_2	$C_{74}H_{99}N_{31}O_{23}$	8.6	1790.0	1791.1
PNA28	H-T*T T*T T*T- Lys NH_2	$C_{75}H_{99}N_{33}O_{22}$	8.8	1814.8	1816.2
PNA29	H-T*T*T*T*T*T- Lys NH_2	$C_{77}H_{99}N_{37}O_{20}$	9.3	1862.8	1863.1

*****Indicates 1,2,3 triazole, T indicates *aeg*T monomer and*T is compound 35

3.5.3 Purification and characterization of the PNA Oligomers

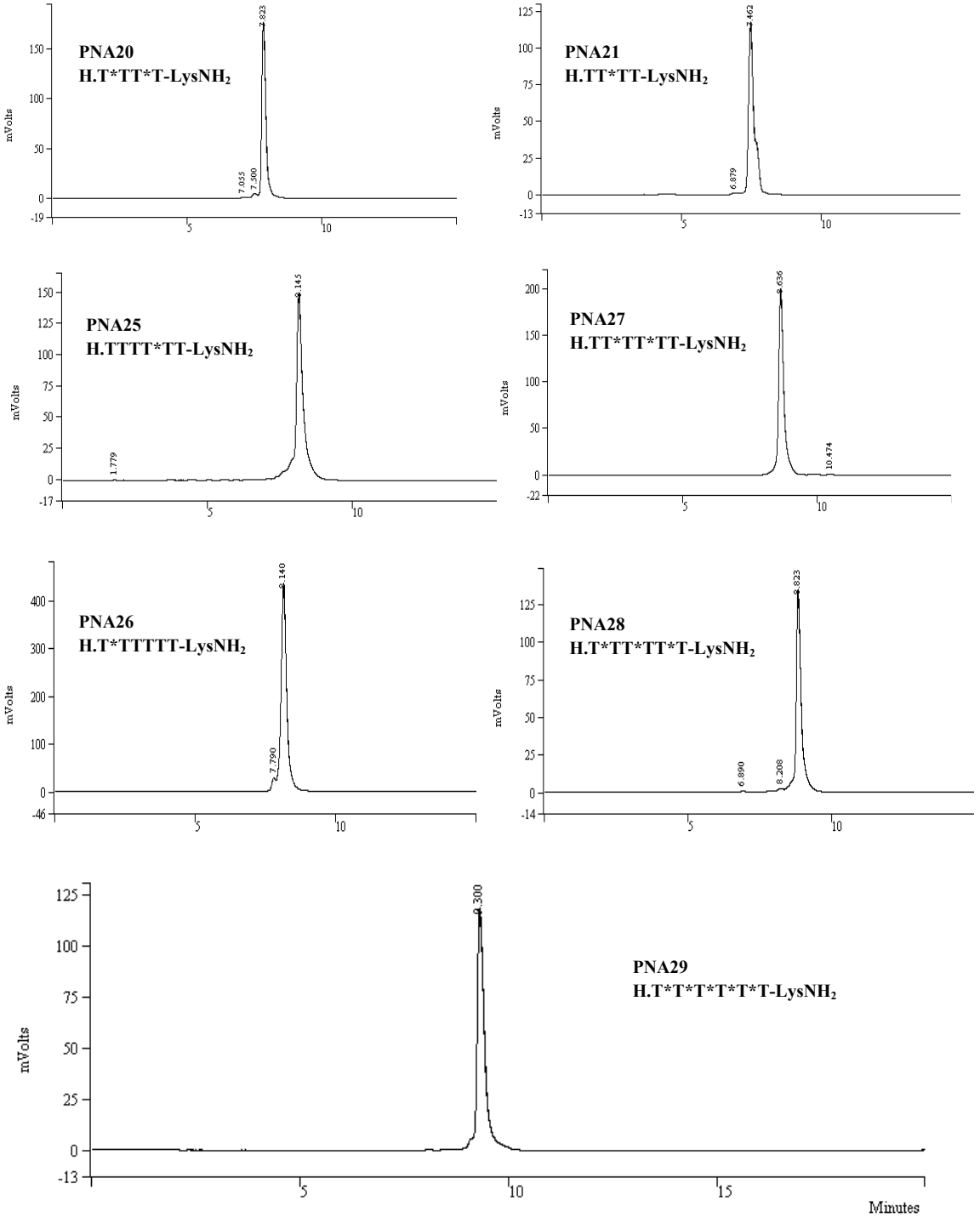

Figure 17: HPLC profile for triazole oligomers

3.6 Biophysical Studies of PNA:DNA Complexes

For the study of binding affinity and specificity of the modified 1,2,3-triazolyl PNA towards complementary DNA, the stoichiometry of the 1,2,3-triazolyl **PNA29**:**DNA30** was first determined using Job's method.[24] The UV and CD-melting studies were then carried out for single stranded **PNA24** to **PNA28** and UV melting studies of the hexamers complexed with complementary DNA. The T_m data of various complexes was compared with that of DNA complexes of unmodified *aeg***PNA23**. The CD spectra of single strands and corresponding complexes with complementary DNA were also examined.

3.6.1 CD spectroscopy of single stranded triazolyl PNA and triazolylPNA:DNA complexes

In circular dichroism spectra, all modified PNAs show normal pattern identical to the unmodified PNA sequence (Figure 18A). The CD spectra for the PNA:DNA complexes were also recorded. All the oligomers hybridized with complementary DNA show positive maxima at 270 nm and 220 nm and a negative minima at 245 nm (Figure 18B).

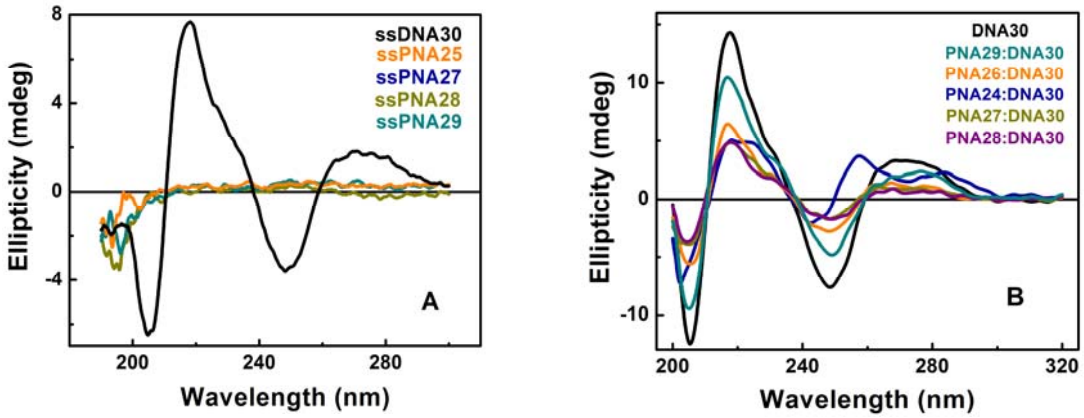

Figure 18: CD spectra for (A) single stranded PNAs and DNA**30** (CGA_8GC) (B) TzNA:DNA complexes

3.6.2 UV and CD Self melting of single stranded triazolyl PNAs

Due to the presence of heterocyclic moiety in the PNA backbone, it was necessary to confirm whether the modified *triazolyl*-PNAs show self organized

structure. It can be determined by temperature dependent UV-experiment. UV melting studies of single stranded *triazolyl*-PNA oligomers (**PNA24-29**) without complexing with complementary DNA was done. Single and double modified PNAs (**PNA25-27**) did not show any melting transition (Figure 19A) suggesting absence of self organized structure. Triple modified **PNA28** and the completely modified PNA hexamer (**PNA29**) showed sigmoidal curves (Figure 19B) which indicate that **PNA29** possesses self organization perhaps due to the presence of heterocycles in the PNA backbone. From the corresponding derivative curves (Figure 19C) melting temperatures (T_m) were found to be 42.9°C and 47.9°C for single stranded **PNA28** and **PNA29** respectively.

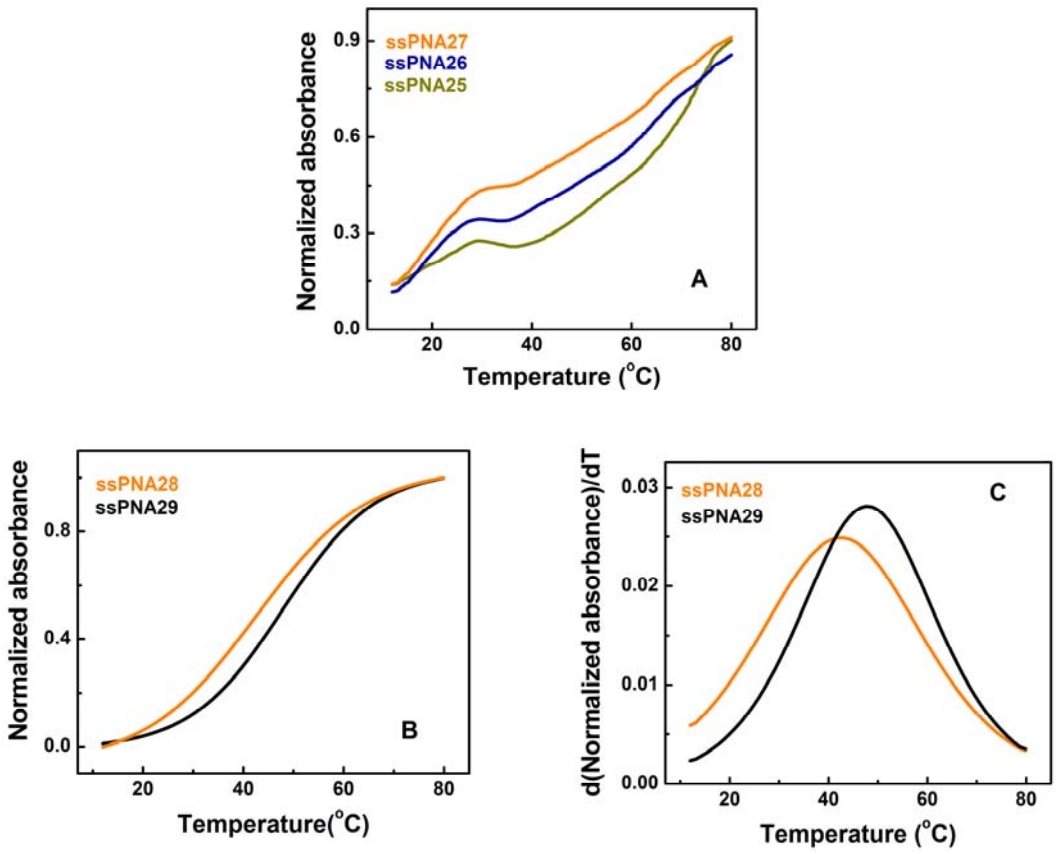

Figure 19: (A) UV self melting of single strand **PNA25-PNA27 (B)** UV self melting for single strand **PNA28** and **PNA29** **(C)** corresponding derivative curve for **B**.

3.6.3 CD and UV Job's plot for 1, 2, 3-triazole PNA:DNA complexes

The CD and UV mixing experiments are carried out by mixing the appropriate oligomers in different molar ratios keeping the total concentration constant. In this experiment, the ellipticity and absorbances of different molar ratios (100:0, 90:10,

80:20, 70:30, 60:40, 50:50 to 0:100) of **PNA27**:**DNA30**, **PNA28**:**DNA30** and **PNA29**:**DNA30** complexes were recorded maintaining overall concentration constant (Figure 20).

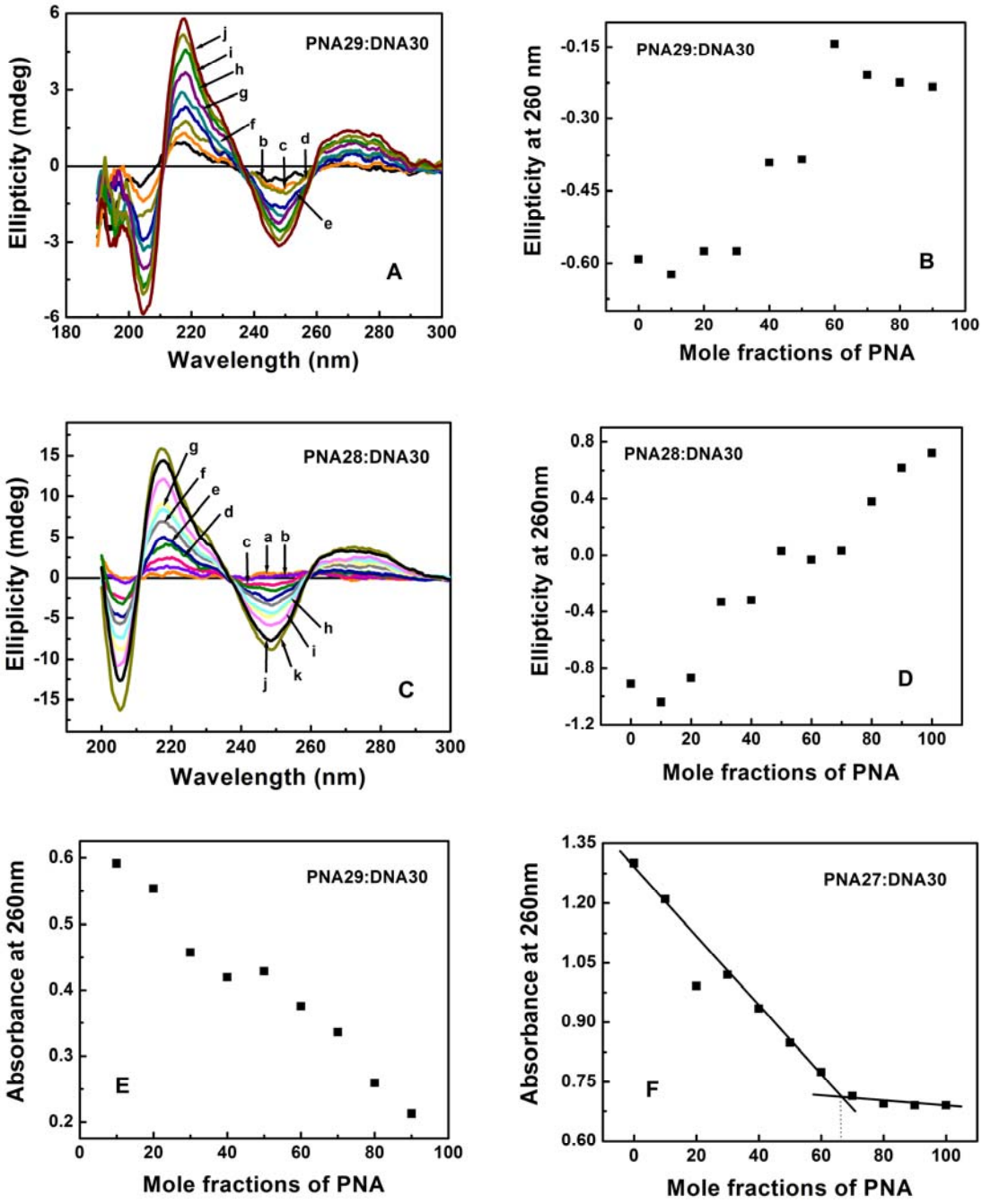

Figure 20: CD job's plot for **(A), (B)** PNA**29**:DNA**30**, **(C), (D)** PNA**28**:DNA**30**; UV Job's plot for **(E)** PNA**29**:DNA**30**, **(F)** PNA**27**:DNA**30** with stoichiometric ratios of (a) 100:0 (b) 90:10 (c) 80:20 (d) 70:30 (e) 60:40 (f) 50:50 (g) 40:60 (h) 30:70 (i) 20:80 (j) 10:90 and (k) 0:100

PNA28 and **PNA29** does not form any duplex/triplex with complementary **DNA30** which is indicated by CD Job's plot (Figure 20A, 20B, 20C and 20D). The UV Job's plot for **PNA29** (Figure 20E) also confirms the failure of complex formation with complementary **DNA30**. But from UV Job's plot, formation of a 2:1 complex of **PNA27** with complementary DNA can be seen, which is shown in Figure 20F. Therefore from the results of CD and UV job's plot it can be concluded that **PNA27** forms a triplex with the complementary **DNA30** and **PNA28**, **PNA29** does not bind to the complementary DNA.

3.6.4 UV-T_m studies of PNA:DNA hybrids

The hybridization of triazole PNAs (**PNA24-PNA29**) with complementary **DNA30** was studied by temperature dependent UV absorbance experiment. The thermal stabilities (T_m) for all the triazole-PNA hexamers (**PNA25-PNA27**) (Figure 21) with complementary **DNA30** were determined and it was found to be stabilized the PNA_2: DNA triplexes compared to the unmodified PNA (Table2).

Table 2: Oligomers synthesized for biophysical studies

Entry	PNA	UV-Tm Single strand	UV-T_m (^oC)	ΔT_m (^oC)
PNA24	H-TTTTTT-$LysNH_2$	---	20.5	---
PNA25	H-TTTTT*T-$LysNH_2$	---	29.8	+8.4
PNA26	H-T*TTTTT-$LysNH_2$	---	31.9	+11.4
PNA27	H- TT*TT*TT-$LysNH_2$	---	34.3	+13.8
PNA28	H- T*TT*TT*T-$LysNH_2$	42.9	43.6	---
PNA29	H-T*T*T*T*T*T-$LysNH_2$	48.1	47.9	---

Complementary **DNA30** is 5' CG A_8 GC 3'

The *aeg*PNA hexamer (PNA**24**) shows a UV-T_m of 20.5^{o}C with the complementary DNA**30** (Figure 21A, 21B). PNA**25** and PNA**26** which have single modification show increase in T_m by +8.4^{o}C and +11.4^{o}C respectively. **PNA27** with two-modifications shows further increase of T_m for triplex by +13.8^{o}C (Figure 21A, 21B). Thus the N-terminus modification stabilizes the PNA:DNA complex more than the C-terminus modification. Two modifications stabilize the hybrid even more as compared to C-terminus and N-terminus modifications. The modification of the peptide bond in the *aeg*PNA backbone with 1,2,3-traizole moiety thus imparts an increase in UV-T_m for the oligomers (**PNA25-PNA27**).

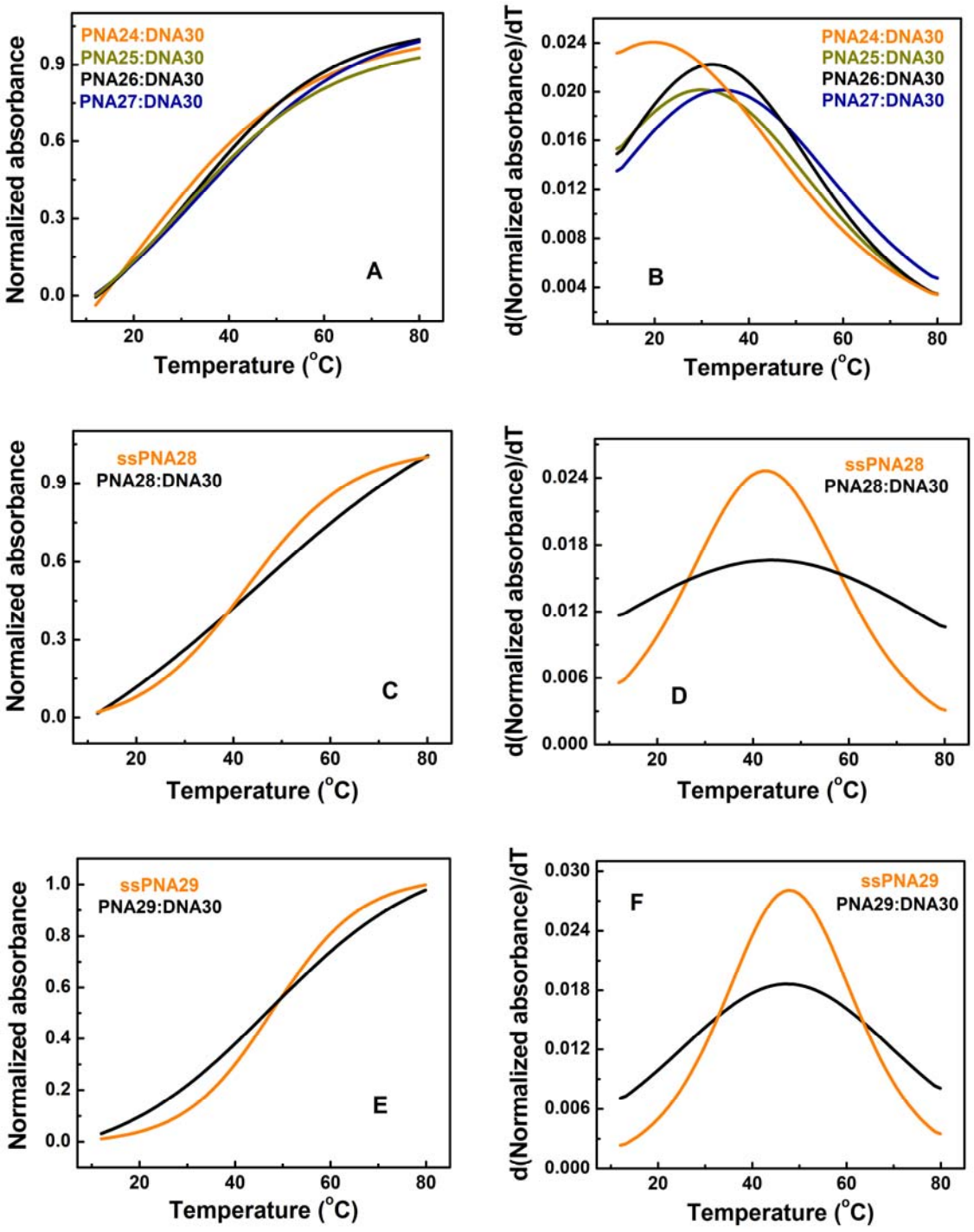

Figure 21: UV melting profile of PNA_2:DNA**30** complexes (**DNA30**: 5'CG A_8 GC 3') **(A) PNA25**:**DNA 30**, **PNA26**:**DNA30** and **PNA27**:**DNA30 (C)** ss**PNA28** and **PNA28**:**DNA30 (E)** ss**PNA29** and **PNA29**:**DNA30;** Derivative curve of **(B) PNA25**:**DNA30**, **PNA26**:**DNA30** and **PNA27**:**DNA30 (D)** ss**PNA28** and **PNA28**:**DNA30 (F)** ss**PNA29** and **PNA29**:**DNA30**.

PNA28 which is modified with three 1,2,3-triazole units has a melting temperature of 42.6°C when hybridized with complementary DNA (Figure 21C, 21D). This melting temperature was same as that of **PNA28** alone, without any hybridization

with complementary DNA. Similarly the melting temperature of triplex of **PNA29** which is fully modified with triazole unit was 47.9^{o}C, almost identical to single strand **PNA29** melting 48.1^{o}C (Figure 21E, 21F). These results suggest that the **PNA28** and **29** do not bind to the complementary DNA, in fact it undergoes self organization due to the presence of more numbers of heterocyclic moiety in the backbone. If such self organization can be obtained with multiple triazole links in PNA backbone, it may lead to a new class of helical PNA oligomers. However, this needs further work with synthesis of PNA oligomers bearing more number of triazole links and use of other characterization techniques to establish the organized structures. These will be analogous to the structures noticed in peptides with triazole links. The dipole moment of triazole ring may be responsible for inducing such structures.

3.7 Conclusion

It is demonstrated here that the amide links in the PNA backbone can be successfully replaced by the isosteric 1,2,3-triazole link, which can be efficiently synthesised in-situ on the resin using "click" reaction. The azide component was synthesized on the resin from the amino function and reacted with the propylene **31** to create the 1,2,3-triazole link. The triazole-hexamer sequence with less than three modifications form triplex with DNA d(CGA$_8$GC) with enhanced stability of 8-14^{o}C. However, **PNA28** where three amide bonds were replaced by 1,2,3-triazole shows a self melting of 42.8^{o}C. **PNA29** where all the amide bonds were replaced by 1,2,3-triazole unit undergoes organization showing a self-melting temperature of 48.1^{o}C. This is perhaps due to some self coiling induced by triazole links. Therefore, it can be concluded that the triazole based oligomers increases the stability towards DNA binding with less number of triazole unit. Increasing number of triazole units make it difficult to bind to the complementary DNA. Further work on the influence of triazole link in backbone on duplex formation is currently in progress, which could be interesting in generation of new oligomers for DNA/RNA hybridization based applications.

3.8 Experimental section

N-propynyl glycine methy ester (16)

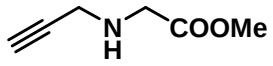

A suspension of glycine **14** (10 g, 133.3 mmol) in anhydrous methanol (100 ml) was stirred at 0°C. Thionyl chloride (11.6 ml, 160 mmol) was added dropwise to the reaction mixture. The stirring was continued at 0°C during the addition of thionyl chloride. After the completion of addition reaction mixture was allowed to come to room temperature followed by reflux for another 6 hrs. Methanol was removed under vacuum till the white solid obtained. The precipitate was washed with diethylether. The residue was dried under vacuum over phosphorus pentoxide which yielded methyl ester hydrochloride **15** as a white solid. This solid was used for the following experiment without further purification. Propargyl bromide (2.5 mL, 28.1 mmol) was added slowly to a cooled solution of salt **15** (5.0 g, 36.9 mmol) in dry CH_3CN (100 mL) containing K_2CO_3 (6.1 g, 44.2 mmol). Reaction mixture was slowly allowed to attain room temperature and stirred for 4 hrs after which CH_3CN was removed under vacuo. The residue was dissolved in water and was extracted with ethyl acetate (40 mL x 3) and the combined organic layer was washed with saturated aqueous $NaHCO_3$ and brine and dried over anhydrous Na_2SO_4. The organic layer upon evaporation in vacuo gave a yellow liquid which was purified by column chromatography (2.1 g, 45%).

^{1}H NMR (200 MHz, $CDCl_3$) δ_H 2.24-2.27 (t, 1H), 3.49-3.5 (d, 2H), 3.53 (s, 2H), 3.76 (s, 3H); **^{13}C NMR** (50 MHz, $CDCl_3$) δ_C 37.4, 48.8, 51.7, 72.0, 81.0, 172.2; **MS (EI)** *m/z* 127.0, Found 128.05 [M+H].

2-chloro-N1-(prop-2-ynyl) glycine methyl ester (17)

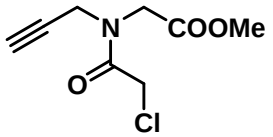

Chloroacetyl chloride (3.7mL, 47.2 mmol) diluted with DCM (5 mL) was added slowly to a stirred solution of the alkylated amine **16** (3.0 g, 23.6 mmol) and Et_3N (13.1 mL, 94.3 mmol) in dry CH_2Cl_2 (35 mL) cooled at 0°C. After 30 min the reaction mixture was washed with water followed by saturated $NaHCO_3$ and by brine. The combined organic layer was removed under vacuo and the residue was purified by

column chromatoghraphy to afford the chloro compound **17** as a yellow liquid (3.1 g, 64%).

^{1}H NMR (200 MHz, $CDCl_3$) δ_H 2.30-2.32 (t, 0.39H), 2.40-2.43 (t, 0.51H), 3.76-3.80 (d, 3H), 4.06 (s, 1H), 4.23 (s, 1H), 4.26 (s, 2H), 4.32-4.35 (t, 2H); **^{13}C NMR** (50MHz, $CDCl_3$) δ_C 35.9, 38.5, 41.0, 47.0, 47.9, 52.2, 52.6, 73.7, 74.3, 166.5, 168.9; **MS (EI)** *m/z* 203.63, Found 226.07 [M+Na^+].

N2-(thyminyl)-N-(prop-2-ynyl) glycine methyl ester (18)

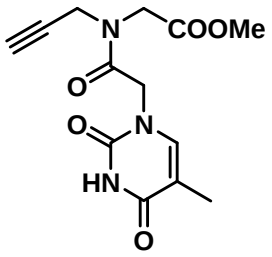

A mixture of the chloro compound **17** (4.5 g, 21.7 mmol), thymine (2.7 g, 21.7 mmol) and anhydrous K_2CO_3 (3.6g, 26.04mmol) in dry DMF (30 mL) was stirred at rt for overnight under inert atmosphere. The mixture was concentrated under reduced pressure and the residue was extracted with ethyl acetate followed by washing with brine and dried over Na_2SO_4. The organic layer was evaporated and the crude product was purified by column chromatography to obtain a colorless solid **18** (4.5g, 72%).

^{1}H NMR (200MHz, $CDCl_3$) δ_H 1.92 (s, 3H), 2.29-2.32 (t, 0.42H), 2.45-2.47 (t, 0.50H), 3.75-3.82 (d, 3H), 4.24-4.26 (d, 2H), 4.32-4.34 (d, 2H), 4.49 (s, 1H), 4.71 (s, 1H), 7.01-7.04 (dd, 1H), 9.13-9.17 (d, 1H); **^{13}C NMR** (50MHz, $CDCl_3$) δ_C 12.1, 35.7, 37.5, 46.6, 47.7, 52.0, 52.5, 73.6, 74.6, 109.9, 140.9, 151.1, 164.7, 167.1, 168.8; **MS (EI)** *m/z* 293.2, Found 316.1 [M+Na^+].

N2-(thyminyl) N-(TMS-prop-2-ynyl) glycine methyl ester (19)

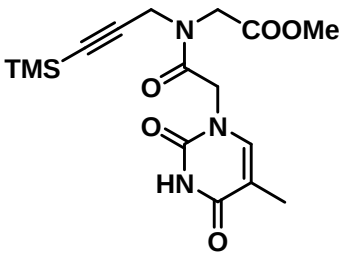

The alkyne **18** (2.0 g, 6.8 mmol) dissolved in freshly dried THF, was taken in 50mL rb flask. The reaction mixture was allowed to attain -78^{o}C. Then *t*-BuLi (1.3 mL, 13.6 mmol) was added slowly to the reaction mixture. Reaction temperature was maintained at -78^{o}C for another 1 hr. After the generation of the nucleophile, TMSCl (1.3 mL, 10.2 mmol) was added dropwise. The reaction mixture was allowed to come to room temperature slowly and it was stirred for overnight. After that reaction was quenched with saturated NH_4Cl solution. The reaction mixture was extracted with

ethyl acetate (50 ml x 3). The combined organic layer was washed with saturated $NaHCO_3$ solution followed by brine. Organic layer was removed under vacuo and was purified by column chromatography to get a colorless solid (0.3g, 12%).

^{1}H NMR (200MHz, $CDCl_3$) δ_H 0.13-0.17 (d, 7H), 1.24 (s, 3H), 1.91 (s, 3H), 3.73-3.8 (d, 3H), 4.22-4.24 (d, 2H), 4.31-4.33 (d, 2H), 4.45 (s, 1H), 4.67 (s,1H), 6.97-7.25 (dd, 1H), 8.72-8.81(d, 1H), **MS (EI)** *m/z* 365.4, Found 366.2 [M+H], 388.2 [M+Na^+].

Ethyl 2-(2-hydroxyethylamino)acetate (24)

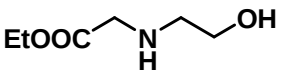

Ethyl bromoacetate (7.2 mL, 65.4 mmol) was added dropwise to an ice cooled mixture of 2-aminoethanol **23** (5.0 g, 81.8 mmol) and triethyl amine (16.5 mL, 163.6 mmol) in acetonitrile (70mL). After complete addition, reaction mixture was allowed to stirr for overnight at ambient temperature. Acetonitrile was removed under vacuo and the residue was dissolved in water. The aqueous layer was extracted with ethyl acetate (40mL x 5). The combined organic layer was then washed with saturated $NaHCO_3$ solution followed by brine and dried over Na_2SO_4. Organic layer was removed under reduced pressure and the crude product was purified by column chromatography to yield the product **24**.

^{1}H NMR (200MHz, $CDCl_3$) δ_H 1.25-1.32 (t, 3H), 2.80-2.85 (t, 2H), 3.46 (s, 2H), 3.6-3.69 (t, 2H), 4.15-4.26 (q, 2H); **MS (EI)** *m/z* 147.0, Found 170.2 [M+Na^+].

Ethyl 2-(2*O*-TBDPS-ethylamino)acetate (25)

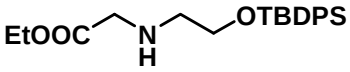

Alcohol **24** (3.5 g, 23.7 mmol) was dissolved in DMF (25 mL). To this mixture imidazole (11.2 g, 165.9 mmol) was added followed by the addition of *t*-butyldiphenylsilylchloride (12.3 mL, 47.4 mmol). The reaction mixture was allowed to stir for 24 hrs at room temperature. DMF was removed under reduced pressure and the residue was extracted with ethyl acetate (30mL x 3). The combined organic layer was washed with brine and dried over Na_2SO_4. The crude product was purified by silica gel column chromatography to afford the product **25** (5.4g, 60%).

^{1}H NMR (200MHz, $CDCl_3$) δ_H 1.06 (s, 9H), 1.25-1.32 (t, 3H), 2.74-2.79 (t, 2H), 3.44 (s, 2H), 3.74-3.8 (t, 2H), 4.1-4.3 (q, 2H), 7.38-7.4 (m, 6H), 7.66-7.69 (m, 4H); **^{13}C**

NMR (50MHz, $CDCl_3$) δ_C 14.3, 19.2, 26.8, 50.9, 51.1, 60.7, 63.3, 127.7, 129.7, 133.5, 135.6, 172.3; **MS (EI)** *m/z* 385.2, Found 286.1 [M+H], 408.0 [M+Na^+].

Ethyl 2-(2*O*-TBDPS-aminoethyl) N-(chloroacetyl)-glycinate (26)

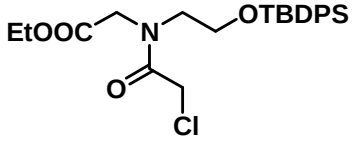

Chloroacetyl chloride (2.0 mL, 25.8 mmol) was added to an ice cooled mixture of the amine **25** (5.0 g, 12.9 mmol) and Et_3N (7.1 mL, 51.6 mmol) in dry DCM (50 mL). Stirring of the reaction mixture was continued for 0.5 hr at 0^{o}C. DCM was washed with water followed by saturated $NaHCO_3$ and brine. The organic layer was removed under vacuo and was purified by column chromatography to obtain the product (4.4 g, 75 %)

^{1}H NMR (200MHz, $CDCl_3$) δ_H 1.05 (s, 9H), 1.21-1.28 (t, 3H), 3.51-3.57 (m, 2H), 3.73-3.86 (m, 2H), 3.96-4.03 (d, 2H), 4.11-4.32 (m, 4H), 7.38-7.47 (m, 6H), 7.6-7.65 (m, 4H); **^{13}C NMR** (50MHz, $CDCl_3$) δ_C 14.1, 19.0, 26.8, 41.0, 47.9, 50.0, 50.8, 61.3, 61.8, 128.0, 130.1, 132.5, 135.5, 167.4, 168.7; **MS (EI)** *m/z* 461.1, Found 483.9 [M+Na^+].

Ethyl -2-(2*O*-TBDPS-aminoethyl) N-thyminyl glycinate (27)

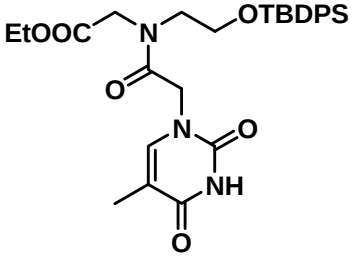

A mixture of compound **26** (2.0 g, 4.3 mmol), thymine (0.54 g, 4.3 mmol) and K_2CO_3 (0.70 g, 5.1 mmol) in DMF (15 mL) was heated at 60^{o}C for 8hrs. DMF was removed under reduced pressure and the residue was dissolved in water. The aqueous layer was extracted with ethyl acetate (40mL x 4). The combined organic layer was washed with saturated $NaHCO_3$ solution followed by brine and then it was removed under vacuo. The residue was purified by silica gel column chromatography to get the pure product (1.5 g, 63%).

^{1}H NMR (200MHz, $CDCl_3$) δ_H 1.05-1.08 (d, 9H), 1.20-1.29 (m, 3H), 1.83-1.92 (d, 2H), 3.54-3.56 (m, 2H), 3.81-3.83 (m, 2H), 4.02 (s, 2H), 4.10-4.32 (m, 2H), 4.42-4.54 (d, 2H), 6.65-7.00 (d, 1H), 7.38-7.44 (m, 6H), 7.60-7.66 (m, 4H); **^{13}C NMR** (50MHz, $CDCl_3$) δ_C 12.3, 14.1, 19.2, 26.9, 47.6, 48.1, 50.2, 61.4, 110.4, 128.0, 130.1, 132.6, 135.5, 140.9, 151.0, 164.3, 167.4, 168.7, 169.3; **MS (EI)** *m/z* 551.7, Found 552.6 [M+H], 574.6 [M+Na^+].

Ethyl 2-(2-hydroxyaminoethyl) N-thyminyl glycinate (28)

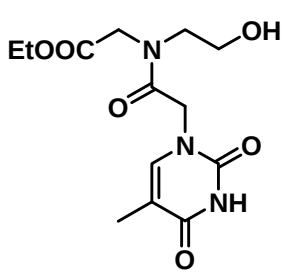

Compound **27** (4 g, 7.2 mmol) was dissolved in THF. To this reaction mixture TBAF (1M solution in THF) was added slowly. After 0.5 hr THF was removed under vacuo and the residue was extracted with ethyl acetate. The organic layer was washed with brine and the crude residue was used as such for the next reaction.

Ethyl 2-(2*O*-mesylaminoethyl)-N-thyminyl glycinate (29)

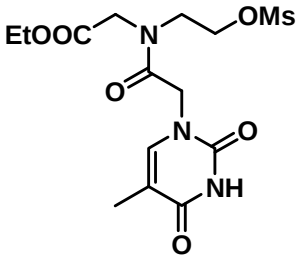

Mesyl chloride (0.55 mL, 7.2 mmol) was added drpowise to a cooled solution of the alcohol **28** (1.0 g, 7.1 mmol) in pyridine (10 mL). The reaction was continued for another 0.5 hr at ice cold temperature. After the completion of the reaction DCM was washed with saturated $NaHCO_3$ solution followed by brine and dried over anhydrous Na_2SO_4. Pyridine was removed under vacuum followed by extraction with ethyl acetate. The organic layer was removed under reduced pressure and the crude mixture was used for next reaction.

Ethyl 2-(2-azidoaminoethyl) N-thyminyl glycinate (30)

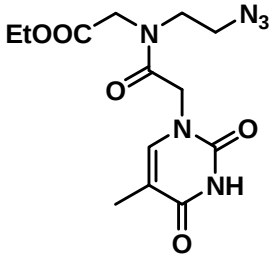

A mixture of crude mesylate **29** and NaN_3 (3.7 g, 57.6 mmol) in DMF (15 mL) was heated at 60^{o}C for 6 hrs. DMF was removed under reduced pressure and the residue was dissolved in water. The aqueous layer was extracted with ethyl acetate (40 mL x 4). The combined organic layer was washed with brine and then it was removed under vacuo. The residue was purified by column chromatography to get the pure product (0.15 g, 15%).

^{1}H NMR (200MHz, $CDCl_3$) δ_H 1.15-1.24 (m, 3H), 1.75 (s, 3H), 3.45-3.63 (m, 4H), 4.04-4.10 (m, 2H), 4.71 (s, 2H), 7.33 (m, 1H), 11.31 (s, 1H); **MS (EI)** *m/z* 338.3, Found 339.8 [M+H].

tert-butyl 2-(prop-2-ynylamino)ethylcarbamate (33)

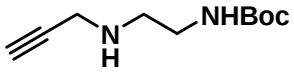

Propargyl bromide (2.5 mL, 28.1 mmol) was added slowly to a cooled solution of *tert*-butyl 2-aminoethylcarbamate **32** (5 g, 31.2 mmol) in dry CH_3CN (70 mL) containing K_2CO_3 (6.5 g, 46.9 mmol). Reaction mixture was slowly allowed to attain room temperature and stirred for 8 hrs after which CH_3CN was removed under vacuo. The residue was dissolved in water and was extracted with ethyl acetate (40 mL x 3) and the combined organic layer was washed with saturated aqueous $NaHCO_3$, brine and dried over anhydrous Na_2SO_4. The organic layer upon evaporation in vacuo gave a yellow liquid which was purified by column chromatography (3.5 g, 56%).

^{1}H NMR (200 MHz, $CDCl_3$) δ_H 1.45 (s, 9H), 2.24 (t, 1H), 2.79 (t, 2H), 3.23 (q, 2H), 3.42 (d, 2H), 5 (bs, 1H); **^{13}C NMR** (50 MHz, $CDCl_3$) δ_C 28.3, 37.6, 39.9, 47.8, 71.5, 79.2, 81.8, 156.1; IR (neat) ν/cm^{-1} 3305, 2977, 2931, 2107, 1699 and 648. **MS (EI**) *m/z* 198.26, Found: 199.25 [M+H], 221.24 [M+Na$^+$].

***tert*-butyl N2-(2-chloro-N^1-(prop-2-ynyl)acetamido)ethylcarbamate (34)**

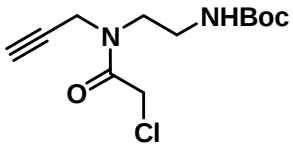

Chloroacetyl chloride (2.8 ml, 35.4 mmol) diluted with DCM (5 mL) was added dropwise to a stirred solution of the amine **33** (3.5 g, 17.7 mmol) and Et_3N (9.8 ml, 70.8 mmol) in dry CH_2Cl_2 (35 mL) cooled at 0^{o}C. After 30 min the reaction mixture was washed with water followed by saturated $NaHCO_3$ and brine. DCM was removed under vacuo and the residue was purified by column chromatoghraphy to afford the chloro compound **34** as a yellow liquid (3.9 g, 81%).

^{1}H NMR (200 MHz, $CDCl_3$) δ_H 1.44 (s, 9H), 2.29 (t, 0.47H), 2.38 (t, 0.39H), 3.33-3.41 (m, 2H), 3.62 (t, 2H), 4.15-4.25 (m, 4H), 4.9 (brs, 1H); **^{13}C NMR** (50 MHz, $CDCl_3$) δ_C 28.3, 35.1, 38.3, 38.6, 41.0, 41.3, 46.7, 47.2, 72.6, 73.7, 78.4, 79.4, 80.0, 156.1, 166.8; **IR** (neat) ν/cm^{-1} 3307, 2979, 2934, 2120, 1659, 663; **MS (EI)** *m/z* 274.74, Found: 275.26 [M+H], 297.28 [M+Na$^+$].

***tert*-butyl-N2-(2-(thyminyl)-N-(prop-2-ynyl)acetamido)ethylcarbamate (35)**

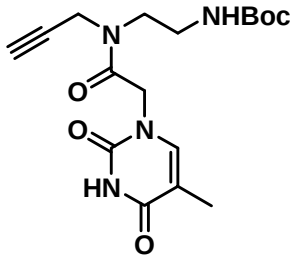

A mixture of the chloro compound **34** (3.9 g, 14.2 mmol), thymine (1.8 g, 14.2 mmol) and anhydrous K_2CO_3 (2.4 g, 17.04 mmol) in dry DMF (20 ml) was stirred at rt for overnight under inert atmosphere. The mixture was concentrated under reduced pressure and the residue was extracted with ethyl acetate followed by washing with brine and dried over anhydrous Na_2SO_4. The organic layer was evaporated and the crude product was purified by column chromatography to obtain a colorless solid (4.3 g, 83%).

^{1}H NMR (200 MHz, $CDCl_3$) δ_H 1.44 (s, 9H), 1.92 (s, 3H), 2.29 (t, 0.53H), 3.31-3.37 (m, 2H), 3.59 (q, 2H), 4.17-4.27 (dd, 2H, J=2.2 Hz, J=2.5 Hz) 4.58 (d, 2H, J= 10.8 Hz), 5.08 (br m, 0.41H), 5.3 (br m, 0.54H), 7.01(s, 1H), 9.33 (s, 1H); **^{13}C NMR** (200 MHz, $CDCl_3$) δ_C 12.3, 28.3, 35.2, 38.0, 38.5, 46.3, 47.4, 48.2, 72.8, 74.0, 78.3, 79.9, 110.6, 141.0, 141.3, 151.4, 156.2, 164.6, 166.7, 167.1; **IR** ($CHCl_3$), ν/cm^{-1} 3306.7, 3019.5, 2400.5, 1683.2, 1506.1, 1470.4, 668.7; **MS (EI)** *m/z* 364.4, Found 365.41 [M+H], 387.44 [M+Na^+]; mp 147.8-150^{o}C.

3.8.1 Synthesis of triflic azide[22]

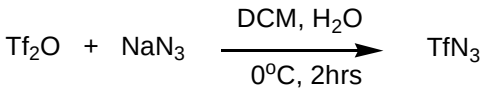

A solution of NaN_3 (3.5 g, 54.0 mmol) in water (8 mL) and CH_2Cl_2 (3 mL) was cooled to 0^{o}C in an ice-water bath. To this vigorously stirred solution, Tf_2O (1.51 mL, 9.0 mmol) was added dropwise through a syringe. After stirring at 0^{o}C for 2 hours, the organic phase was separated and the aqueous phase was extracted with 3 mL CH_2Cl_2. The combined organic layer was washed with 10 mL saturated aqueous $NaHCO_3$ and dried over anhydrous Na_2SO_4 for use in the next step. (**Note**: Although we have not experienced any problem in handling this compound, precaution should be taken due to its explosive nature).

3.8.2 Synthesis of azide on solid support

The free amine was converted to azide by reacting the resin (100 mg, loading value 0.35 meqg^{-1}) with freshly prepared TfN_3. A mixture of Et_3N (0.2 μL 3.5 eq), catalytic amount of $CuSO_4$ and freshly prepared TfN_3 in DCM was added to the resin bound amine. This mixture was brought to homogeneity by adding MeOH. Conversion was completed within 2-4 hrs as monitored by Kaiser test.

3.8.3 1, 2, 3- triazole on solid support

The resin bound azide was then reacted with the alkyne functionalized monomer **35** to get the 1,2,3-triazole unit. To the solid supported azide, a mixture of alkyne (9.0 mg, 7 eq), CuI (15.0 mg, 13 eq), ascorbic acid (4.3 mg, 7 eq) and DIPEA (10 μL, 17 eq) in DMF:pyridine (5:3) was added. The reaction was completed within 24 hrs with more than 90% yield in all the steps as confirmed by RP- HPLC.

3.8.4 UV-T_m measurements

The concentration of PNA and DNA oligomers were calculated on the basis of absorbance from the molar extinction coefficient of the corresponding nucleobases. The hybridized complexes was constituted in sodium phosphate buffer (pH 7.4, 10 mM), containing NaCl (100 mM) and by annealing the samples at 85^{o}C for 2 min followed by slow cooling to 4^{o}C over 7-8 hrs. The absorbance versus temperature profiles were obtained by monitoring UV absorbance at 260 nm with Perkin-Elmer Lambda 35 UV-vis spectrometer equipped by peltier leading in the range 10^{o}C to 85^{o}C with ramping rate of 0.5^{o}C per minute. The data were processed using Microcal origin 6.1 and T_m values obtained from the derivative curves.

3.9 References

1. (a) Egholm, M.; Buchardt, O.; Nielsen, P. E.; Berg, R. H. Peptide nucleic acids (PNAs): Oligonucleotide analogues with an achiral peptide backbone. *J. Am. Chem. Soc*. **1992**, *114*, 1895-1897. (b) Nielsen, P. E.; Egholm, M.; Berg, R. H.; Buchardt, O. Sequence-selective recognition of DNA by strand displacement with a thymine-substituted polyamide. *Science*, 1991, *254*, 1497-1500.

2. (a) Ganesh, K. N.; Nielsen, P. E. Peptide Nucleic Acids: analogs and derivatives. *Curr. Org. Chem.* **2000**, *4*, 931-943. (b) Kumar, V. A.; Ganesh, K. N. Conformationally constrained PNA analogues: Structural evolution toward DNA/RNA binding selectivity. *Acc. Chem. Res*. **2005**, *38*, 404-412. (c) Kumar, V. A. Structural preorganization of peptide nucleic acid: chiral cationic analogues with five-or six-membered ring structures. *Eur. J. Org. Chem.* **2002**, 2021-2032. (d) Kumar, V. A.; Ganesh, K. N. Structure-editing of nucleic acids for selective targeting of RNA. *Curr. Med. Chem*. **2007**, *7*, 715-726.
3. Vagner, J.; Qu, H.; Hruby, V. J. Peptidomimetics, a synthetic tool of drug discovery. *Curr. Opin. Chem. Bio.* **2008**, *12*, 292–296.

4. (a) Kolb, H. C.; Finn, M. G.; Sharpless, K. B. Click Chemistry: Diverse chemical function from a few good reactions. *Angew. Chem. Int. Ed*. **2001**, *40*, 2004-2021. (b) Huisgen, R. in *1,3-Dipolar Cycloaddition chemistry*, Padwa, A., Ed.; Wiley: New York, 1984. (c) Moses, J. E.; Moorhouse, A. The growing applications of click chemistry. *Chem. Soc. Rev*. **2007**, *36*, 1249-1262.

5. (a) Hlasta, P. D. J.; Ackerman, J. A. Steric Effects on the regioselectivity of an azide-alkyne dipolar cycloaddition reaction: The synthesis of human leukocyte Elastase inhibitors. *J. Org. Chem*. **1994**, *59*, 6184-6189. (b) Booth, C. A.; Philp, D. Efficient recognition-induced acceleration of a [3+2] dipolar cycloaddition reaction. *Tetrahedron Lett.* **1998**, *39*, 6987-6990. (c) Howell, S. J.; Spencer, N.; Philp, D. Recognition-mediated regiocontrol of a dipolar cycloaddition reaction. *Tetrahedron,* **2001**, *57*, 4945-4954. (d) Mock, W. L.; Irra, T. A.; Wepsiec, J. P.; Adhya, M. Catalysis by cucurbituril: The significance of bound-substrate destabilization for induced triazole formation. *J. Org. Chem.* **1989**, *54*, 5302-5308. (e) Chen, J.; Rebek, J. Jr. Selectivity in an Encapsulated cycloaddition reaction. *Org. Lett*. **2002**, *4*, 327-329.

6. Rostovtsev, V. V.; Green, L. G.; Fokin, V. V.; Sharpless K. B. A Stepwise Huisgen cycloaddition process: Copper(I)-catalyzed regioselective "Ligation" of azides and terminal alkynes. *Angew. Chem. Int. Ed.* **2002**, *41*, 2596-2599.

7. (a) Rodionov, V. O.; Fokin, V. V.; Finn, M. G.; Mechanism of the ligand-free CuI-catalyzed azide-alkyne cycloaddition reaction. *Angew. Chem. Int. Ed.*, **2005**, *44*, 2210-2215. (b) Himo, F.; Lovell, T.; Hilgraf, R.; Rostovtsev, V. V.; Noodleman, L.; Sharpless, K. B.; Fokin, V. V. J. Copper(I)-catalyzed synthesis of azoles. DFT

study predicts unprecedented reactivity and intermediates. *J. Am. Chem. Soc*. **2005**, *127*, 210-216.

8. Angell, Yu. L.; Burgess, K. Peptidomimetics via copper-catalyzed azide-alkyne cycloadditions. *Chem. Soc. Rev.* **2007**, *36*, 1674-1689.
9. Bock, V. D.; Perciaccante, R.; Jansen, T. P.; Hiemstra, H.; Maarseveen, J. H. V. Click chemistry as a route to cyclic tetrapeptide analogues: Synthesis of cyclo-[Pro-Val-*ã*(triazole)-Pro-Tyr]. *Org. Lett*. **2006**, *8*, 919–922.
10. Angelo, N. G.; Arora, P. S. Nonpeptidic foldamers from amino acids: Synthesis and characterization of 1,3-Substituted triazole oligomers. *J. Am. Chem. Soc.* **2005**, *127*, 17134–17135.
11. Horne, W. S.; Yadav, M. K.; Stout, C. D.; Ghadiri, M. R. Heterocyclic peptide backbone modifications in an α-helical coiled coil. *J. Am. Chem. Soc*. **2004**, *126*, 15366-15367.
12. Oh, K.; Guan Z. A convergent synthesis of new b-turn mimics by click chemistry. *Chem. Commun.* **2006**, 3069–3071.
13. Holub, J. M.; Jang, H.; Kirshenbaum, K. Clickity-Click: highly functionalized peptoid oligomers generated by sequential conjugation reactions on solid support. *Org. Biomol. Chem*. **2006**, *4*, 1497-1502.
14. Pokorski, J. K.; Jenkins, L. M. M.; Feng, H.; Durell, S. R.; Bai, Y.; Appella, D. H. Introduction of a triazole amino acid into a peptoid oligomer induces turn formation in aqueous solution. *Org. Lett*. **2007**, *9*, 2381-2383.
15. Nakane, M.; Ichikawa, S.; Matsuda, A. Triazole-linked dumbbell oligodeoxynucleotides with NF-kB binding ability as potential decoy molecules. *J. Org. Chem.* **2008**, *73*, 1842-1851.
16. Isobe, H.; Fujino, T.; Yamazaki, N.; Guillot-Nieckowski, M.; Nakamura. E. Triazole-linked analogue of deoxyribonucleic acid (^{TL}DNA): design, synthesis, and double-strand formation with natural DNA. *Org. Lett*. **2008**, *10*, 3729-3732.
17. Gasser, G.; Husken, N.; Koster, S. D.; Metzler-Nolte, N. Synthesis of organometallic PNA oligomers by click chemistry. *Chem. Commun.* **2008**, 3675-3677.
18. Bourne, Y.; Kolb, H. C.; Radic, Z.; Sharpless, K. B.; Taylor, P.; Marchot, P. Freeze-frame inhibitor captures acetylcholinesterase in a unique conformation. *Proc. Natl. Acad. Sci. U.S.A*. **2004**, *101*, 1449-1454.
19. (a) Tornoe, C. W.; Sanderson, S. J.; Mottram, J. C.; Coombs, G. H.; Meldal, M. Combinatorial Library of Peptidotriazoles: Identification of [1,2,3]-Triazole inhibitors against a recombinant *Leishmania mexicana* cysteine protease. *J. Comb. Chem.* **2004**, *6*, 312–324. (b) Bettinetti, L.; Lober, S.; Hubner, H.; Gmeiner, P.

Parallel synthesis and biological screening of dopamine receptor ligands taking advantage of a click chemistry based BAL linker. *J. Comb. Chem*. **2005**, *7*, 309–316.

20. (a) Egholm, M.; Nielsen, P. E.; Buchardt, O.; Berg, R. H. Recognition of guanine and adenine in DNA by cytosine and thymine containing peptide nucleic acids (PNAs). *J. Am. Chem. Soc*. **1992**, *114*, 9677-9678. (b) Dueholm, K. L.; Egholm, M.; Behrens, C.; Christensen, L.; Hansen, H. F.; Vulpius, T.; Petersen, K. H.; Berg, R. H.; Nielsen, P. E.; Buchardt, O. Synthesis of peptide nucleic acid monomers containing the four natural bases: Thymine, cytosine, adenine, and guanine and their oligomerization. *J. Org. Chem*. **1994**, *59*, 5767-5773.
21. Matsueda, G. R.; Stewart, J. M. *p*-Methylbenzhydrylamine resin for improved solid-phase synthesis of peptide amides. *Peptides*, **1981**, *2*, 45-50.
22. (a) Yan, R-B.; Yang, F.; Wu, Y.; Zhang, L. H.; Ye, X-S. An efficient and improved procedure for preparation of triflyl azide and application in catalytic diazotransfer reaction. *Tetrahedron Lett.* **2005**, *46*, 8993-8995. (b) Liu, Q.; Tor, Y. Simple conversion of aromatic amines into azides. *Org. Lett.* **2003**, *5*, 2571-2572.
23. Christensen, L.; Fitzpatrick, R.; Gildea, B.; Petersen, K. H.; Hansen, H. F.; Koch, T.; Egholm, M.; Buchardt, O.; Nielsen, P. E.; Coull, J.; Berg, R. H. Solid-phase synthesis of peptide nucleic acids. *J. Peptide Sci*. **1995**, *3*, 175-183.
24. (a) Job, P. *Ann. Chim*. **1928**, *9*, 113-203. (b) Cantor, C. R.; Schimmel, P. R. *Biophys. Chem. Part III,* **1980**, 624.

3.10 Appendix

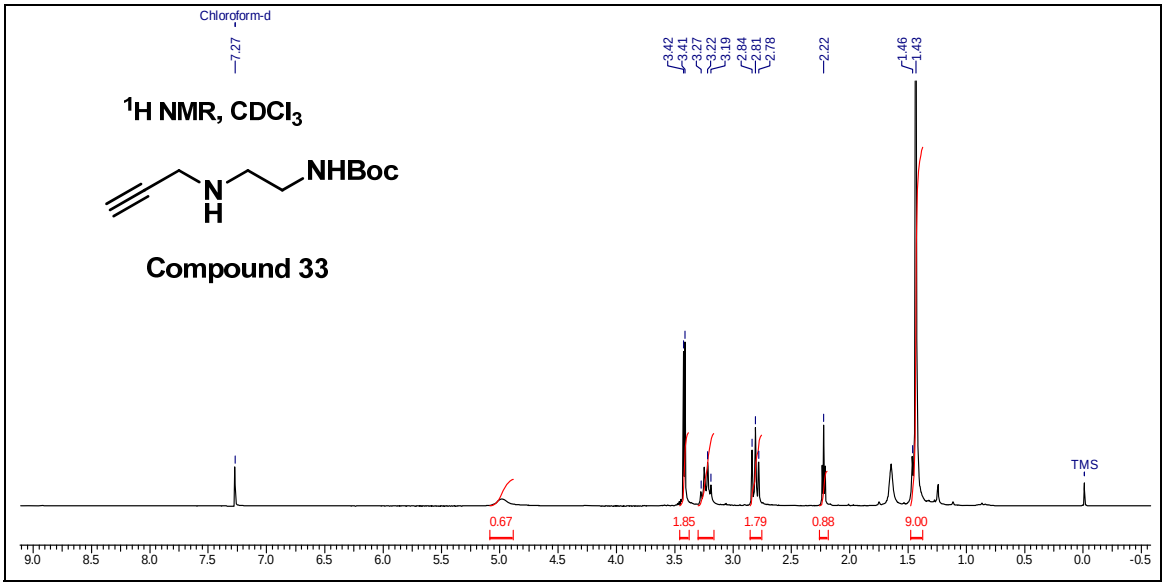
Chloroform-d
7.27
3.42
3.41
3.27
3.22
3.19
2.84
2.81
2.78
2.22
1.46
1.43
^{1}H NMR, CDCl$_3$
NHBoc
N
H
Compound 33
TMS
0.67
1.85
1.79
0.88
9.00

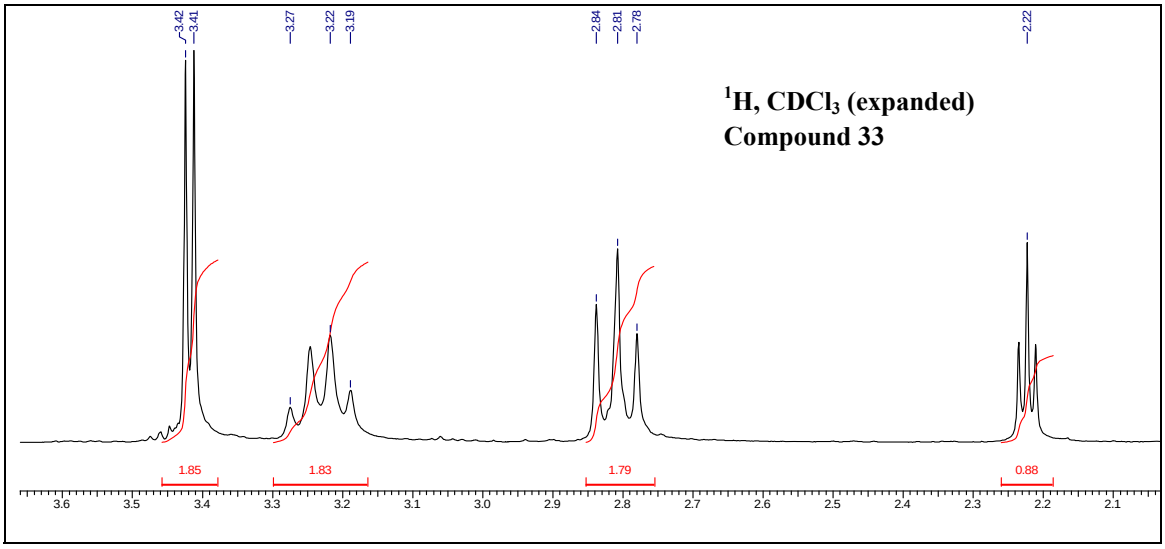
3.42
3.41
3.27
3.22
3.19
2.84
2.81
2.78
2.22
^{1}H, CDCl$_3$ (expanded)
Compound 33
1.85
1.83
1.79
0.88

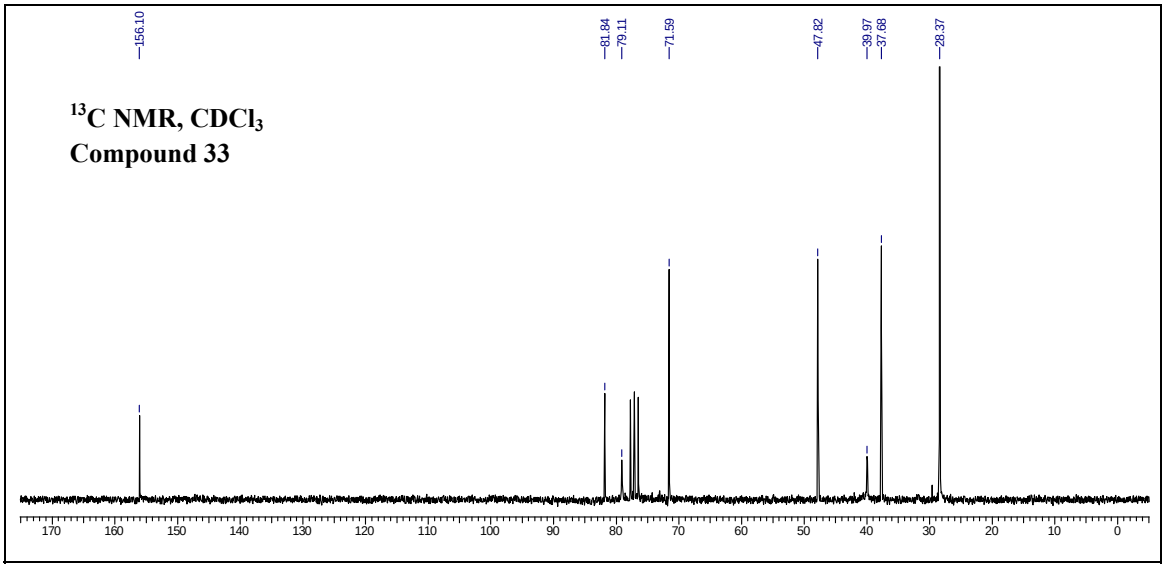
156.10
81.84
79.11
71.59
47.82
39.97
37.68
28.37
^{13}C NMR, CDCl$_3$
Compound 33

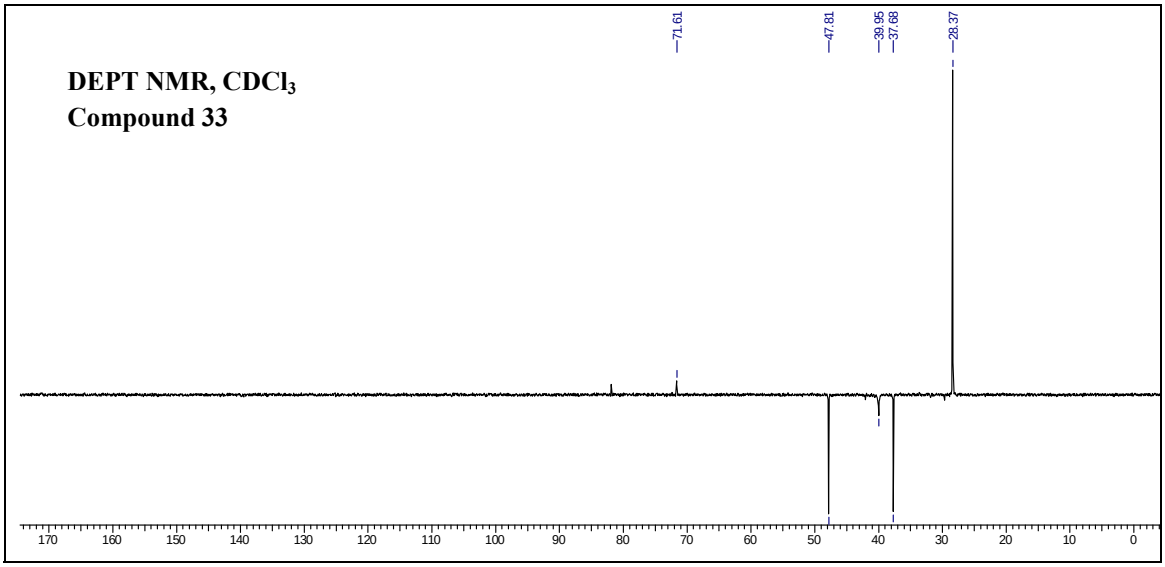
DEPT NMR, CDCl3
Compound 33
71.61
47.81
39.95
37.68
28.37

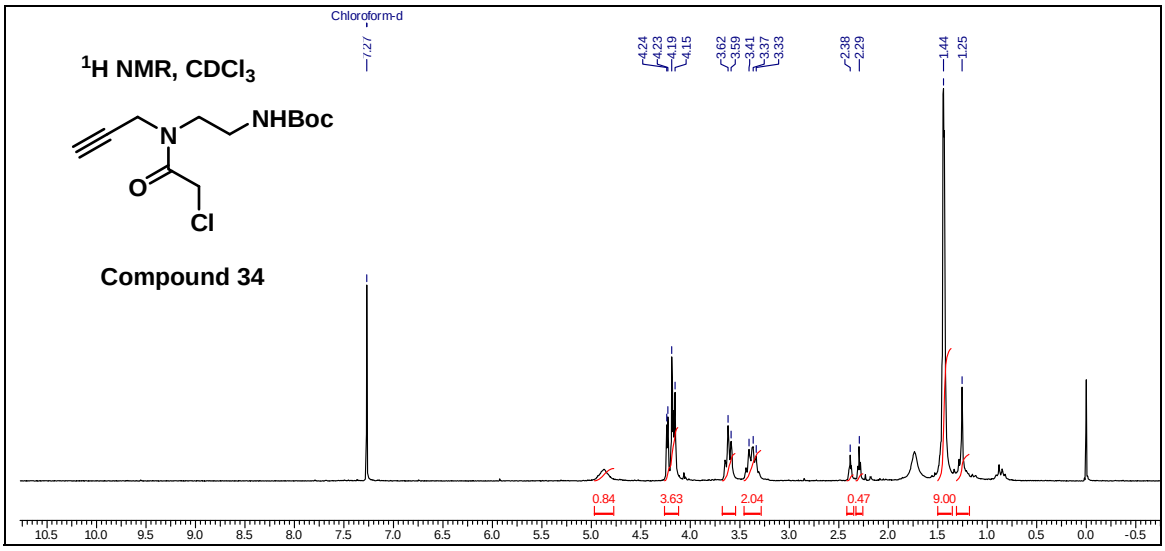
1H NMR, CDCl3
NHBoc
N
O
Cl
Compound 34
Chloroform-d
7.27
4.24
4.23
4.19
4.15
3.62
3.59
3.41
3.37
3.33
2.38
2.29
1.44
1.25
0.84
3.63
2.04
0.47
9.00

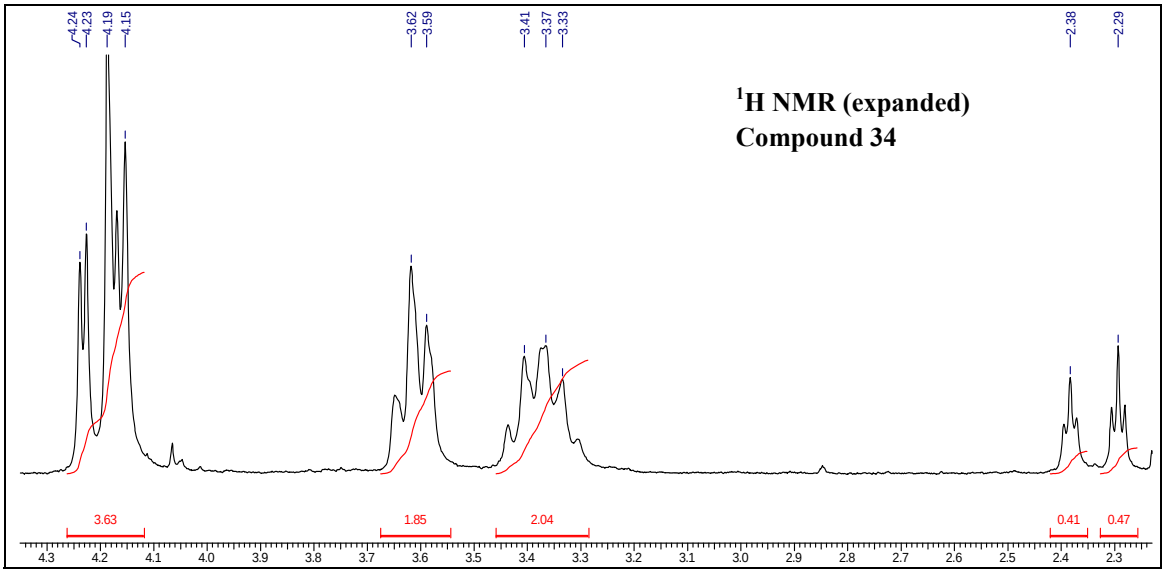
4.24
4.23
4.19
4.15
3.62
3.59
3.41
3.37
3.33
2.38
2.29
1H NMR (expanded)
Compound 34
3.63
1.85
2.04
0.41
0.47

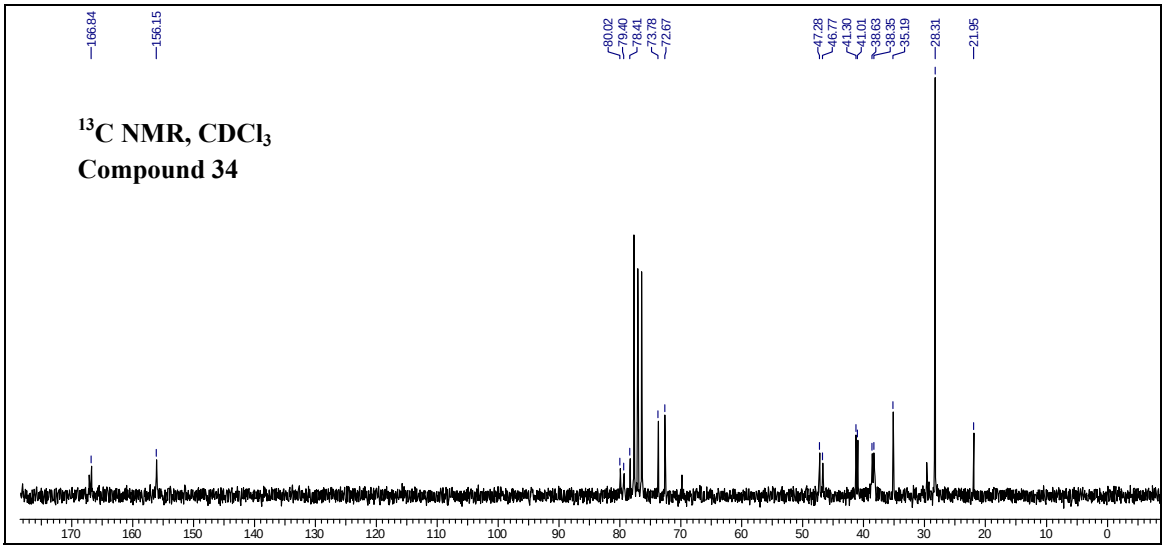
166.84
156.15
80.02
79.40
78.41
73.78
72.67
47.28
46.77
41.30
41.01
38.63
38.35
35.19
28.31
21.95
^{13}C NMR, CDCl$_3$
Compound 34

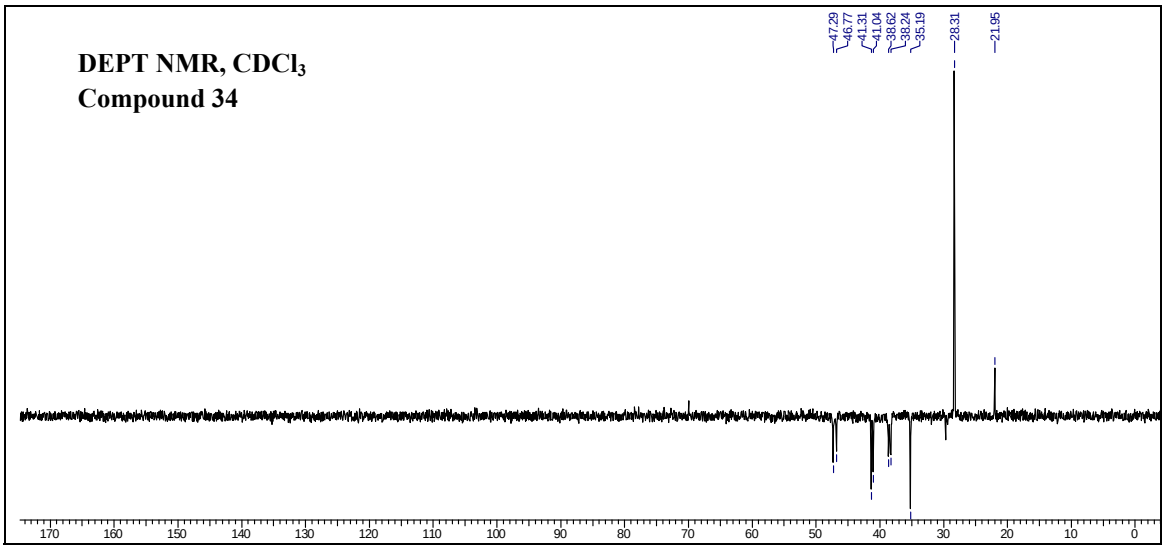
47.29
46.77
41.31
41.04
38.62
38.24
35.19
28.31
21.95
DEPT NMR, CDCl$_3$
Compound 34

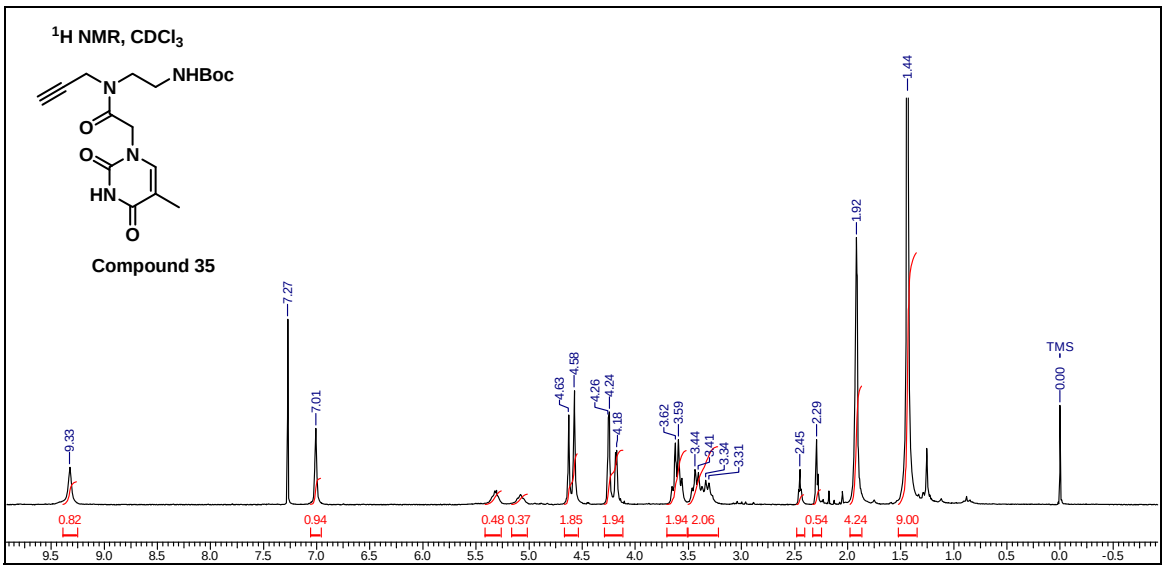
^{1}H NMR, CDCl$_3$
NHBoc
Compound 35
9.33
7.27
7.01
4.63
4.58
4.26
4.24
4.18
3.62
3.59
3.44
3.41
3.34
3.31
2.45
2.29
1.92
1.44
TMS
0.00
0.82
0.94
0.48
0.37
1.85
1.94
1.94
2.06
0.54
4.24
9.00

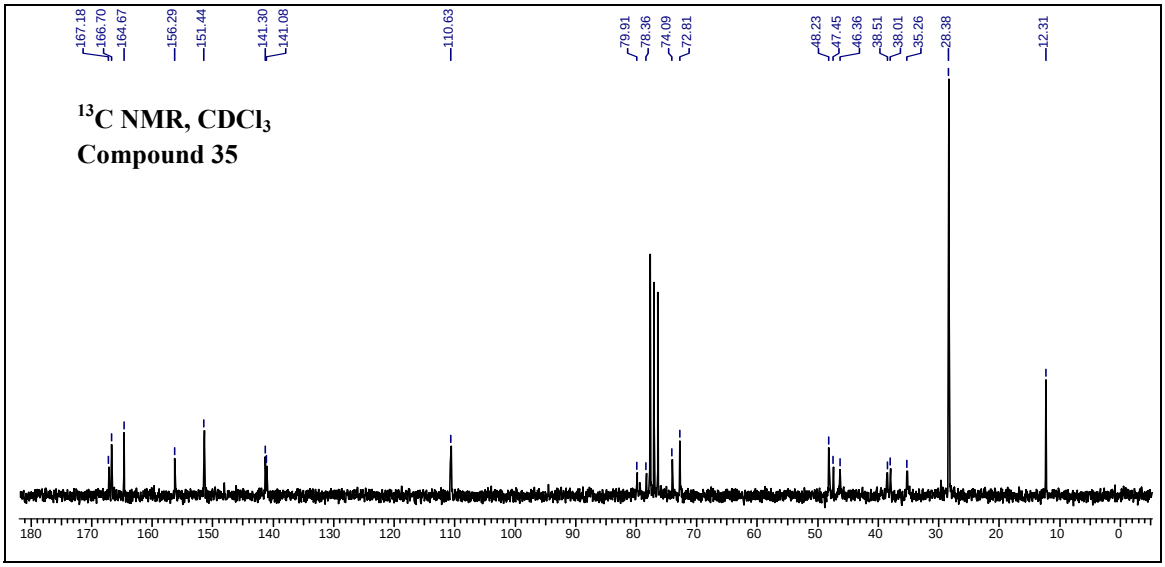
167.18
166.70
164.67
156.29
151.44
141.30
141.08
110.63
79.91
78.36
74.09
72.81
48.23
47.45
46.36
38.51
38.01
35.26
28.38
12.31
13C NMR, CDCl3
Compound 35

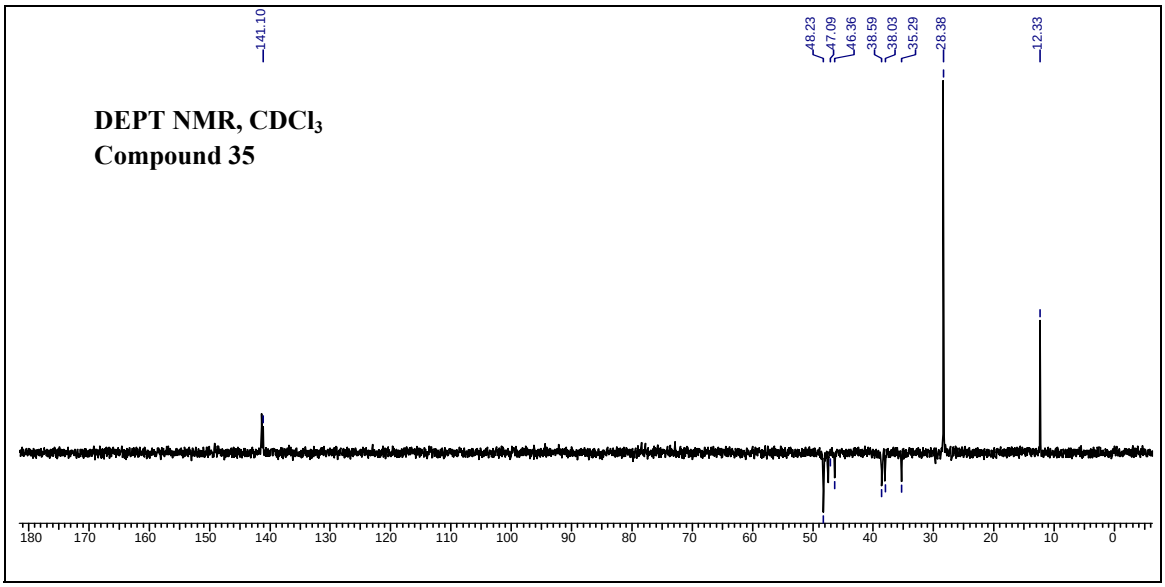
141.10
48.23
47.09
46.36
38.59
38.03
35.29
28.38
12.33
DEPT NMR, CDCl3
Compound 35

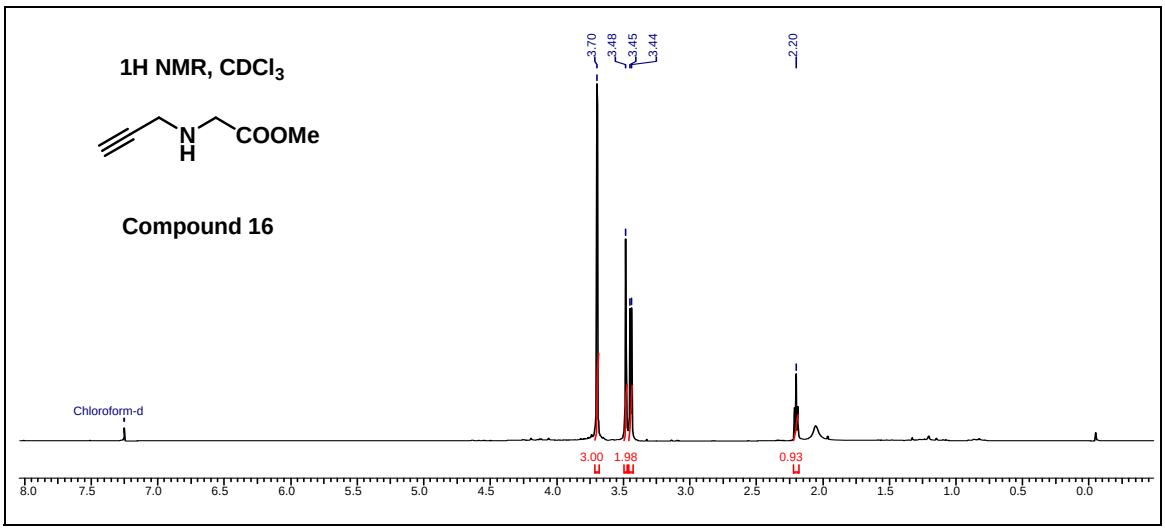
1H NMR, CDCl3
N
H
COOMe
Compound 16
3.70
3.48
3.45
3.44
2.20
Chloroform-d
3.00
1.98
0.93

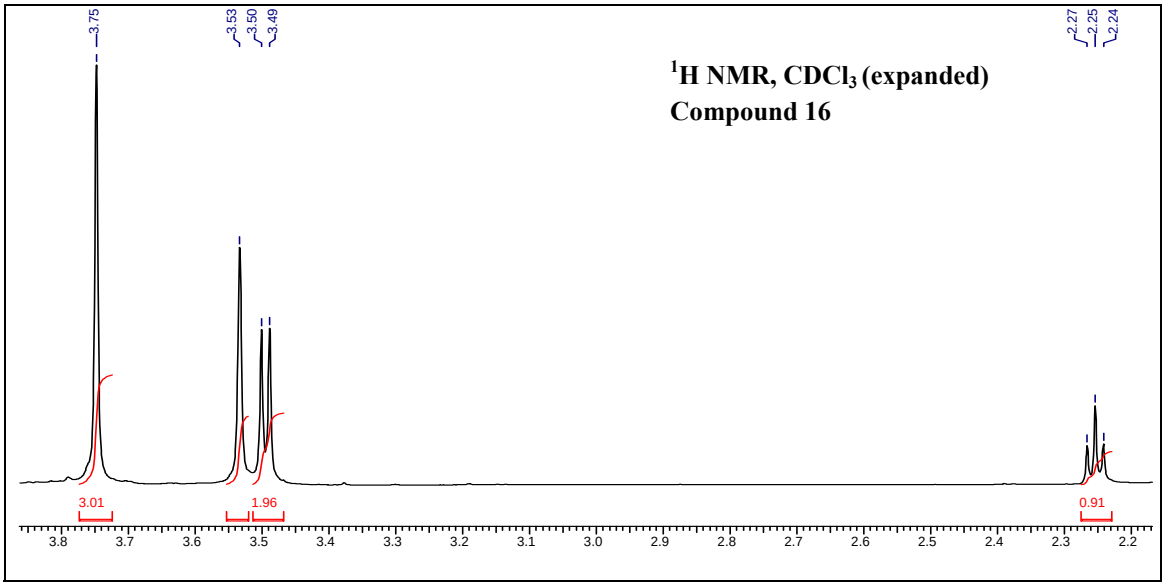
3.75
3.53
3.50
3.49
2.27
2.25
2.24
^{1}H NMR, CDCl$_3$ (expanded)
Compound 16
3.01
1.96
0.91

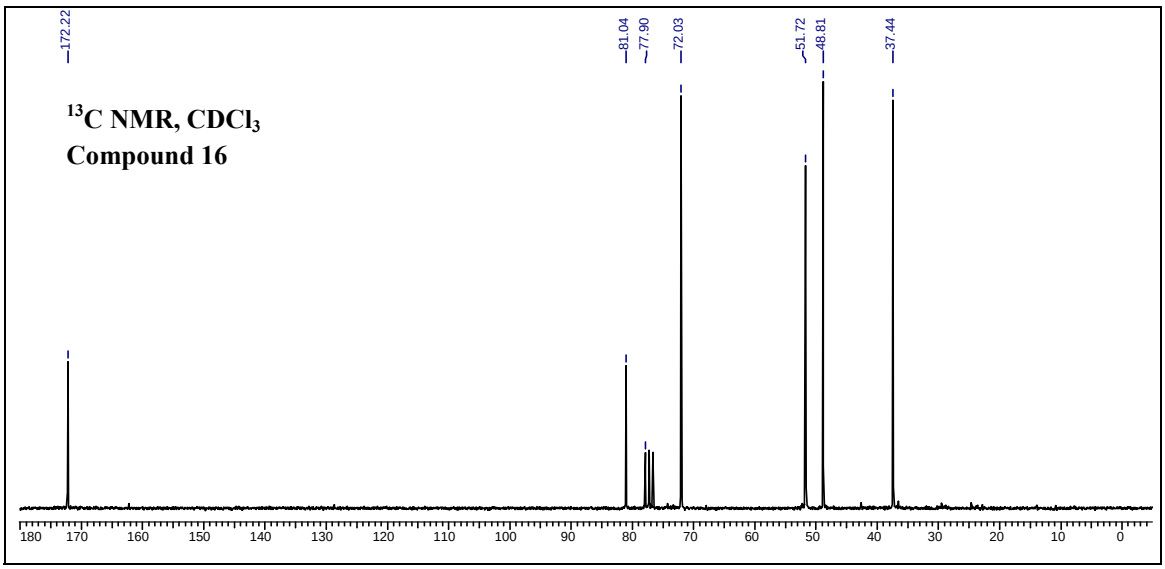
172.22
81.04
77.90
72.03
51.72
48.81
37.44
^{13}C NMR, CDCl$_3$
Compound 16

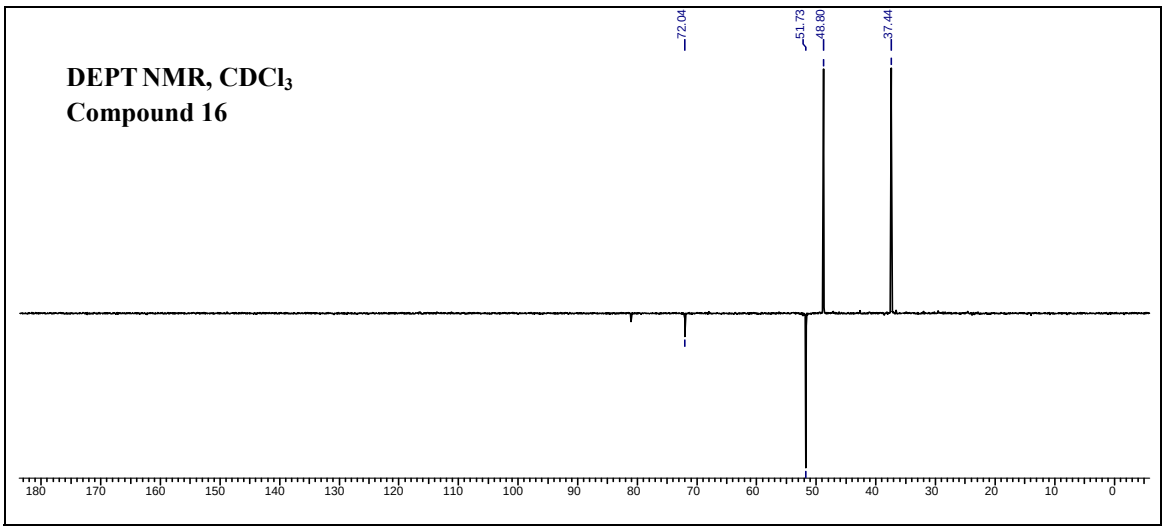
72.04
51.73
48.80
37.44
DEPT NMR, CDCl$_3$
Compound 16

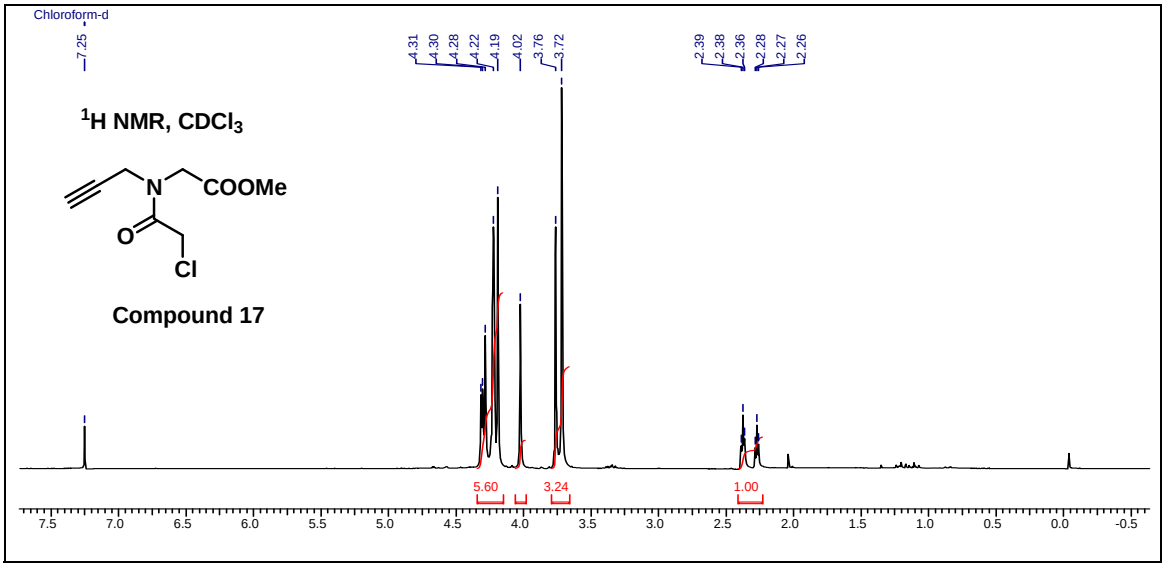
Chloroform-d
7.25
4.31
4.30
4.28
4.22
4.19
4.02
3.76
3.72
2.39
2.38
2.36
2.28
2.27
2.26
^{1}H NMR, CDCl$_3$
N
COOMe
O
Cl
Compound 17
5.60
3.24
1.00

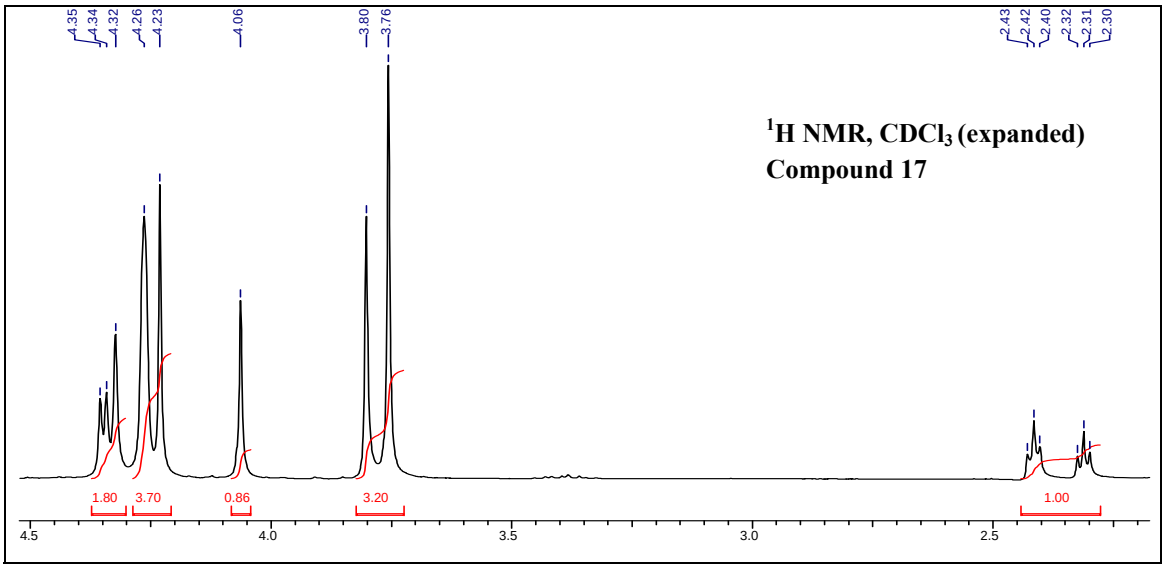
4.35
4.34
4.32
4.26
4.23
4.06
3.80
3.76
2.43
2.42
2.40
2.32
2.31
2.30
^{1}H NMR, CDCl$_3$ (expanded)
Compound 17
1.80
3.70
0.86
3.20
1.00

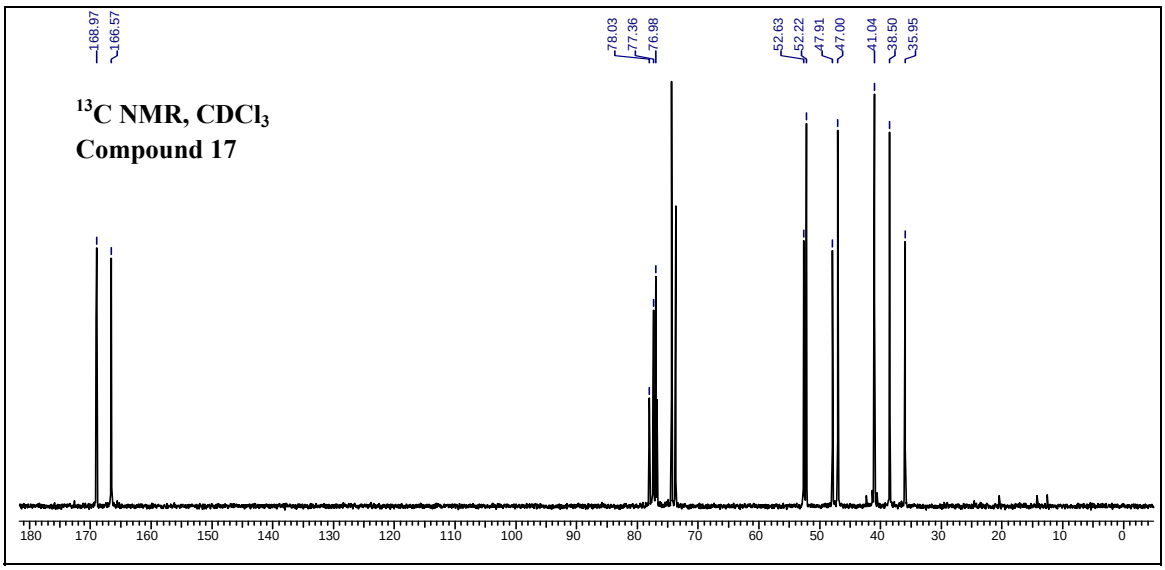
168.97
166.57
78.03
77.36
76.98
52.63
52.22
47.91
47.00
41.04
38.50
35.95
^{13}C NMR, CDCl$_3$
Compound 17

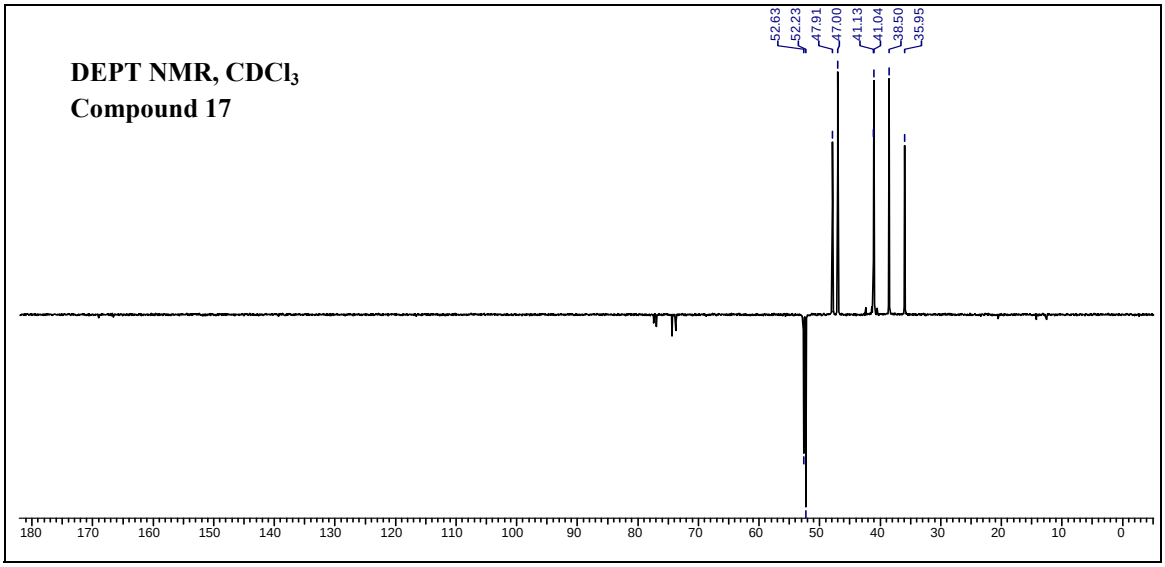
DEPT NMR, CDCl3
Compound 17
52.63
52.23
47.91
47.00
41.13
41.04
38.50
35.95

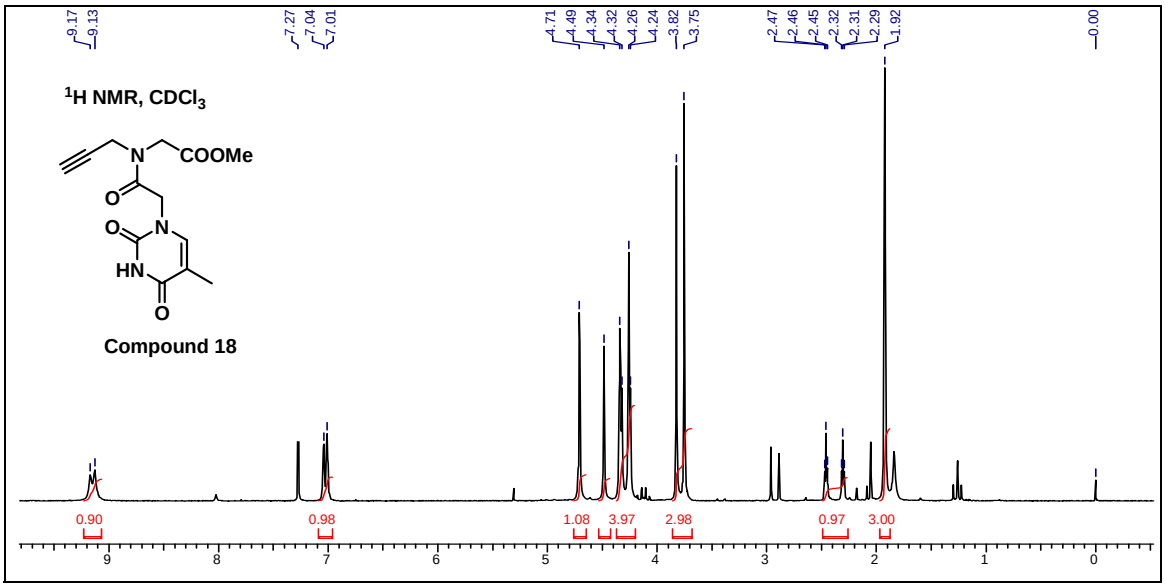
1H NMR, CDCl3
COOMe
Compound 18
9.17
9.13
7.27
7.04
7.01
4.71
4.49
4.34
4.32
4.26
4.24
3.82
3.75
2.47
2.46
2.45
2.32
2.31
2.29
1.92
0.00
0.90
0.98
1.08
3.97
2.98
0.97
3.00

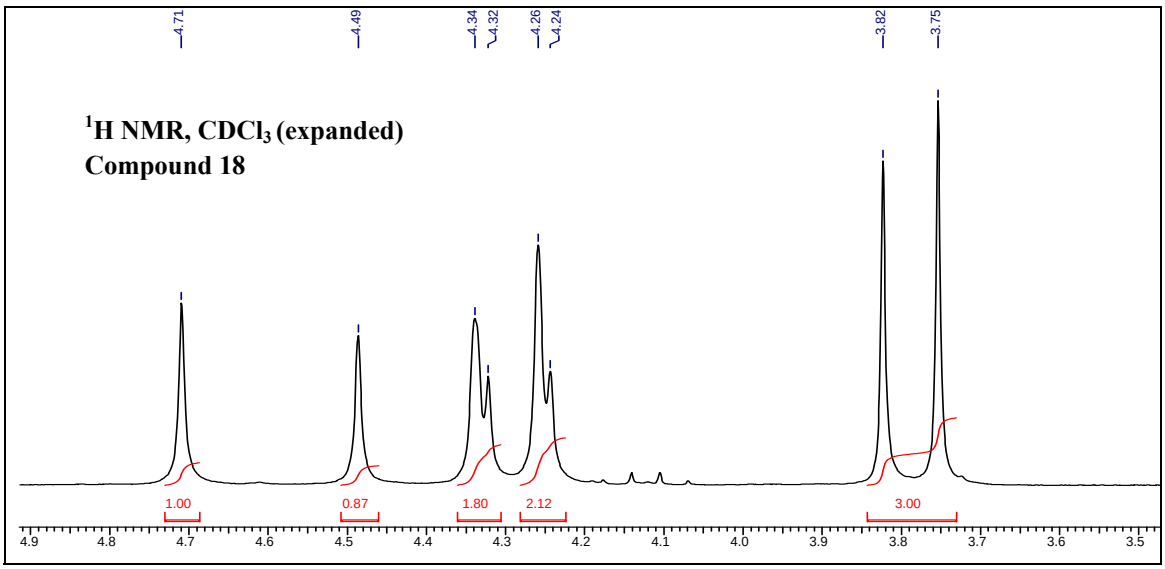
1H NMR, CDCl3 (expanded)
Compound 18
4.71
4.49
4.34
4.32
4.26
4.24
3.82
3.75
1.00
0.87
1.80
2.12
3.00

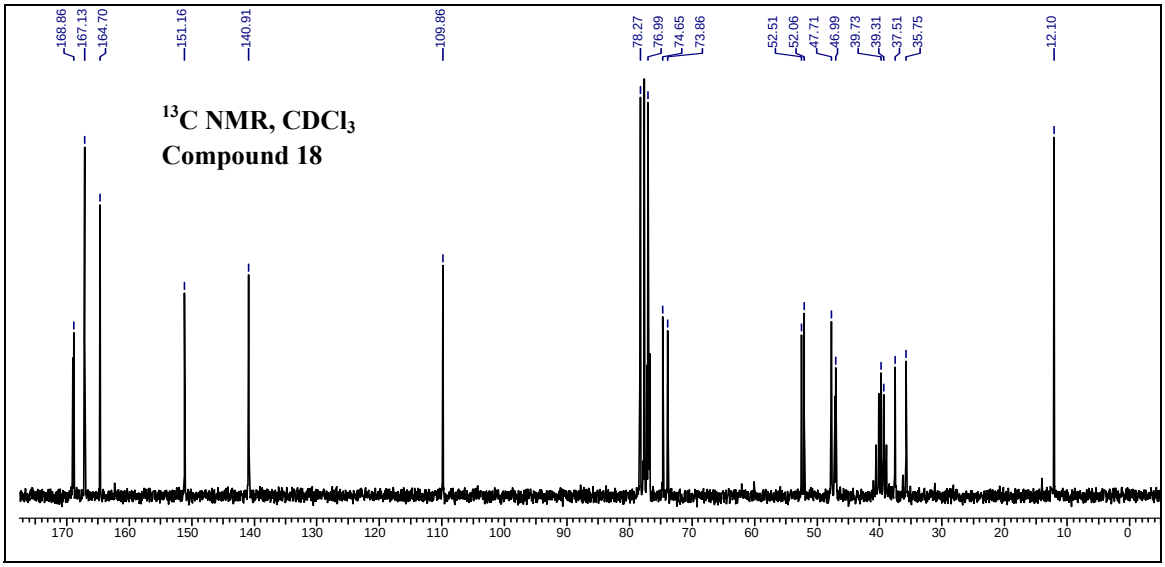
168.86
167.13
164.70
151.16
140.91
109.86
78.27
76.99
74.65
73.86
52.51
52.06
47.71
46.99
39.73
39.31
37.51
35.75
12.10
13C NMR, CDCl3
Compound 18

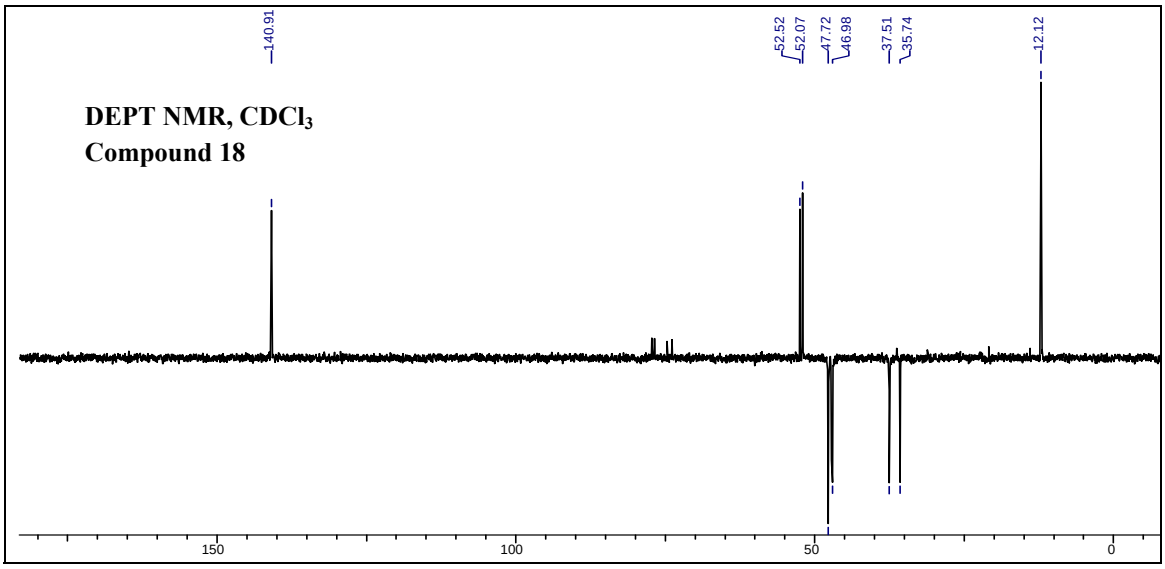
140.91
52.52
52.07
47.72
46.98
37.51
35.74
12.12
DEPT NMR, CDCl3
Compound 18

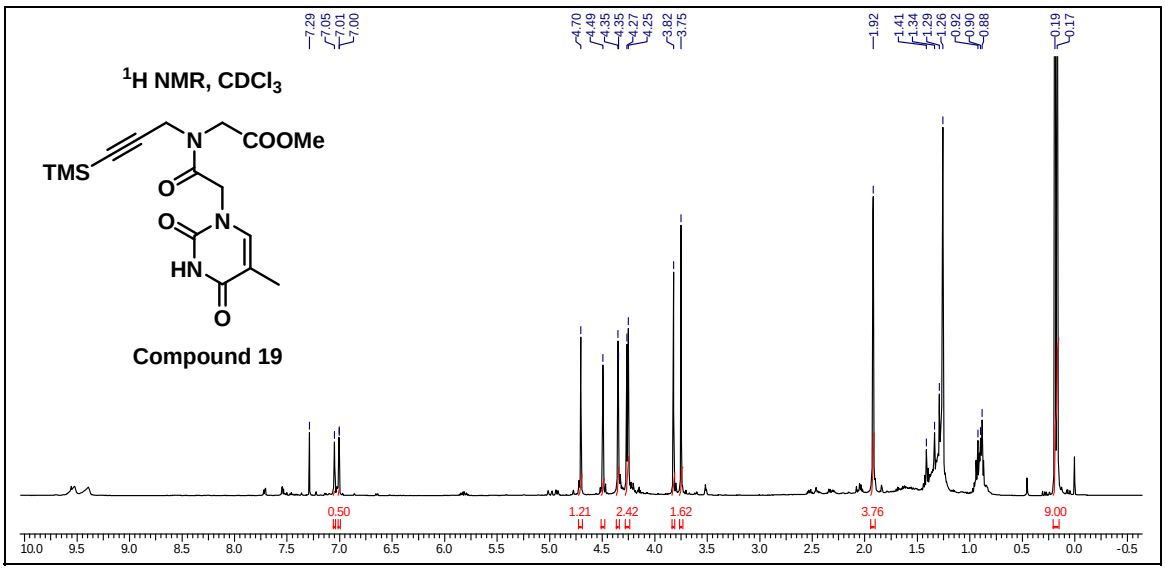
7.29
7.05
7.01
7.00
4.70
4.49
4.35
4.27
4.25
3.82
3.75
1.92
1.41
1.34
1.29
1.26
0.92
0.90
0.88
0.19
0.17
1H NMR, CDCl3
TMS
N
COOMe
O
O
N
HN
O
Compound 19
0.50
1.21
2.42
1.62
3.76
9.00

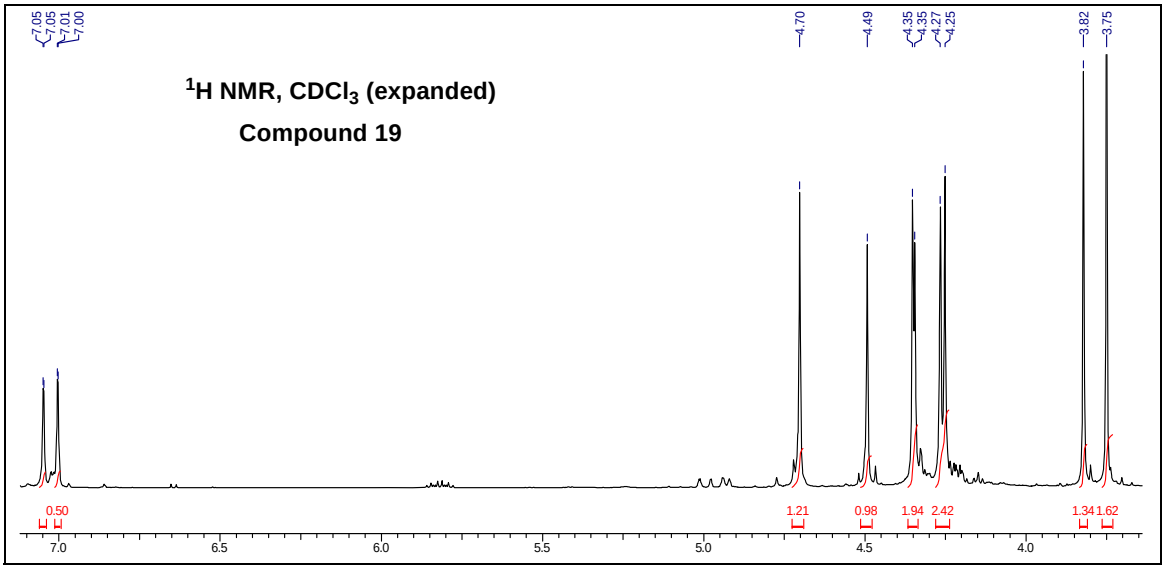
^{1}H NMR, $CDCl_3$ (expanded)
Compound 19

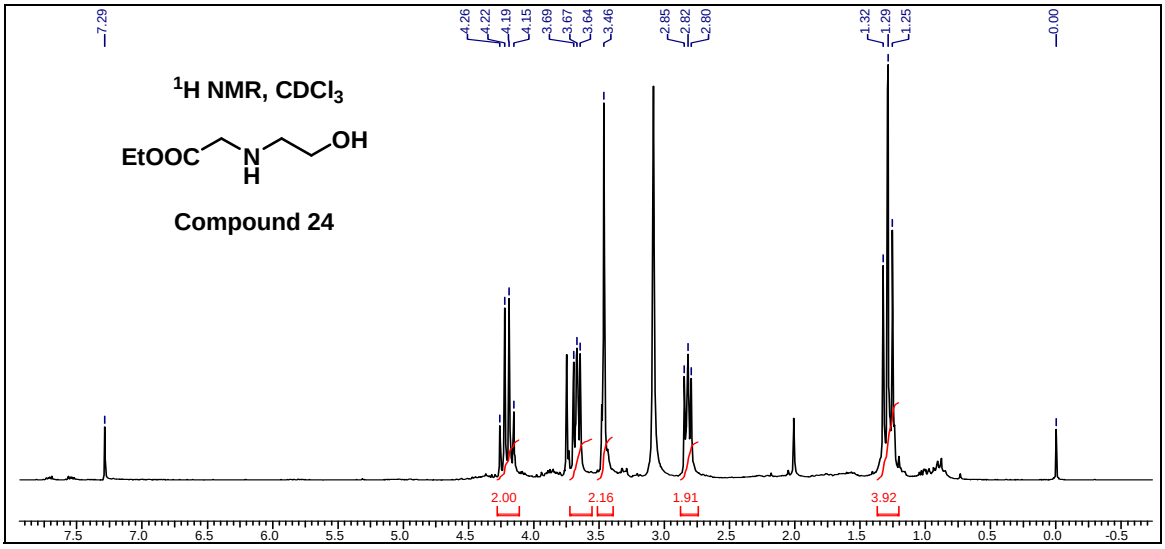
^{1}H NMR, $CDCl_3$
EtOOC
N
H
OH
Compound 24

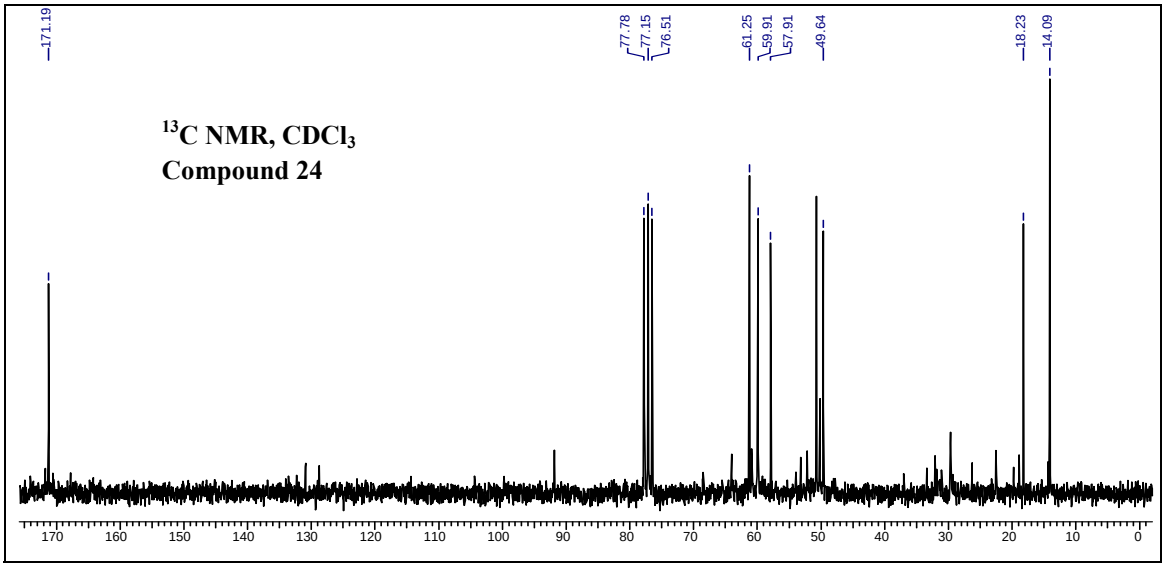
^{13}C NMR, $CDCl_3$
Compound 24

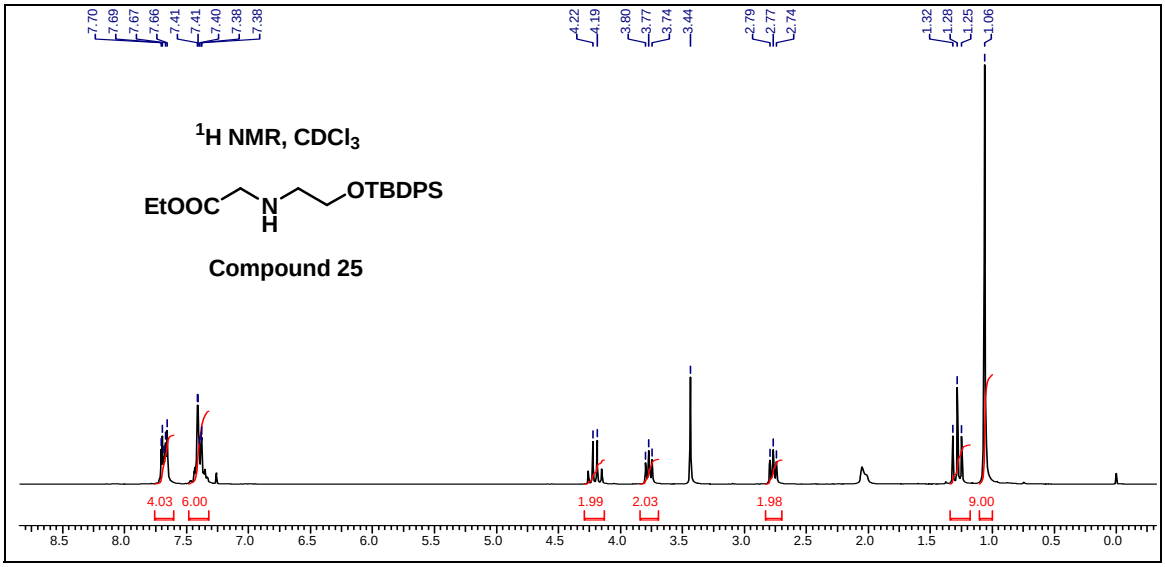
7.70
7.69
7.67
7.66
7.41
7.41
7.40
7.38
7.38
4.22
4.19
3.80
3.77
3.74
3.44
2.79
2.77
2.74
1.32
1.28
1.25
1.06
^{1}H NMR, CDCl$_3$
EtOOC
N
H
OTBDPS
Compound 25
4.03
6.00
1.99
2.03
1.98
9.00
8.5
8.0
7.5
7.0
6.5
6.0
5.5
5.0
4.5
4.0
3.5
3.0
2.5
2.0
1.5
1.0
0.5
0.0

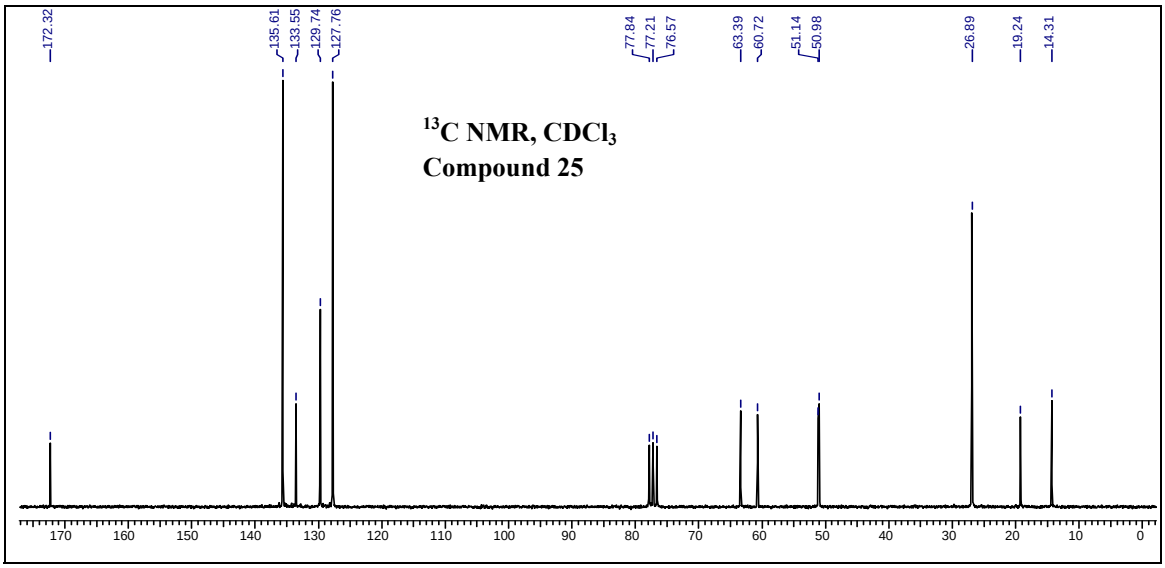
172.32
135.61
133.55
129.74
127.76
77.84
77.21
76.57
63.39
60.72
51.14
50.98
26.89
19.24
14.31
^{13}C NMR, CDCl$_3$
Compound 25
170
160
150
140
130
120
110
100
90
80
70
60
50
40
30
20
10
0

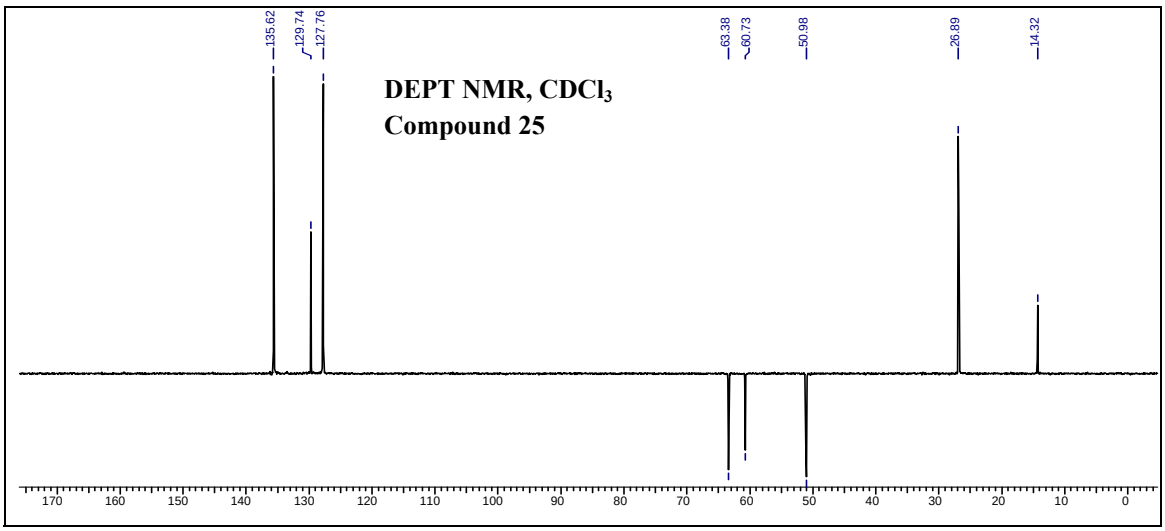
135.62
129.74
127.76
63.38
60.73
50.98
26.89
14.32
DEPT NMR, CDCl$_3$
Compound 25
170
160
150
140
130
120
110
100
90
80
70
60
50
40
30
20
10
0

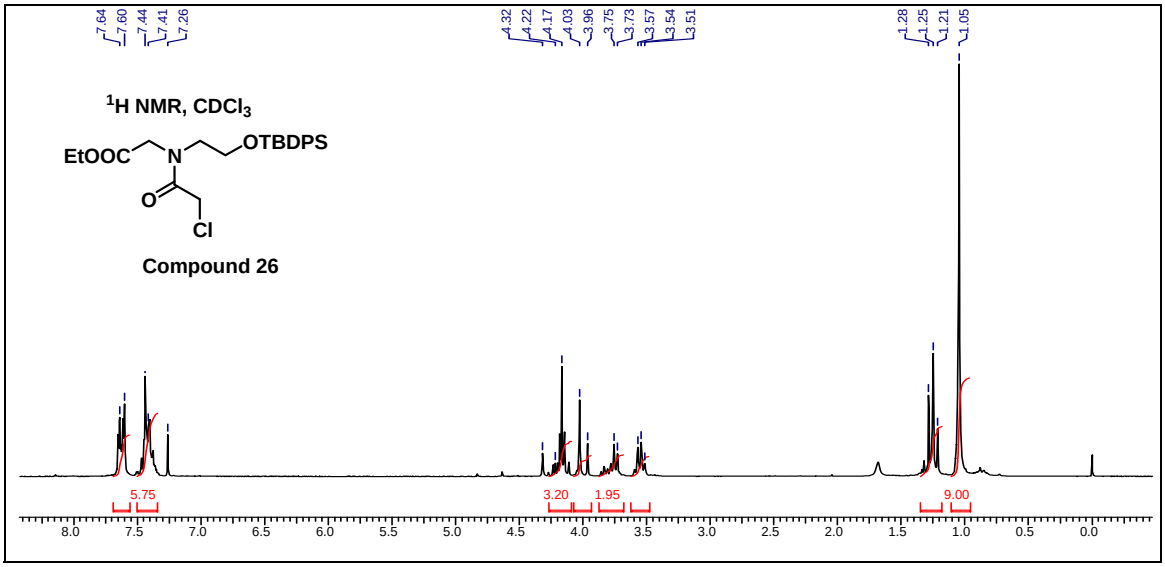
7.64
7.60
7.44
7.41
7.26
4.32
4.22
4.17
4.03
3.96
3.75
3.73
3.57
3.54
3.51
1.28
1.25
1.21
1.05
^{1}H NMR, CDCl$_3$
EtOOC
N
OTBDPS
O
Cl
Compound 26
5.75
3.20
1.95
9.00

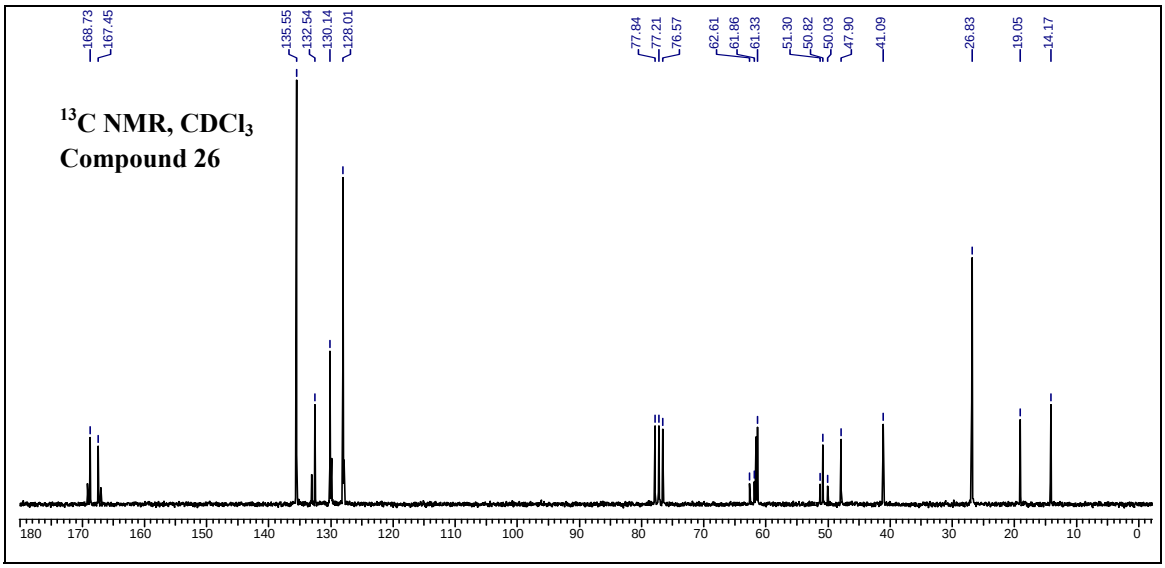
168.73
167.45
135.55
132.54
130.14
128.01
77.84
77.21
76.57
62.61
61.86
61.33
51.30
50.82
50.03
47.90
41.09
26.83
19.05
14.17
^{13}C NMR, CDCl$_3$
Compound 26

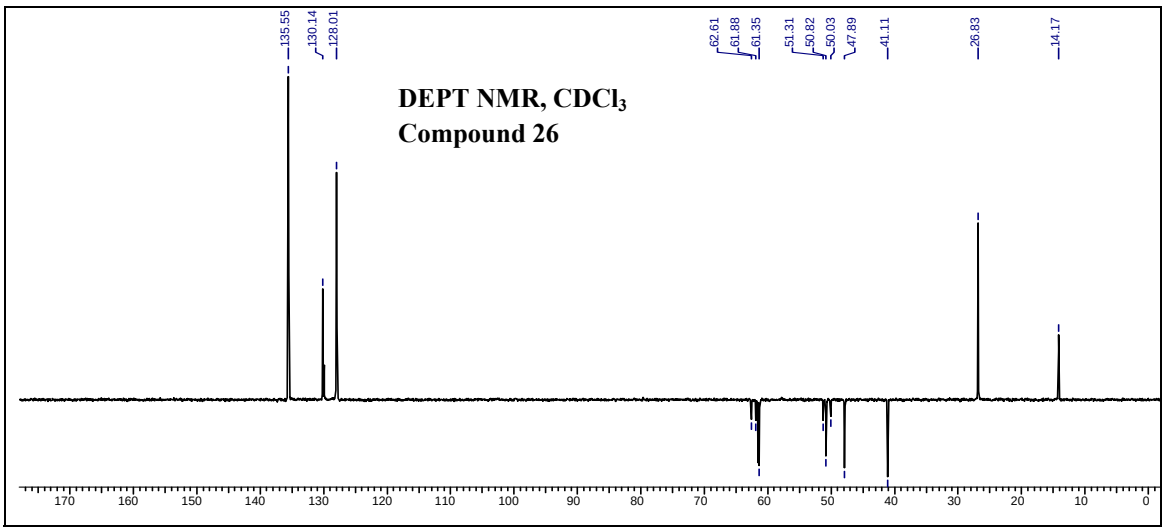
135.55
130.14
128.01
62.61
61.88
61.35
51.31
50.82
50.03
47.89
41.11
26.83
14.17
DEPT NMR, CDCl$_3$
Compound 26

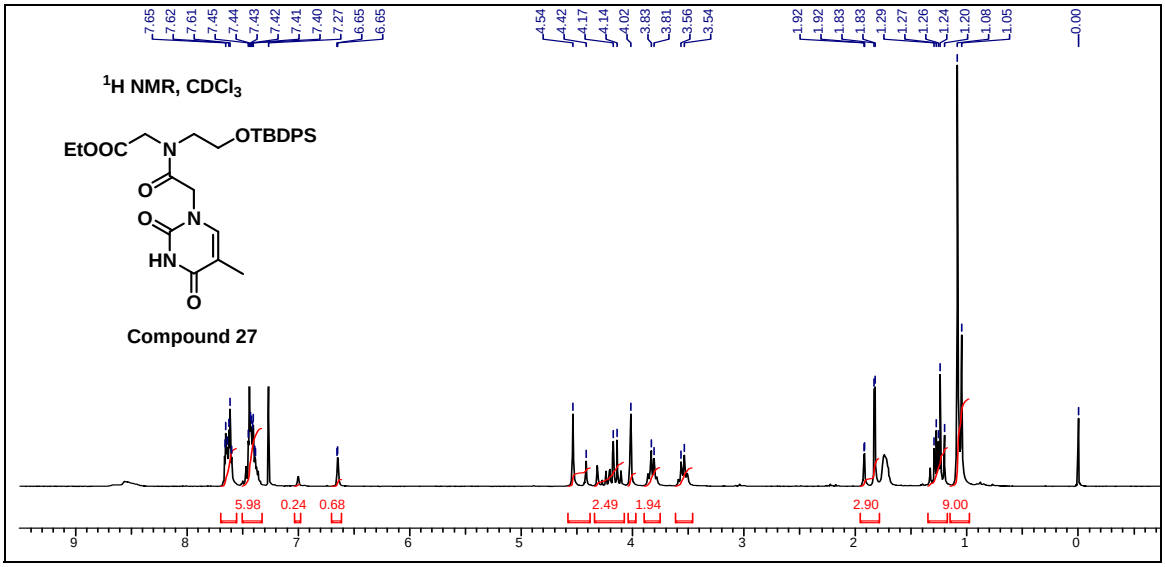
7.65
7.62
7.61
7.45
7.44
7.43
7.42
7.41
7.40
7.27
6.65
6.65
4.54
4.42
4.17
4.14
4.02
3.83
3.81
3.56
3.54
1.92
1.92
1.83
1.83
1.29
1.27
1.26
1.24
1.20
1.08
1.05
0.00
^{1}H NMR, CDCl$_3$
EtOOC
N
OTBDPS
O
O
N
HN
O
Compound 27
5.98
0.24
0.68
2.49
1.94
2.90
9.00

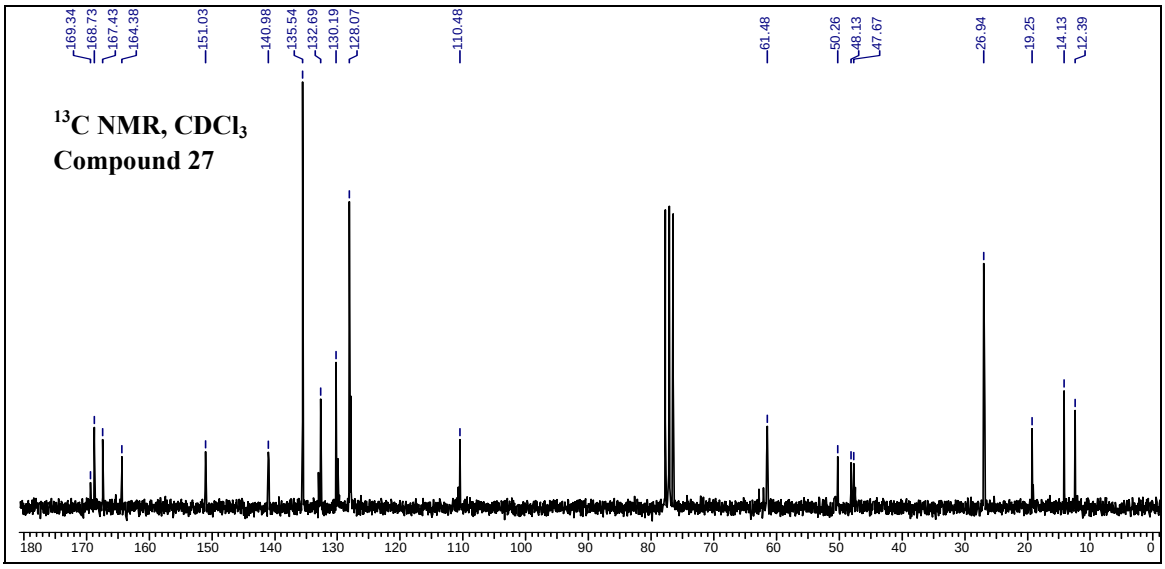
169.34
168.73
167.43
164.38
151.03
140.98
135.54
132.69
130.19
128.07
110.48
61.48
50.26
48.13
47.67
26.94
19.25
14.13
12.39
^{13}C NMR, CDCl$_3$
Compound 27

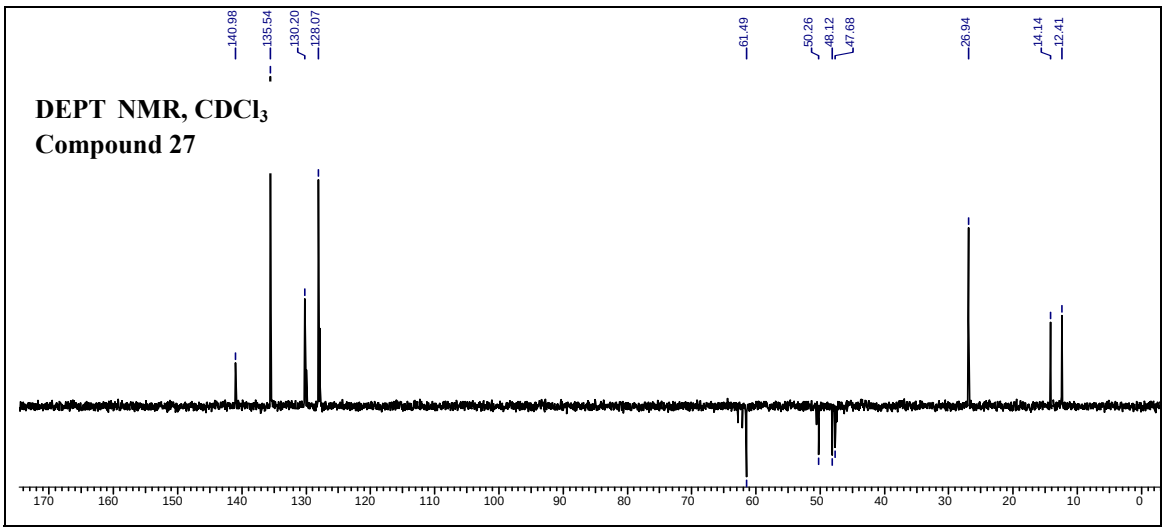
140.98
135.54
130.20
128.07
61.49
50.26
48.12
47.68
26.94
14.14
12.41
DEPT NMR, CDCl$_3$
Compound 27

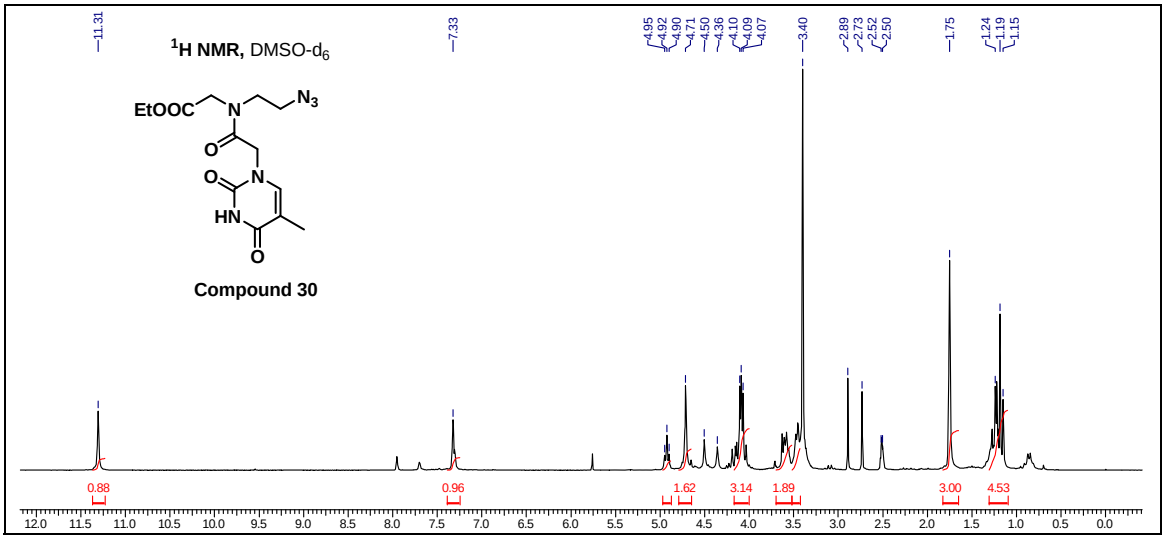
11.31
7.33
4.95
4.92
4.90
4.71
4.50
4.36
4.10
4.09
4.07
3.40
2.89
2.73
2.52
2.50
1.75
1.24
1.19
1.15
1H NMR, DMSO-d6
EtOOC
N
N3
O
O
N
HN
O
Compound 30
0.88
0.96
1.62
3.14
1.89
3.00
4.53
12.0
11.5
11.0
10.5
10.0
9.5
9.0
8.5
8.0
7.5
7.0
6.5
6.0
5.5
5.0
4.5
4.0
3.5
3.0
2.5
2.0
1.5
1.0
0.5
0.0

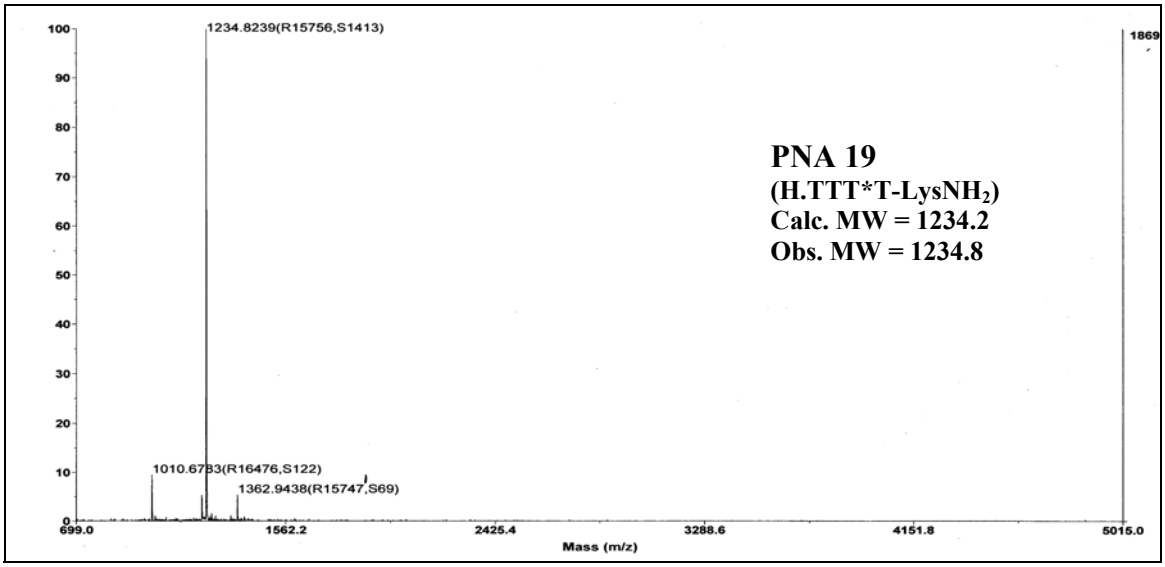

PNA 19
(H.TTT*T-LysNH$_2$)
Calc. MW = 1234.2
Obs. MW = 1234.8

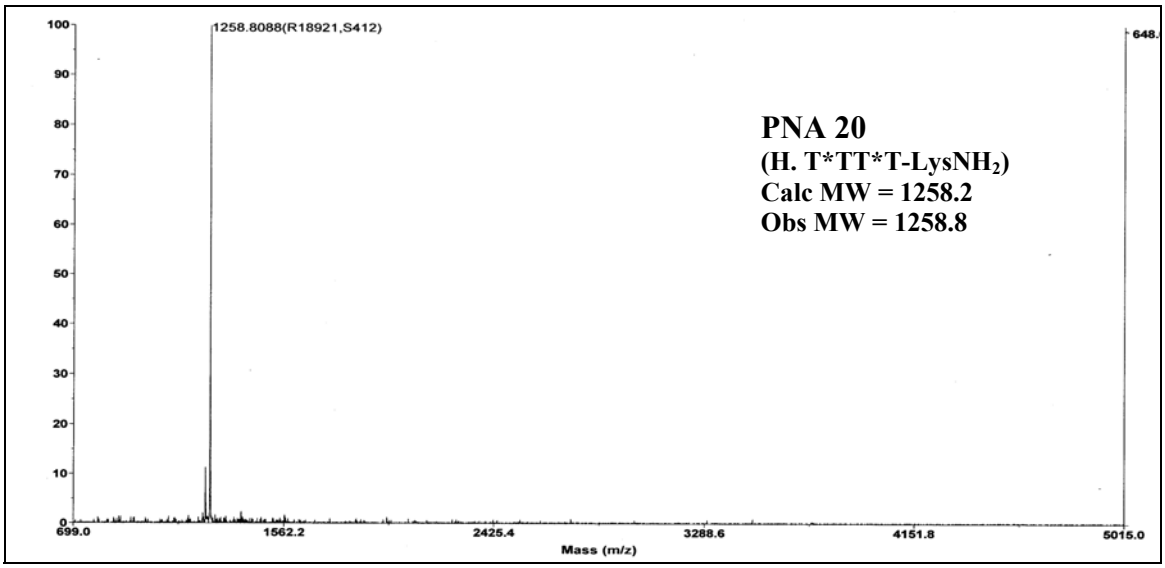

PNA 20
(H. T*TT*T-LysNH$_2$)
Calc MW = 1258.2
Obs MW = 1258.8

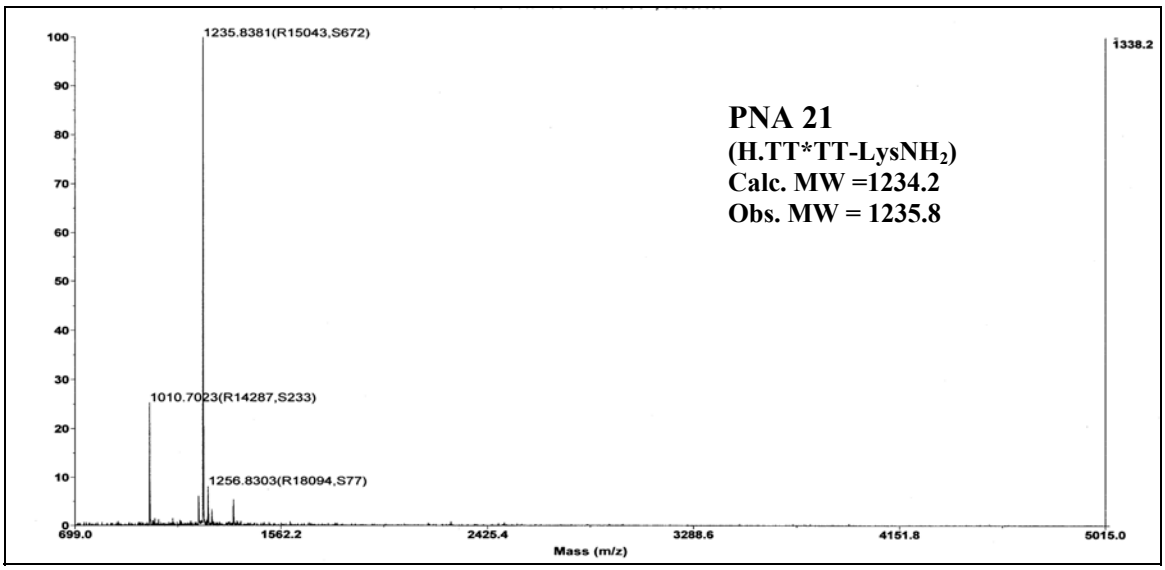

PNA 21
(H.TT*TT-LysNH$_2$)
Calc. MW =1234.2
Obs. MW = 1235.8

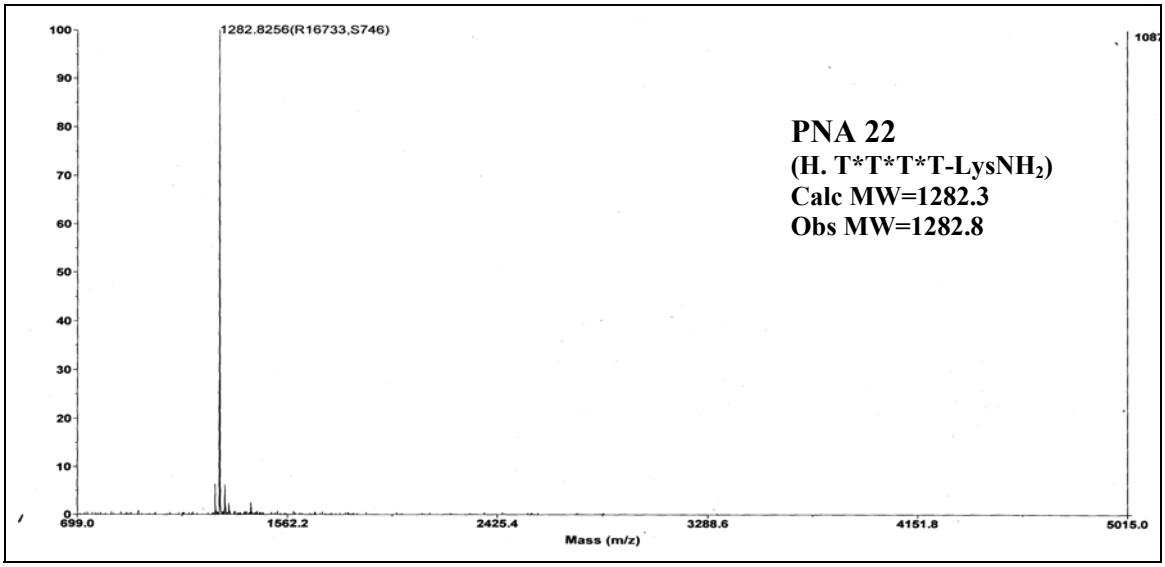

PNA 22
(H. T*T*T*T-LysNH$_2$)
Calc MW=1282.3
Obs MW=1282.8

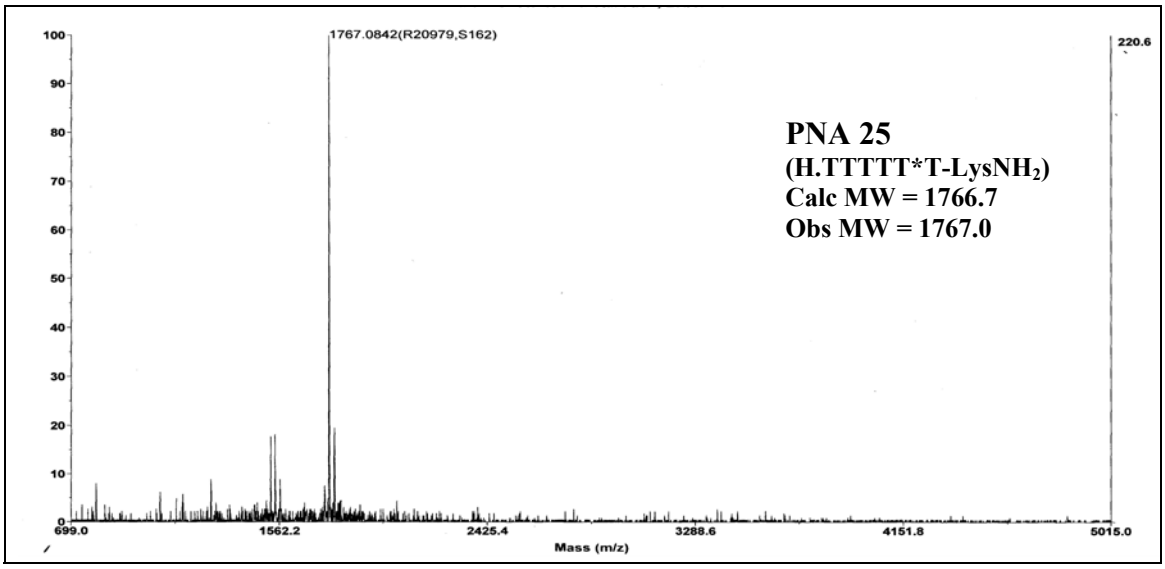

PNA 25
(H.TTTTT*T-LysNH$_2$)
Calc MW = 1766.7
Obs MW = 1767.0

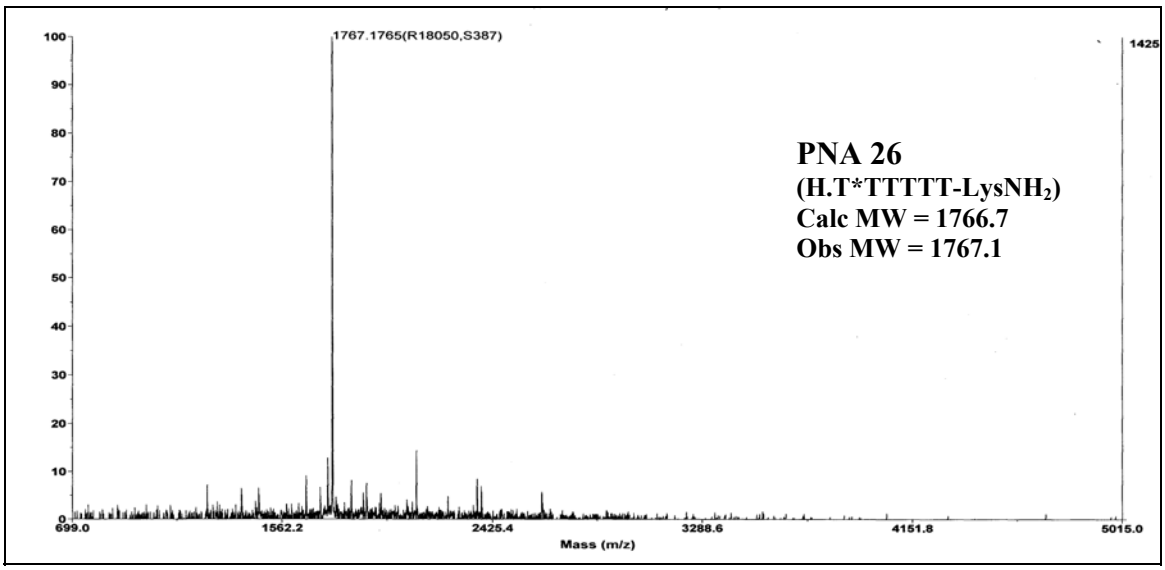

PNA 26
(H.T*TTTTT-LysNH$_2$)
Calc MW = 1766.7
Obs MW = 1767.1

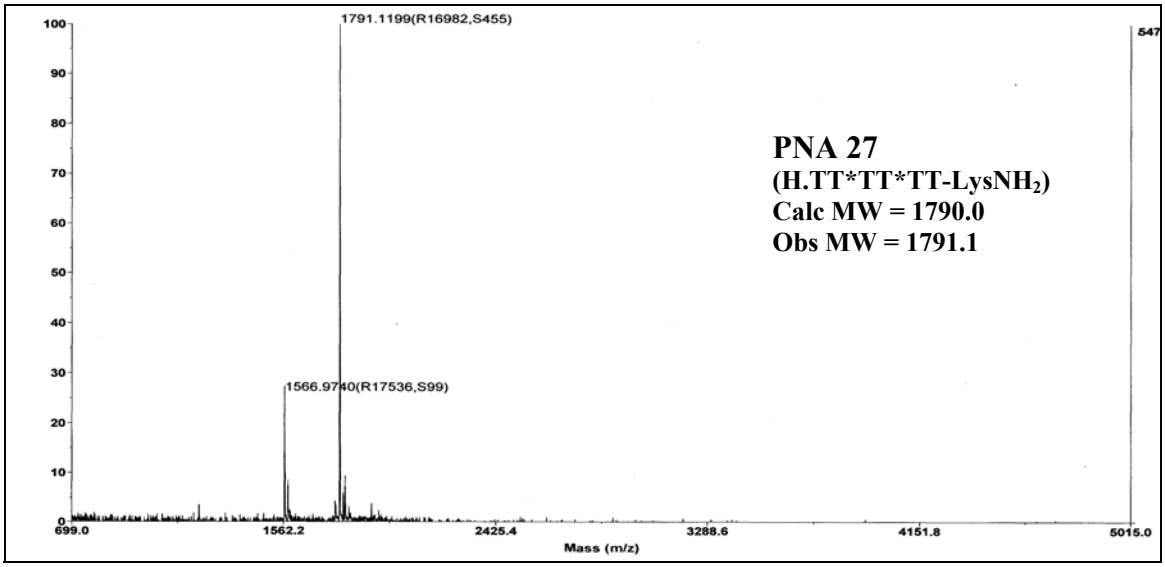

PNA 27
(H.TT*TT*TT-LysNH$_2$)
Calc MW = 1790.0
Obs MW = 1791.1

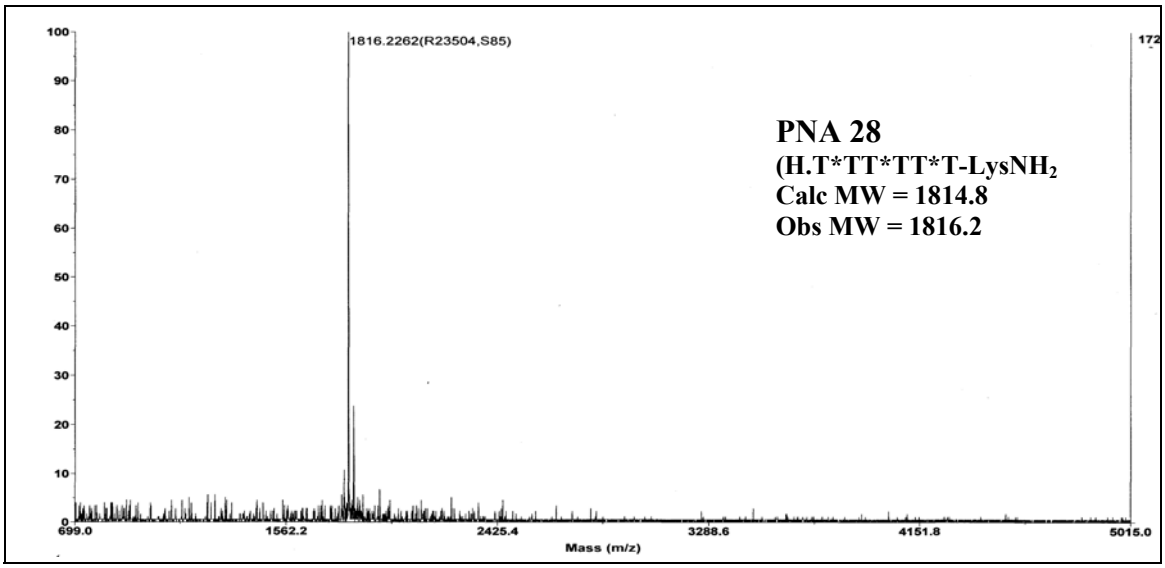

PNA 28
(H.T*TT*TT*T-LysNH$_2$
Calc MW = 1814.8
Obs MW = 1816.2

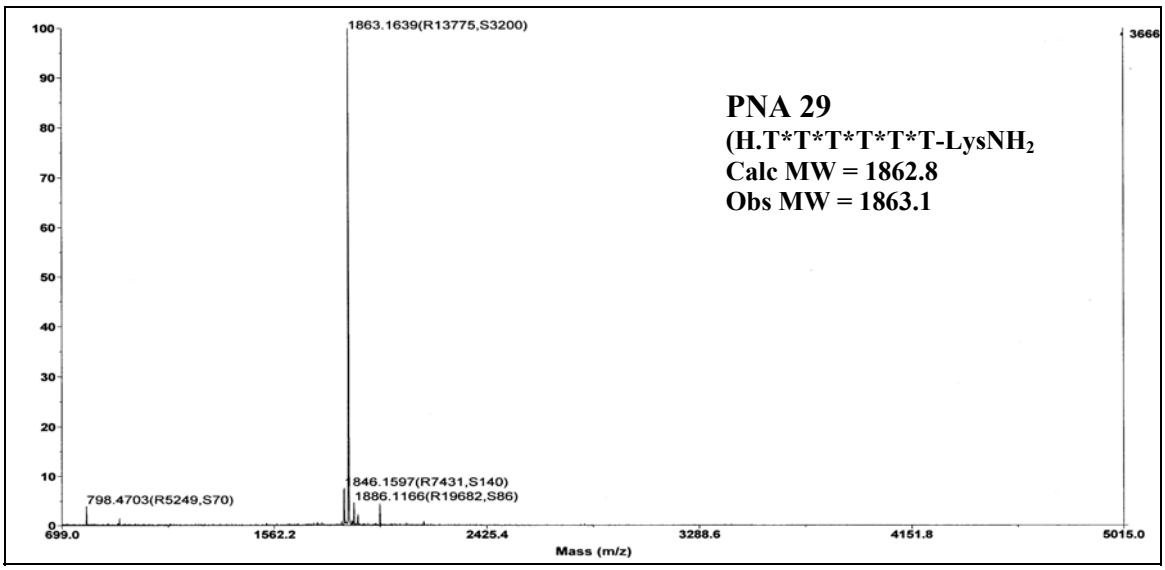

PNA 29
(H.T*T*T*T*T*T-LysNH$_2$
Calc MW = 1862.8
Obs MW = 1863.1

Chapter 4

Synthesis and enzyme mimetic hydrolytic studies of imidazolyl PNA

4 Introduction

Ribozymes are RNA molecules that possess a catalytic activity and therefore behave as enzymes. Those that occur in nature can catalyze the formation and breaking of a phosphodiester bond between two nucleotides. Ribozymes from plant pathogens or the human hepatitis delta virus (HDV) are self cleaving RNAs[1] that undergo an intramolecular reaction called as transesterification leading to 5'-hydroxyl group and 2', 3'-cyclic phosphate products and this self-cleaving reaction is necessary for replication of the single-stranded RNA genome of viral pathogens.

There has been a long standing interest in the development of ribozyme mimics and such ribonuclease mimics may be used as artificial restriction enzymes for sequence-selective manipulation of large RNA molecules *in vitro*. The potential applications of these artificial ribonucleases as catalytic antisense oligonucleotides in chemotherapy have attracted more attention.[2] Gene silencing by antisense oligonucleotides could benefit from artificial ribonucleases due to the reason that the oligodeoxyribonucleotides (ODN) and their phosphorothioate analogs activate an intracellular enzyme, RNase H, which degrades the RNA component of an RNA-ODN duplex, releasing the antisense ODN (Figure 1). In other words, mRNA hybridized with these kinds of antisense oligonucleotides is destroyed by the cells' own machinery.

Figure 1: The RNase H pathway for catalytic destruction of specific mRNA with antisense DNA probes.

4.1 Mechanism for RNA cleavage

Although there are similarities in the RNA cleavage products, the three dimensional architectures of the characterized self-cleaving ribozymes[3] do not appear to be similar, which indicates a chemical diversity in the mechanisms of cleavage.[4] The HDV ribozyme proceeds through a base catalytic mechanism[5] during self cleavage, where a base abstracts a proton from the 2'-hydroxyl group by increasing the electron

density on oxygen atom of the 2'-position of ribose to initiate the cleavage reaction. Another mechanism in which the phosphodiester is activated by a proton transfer from an acid to initiate the reaction. In this case the proton transfer to the 5'-OH occurs either prior to or simultaneously with nucleophilic attack by the 2'-OH group. This is the mechanism that also yields migration product **5** (Figure 2)**.**

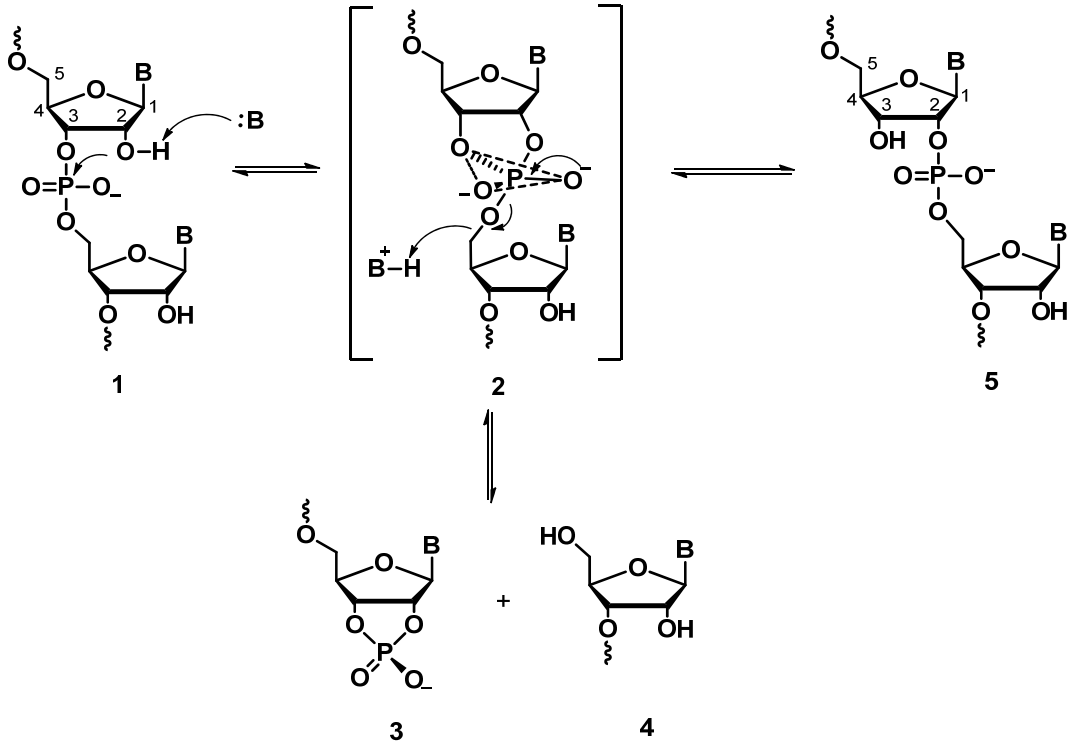

Figure 2: Acid base catalytic mechanism for RNA cleavage proceeding via trigonal bipyramidal dianionic phosphorane.

The self cleavage of RNA follows specific acid base catalytic mechanism and this mechanism for RNA self cleavage requires a base for abstracting the proton from the 2'-hydroxyl group of the ribose and an acid for protonating the departing 5'-hydroxyl group to give the 2', 3'-cyclic phosphate **3** along with the alcohol **4** (Figure 2). As nucleic acids carry negative charges, it requires metal ions for folding and stabilization and these metal ions can be a good source of hydroxide ions at neutral pH. Hence the cleavage process is facilitated by the presence of divalent ions in natural systems. This is the reason why RNA is randomly cleaved and degraded into its constituent nucleotides at basic pHs.

The RNA cleavage reaction may be accelerated by facilitating the proton transfer from the attacking nucleophile, 2'-OH, to the leaving nucleophile, 5'-O^-. Accordingly, possible candidates for cleaving agents are molecules or ions that (i) enhance deprotonation of the 2'-OH, (ii) reduce the electron density at the phosphorus atom upon formation of the phosphorane intermediate, or (iii) reduce the electron density at the departing 5'-oxygen atom upon cleavage of the P-O5' bond.

4.2 Development of artificial ribozyme based on antisense strategy

The first DNAzyme was reported in 1994 which cleaves the RNA.[6] Since that time, many other RNA-cleaving deoxyribozymes have been identified. A promising approach has been to covalently link a DNA oligonucleotide with a chemical cleaving head which may be metallated or metal-free. More recently acridine derivatised oligonucleotides have been used as cofactors for free metal ion cleavage.[7] The 5-amino-2,9-dimethyl-1,10-phenanthroline Zn^{2+} complex has been shown to work as an RNA cleaving group in several artificial ribonuclease studies.[8] On the other hand, the Cu^{2+} complex of the 2,9-diamino-1,10- phenanthroline has been reported to hydrolyze 2',3'-cAMP substantially faster than the Cu^{2+} complex of the 2,9-dimethyl-1,10-phenanthroline.[9]

Synthesis of 2,9-diamino-1,10-phenanthroline PNA conjugates as well as their action in cleavage of a target RNA has been reported.[10] PNA conjugates bearing phenanthroline either to the amino-end or to a centrally positioned diaminopropionic acid in the PNA via a urea linker cleaves the target RNA. PNA based artificial nucleases were designed to create a bulge in the target RNA, which is a model of leukemia related bcr/ab1 mRNA.[11] In the presence of zinc ions, PNA-Dap-PNA neocuproine conjugates cleave the target RNA sequence.

4.2.1 Metal ions used for transesterification and hydrolysis of RNA

Metal ions, including transition metals and rare earths are well known to catalyze the transesterification at phosphodiester bond of mRNA.[12] Among various metal ions, lanthanide ions are exceptionally effective in this respect.[13] Conjugates of lanthanide ion complexes have received interest as artificial ribonucleases, and most efficient nucleases so far described.[14] The Cu^{2+}-based artificial nucleases[15] introduced

so far are less efficient than their lanthanide ion counterparts. The interest for this metal ion is due to the reason that Cu^{2+} is present in intracellular fluids. Ligands that bind Cu^{2+} very tightly may, hence, be expected to occur as Cu^{2+} complexes even in an intracellular environment. Another 3d transition metal ion Zn^{2+}, has received attention in the design of artificial ribonucleases.[16]

4.2.2 Imidazole and metal ion dependent artificial ribonucleases

Breslow et al.[17] have shown that imidazole ring in the side chain of histidine plays an important role in many enzymes. Imidazole and Zn^{2+} more effectively can catalyze a cleavage reaction than the catalysis by imidazole alone.[18] In a separate investigation, catalysis of RNA was observed by imidazole buffer.[19] Imidazoles act as both acids and bases at physiological pH.

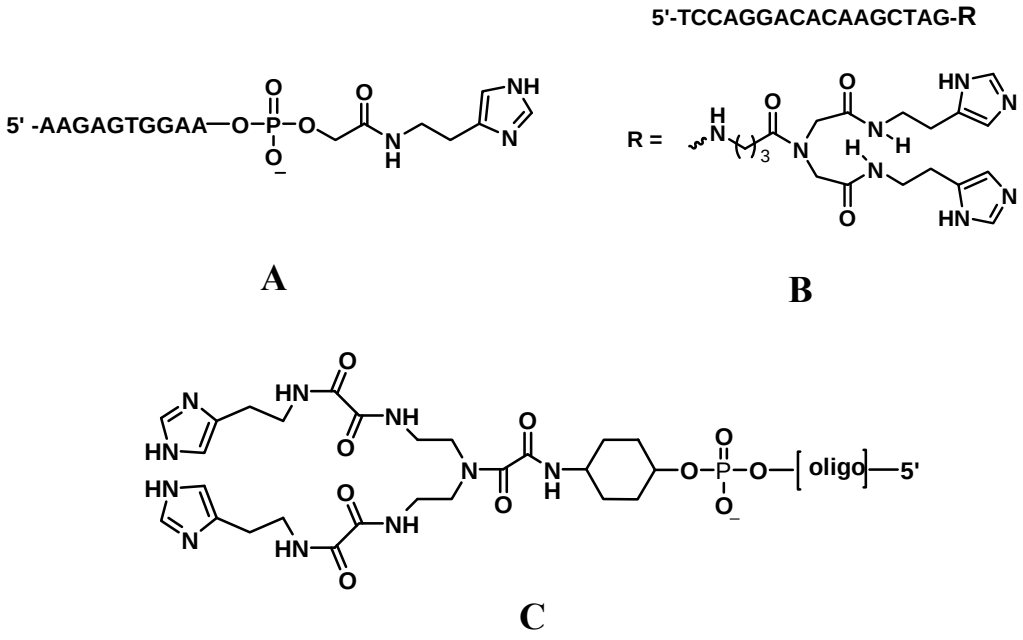

Figure 3: Imidazole-containing oligonucleotide conjugates.

Lonnberg et al.[20] developed a sequence specific RNA cleavage agent by tethering a histamine group to the 3'-terminus of a 10-mer deoxyoligonucleotide (Figure 3A). This was accomplished by attaching an ester function to the deoxyoligonucleotide during chain assembly. Treatment of the deoxyoligonucleotide with the appropriate primary amine afforded the desired conjugate. Site-specific

cleavage of a synthetic 16-mer RNA target was observed only in the presence of zinc (II) ion. Remarkable site-specific cleavage was obtained for deoxyoligonucleotide derivatives conjugated with moieties containing two histamine residues that mimic the catalytic active site of RNase A.[21] (Figure 3B and 3C). Deoxyoligonucleotides with the modifications at either the 3'- or 5'-ends, separately or together, site specifically cleaved RNA. A maximum cleavage (60%) of the target was attained after 8 hrs at 37 °C (pH 7.0).

An imidazole-based antisense methylphosphonate oligonucleotide (MPO) synthetic ribonuclease has been synthesized by Reynolds et al.[22] This bears a non-nucleotide-linker with an attached imidazole group in place of one of the complementary bases (Figure 4). Covalent attachment of a catalyst to an oligonucleotide via a non-nucleotide-based linker enables it to be directed toward a hydrolytically sensitive site on the RNA thereby allowing it to adopt a conformation more favorable for transesterification.

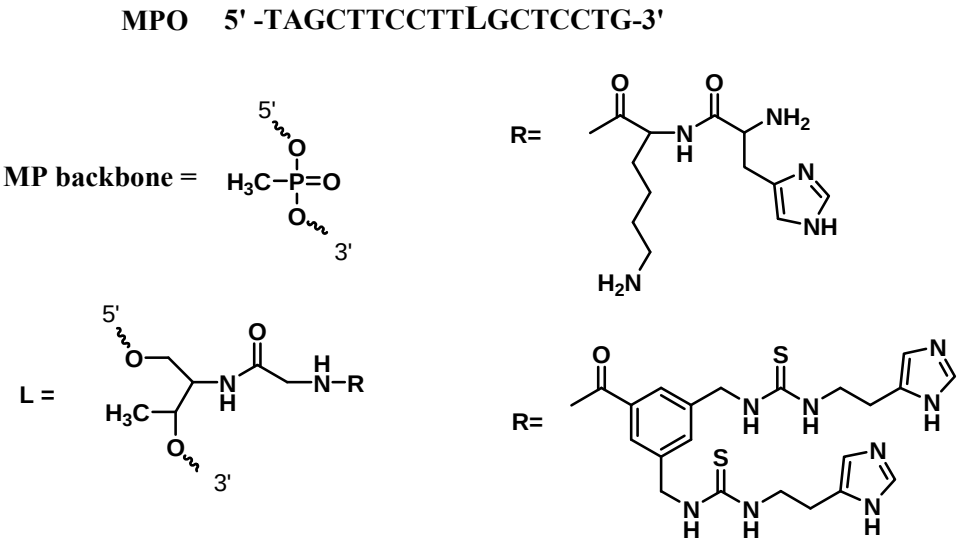

Figure 4: Structure of imidazole-based antisense methylphosphonate oligonucleotide.

4.2.2a Role of imidazole in RNA cleavage mechanism

In the protein universe, the ribonucleases cleave RNAs using amino acid such as histidine, which carries an imidazole side chain that has a nitrogen atom with a p*K*a around 6. At this p*K*a imidazole ring can exist at least partially unprotonated in

biological solution, while in its protonated form that can exist at physiological pH, the imidazolium ion is the strongest acid. During acid- base catalysis, the nitrogen of the histidine attacks the ribose hydroxyl, whereas another histidine gives off a proton to the departing 5'-hydroxyl group (Figure 5). Thus imidazole acts as a base catalyst in many enzymatic reactions, while imidazolium ion acts as an acid catalyst. The two imidazole rings of His-12 and His-119 in the enzyme ribonuclease A act as the acid and base catalysts in the hydrolytic cleavage of RNA.

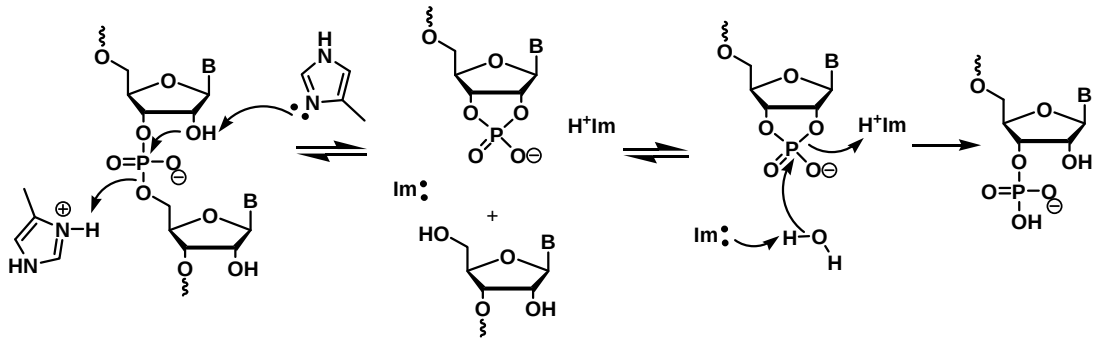

Figure 5: Acid base catalysis mechanism of imidazole in RNA cleavage

4.2.2b Role of Zn^{2+} in RNA cleavage

The most important characteristic of a metal ion promoted reaction is its positive charge. For maximal effects, the metal ion should be directly associated with a substrate molecule and electronically linked to the reactive bond of substrate to be broken. A metal ion has advantages over a proton as it can introduce multiple positive charges whereas a proton introduces only a positive charge. Metal ion Zn^{2+} can catalyze a reaction either in one or a combination of the following effects: (i) it can act as an electrophilic catalyst by neutralization of anionic charge ($P\text{-}O^-$) of phosphate and thereby enhance the intramolecular nucleophilic attack on phosphorous by $2'\text{-}O^-$ (Figure 6) (ii) it may enhance the leaving group tendency of $5'\text{-}O^-$ through stabilization via coordination and (iii) it may simultaneously complex with phosphate and imidazole to activate phosphate for receiving a nucleophilic attack. Although (i) is more reasonable explanation, (ii) and (iii) cannot be ruled out.

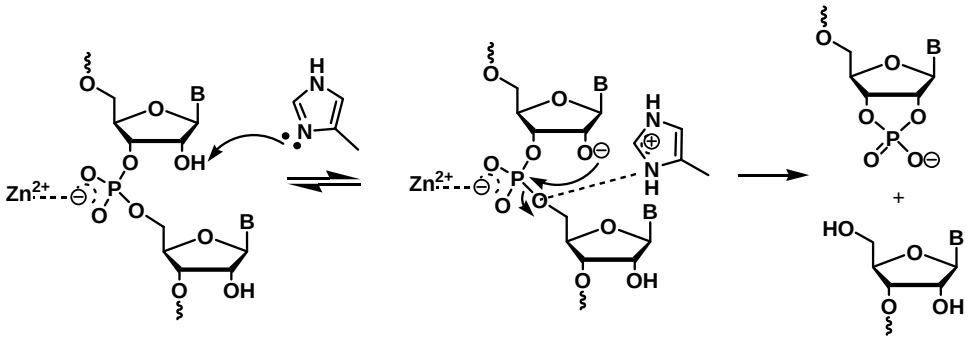

Figure 6: RNA cleavage mechanism in presence of metal ion

4.3 Rationale and Objectives of present work

Structurally modified antisense oligonucleotides do not usually trigger a similar activity as their antisense effect remains stoichiometric, unless they bear a catalyst that is able to destroy the target RNA and hence, release the intact antisense oligomer. Therefore the process of designing ribozyme mimics involves a series of steps. The first step involves the identification of RNA cleavage catalysts that function by transesterification/hydrolysis mechanisms and that are suitable for covalent incorporation into ODN. Second step required the use of preliminary molecular designs that controlled features such as the vertical approach of the catalyst to the substrate. Third, candidate molecules were tested for sequence-specific cleavage activity, and the structures of mimic-RNA complexes were investigated.

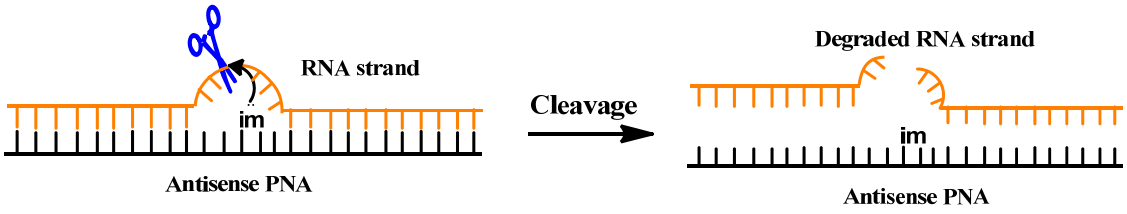

Figure 7: RNA cleavage strategy by catalytic PNA

In view of the above mentioned strategy for designing an antisense oligonucleotide as artificial ribonuclease, it was proposed to synthesize imidazole *N*1-acetyl PNA **5** and imidazole *C*4-acetyl PNA **6** monomers (Figure 8), which can be incorporated at the desired positions of the *aeg*PNA oligomer. The imidazole based oligomer designed for the cleavage study will bind to the complementary RNA oligonucleotide and the imidazole unit acts either as acid-base or as base catalyst for

RNA cleavage. The imidazole *N*1-acetyl PNA can act only as base catalyst whereas imidazole *C*4-acetyl PNA can act as acid-base catalyst. The lone pair of electron on imidazole can site specifically attack on the 2'-OH of the ribose of the opposite RNA strands and gives rise to the degraded RNA (Figure 7).

Further these oligomers can be characterized and subjected for biophysical studies along with the enzyme mimetic hydrolytic studies.

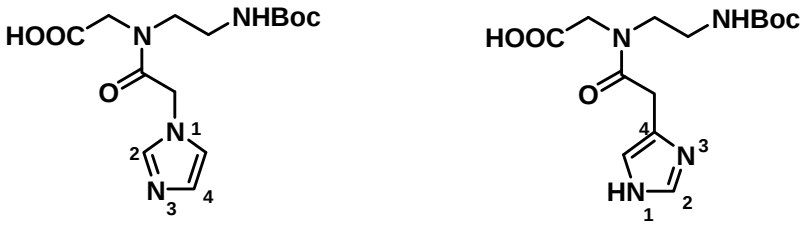

imidazole *N*1-acetyl PNA monomer (5) **imidazole *C*4-acetyl PNA monomer (6)**

Figure 8: Structure of imidazole *N*1- acetyl and imidazole *C*4-acetyl PNA monomer

PNA oligomer containing imidazole *C*4-acetyl unit (Figure 9) at the N-terminus also designed for enzyme mimetic hydrolytic studies.

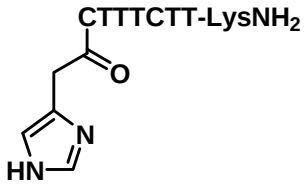

Figure 9: Chemical structure of imidazole *C*4-acetyl PNA oligomer

4.3.1 Results and Discussion

The synthesis of imidazole *N*1-acetyl PNA and imidazole *C*4-acetyl PNA monomers are described in the following section.

4.3.1a Synthesis of imidazole *N*1-acetyl PNA monomer

The synthesis of imidazole *N*1-acetyl PNA monomer **5** starts from commercially available 1,2-diaminoethane **7** (Scheme 1). The amine was protected with *t*-Boc under high dilution condition to get mono Boc- protected compound **8** along with the di-Boc

compound which being insoluble in water can be removed by filtration through celite. The mono-Boc protected compound **8** was further alkylated with ethyl bromoacetate to obtain the mono alkylated product **9**, which can be confirmed by ^{1}H NMR as it appears ethyl ester protons and the singlet proton for the glycine unit at δ 4.02 ppm. It was further acylated with chloroacetyl chloride in presence of triethyl amine to get the product **10**, which was used for alkylation using imidazole to obtain product **11**. The formation of the product was confirmed by the appearance of the three olefinic protons at the range of δ 6.95-7.51ppm in ^{1}H NMR. The hydrolysis of ester **11** was done using 1N aqLiOH to give the corresponding acid **5**.

Scheme 1: Synthesis of imidazole-*N*1-acetyl PNA monomer

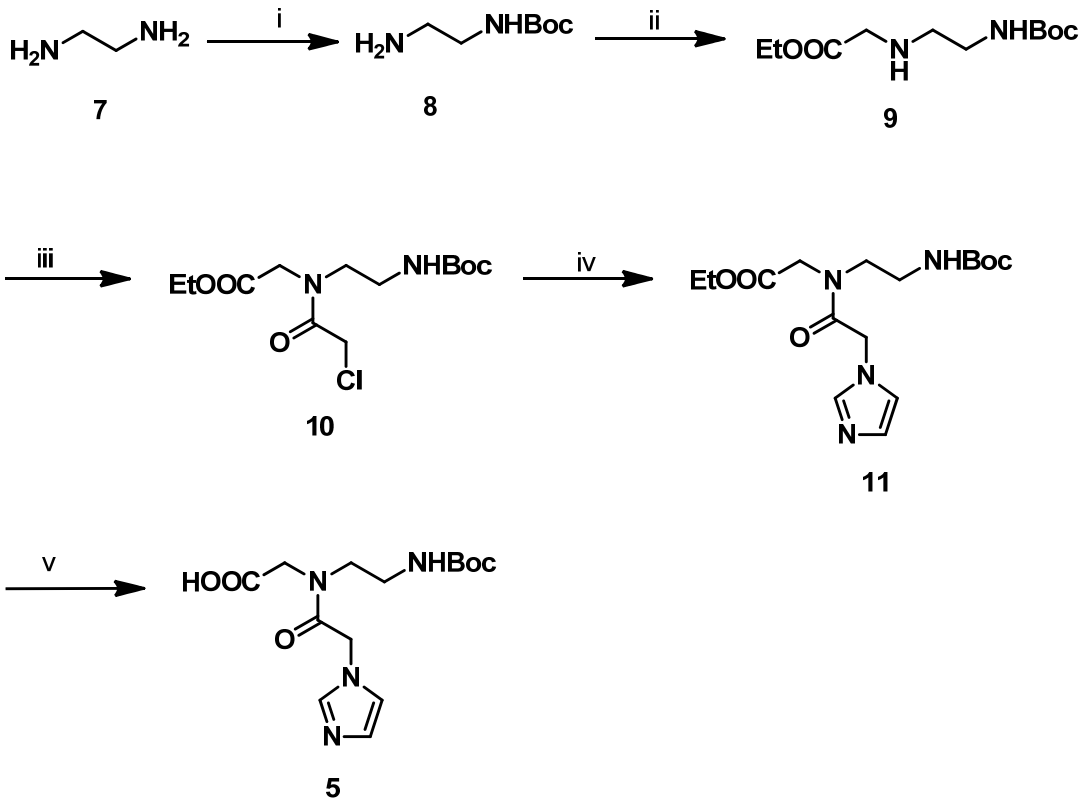

Reagents and conditions: i. Boc anhydride, THF, 60% ii. $BrCH_2COOEt$, Et_3N, ACN, 81% ii. $ClCH_2COCl$, Et_3N, DCM, 80% iii. Imidazole, K_2CO_3, 60^{o}C, 79%, iv. 1N aq LiOH, THF, 86%

4.3.1b Synthesis of imidazole *C*4-acetyl PNA monomer

The imidazole *C*4-acetyl PNA monomer **6** was synthesized by a similar reaction sequence followed for the synthesis of imidazole *N*1-acetyl PNA monomer. The mono *N*-alkylated product **9** obtained from the mono Boc protected compound **8** (Scheme 1)

was subjected to EDC/DIPEA coupling reaction with the commercially available imidazole 4-acetic acid monohydrochloride to get the product **12** (Scheme 2). Here the acid to be coupled was activated initially by EDC and DIPEA, followed by the addition of the amine **9** to the reaction mixture. The success of the coupling reaction was confirmed by ^{1}H and ^{13}C NMR. In ^{1}H NMR two singlets appear at δ 6.88 ppm and 7.52 ppm for two olefinic protons indicating the presence of imidazole ring in the compound. One broad singlet at δ 8.02 ppm also shows the presence of free amine in *C*4-imidazole ring. The ester **12** was hydrolyzed with 1N aqLiOH to yield the product **6**. Disappearance of the ethyl ester protons at δ 4.17-4.24 ppm and δ 1.23-1.21 ppm indicates the formation of the final imidazole *C*4-acetyl monomer **6**.

Scheme 2: Synthesis of imidazole *C*4-acetyl PNA monomer

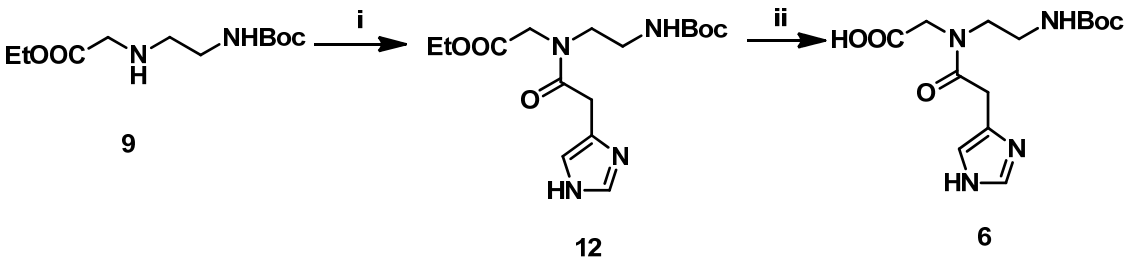

9 12 6

Reagents and conditions: i. imidazole-4-acetic acid monohydrochloride, EDC, DIPEA, DMF, 22% ii. 1N LiOH, THF, 78%

4.3.1c Solid phase PNA synthesis

The Boc protected imidazole *N*1-acetyl PNA monomer **5** was incorporated to solid support for synthesis of desired PNA oligomers. Similar to the peptide synthesis mentioned in the previous chapters, MBHA resin (4-methyl benzhydrylamine resin) was used as the solid support on which the oligomers were elongated. The monomer was subjected to coupling reaction by *in situ* activation with HBTU/HOBt/DIEA. Orthogonally protected L-lysine was selected as the *C*-terminal spacer-amino acid for the synthesis of all the oligomers and it is linked to the resin through amide bond. The amine content on the resin was determined by the Kaiser test and was found to be 2.00mmol/g. This loading value was suitably lowered to approximately 0.35 mmol/g by partial acetylation of amine content using calculated amount of acetic anhydride.

The PNA oligomers were synthesized using repetitive cycles, each containing the following steps

Step 1: Deprotection of the *N*-Boc-group using 50% TFA in CH_2Cl_2.

Step 2: Neutralization of the TFA salt formed with 5% DIPEA in DCM to liberate the free amine.

Step 3: Coupling of the free amine on the resin with the free carboxylic acid group of the added monomer using HBTU and HOBt as the coupling reagent.

4.3.1d Cleavage of the oligomers from solid support

All the synthesized oligomers which are derivatized with L-lysine at the C-terminus were cleaved from the solid support, using trifluoromethanesulphonic acid (TFMSA) in the presence of trifluoroacetic acid (TFA) (Low, High TFMSA-TFA method)[22] (Table 1). For the cleavage of the oligomer from the solid support, the resin was kept for 1.5-2 h in TFA-TFMSA at room temperature. The side chain protecting groups were also cleaved during this cleavage process. After cleavage reaction, the oligomer was precipitated out by diethylether. Various oligomers synthesized for imidazole *N*1-acetyl PNA for the biophysical studies are depicted in Table 1.

The polypyrimidine (thymine) octamers (**PNA31** and **PNA32,** entry 2 and 3) were synthesized to study the effect of the imidazole in PNA side chain for the triplex forming ability. The mixed purine-pyrimidine oligomers (**PNA33-PNA36,** entry 5-8) were synthesized for comparative studies with mixed *aeg*PNA (**PNA10**) oligomer.

Table 1: Oligomers synthesized for imidazole *N*1-acetyl PNA monomer

S No	Entry	PNA sequences
1	**PNA 1**	H. TTTTTTTT-LysNH_2
2	**PNA 31**	H. $\mathbf{I_m}$TTTTTTT-LysNH_2
3	**PNA 32**	H. TTT $\mathbf{I_m}$ TTTT-LysNH_2
Mixed Sequences		
4	**PNA 10**	H.T ATT ATT ATT-LysNH_2
5	**PNA 33**	H. $\mathbf{I_m}$ ATT ATT ATT-LysNH_2
6	**PNA 34**	H.T ATT A$\mathbf{I_m}$T ATT-LysNH_2
7	**PNA 35**	H. $\mathbf{I_m}$ ATT A$\mathbf{I_m}$T ATT-LysNH_2
8	**PNA 36**	H.T ATT ATT AT$\mathbf{I_m}$-LysNH_2

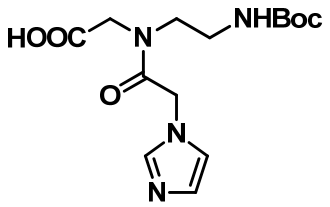

imidazole *N*1-acetyl PNA monomer ($\mathbf{I_m}$)

Purification of oligomers

The oligomers cleaved from solid support were dissolved in water and were subjected for gel filtration. Further the purity of the oligomers was ascertained by RP-HPLC method followed by purification with preparative HPLC using C18 column. Purity of the oligomers containing L-lysine side chain at the C-terminus were checked by RP-HPLC (Figure 10 and 11) and characterized by MALDI-TOF experiment shown in Table 2

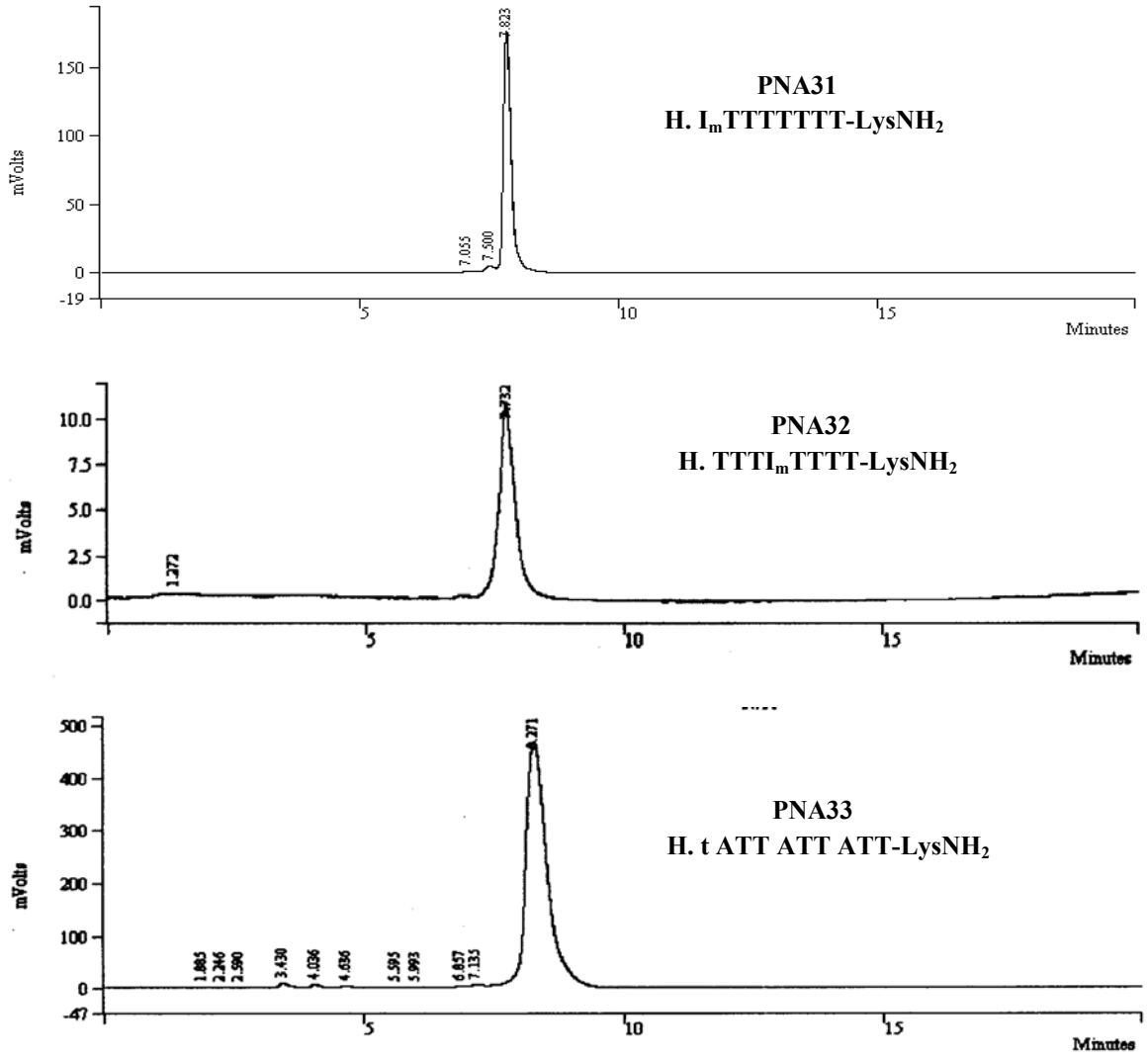

Figure 10: HPLC profile for **PNA 31-33**

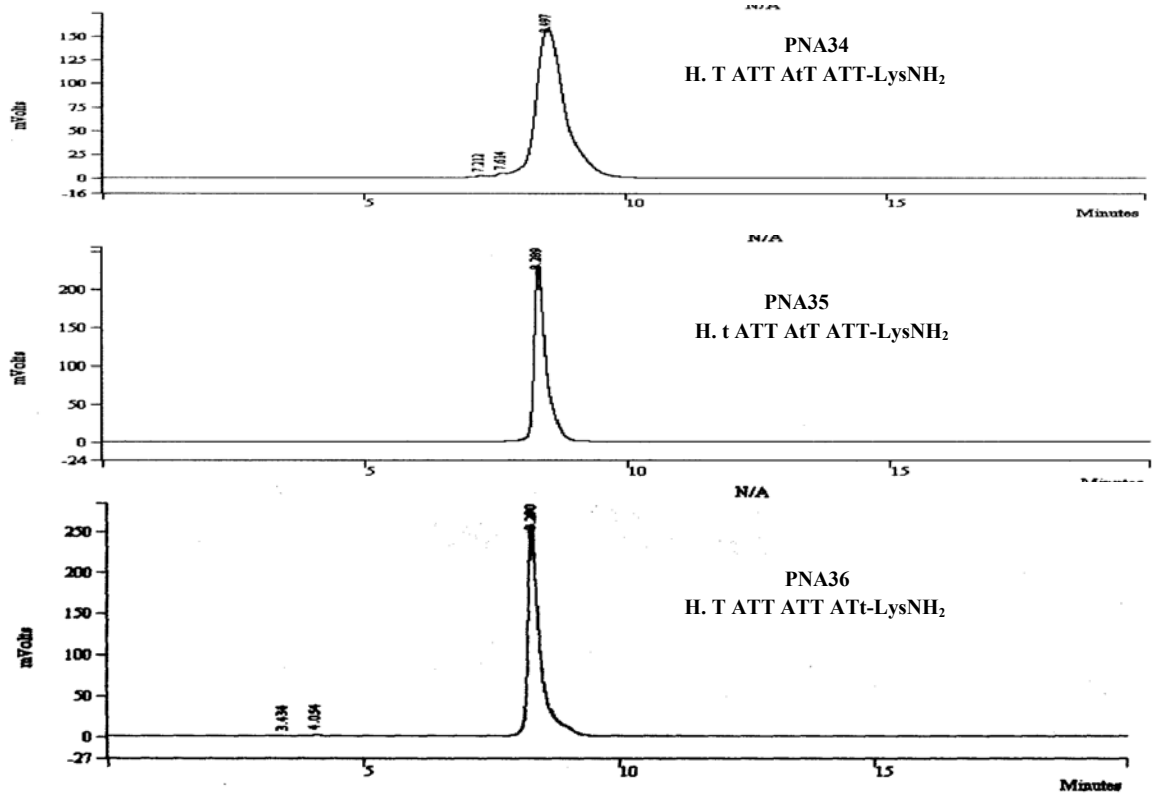

Figure 11: HPLC profile for **PNA34-36**

After purification, the HPLC purity for all the oligomers is shown in Table 2. The calculated and observed molecular weights are shown along with the molecular formula for all the synthesized oligomers in the Table 2. The MALDI-TOF spectra showing the molecular weight of each are shown in the experimental section.

Table 2: PNA oligomers with imidazole- N-acetyl PNA monomer

S. No	Entry	Mol. Formula	RP-HPLC R_t	Calc. MW*	Obs. MW
1	**PNA 31**	$C_{92}H_{125}N_{35}O_{31}$	7.9	2215.93	2215.23
2	**PNA 32**	$C_{92}H_{125}N_{35}O_{31}$	7.7	2215.93	2215.64
3	**PNA 33**	$C_{117}H_{153}N_{49}O_{33}$	8.2	2773.83	2774.66
4	**PNA 34**	$C_{117}H_{153}N_{49}O_{33}$	8.4	2773.83	2774.66
5	**PNA 35**	$C_{115}H_{151}N_{49}O_{31}$	8.2	2715.80	2716.75
6	**PNA 36**	$C_{117}H_{153}N_{49}O_{33}$	8.2	2773.83	2774.55

*MW calculated using Chem Draw ultra 8.0, MALDI-TOF spectra are shown in experimental section

4.3.2 Biophysical Studies

4.3.2a UV melting experiment

For the study of binding selectivity, specificity and discrimination in parallel and antiparallel biding of the modified PNA towards complementary DNA, UV-melting studies were carried out with all the synthesized oligomers and T_m data were compared with that of control *aeg*PNA. The stability of the imidazole *N*1-acetyl PNA duplexes with DNA was also studied. The hybridization studies of modified imidazole *N*1-acetyl PNA oligomers with complementary **DNA1, DNA2 and DNA3** were done by temperature dependent UV-absorbance experiments.

Results and Discussion

Similar to the results which were discussed in Chapter 2, no double transition were observed in temperature dependent UV spectra for triplex forming oligomers. The melting curves for polypyrimidine and mixed purine-pyrimidine PNA:DNA complexes are shown in Figure 12 and 13.

The homopyrimidine **PNA31** with N-terminus imidazole *N*1-acetyl modification shows a melting transition of 28.3^{o}C when it is hybridized with complementary **DNA1** (Table 3, entry 2, Figure 13A, B). PNA**32** with incorporation of the imidazolyl-*N*1-acetyl PNA modification (Table 3, entry1) shows the melting temperature of complex to be 28.3^{o}C which is identical with that for N-terminus modified PNA oligomer. Thus in comparison with unmodified homothymine PNAs, a destabilization of 16.7^{o}C was observed for imidazole *N*1-acetyl modified PNA irrespective of the position of modification. This is in contrast with the T_m of the control, unmodified PNA_2:DNA triplex which was 45^{o}C. It should be noted that one modification per strand is equivalent to two modifications in triplexes. Thus ΔT_m per modification is -8.3^{o}C.

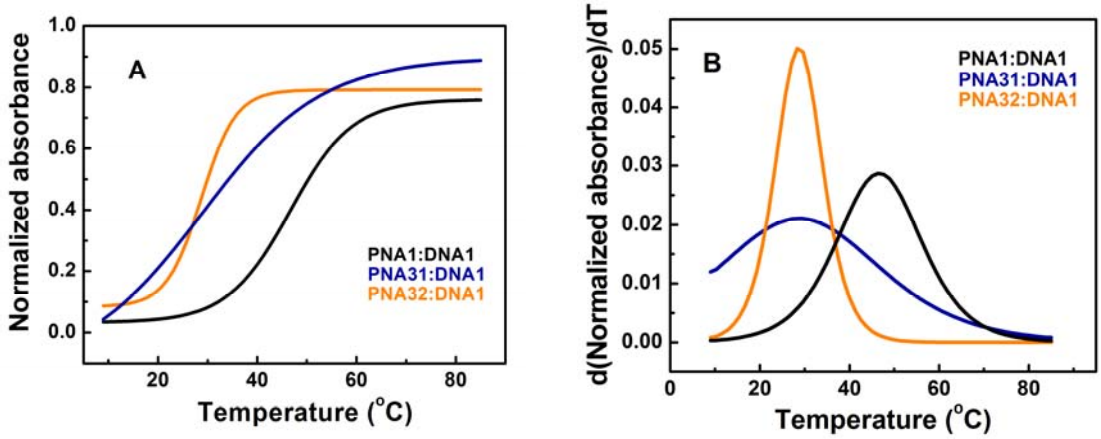

Figure 12: UV melting curves for homopyrimidine **PNA31** and **PNA32** hybridized with complementary **DNA1**

Table 3: UV melting data for homopyrimidine oligomers

S. No.	Entry	Triplex PNA_2:DNA	UV-T_m (^oC)	ΔT_m (^oC)
1	**PNA1** **DNA1** **PNA1**	H. TTTTTTTT-LysNH_2 5' CGAAAAAAAAGC 3' H_2N Lys-TTTTTTTT.H	45.0	-----
2	**PNA31** **DNA1** **PNA31**	H. $\mathbf{I_m}$TTTTTTT-LysNH_2 5' CGAAAAAAAAGC 3' H_2N Lys-TTTTTTT$\mathbf{I_m}$.H	28.3	-16.7
3	**PNA32** **DNA1** **PNA32**	H. TTT $\mathbf{I_m}$TTTT-LysNH_2 5' CGAAAAAAAAGC 3' H_2N Lys-TTTT$\mathbf{I_m}$TTT.H	28.3	-16.7

Mixed purine-pyrimidine oligomers such as **PNA33-36** will form duplexes. The PNA oligomers were studied for their ability to form duplexes. The UV melting experiments were carried out for mixed purine-pyrimidine oligomers **PNA33-PNA36** (Table 4, entry 3-9). The N-terminus modified **PNA 33**, shows a melting transition at 23.1°C for parallel (Table 4, entry 4) and 23.3°C for antiparallel (Table 4, entry 3) binding thus showing no discrimination among the parallel/antiparallel orientations. This is in contrast to that of control *aeg***PNA10** duplex which shows melting temperatures 10.2°C and 23.9°C for parallel and antiparallel binding orientations respectively (Table 4, entry 2, 1). A destabilization of only 0.6°C is therefore observed

for the antiparallel binding mode compared to the corresponding unmodified **PNA10**, while more destabilization was seen for parallel binding.

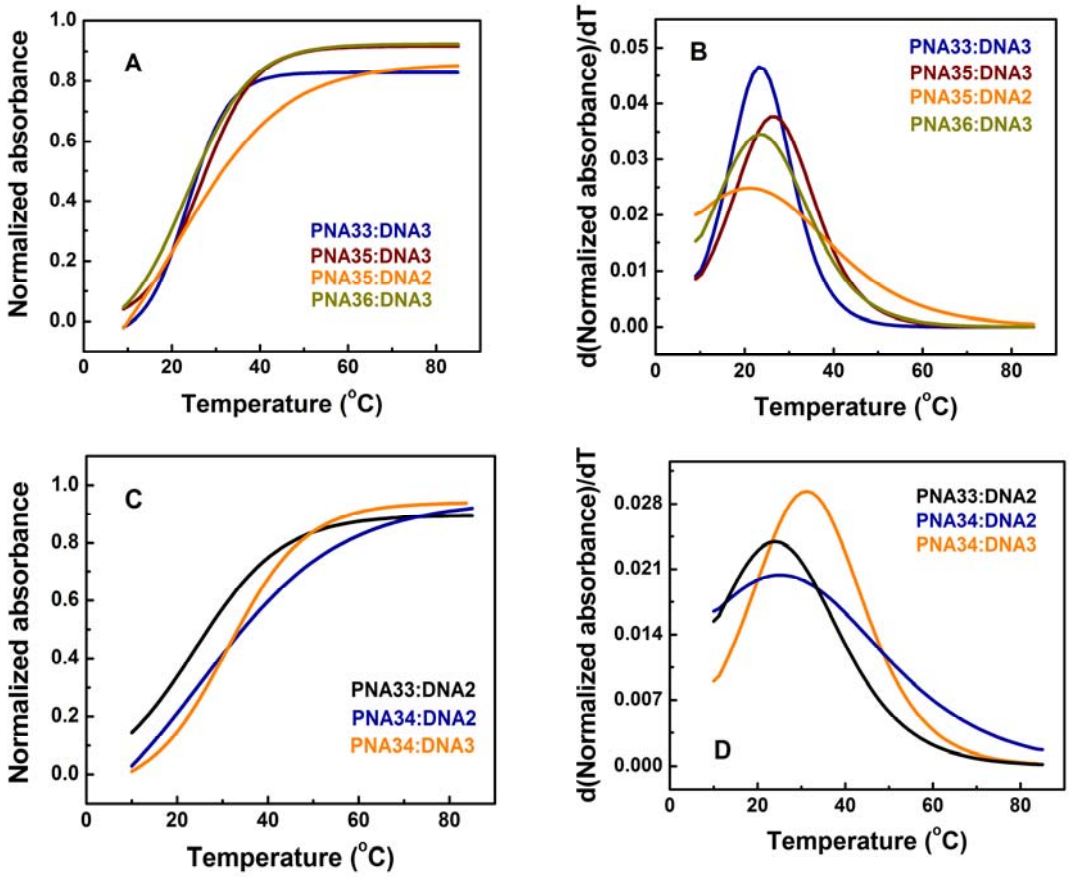

Figure 13: UV melting curves for purine-pyrimidine PNAs with complementary **DNA2** and **DNA3** in parallel and antiparallel orientation and the corresponding derivative curves**.**

The middle and double modified PNAs (**PNA34** and **PNA35**, Table 4, entry 5, 7) when hybridized with complementary antiparallel **DNA3**, showed melting temperatures of 31.2°C and 26.7°C, amounting to stabilization of +7.3°C and +2.7°C respectively over the control duplex. For parallel duplexes of **PNA34** (Table 4, entry 6) and **PNA35** (Table 4, entry 8) stabilization of 14.8°C and 11.6°C respectively were observed as compared to that of unmodified **PNA10**. Similarly the C-terminus modified duplex (**PNA36**, Table 3, entry 9) gave a melting temperature 24.0°C for antiparallel binding mode with destabilization of 0.7°C.

Table 4: UV-Tm of mixed purine/pyrimidine oligomers

S. No.	PNA	Duplex PNA:DNA	Binding orientation	UV T_m	ΔT_m
1	**PNA 10** **DNA 3**	H. T ATT ATT ATT-LysNH_2 5' AAT AAT AAT A 3'	Antiparallel	23.9	-----
2	**PNA 10** **DNA 2**	H. T ATT ATT ATT-LysNH_2 5' A TAA TAA TAA 3'	Parallel	10.2	-----
3	**PNA 33** **DNA 3**	H.**I_m** ATT ATT ATT- LysNH_2 5' AAT AAT AAT A 3'	Antiparallel	23.3	-0.6
4	**PNA 33** **DNA 2**	H. **I_m** ATT ATT ATT- LysNH_2 5' A TAA TAA TAA 3'	Parallel	23.1	+12.9
5	**PNA 34** **DNA 3**	H.T ATT A**I_m**T ATT- LysNH_2 5' AAT AAT AAT A 3'	Antiparallel	31.2	+7.3
6	**PNA 34** **DNA 2**	H.T ATT A**I_m**T ATT- LysNH_2 5' A TAA TAA TAA 3'	Parallel	25.0	+14.8
7	**PNA 35** **DNA 3**	H. **I_m**ATT A**I_m**T ATT- LysNH_2 5' AAT AAT AAT A 3'	Antiparallel	26.7	+2.8
8	**PNA 35** **DNA 2**	H. **I_m**ATT A**I_m**T ATT- LysNH_2 5' A TAA TAA TAA 3'	Parallel	21.8	+11.6
9	**PNA 36** **DNA 3**	H.T ATT ATT AT**I_m**- LysNH_2 5' AAT AAT AAT A 3'	Antiparallel	24.0	-0.7

T_m = melting temperature PNA:DNA complexes (measured in the buffer 10 mM sodium phosphate, 100 mM NaCl, pH = 7.4)

From the above UV melting experiments it is observed that none of the oligomers synthesized from imidazole *N*1-acetyl PNA monomer exhibited stabilization towards the complementary DNA oligomers for triplex formation. However duplex from the mixed purine-pyrimidine PNA oligomers with middle and double modifications exhibited some stabilization.

4.4 Enzyme Mimetic Hydrolytic Studies

4.4.1 Introduction

Over the last decade, many catalytically active DNA molecules (DNA enzyme) have been identified that cleave RNA substrate.[6] These enzyme mimics can be constructed by covalently incorporating nucleophilically active RNA cleavage catalysts

into DNA. Based on work spanning 50 years, several groups have recently achieved the specific cleavage of RNA by attaching RNA-cleaving chemical moieties to antisense oligonucleotides.[14d] Such artificial chemical ribonucleases have potential as a possible next generation antisense compounds and also as probes for structural and functional investigations of RNA. Different chemical moieties,[7-11] such as polyamines, imidazoles, and metal complexes, have been used as the catalytic part of the artificial nucleases. To be of practical use as therapeutics, however, the conjugates must fulfill a number of requirements, such as ease of preparation, chemical stability, selectivity, nontoxicity. In addition, high cleavage efficiency and specificity is essential to overcome short lifetimes of cellular mRNA targets and the reaction should happen under physiological conditions without requirement of additional cofactors.

4.4.2 Rationale and Objectives

The rationale behind the incorporation of imidazole *C*4-acetyl unit was to use them as bifunctional acid-base catalytic unit to cleave complementary DNA/RNA sequence through hydrolysis of phosphodiester units. An efficient antisense artificial ribonuclease consists of two moieties, a catalytic group and a probe for sequence recognition. The oligonucleotide sequence brings the sequence selectivity through hybridization and the catalytic group cleaves the phosphodiester bond (Figure 14). Due to the hybridization of the artificial ribonuclease with the target RNA, the local concentration of the catalytic moiety increases in the vicinity of one particular phosphodiester bond, instead of random cleavage of the target.

Another role of oligonucleotide moiety is that the duplex formation between the artificial nuclease and the target may be exploited to shape the secondary structure and chain folding of the target optimal for cleavage. The site of tethering of the conjugate group within the artificial nuclease and the length of the complementary region(s) with the target, in turn affects the efficiency of turnover. The overall construct should be such that it binds the intact target chain more tightly than the cleavage products. With this rationale in mind, PNA oligomers (**PNA38** and **PNA39**) having imidazole unit at side chain and in the middle of the oligomer were specifically designed and synthesized. The next section will report on experiments towards their utility in site specific cleavage of target complementary srtands.

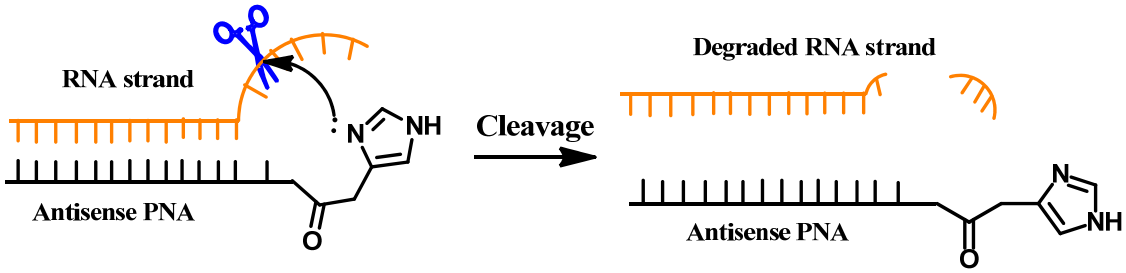

Figure 14: Strategy for RNA cleavage by N-terminus modified antisense PNA

4.4.3 Results and Discussion

4.4.3a Synthesis of PNA oligomers on solid support

The PNA oligomers **PNA37-39** (Table 5) which were derivatized with L-lysine at the C- terminus synthesized for examining enzyme catalytic study. The incorporation of the imidazole 4-acetic acid unit to the N-terminus of the PNA backbone (**PNA38**) was done by using HBTU/HOBt/DIEA as the coupling reagent. These were synthesized on MBHA resin and cleaved from the solid support, using trifluoromethanesulphonic acid (TFMSA) in the presence of trifluoroacetic acid (TFA) (Table 1). The duration for cleavage was 1.5-2 h and was kept in TFA-TFMSA at room temperature. The side chain protecting groups were also cleaved during this cleavage process. The complementary RNAs are shown in Table 5.

Table 5 : oligomers synthesized for enzyme catalysis study

S. No.	Entry	PNA sequence
1	**PNA37**	H. C TTT CTT-LysNH_2
2	**PNA38**	H. **I_{mC4}**-C TTT CTT-LysNH_2
3	**PNA39**	H. G**I_m**A GAT CAC T-LysNH_2
		RNA sequence
4	**RNA40**	5’ AAG AAA GAG A 3’
5	**RNA41**	5’ AGU GAU CUA C 3’

RNA40 is complementary to **PNA37** and **PNA38**
RNA41 is complementary to **PNA 39**

I_{mC4} =

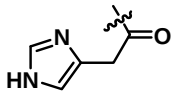

I_m =

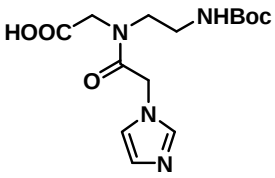

4.4.3b Purification and characterization of oligomers

The purity of the PNA oligomers (**PNA37-PNA39**) dissolved in water was checked by RP-HPLC analysis using C18 column. These were subjected to gel filtration, further purified by semi-preparative column and characterized by MALDI-TOF spectra (Figure 16).

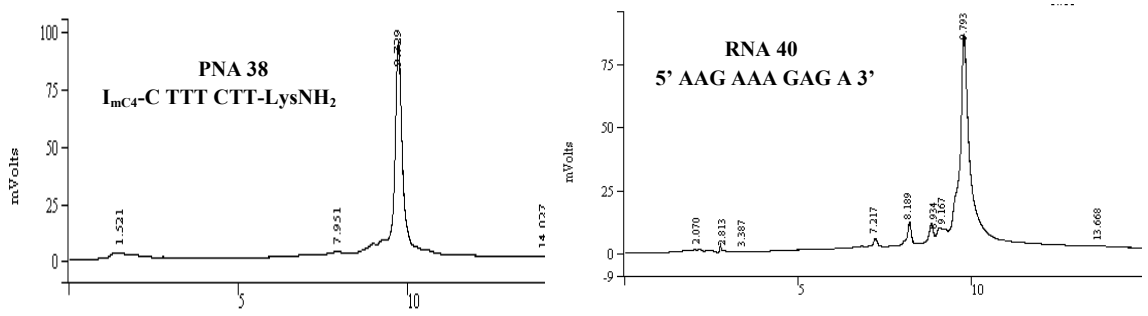

Figure 15: HPLC profile for **PNA38** and **RNA40**

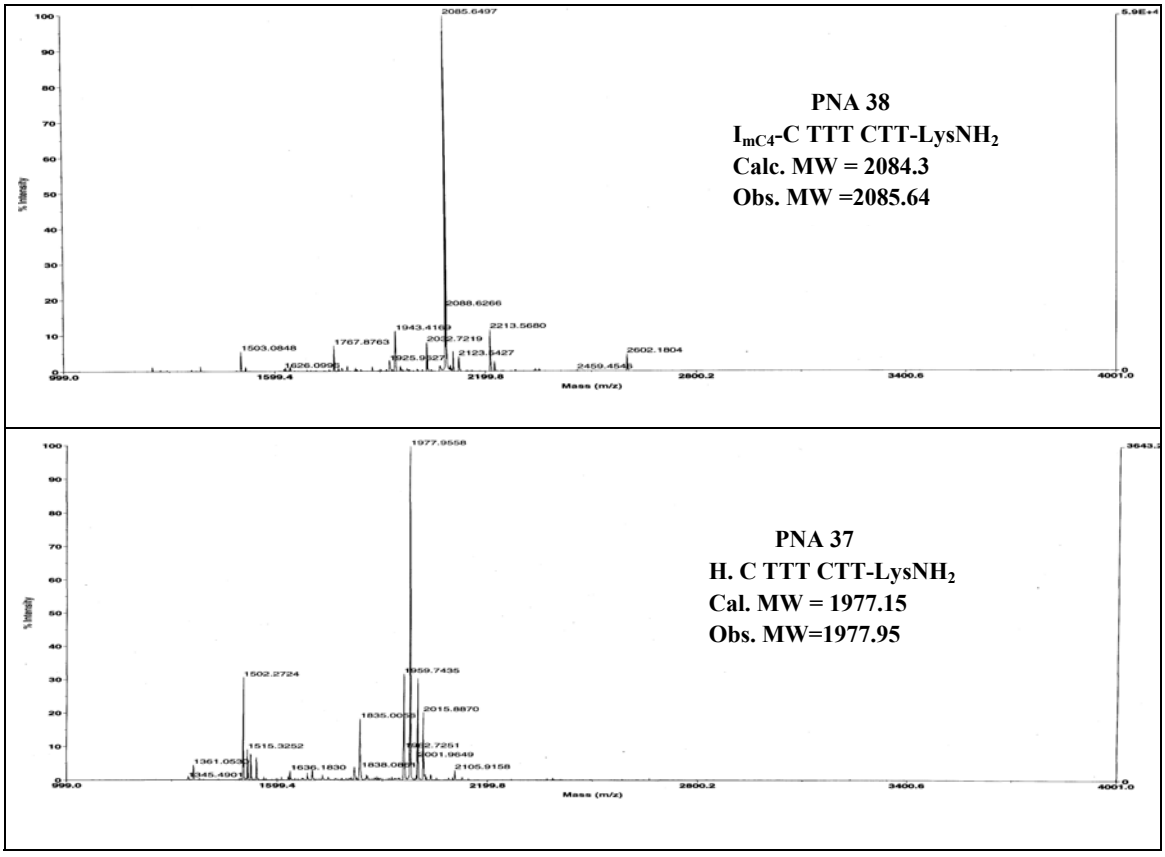

Figure 16: MALDI-TOF spectra of **PNA37** and **PNA38**

4.4.3c UV-T_m studies of PNA:RNA hybrids

The hybridization of imidazole *C*4-acetyl **PNA38** with complementary **RNA40** was studied by temperature dependent UV absorbance experiments. The thermal stability (T_m) of duplexes of control **PNA37** and imidazole *C*4-acetyl **PNA38** with the complementary **RNA40** was found to be 69°C, identical for both duplexes (Figure 17).

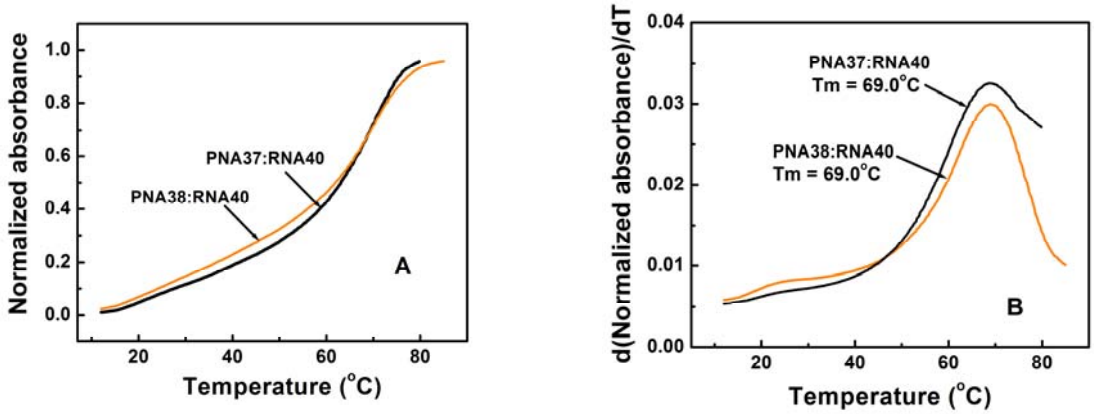

Figure 17: (A) UV melting profile for **PNA37: RNA40** and **PNA38:RNA40** (B) derivative curve of **PNA37: RNA40** and **PNA38:RNA40**.

4.4.3d Experimental conditions for enzyme mimetic hydrolytic studies

The cleavage reaction was carried out using equimolar and double concentration of **PNA38** to that of the RNA target (**RNA40**). Individual reactions were done at temperatures below the T_m (37°C) and around the T_m (70°C) using with 3 μM, 4 μM and 8 μM concentration of PNA and 3 μM, 4 μM concentration of RNA in 10 mM HEPES buffer, pH 7.0) containing 100 mM NaCl and varying amount of 10 μM, 100 μM, 1 mM $ZnCl_2$. Different reaction mixtures were prepared individually with different molar concentrations of PNA, RNA and the metal ion. All fractions of reaction mixture were incubated separately at 37°C and 70°C at pH 7. At regular time intervals, small fractions of aliquots was removed and subjected for RP-HPLC analysis using triethyl amine acetate buffer (pH 6.2) as the mobile phase on Merck C18 column.

As control reaction, **RNA40** and **PNA38** were individually incubated for 0-48 hrs at 37°C and 70°C with varying concentration of Zn^{2+} ion (Table 6, entry 1-8, Figure 18). **PNA38** was also stable under these reaction conditions suggesting no self cleavage. **RNA40** was stable at room temperature and at 37°C in the presence or absence of metal

ion (Table 6, entry 3-6). With increased concentration of Zn^{2+} (1 mM, 37°C) (Table 6, entry 7) and (100 μM, 70°C) (Table 6, entry 8), RNA underwent degradation. This may be due to the fact that the metal ion alone catalyzes the scission of RNA phosphodiester bond. These conditions could not be optimized Therefore, these two reaction conditions were not selected for further experiments.

PNA38 bearing the imidazole *C*4-acetyl unit at the N-terminus was subjected to cleavage reaction at 37°C for 48 hrs with the complementary **RNA40** to determine its catalytic activity (Table 6, entry 9). This reaction was done in absence of any metal ion using an equimolar concentration of both PNA and RNA substrate. The reaction mixture was incubated for 48 hrs and RP-HPLC analysis was done at a regular time intervals as mentioned in Table 6. No cleavage product was seen during the complete reaction period. Concentration **PNA38** was increased to 8 μM keeping the RNA concentration constant (Table 6, entry 10) and no change was observed in RP-HPLC analysis of the reaction.

Equimolar concentration of **PNA38** and **RNA40** were incubated with Zn^{2+} metal ion (10 μM, Table 6, entry 11) at 37°C for 48 hrs and HPLC analysis indicated no change. The concentration of **PNA38** was doubled to 8 μM and the reaction mixture was incubated for 48 hrs at 37°C (Table 6, entry 12). However no cleavage was observed as in the earlier case. Initially, **PNA38** (4 μM) and **RNA40** (4 μM) was taken in HEPES buffer (pH 7.0) containing Zn^{2+}(100μM) and was incubated for 48 hrs and RP-HPLC analysis indicated no change (Table 6, entry 13). The concentration of **PNA38** was then increased two fold to that of the **RNA40** maintaining all the conditions same as the previous (Table 6, entry 14). After this experiment the temperature of the reaction mixture was increased to 70°C without addition of metal ion (Table 6, entry 15). But none of the cases show a cleavage product in RP-HPLC analysis.

Table 6 : Different fractions of reaction mixture prepared for enzyme catalytic study

S No	PNA38 Conc.	RNA40 Conc.	Zn^{2+} concentration			Incubation temperature (°C)	Time interval (hr)	Remarks
			1mM	10µM	100µM			
1	4µM	-----	----	-----	✓	37	0,12, 24, 48	No cleavage
2	4µM	-----	----	----	----	37	0,12, 24, 48	No cleavage
3	-----	4µM	-----	-----	-----	37	0,12, 24, 48	No cleavage
4	-----	3µM	-----	✓	-----	37	0,12, 24, 48	No cleavage
5	-----	3µM	-----	-----	✓	rt	0,12, 24, 48	No cleavage
6	-----	3µM	-----	-----	✓	37	0,12, 24, 48	No cleavage
7	-----	4µM	✓	-----	-----	37	0,12, 24, 48	Non specific cleavage
8	-----	4µM	----	----	✓	70	12	Non specific Cleavage
9	4µM	4µM	-----	-----	-----	37	0,12, 24, 48	No cleavage
10	8µM	4µM	-----	-----	-----	37	0,3,6,9,12, 24	No cleavage
11	4µM	4µM	-----	✓	-----	37	0,12, 24, 48	No cleavage
12	8µM	4µM	-----	✓	-----	37	0,3,6,9,12, 24	No cleavage
13	4µM	4µM	-----	-----	✓	37	0,12, 24, 48	No cleavage
14	8µM	4µM	-----	-----	✓	37	0,3,6,9,12, 24	No cleavage
15	8µM	4µM	-----	-----	✓	70	0,3,6,9,12, 24	No cleavage

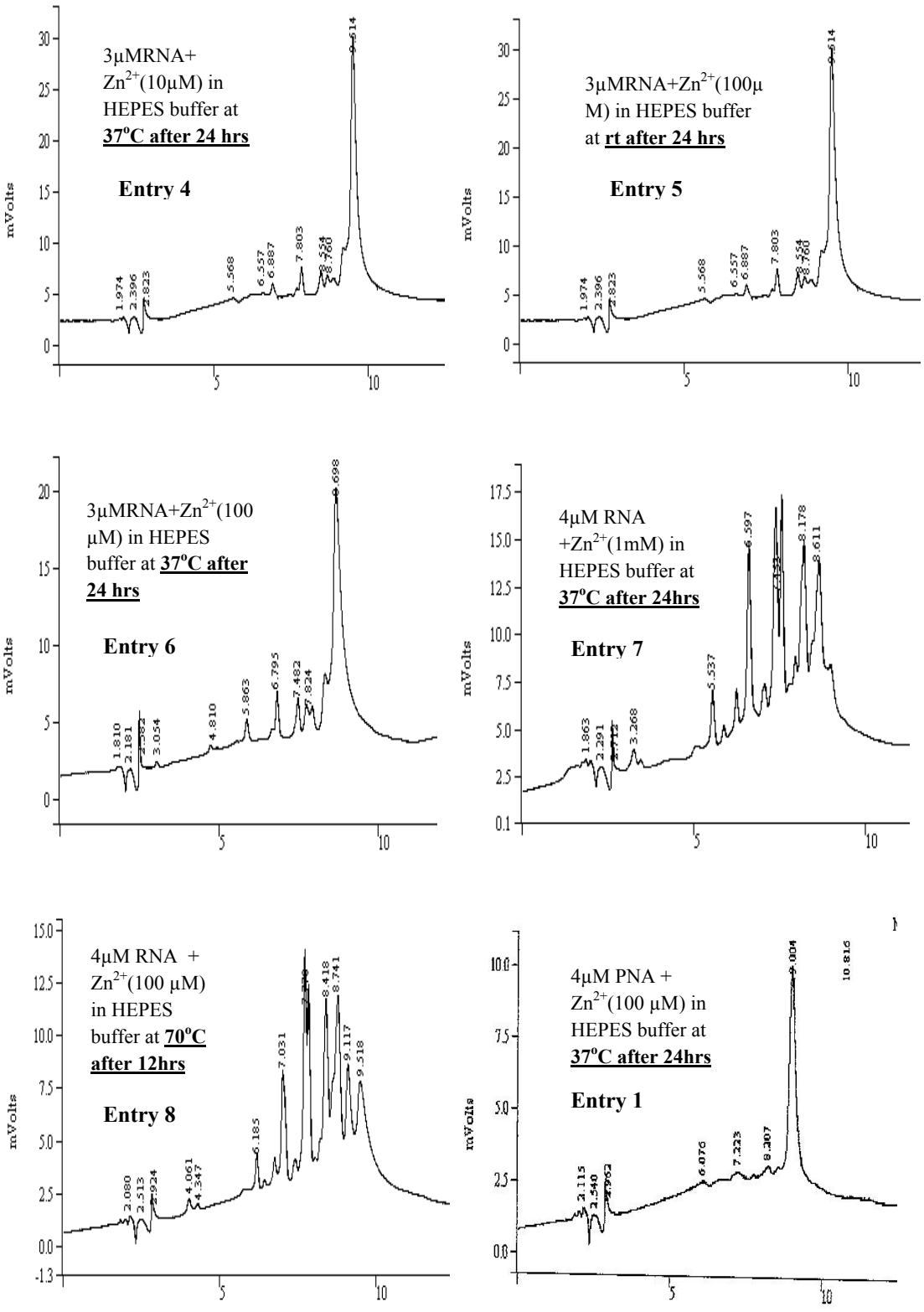

Figure 18: RP-HPLC spectra for **PNA38** and **RNA40**with Zn^{2+} for the control experiment

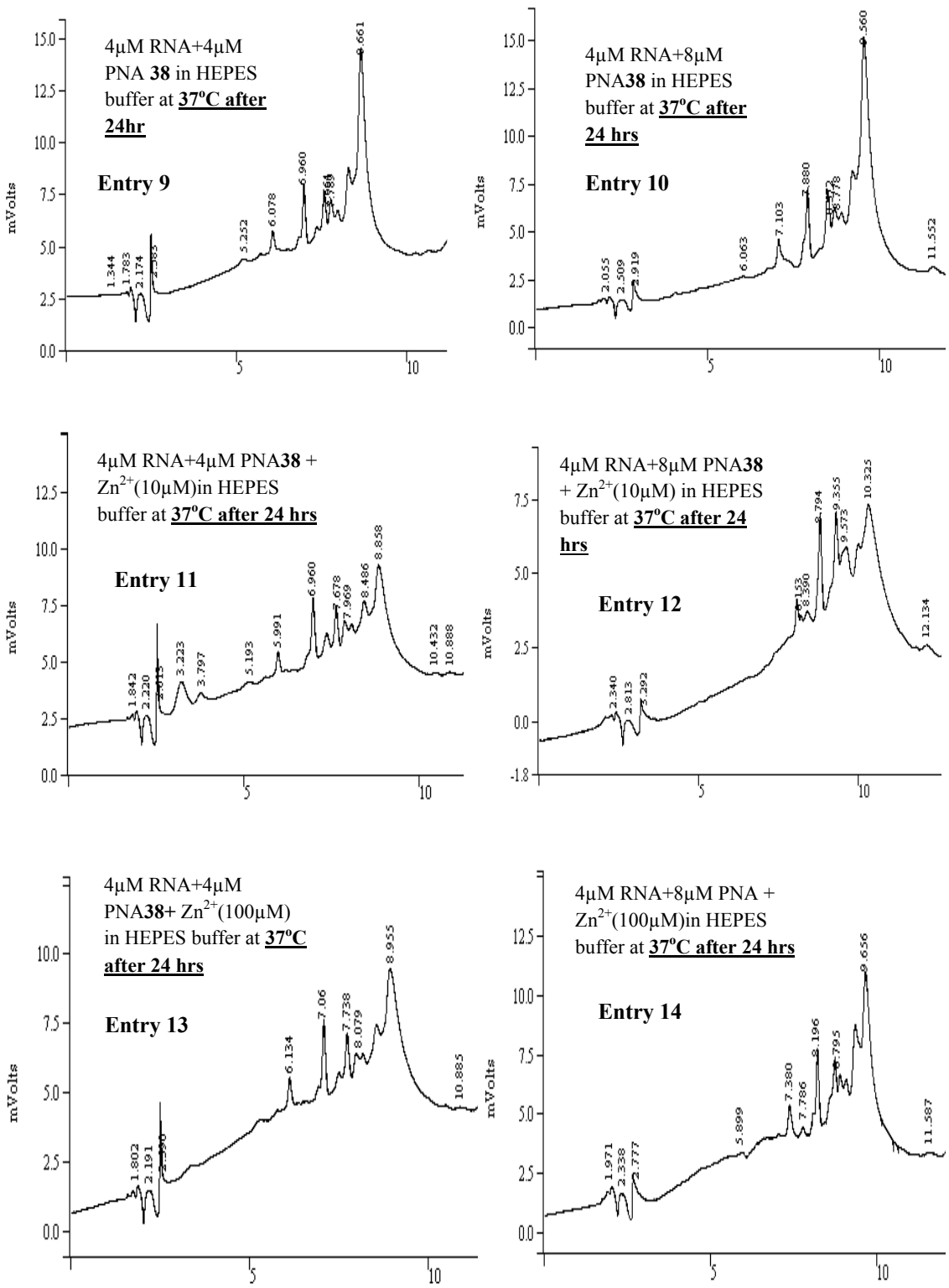

Figure 19: RP-HPLC spectra for the mixture of RNA**40** and PNA**38** with varying reaction conditions.

Therefore, from the above experiments it can be summarized that designed imidazole *C*4-acetyl modified **PNA38** does not cleave the phosphodiester bond of the complementary RNA**40** irrespective of the presence and absence of metal ion. The scission of the RNA phosphodiester bond happens with higher concentration of metal ion alone. It is possible that the terminally modified imidazole PNA does not align the catalytic imidazole unit in proper orientation and vicinity to approach the RNA phosphodiester group. Hence experiments need to be done in centrally modified PNA oligomers.

4.5 Conclusion

Imidazole *N*1-acetyl and imidazole *C*4-acetyl PNA monomers have been synthesized. The oligomers were synthesized from Imidazole *N*1-acetyl PNA monomer and UV-T_m was determined for the oligomers. Destabilization was observed for all the homothymine oligomers.

RNA cleavage experiments were performed for catalytic **PNA38** which bears an imidazole moiety at the N-terminus of the oligomer. Various reaction conditions was preapared to carry out the cleavage experiment by varying the concentration of PNA, reaction temperature and the metal ion. But under none of the conditions any specific RNA cleavage was observed. Under slightly high Zn^{2+} concentration, RNA got completely degraded. Further studies are required in terms of different RNA sequences (longer), PNA sequence (mixed purine-pyrimidine) to optimize and test the hypothesis.

4.6 Experimental

***N*-(Boc-aminoethylglycyl) imidazole-*N*-acetyl ethyl ester (11)**

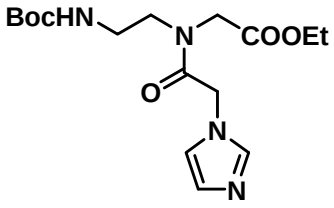

A mixture of ethyl *N*-(Boc-aminoethyl)- *N* (chloroacetyl)-glycinate **10** (2.0 g, 6.2 mmol), K_2CO_3 (0.94 g, 6.8 mmol) and imidazole (0.42 g, 6.2 mmol) in anhydrous DMF, was stirred with anhydrous in DMF at 60^{o}C for 6-8 hrs. DMF was removed under reduced pressure and the residue obtained was extracted with ethyl acetate (30 mL x 3) and washed with brine. The mixture obtained after removal of combined organic layer was purified by column chromatography to afford **11** (1.7 g, 79 %).

^{1}H NMR (200MHz, $CDCl_3$) δ 1.23-1.30 (t, 3H), 1.44 (s, 9H), 3.27-3.32 (m, 2H), 3.47-3.53(m, 2H), 4.02 (s, 2H), 4.14-4.21 (m, 2H), 4.84 (s, 2H), 5.67 (bm, 1H), 6.95 (s, 1H), 7.07 (s, 1H), 7.51 (s, 1H) **^{13}C NMR** (50MHz, $CDCl_3$) δ 14.0, 28.3, 38.5, 47.3, 48.5 (maj), 48.8 (min), 61.6 (maj), 62.2 (min), 79.9, 120.4, 128.8, 138.1, 156.2, 167.3, 169.5; **MS (EI)** *m/z* 354.4, Found 355.5 [M+H].

***N*-(Boc-aminoethylglycyl) imidazole-*N*- acetyl acid (5)**

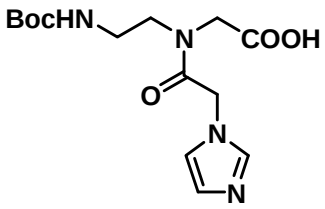

Compound **11** (1.0 g, 28 mmol) was dissolved in THF and 1N LiOH solution was added to this reaction mixture and stirred at rt for 1hr. After completion of the reaction it was neutralized by using Dowex H^+ resin and was isolated the product **5** (0.79 g, 86 %) from the aqueous reaction medium.

^{1}H NMR (200MHz, MeOH-d_4) δ 1.36 (s, 9H), 1.91 (s, 1H), 3.01-3.41 (m, 4H), 3.94-4.02 (d, 2H), 5.04 (s, 2H), 6.87 (s, 1H), 7.04 (s, 1H), 7.55 (s, 1H). **MS (EI)** m/z 326.3, Found 349.7 [M+Na^+]

***N*-(Boc-aminoethylglycyl) imidazole-4-acetyl ethyl ester (12)**

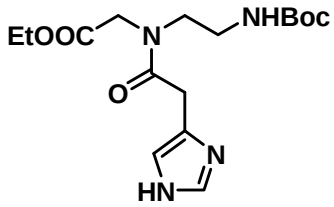

Imidazole 4-acetic acid (0.85 g, 4.8 mmol) was activated by coupling reagent EDC (0.74 g, 4.8 mmol) and DIPEA (0.85 mL, 4.8 mmol) in DMF under argon atmosphere. Compound **9** (1.0 g, 4.0 mmol) dissolved in DMF was then added to the reaction mixture. Reaction was stirred at

room temperature for 6 hrs. DMF was evaporated under reduced pressure and the left residue was extracted with ethyl acetate (30 mL x 3). Combined organic layer was washed with saturated Na_2HCO_3 solution followed by brine. Organic layer was evaporated in rota vapour and the compound was purified by column chromatography. (0.3 g, 22%)

^{1}H NMR (200MHz, $CDCl_3$) δ 1.23-1.31 (m, 3H), 1.43 (s, 9H), 3.25-3.28 (m, 2H), 3.53-3.61 (m, 2H), 3.77 (s, 2H), 4.04 (s, 2H), 4.17-4.24 (m, 2H), 5.83 (bm, 1H), 6.88 (s, 1H), 7.52 (s, 1H), 8.02 (bs, 1H); **^{13}C NMR** (50MHz, $CDCl_3$) δ 14.0, 28.3, 32.0, 38.8, 48.6, 49.4, 61.4 (maj), 61.8 (min), 79.4, 117.2, 131.1, 135.1, 156.2, 169.6 (min), 169.9 (maj), 171.8 (maj), 172.1; **MS (EI)** *m/z* 354.4, Found 355.5 [M+H].

***N*-(Boc-aminoethylglycyl) imidazole *C*4-acetyl acid (6)**

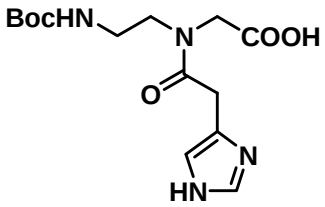

Ester **12** (0.3 g, 0.84 mmol) was taken in THF and 1N LiOH solution was added to this reaction mixture. It was then stirred at rt for 1hr. Neutralization was done by using Dowex H^+ resin after completion of the reaction. The product was isolated from aqueous medium in a good yield (0.21 g, 78%)**.**

^{1}H NMR (200MHz, $CDCl_3$) δ 1.46 (s, 9H), 3.27-3.35 (m, 2H), 3.5-3.7 (m, 2H), 3.85 (s, 1H), 4.0 (s, 1H), 4.08-4.12 (d, 2H), 7.36 (s, 1H), 8.60-8.68 (d, 1H); **MS (EI)** *m/z* 326.3, Found 349.2 [M+Na^+].

4.7 References

1. Been, M. D.; Wickham, G. S. Self-cleaving ribozymes of hepatitis delta virus RNA. *Eur. J. Biochem*. **1997**, 247, 741-753.

2. (a) Zelphati, O.; Imbach, J.-L.; Signoret, N.; Zon, G.; Rayner, B.; Leserman. L. Antisense oligonucleotides in solution or encapsulated in immunoliposomes inhibit replication of HIV-1 by several different mechanisms. Nucleic Acids Research, **1994**, *22*, 4307-4314. (b) Tavitian, B.; Terrazzino, S.; Kühnast, B.; Marzabal, S.; Stettler, O.; Dolle, F.; Deverre, J.-R.; Jobert, A.; Hinnen, F.; Bendriem, B.; Crouzel, C.; Giamberardino, L-D. *In vivo* imaging of oligonucleotides with positron emission tomography. *Nature Medicine*, **1998**, *4*, 467- 471.

3. (a) Pley, H. W.; Flaherty, K. M.; McKay, D. B. Three-dimensional structure of a hammerhead ribozyme. *Nature*, **1994**, *372*, 68-74. (b) Scott, W. G.; Finch, J. T.; Klung, A. The crystal structure of an all-RNA hammerhead ribozyme: a proposed mechanism for RNA catalytic cleavage. *Cell*, **1995**, *81*, 991-1002.

4. (a) Prakash, T. P.; Kunte, S. S.; Ganesh, K. N. Self cleavage of CS-histamine-r(UpA) promoted by $ZnCl_2$: Mechanistic studies on a designed ribonuclease mimic. *Tetrahedron*, **1994**, *50*, 11699-l 1708. (b) Nesbitt, S.; Hegg, L. A.; Fedor, M. J. *Chem. Biol.* **1998**, *4*, 619-630.

5. Perreault, D. M.; Anslyn, E. V. Unifying the current data on the mechanism of cleavage- transesterification of RNA. *Angew. Chem. Int. Ed. Eng.* **1997**, *36*, 432-450.

6. Prudent, J. R.; Uno, T.; Schultz, P. G. Expanding the Scope of RNA Catalysis. *Science,* **1994**, *264*, 1924-1927.

7. Kuzuya, A.; Mizoguchi, R.; Morisawa, F.; Machida, K.; Komiyama, M. Metal ion-induced site-selective RNA hydrolysis by use of acridine-bearing oligonucleotide as cofactor. *J. Am. Chem. Soc.* **2002**, *124*, 6887-6894.

8. (a) Whitney, A.; Gavory, G.; Balasubramanian, S. Site-specific cleavage of human telomerase RNA using PNA-neocuproine-Zn(II) derivatives. *Chem. Commun.* **2003**, 36-37. (b) Astrom, H.; Williams, N. H.; Stromberg, R. Oligonucleotide based artificial nuclease (OBAN) systems. Bulge size dependence and positioning of catalytic group in cleavage of RNA-bulges. *Org. Biomol. Chem.* **2003**, 1, 1461-1465. (c) Astrom, H.; Stromberg, R. Synthesis of new OBAN's and further studies on positioning of the catalytic group. *Org. Biomol. Chem.* **2004**, 2, 1901-1907.

9. Wall, M.; Linkletter, B.; Williams, D.; Lebuis, A.-M.; Hynes, R.C.; Chin, J. Rapid hydrolysis of 2',3'- cAMP with a Cu(II) complex: Effect of intramolecular hydrogen bonding on the basicity and reactivity of a metal-bound hydroxide. *J. Am. Chem. Soc.* **1999**, *121*, 4710-4711.

10. Murtola, M.; Ossipov, D.; Sandbrink, J.; Strömberg, R. RNA Cleavage by 2,9-Diamino-1,10 Phenanthroline PNA Conjugates. *Nucleosides & Nucleotides*, **2007**, *26*, 1479-1483.
11. Murtola, M.; Stromberg, R. PNA based artificial nucleases displaying catalysis with turnover in the cleavage of leukemia related RNA model. *Org. Biomol. Chem.* **2008**, *6*, 3837-3842.
12. (a) Eichhorn, G. L.; Tarien, E.; Butzow, J. J. Interaction of metal ions with nucleic acids and related compounds. XVI. Specific cleavage effects in the depolymerization of ribonucleic acids by Zinc(II) ions. *Biochemistry*, **1971**, *10*, 2014-2019. (b) Shelton, V. M.; Morrow, J. R. Catalytic transesterification and hydrolysis of RNA by Zinc(II) Complexes. *Inorg. Chem.* **1991**, *30*, 4295-4299.
13. Morrow, J. R.; Buttery, L. A.; Shelton, V. M.; Berback, K. A. Efficient catalytic cleavage of RNA by Lanthanide(III) macrocyclic complexes: Toward synthetic nucleases for in vivo applications. *J. Am. Chem. Soc.* **1992**, *114*, 1903-1905.
14. (a) Magda, D.; Miller, R. A.; Sessler, J. L.; Iverson, B. L. Site-specific hydrolysis of RNA by Europium(III) texaphyrin conjugated to a synthetic oligodeoxyriboaucleotide. *J. Am. Chem. Soc.* **1994**, *116*, 7439-7440. (b) Magda, D.; Crofts, S.; Lin, A.; Miles, D.; Wright, M.; Sessler, J. L. Synthesis and kinetic properties of Ribozyme Analogues Prepared Using Phosphoramidite Derivatives of Dysprosium(III) texaphyrin. *J. Am. Chem. Soc.* **1997**, *119*, 2293-2294. (c) Magda, D.; Wright, M.; Crofts, S.; Lin, A.; Sessler, J. L. Metal complex conjugates of antisense DNA which display ribozyme-like activity. *J. Am. Chem. Soc.* **1997**, *119*, 6947-6948. (d) Hall, J.; Husken D.; Haner, R. Towards artificial ribonucleases: the sequence-specific cleavage of RNA in a duplex. *Nucleic Acids Res.*, **1996,** *24*, 3522-3526.
15. (a) Bashkin, J. K.; Frolova, E. I; Sampath, U. Sequence-specific cleavage of HIV mRNA by a ribozyme mimic. *J. Am. Chem. Soc.* **1994**, *116*, 5981. (b) Daniher, A. T.; Bashkin, J. K. Precise control of RNA cleavage by ribozyme mimics. *Chem. Commun.* **1998**, 1077-1078. (c) Putnam, W. C.; Bashkin, J. K. *De novo* synthesis of artificial ribonucleases with benign metal catalysts. *Chem. Commun.* **2000**, 767-768. (e) Inoue, H.; Furukawa, T.; Tamura, T.; Kamada, A.; Ohtsuka, E. Rapid RNA cleavage using an antisense system with two terpyridine Cu(II) complexes. *Nucleosides & Nucleotides*, **2001**, *20*, 833-835. (f) Sakamoto, S.; Tamura, T.; Furukawa, T.; Komatsu, Y.; Ohtsuka, E.; Kitamura, M.; Inoue, H. Highly efficient catalytic RNA cleavage by the cooperative action of two Cu(II) complexes embodied within an antisense oligonucleotide. *Nucleic Acids Res.* **2003**, *31*, 1416-1425.
16. (a) Astrom, H.; Williams, N. H.; Stromberg, R. Oligonucleotide based artificial nuclease (OBAN) systems. Bulge size dependence and positioning of catalytic group in cleavage of RNA-bulges. *Org. Biomol. Chem.* **2003**, *1*, 1461-1465. (b)

Astrom, H.; Stromberg, R. Synthesis of new OBAN's and further studies on positioning of the catalytic group. *Org. Biomol. Chem.* **2004**, *2*, 1901-1907.

17. Breslow, R.; Anslyn, E.; Huang, D.-L. Ribonuclease mimics. *Tetrahedron*, **1991**, *47*, 2365-2376.

18. Breslow, R.; Huang, D.-L.; Anslyn, E. On the mechanism of action of ribonucleases: Dinucleotide cleavage catalysed by imidazole and Zn^{2+}. **1989**, *88*, 1746-1750.

19. Breslow, R.; Labelle, M. Sequential general base-acid catalysis in the hydrolysis of RNA by imidazole. *J. Am. Chem. Soc*. **1986**, *108*, 2655-2659.

20. Hovinen, J.; Guzaev, A.; Azhayeva, E.; Azhayev, A.; Lonnberg, H. Imidazole tethered oligodeoxyribonucleotides: synthesis and RNA cleaving activity. *J. Org. Chem.* **1995**, *60*, 2205-2209.

21. (a) Vlassov, V.; Abramova, T.; Godovikova, T.; Giege, R.; Silnikov, V. Sequence-specific cleavage of yeast tRNA(Phe) with oligonucleotides conjugated to a diimidazole construct. *Antisense Nucleic Acid Drug Dev*. **1997**, *7*, 39-42. (b) Beloglazova, N. G.; Fabani, M. M.; Zenkova, M. A.; Bichenkova, E. V.; Polushin, N.N.; Silnikov, V. V.; Douglas, K. T.; Vlassov, V. V. Sequence-specific artificial ribonucleases. I. Bis-imidazole-containing oligonucleotide conjugates prepared using precursor-based strategy. *Nucleic Acids Res.* **2004**, *32*, 3887-3897. (c) Yurchenko, L.; Silnikov, V.; Godovikova, T.; Shishkin, G.; Toulme J.-J.; Vlassov, V. Cleavage of leishmania mini-exon sequence by oligonucleotides conjugated to a dimidazole construction. *Nucleosides & Nucleotides*, **1997**, *16*, 1721-25.

22. Reynolds, M. A.; Beck, T. A.; Say, P. B.; Schwartz, D. A.; Dwyer, B. P.; Daily, W. J.; Vaghefi, M. M.; Metzler, M. D.; Klem, R. E.; Arnold Jr., L. J. Antisense oligonucleotides containing an internal, non-nucleotide-based linker promote site-specific cleavage of RNA. *Nucleic Acids Res.* **1996**, *24*, 760-765.

4.8 Appendix

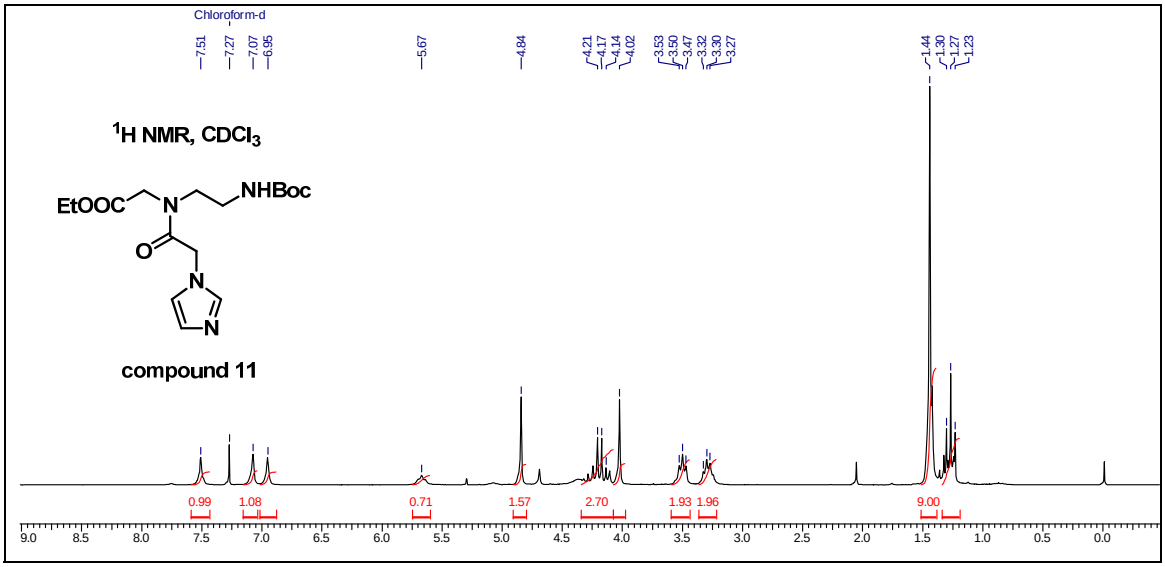
Chloroform-d
7.51
7.27
7.07
6.95
5.67
4.84
4.21
4.17
4.14
4.02
3.53
3.50
3.47
3.32
3.30
3.27
1.44
1.30
1.27
1.23
^{1}H NMR, CDCl$_3$
EtOOC
N
NHBoc
O
N
N
compound 11
0.99
1.08
0.71
1.57
2.70
1.93
1.96
9.00

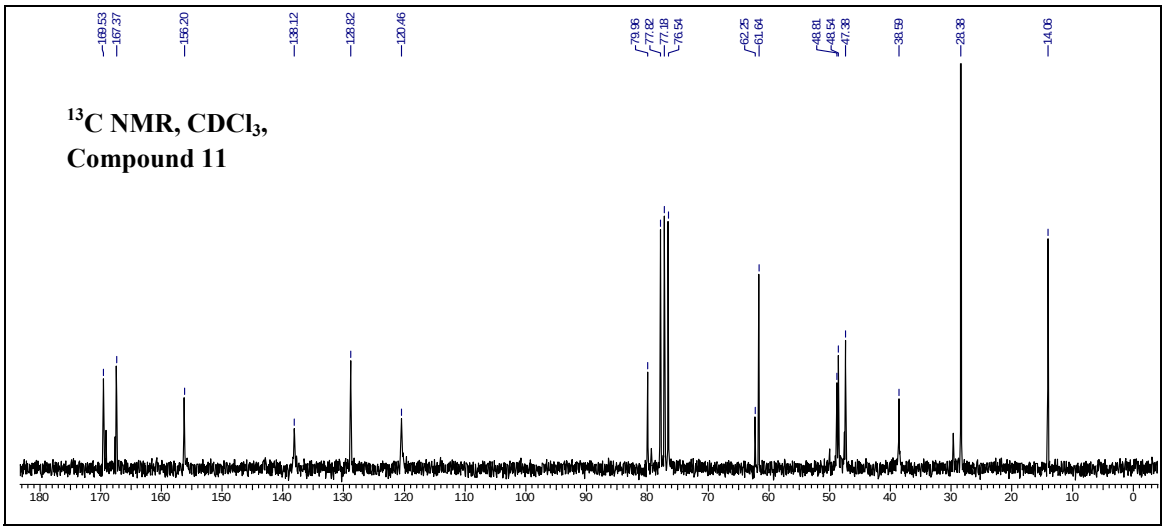
169.53
167.37
156.20
138.12
128.82
120.46
79.96
77.82
77.18
76.54
62.25
61.64
48.81
48.54
47.38
38.59
28.38
14.06
^{13}C NMR, CDCl$_3$,
Compound 11

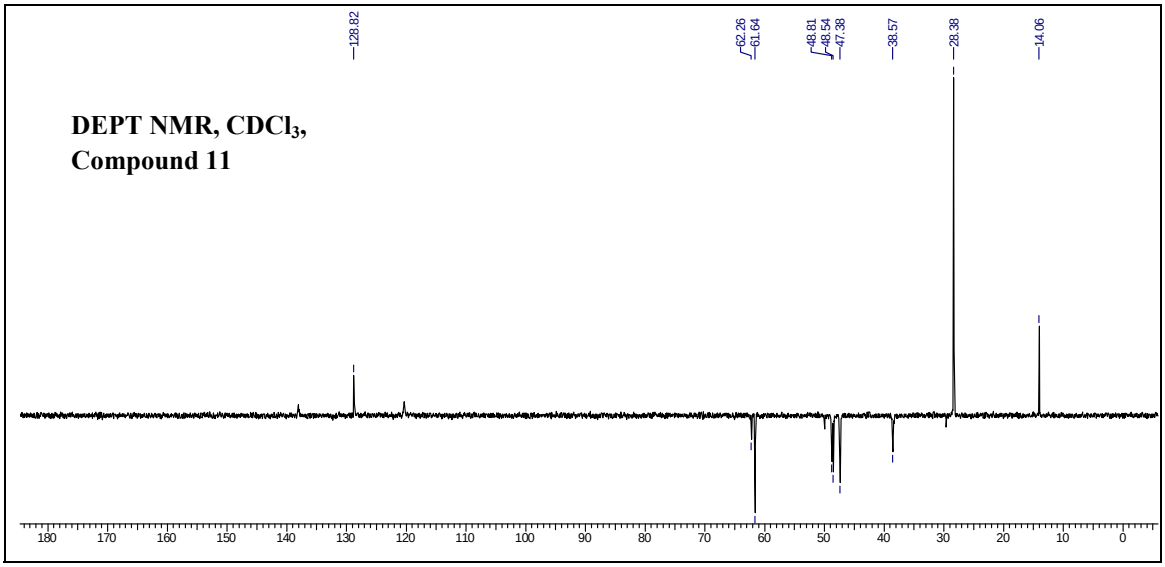
128.82
62.26
61.64
48.81
48.54
47.38
38.57
28.38
14.06
DEPT NMR, CDCl$_3$,
Compound 11

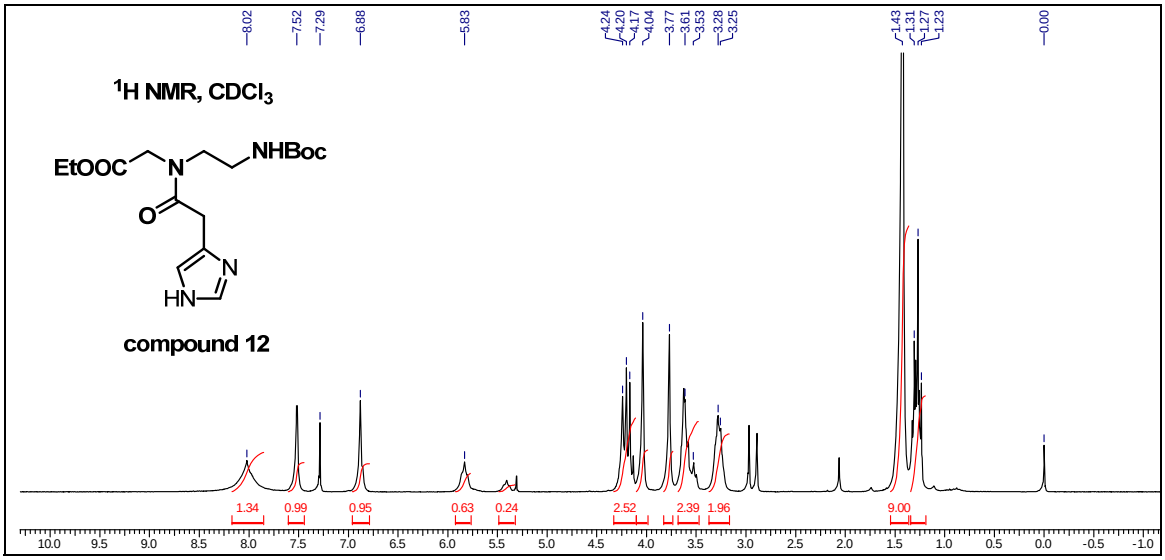
8.02
7.52
7.29
6.88
5.83
4.24
4.20
4.17
4.04
3.77
3.61
3.53
3.28
3.25
1.43
1.31
1.27
1.23
0.00
1H NMR, CDCl3
EtOOC
N
NHBoc
O
N
HN
compound 12
1.34
0.99
0.95
0.63
0.24
2.52
2.39
1.96
9.00

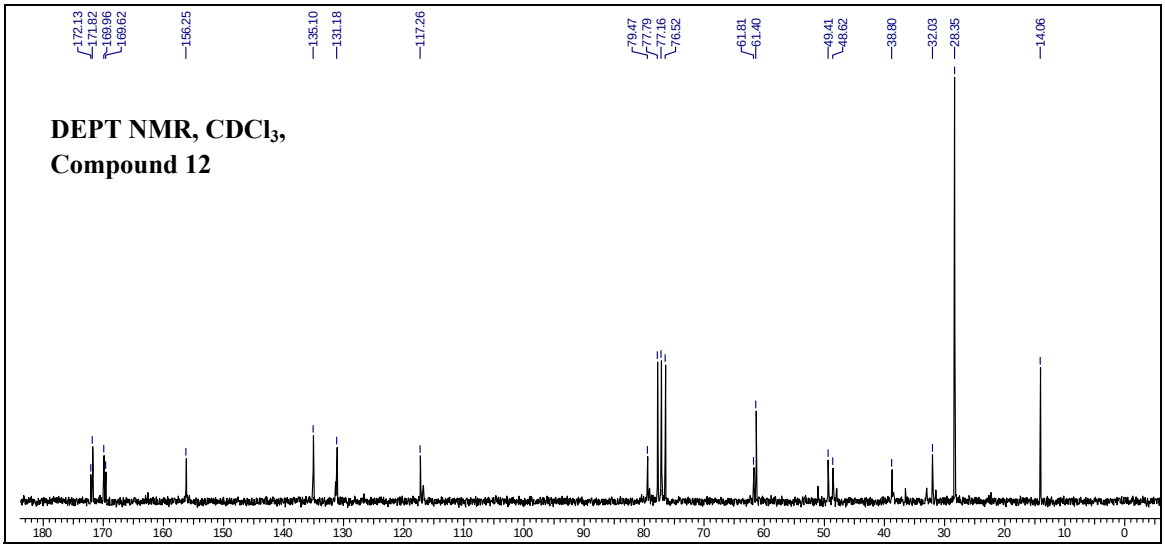
172.13
171.82
169.96
169.62
156.25
135.10
131.18
117.26
79.47
77.79
77.16
76.52
61.81
61.40
49.41
48.62
38.80
32.03
28.35
14.06
DEPT NMR, CDCl3,
Compound 12

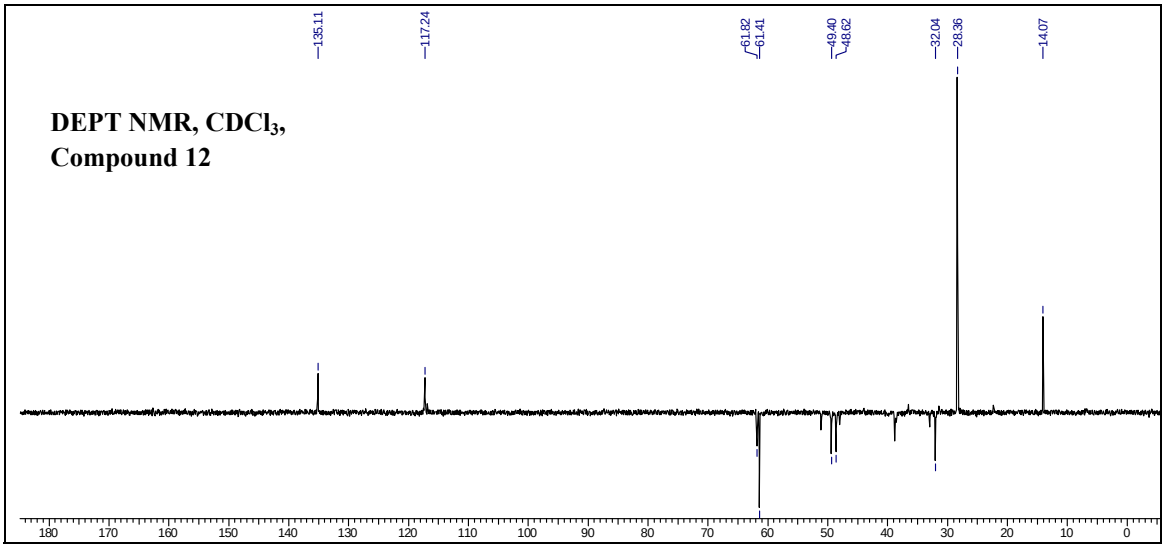
135.11
117.24
61.82
61.41
49.40
48.62
32.04
28.36
14.07
DEPT NMR, CDCl3,
Compound 12

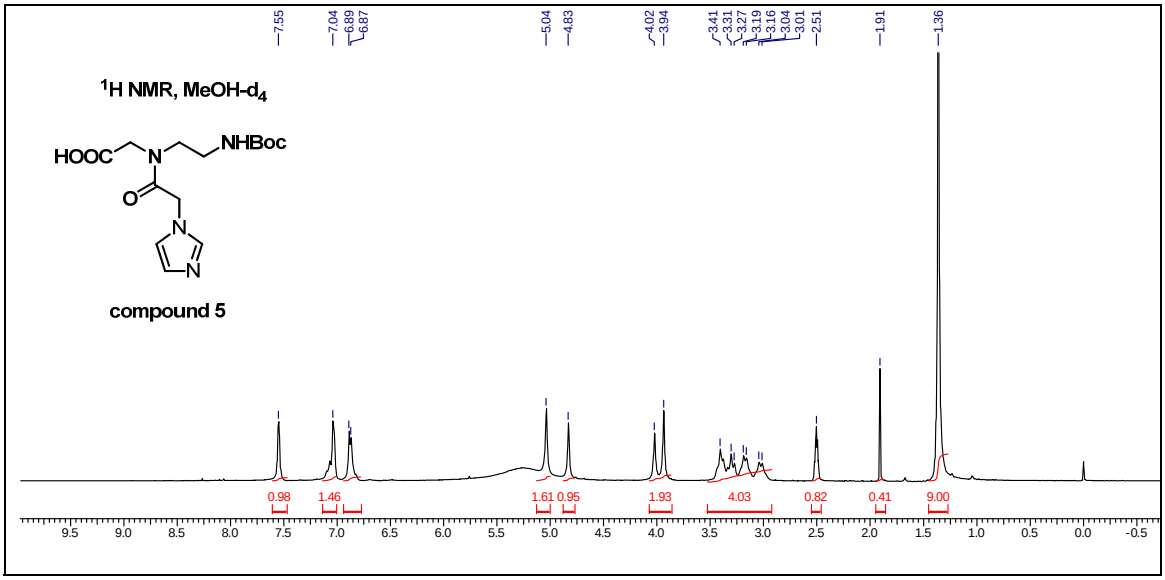
7.55
7.04
6.89
6.87
5.04
4.83
4.02
3.94
3.41
3.31
3.27
3.19
3.16
3.04
3.01
2.51
1.91
1.36
^{1}H NMR, MeOH-d$_4$
HOOC
N
NHBoc
O
N
N
compound 5
0.98
1.46
1.61
0.95
1.93
4.03
0.82
0.41
9.00

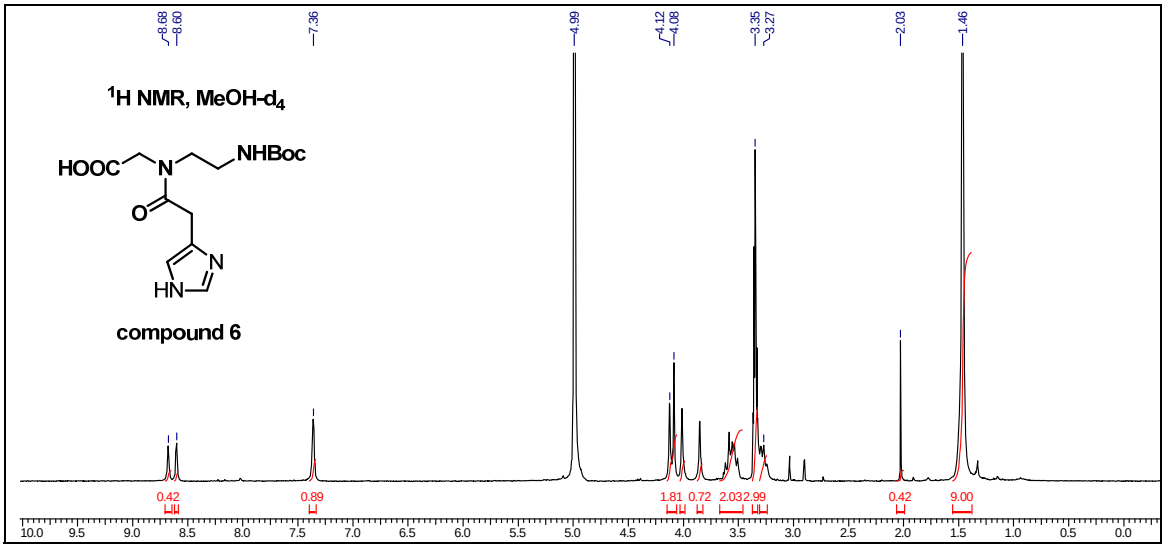
8.68
8.60
7.36
4.99
4.12
4.08
3.35
3.27
2.03
1.46
^{1}H NMR, MeOH-d$_4$
HOOC
N
NHBoc
O
N
HN
compound 6
0.42
0.89
1.81
0.72
2.03
2.99
0.42
9.00

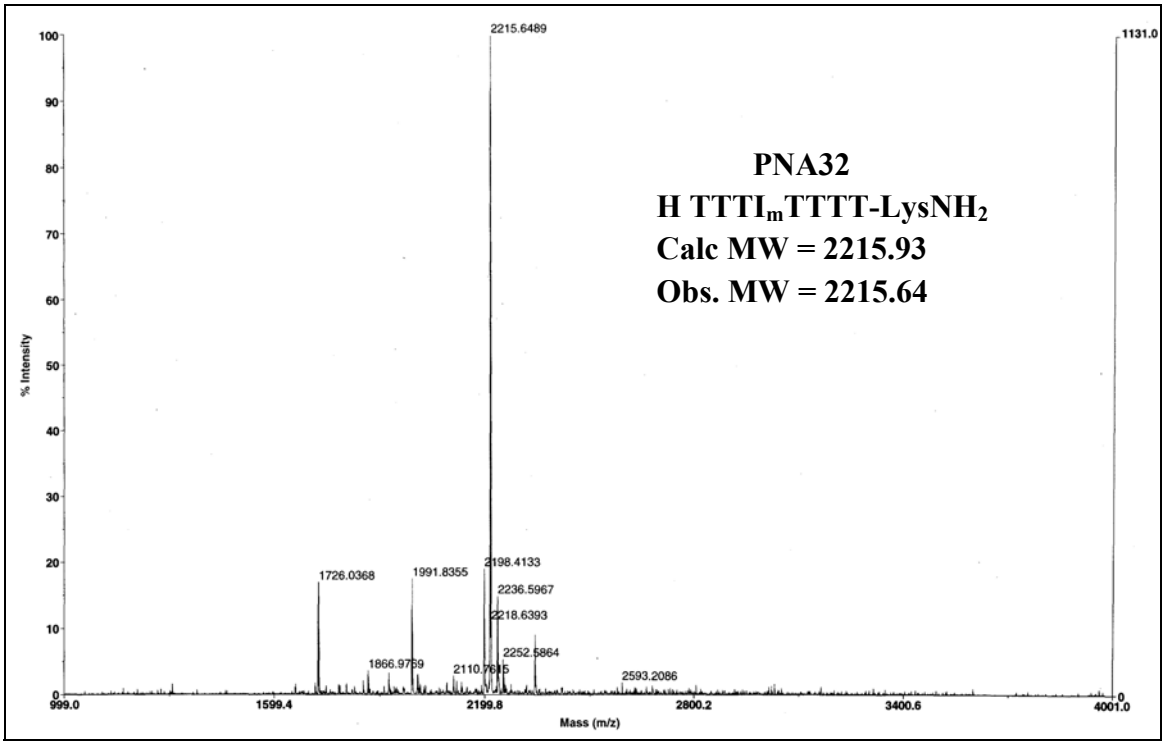
PNA32
H TTTI$_m$TTTT-LysNH$_2$
Calc MW = 2215.93
Obs. MW = 2215.64
2215.6489
1131.0
1726.0368
1991.8355
2198.4133
2236.5967
2218.6393
2252.5864
1866.9759
2110.7615
2593.2086
% Intensity
Mass (m/z)
999.0
1599.4
2199.8
2800.2
3400.6
4001.0

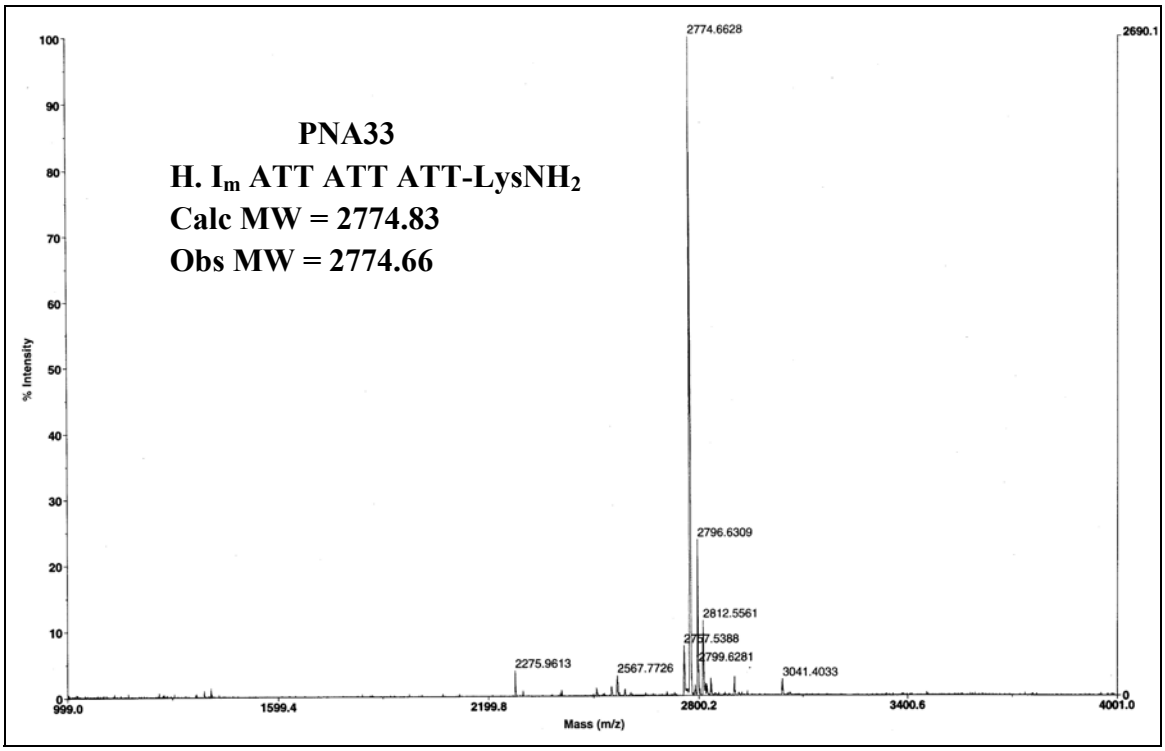
PNA33
H. I$_m$ ATT ATT ATT-LysNH$_2$
Calc MW = 2774.83
Obs MW = 2774.66
2774.6628
2690.1
2796.6309
2812.5561
2757.5388
2799.6281
2275.9613
2567.7726
3041.4033
% Intensity
Mass (m/z)
999.0
1599.4
2199.8
2800.2
3400.6
4001.0

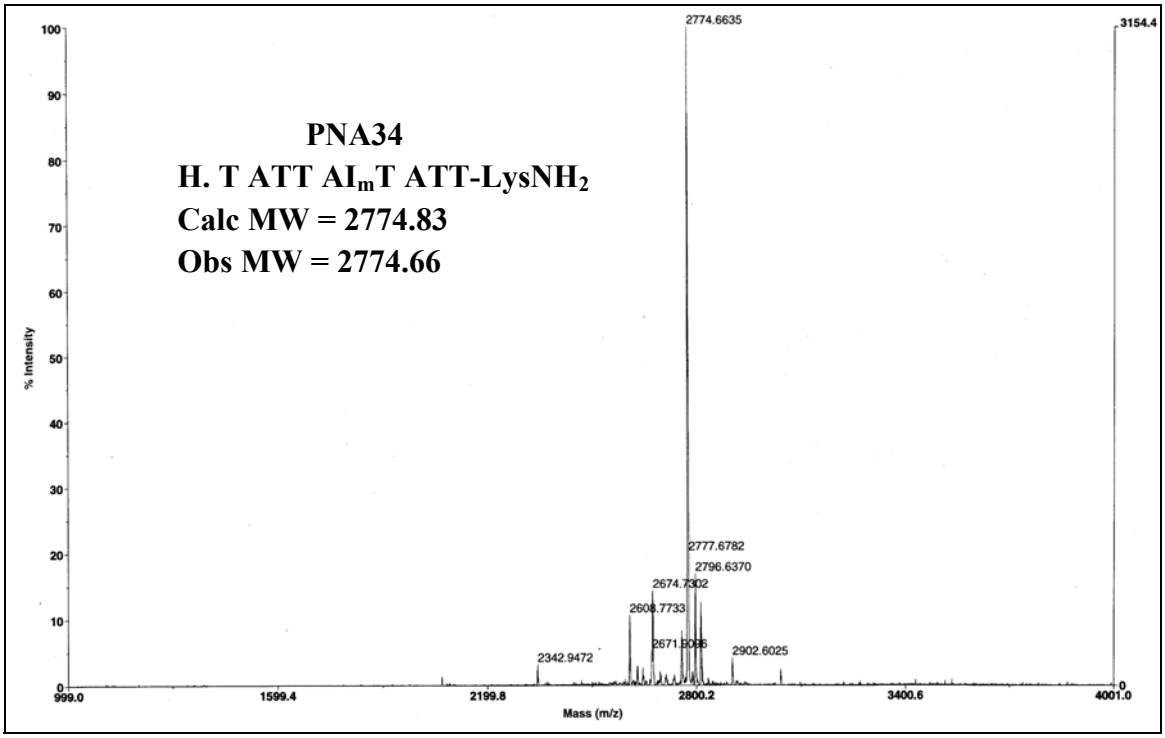
PNA34
H. T ATT AI$_m$T ATT-LysNH$_2$
Calc MW = 2774.83
Obs MW = 2774.66
2774.6635
3154.4
2777.6782
2796.6370
2674.7302
2608.7733
2671.9066
2902.6025
2342.9472
% Intensity
Mass (m/z)
999.0
1599.4
2199.8
2800.2
3400.6
4001.0

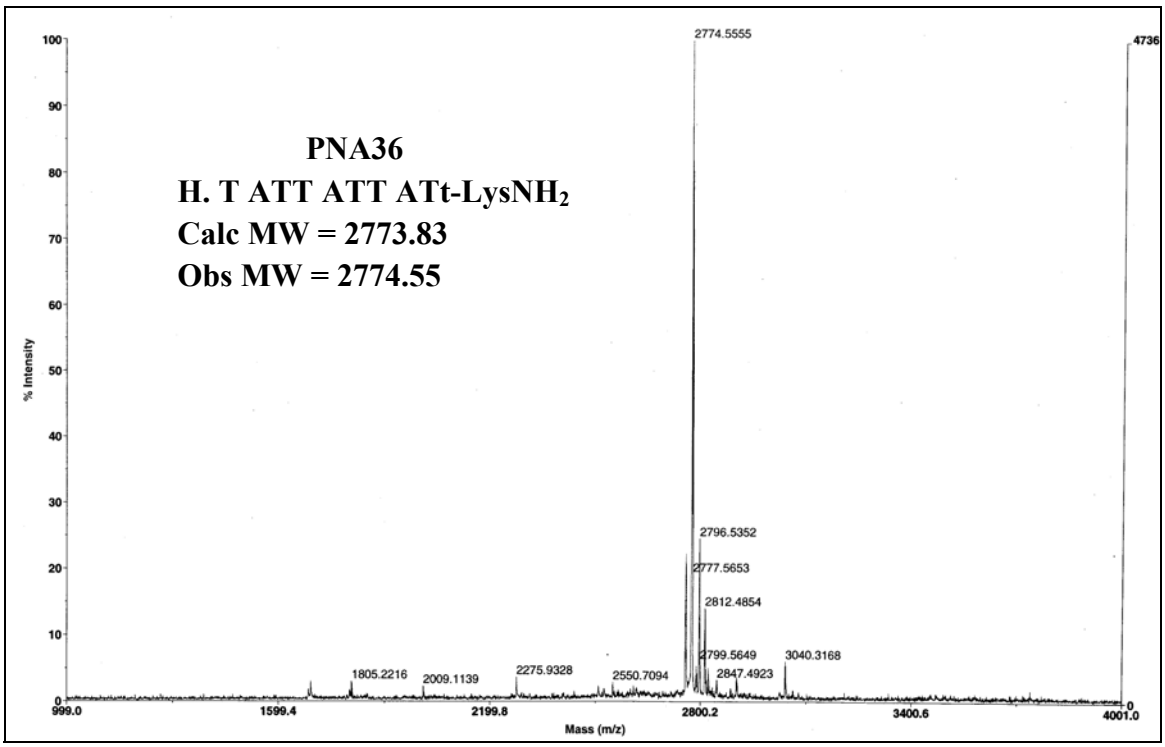
PNA36
H. T ATT ATT ATt-LysNH$_2$
Calc MW = 2773.83
Obs MW = 2774.55
2774.5555
4736
2796.5352
2777.5653
2812.4854
2799.5649
3040.3168
2847.4923
1805.2216
2009.1139
2275.9328
2550.7094
% Intensity
Mass (m/z)
999.0
1599.4
2199.8
2800.2
3400.6
4001.0